NEUROPROTECTION AND FUNCTIONAL ALTERATIONS IN MICE OVER-EXPRESSING HEAT SHOCK PROTEIN 70i

STEPHEN KELLY B.Sc. (Hons)

A thesis submitted for the degree of Doctor of Philosophy to the Faculty of Medicine,

University of Glasgow

Wellcome Surgical Institute and Hugh Fraser Neuroscience Laboratories,

University of Glasgow,

Garscube Estate, Bearsden Road, Glasgow, G61 1QH.

ProQuest LLC.
789 East Eisenhower Parkway
P.O. Box 1346
Ann Arbor, MI 48106 – 1346

DECLARATION

I do solemnly declare that this thesis comprises of my own original work and has not been accepted in any previous application for a degree. The work, of which this thesis is a record, was carried out by myself, except where acknowledged. All sources of information have been specifically referenced.

Stephen Kelly

ACKNOWLEDGEMENTS

Throughout my three and a half years at the Wellcome Surgical Institute, compiling and completing this thesis, I was fortunate to work and associate myself with some truly special people. I would like to take this opportunity to acknowledge the help, guidance, support, harassment, criticism (various forms) and systematic abuse I received from many of these sources, which have helped shape this thesis. To do this I have adopted the seven orders of the celestial hierarchy according to St Jerome.

Achieving the rank of seraphim, I would like to thank my supervisor Professor Jim McCulloch. First, for his never failing support, guidance and access to his knowledge of the field of cerebrovascular research (even when I could have done without it). Second, his energy and drive for matters of cerebrovascular research, which I feel have imparted upon me somewhat. Third, telling me about the rule of three. Achieving the order of cherubin, I would like to thank Dr Karen Horsburgh for her consistent support, guidance, availability for scientific consultation at short notice and her expert involvement (practical; Section 3.1, Appendix G – upon which I was fortunate to collaborate) and (theoretical; Section 3.2). Achieving the rank of Powers, I would like to thank Dr James Uney and his colleagues at the University of Bristol (notably Ali Fryer) for providing me with my transgenic mice and adenovirus vectors, which formed the basis of several studies within this thesis. Achieving the rank of Dominion, I would like to thank the many pre and post-doctoral scientists (notably Dr Lawrence Dunn - my advisor, Dr Nobuhiro Hakuba – with whom I collaborated on appendices I, J and K, Dr Amy Lam, Louise Marks, Dr Eileen McCracken, Dr Iain Murdoch, Dr Elaine Peters, Dr Marc Soriano and Dr Omar Touzani) with whom I have been fortunate enough to work, rest and play. Achieving the order of Thrones, I would like to thank all the other staff of the Wellcome Surgical Institute (be they technical or secretarial) and the staff of biological services (at the veterinary research facility and the parasitology animal house) for all of their help and assistance. Achieving

the order of archangel, I would like to thank Professor David Graham (Department of Neuropathology) for his expert opinion and guidance, Professor Ian Griffiths (Veterinary Clinical Studies) for allowing me to use his image capture system, Dr Christine Thompson for the use of her microscope and Dr Julia Edgar for her instruction in operating both of the aforementioned. Achieving the order of angel, I would like to thank my family (predominantly for their profound words of empathy and encouragement in times of stress- 'well you'll just need to do it' and the occasional hot meal), the Wilsons (for taking me in for the last two months of the production of this thesis) and my pals John and Derek (for providing minimal resistance at snooker and to self-induced inebriation).

Finally, achieving an order somewhere between seraphim and the almighty, I would like to thank Mairi for all her efforts and support over the last several years by way of dedicating this thesis to her, as she has paid heavily for it in both mental and monetary terms.

LIST OF CONTENTS

CHAPTER TWO: MATERIALS AND METHODS

LIST OF FIGURES

LIST OF TABLES

LIST OF ABBREVIATIONS

ACA	anterior cerebral artery
ad	adenovirus
AMPA	α-amino-2, 3-dihydro-5-methyl-3-oxo-4-isoxalepropanoic acid
apoE	apolipoprotein E
BA	basilar artery
BCCAo	bilateral common carotid artery occlusion
CMV	cytomegalovirus
CNS	central nervous system
DNA	deoxyribonucleic acid
egfp	enhanced green fluorescing protein
ES cell	embryonic stem cell
HPRT	hypoxanthine guanine phosphorybosil transfecrase
hsc	heat shock cognate
hse	heat shock element
hsf	heat shock factor
hsp	heat shock protein
hsv	herpes simplex virus
IL-18	interleukin-18
LCGU	local cerebral glucose utilisation
MABP	mean arterial blood pressure
MCA	middle cerebral artery
MCAo	middle cerebral artery occlusion
mins	minutes
mM	millimolar
mmHg	millimeters mercury
mRNA	messenger ribonucleic acid
nCi/g	nanocuries per gram
NMDA	*N*-methyl-D-aspartate
PCA	posterior communicating artery
PcomA	posterior communicating artery
SCA	superior cerebellar artery

SUMMARY

Heat Shock proteins (hsps) are induced and expressed in response to cerebral ischaemia. Pre-conditioning and cell culture studies have indicated that hsp 70i (the major inducible hsp) may be involved in reducing ischaemic neuronal damage induced by cerebral ischaemia and simulated ischaemia, respectively. Moreover, genetically modified mice and viral vectors are being increasingly employed to investigate the roles of various genes and gene products in cerebral ischaemia. The studies of this thesis were designed to address two major themes. First, the influence of hsp 70i upon ischaemic neuronal damage following global cerebral ischaemia was investigated using transgenic mice over-expressing hsp 70i and intrastriatal adenovirus (ad) hsp 70i gene transfer. Second, the functional consequences of transgene introduction into the brain were investigated, in transgenic mice over-expressing hsp 70i and in mice with intrastriatal ad enhanced green fluorescing protein (egfp, reporter gene) gene transfer.

Global cerebral ischaemia in MF1 and C57bl/6 strain mice

A mouse model of global cerebral ischaemia (bilateral common carotid artery occlusion, BCCAo) was established to investigate the influence of hsp 70i over-expression in the pathophysiology of cerebral ischaemia. The pathologic consequences of BCCAo in MF1 mice (the background strain of the hsp 70i transgenic mice used in this thesis) were compared with those in C57bl/6 mice (the strain most susceptible to BCCAo). Ischaemic neuronal damage in MF1 strain mice was significantly less extensive and widespread than that observed in C57bl/6 strain mice (even after extended BCCAo in MF1 mice). Significantly increased posterior communicating artery (PcomA) plasticity in the circle of Willis and significantly increased mean arterial blood pressure (MABP) in MF1 strain mice during BCCAo were the most likely reasons for reduced susceptibility to BCCAo compared with C57bl/6 strain mice.

Ischaemic neuronal damage in transgenic mice over-expressing hsp 70i

Hsp 70i is induced in the brain by several stimuli (including cerebral ischaemia) and has been postulated to play a beneficial role in damaged cells. Following BCCAo, transgenic mice over-expressing hsp 70i displayed significantly reduced ischaemic neuronal damage in the medial caudate nucleus, lateral caudate nucleus and posterior thalamus than wild type littermate mice. PcomA plasticity and MABP during BCCAo were similar in hsp 70i transgenic and wild type littermate mice. These data indicate that transgenic hsp 70i over-expression reduces ischaemic neuronal damage induced by BCCAo.

Ischaemic neuronal damage following ad hsp 70i and ad egfp gene transfer

Gene transfer of therapeutic molecules by viral vectors has been shown to reduce ischaemic neuronal damage induced by both global and focal cerebral ischaemia. Intrastriatal injection of ad hsp 70i and ad egfp significantly reduced ischaemic neuronal damage in ipsilateral caudate nucleus compared with contralateral nucleus following 20-minute BCCAo, but not 10-minute BCCAo. Although ad hsp 70i and ad egfp gene transfer reduced ischaemic neuronal damage following 20-miunte BCCAo it is unlikely that they did so by the same mechanism, although this could not be concluded.

Local cerebral glucose utilisation in transgenic mice over-expressing hsp 70i

To investigate the impact of hsp 70i over-expression on local cerebral glucose utilisation (LCGU), ^{14}C-2-deoxyglucose autoradiography was employed. LCGU in transgenic mice over-expressing hsp 70i was not significantly different from LCGU in wild type littermate mice in any of 35 brain regions analysed (including brain regions known to over-express hsp 70i) in the basal state. Following metabolic activation with dizocilpine (1mg/kg) however, LCGU in transgenic mice over-expressing hsp 70i was significantly increased in three brain regions (anterior thalamus, hippocampus CA1 stratum lacunosum moleculare and hippocampus CA1 stratum oriens) and significantly decreased in two brain regions

(superior olivary body and nucleus of the lateral lemniscus) compared to wild type littermate mice. These data suggest transgenic hsp 70i over-expression does not affect brain function in the basal state, but can influence brain function following metabolic activation.

Local cerebral glucose utilisation following intrastriatal ad egfp gene transfer

To investigate the impact of ad egfp gene transfer on LCGU, ^{14}C-2-deoxyglucose autoradiography was employed. LCGU in areas of ad egfp transfection in ipsilateral caudate nucleus was significantly reduced compared to LCGU in the contralateral caudate nucleus at seven and 28-days post-injection. The absence of any significant differences in LCGU between hemispheres in saline injected mice at seven and 28-days post-injection, suggests that ad egfp transfer actively reduces LCGU.

CHAPTER ONE : INTRODUCTION

1.1 Cerebral ischaemia

Only cardiovascular disease and cancer end more human lives than cerebrovascular disease (cerebral ischaemia) in the Western world today (Camamarta *et al.*, 1994). Cerebral ischaemia is also the major cause of incapacity in adults (Camamarta, *et al.*, 1994). It is estimated that approximately 500,000 people in the United Kingdom are severely debilitated by the neurological consequences of cerebral ischaemia (Bamford *et al.*, 1990). The incidence of cerebral ischaemia and the impact of its sequelae upon society serve to highlight the importance of research into the understanding of the mechanisms involved in cerebral ischaemia. The studies, which constitute this thesis, were primarily designed and executed to investigate the influence of heat shock protein 70i (hsp 70i) in cerebral ischaemia and to explore and extend the use of transgenic mice and viral vectors in cerebral ischaemia research.

Ischaemia (from the Greek *ischo*, to hold back, and *hamia*, blood) is, by definition, the complete loss of blood flow in a region of a bodily organ. In cerebral ischaemia research however, ischaemia is generally defined as a decrease in cerebral blood flow to the point that metabolic substrate (chiefly oxygen and glucose) fails to meet the metabolic demand of the tissue, which perturbs function. The level of cerebral blood flow at which this occurs varies with brain region and the ischaemic insult involved (Siesjö *et al.*, 1995). Anatomically, cerebral ischaemia can be classified as global (the loss or reduction of blood flow to the entire brain) or focal (the loss or reduction in blood flow to a specific vascular territory).

Clinically, global and focal cerebral ischaemia are very different. Global cerebral ischaemia in man is most frequently observed following cardiac arrest (stagnant hypoxia). Increased intracranial pressure, hypotension, hypoxia (hypoxic and histotoxic), hypoglycaemia and carbon monoxide can all also produce global cerebral ischaemic

damage to varying degrees. Permanent global cerebral ischaemia results in death. Prolonged global cerebral ischaemia (approximately 10 minutes or greater) is generally incompatible with survival beyond the vegetative state. Transient global cerebral ischaemia (less than 10 minutes) can go unnoticed or cause varying degrees of mental and physical disability. Focal cerebral ischaemia (stroke) in man is most frequently encountered following occlusion of a cerebral artery (in particular the middle cerebral artery, MCA) by thrombus or embolus. Cerebral haemorrhage can also induce focal cerebral ischaemia, although this is less common. Approximately 40% of first strokes are fatal (Camamarta *et al.*, 1994). Increased duration of focal occlusion is intimately related to the volume of infarction (brain tissue in which all components die). Transient focal cerebral ischaemia (that is to say the source of occlusion has moved, been reduced or been removed) has wide-ranging effects depending upon the severity of the insult. Transient focal cerebral ischaemia, like global cerebral ischaemia, can pass unnoticed or cause varying degrees of mental and physical debilitation.

Pathologically, global and focal cerebral ischaemia are also very different (Figure 1). Global cerebral ischaemia results in cell death in selectively vulnerable brain regions (see Section 1.3.4). Classically, hippocampus, cortex, thalamus, basal ganglia, cerebellum and brainstem are affected in both humans and animals alike (Auer and Beneviste, 1997; Auer 1998). Moreover, ischaemic neuronal damage following global cerebral ischaemia occurs over a period of a few hours to a few days (Ito *et al.*, 1975; Pulsinelli and Brierly, 1979; Kirino, 1982; Kirino and Sano, 1984; Smith *et al.*, 1984; Petito *et al.*, 1987; Bonnekoh *et al.*, 1990; Horn and Scholte, 1992). This maturation phenomenon is known as delayed neuronal death (see Section 1.3.4). Focal cerebral ischaemia results in infarction of brain tissue. The densely ischaemic core of infarction varies with the degree and duration of the ischaemic insult and matures quickly (a few hours). Surrounding the core of infarction is a margin of tissue known as the penumbra. Penumbra consists of neurones and glial cells

Figure 1 Global and focal cerebral ischaemia pathology

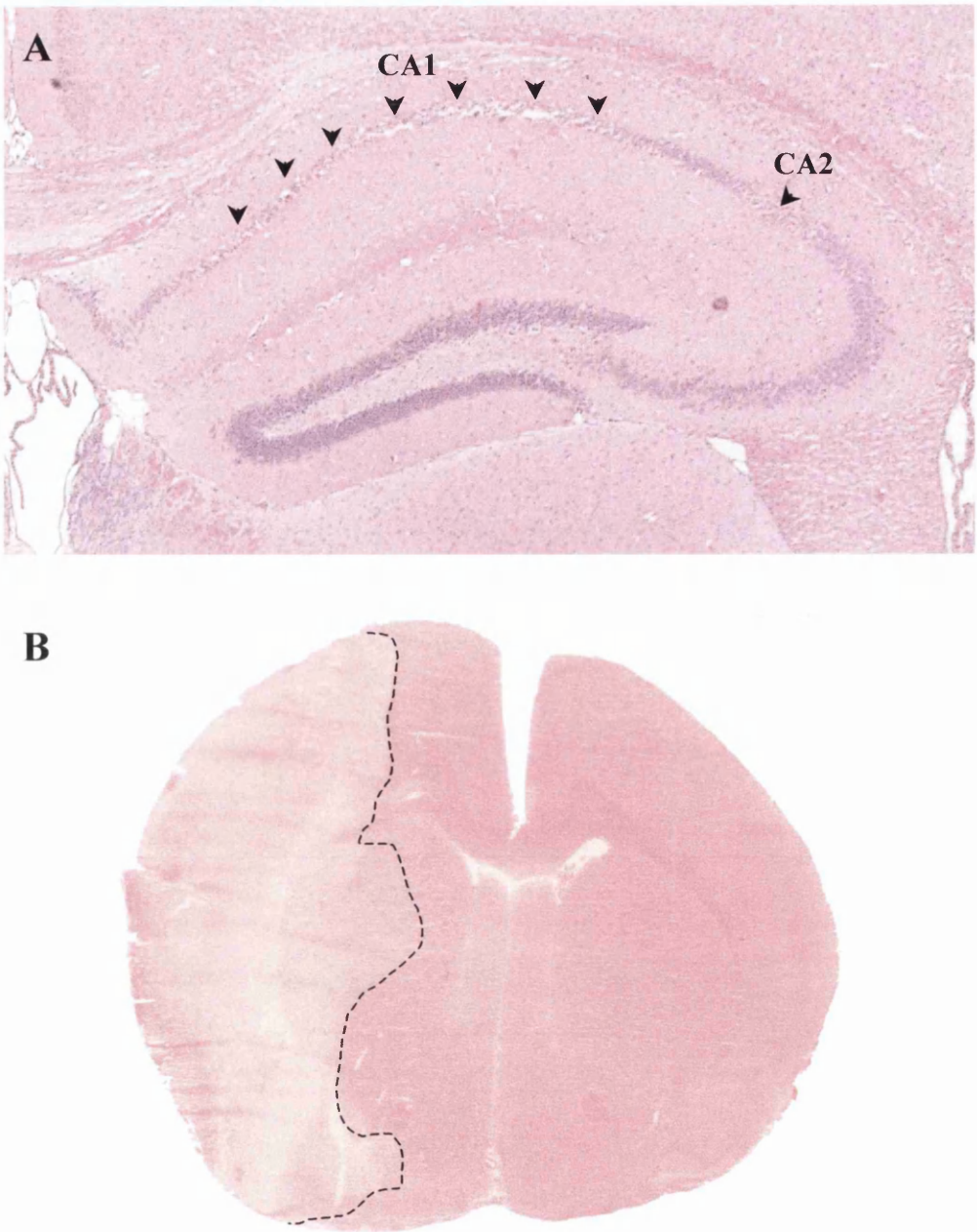

Twenty-minutes of global cerebral ischaemia (BCCAo) in C57bl/6 mouse induced ischaemic neuronal damage in selectively vulnerable neurones in hippocampus CA1 and CA2 at 72-hours survival (A). Permanent distal MCAo (24-hour diathermy) produces ischaemic neuronal damage in the MCA territory including cortex and striatum (B, lighter pallor to left of dotted line). (Original magnification A = X40, B = X8).

subjected to varying degrees of ischaemia, which may or may not die; that is to say it might be possible to intervene and save some of these cellular components.

1.2 Animal models of cerebral ischaemia

Several large animal species have been used to model global and focal cerebral ischaemia (notably sub-human primates, dogs, cats, pigs and rabbits). Major advantages of using large animals are first, their homology with humans, and second, the ease with which they can be resuscitated and recovered. The major disadvantages to the use of large animals are their high cost and high associated costs (such as large volumes of anaesthesia, drugs, fixation materials, etcetera) and the considerable ethical and quasi-political concerns over the use of higher vertebrates as experimental models. Rodents have been employed to model cerebral ischaemia since the 1960's. There are several major advantages of using rodents as models of cerebral ischaemia. First, their low cost and low associated costs (i.e., less reagents and drugs are required). Second, their small brain size is better suited to fixation procedures, such as *in vivo* and *in vitro* freezing. Third, ethical and quasi-political concerns over their use are less contentious than those raised about large animals. In this thesis bilateral common carotid artery occlusion (BCCAo) was established in the mouse as a model of global cerebral ischaemia. It should be made clear at this point, that BCCAo in mouse does not induce complete global cerebral ischaemia (as the vertebro-basilar arterial branches are not occluded). However, the term global cerebral ischaemia is used in this thesis to describe a loss or reduction in cerebral blood flow to the forebrain (as well as the entire brain). This thesis focuses predominantly upon the mechanisms and pathology of global cerebral ischaemia, with occasional consideration aspects involved in focal cerebral ischaemia.

1.2.1 Rodent models of global cerebral ischaemia

Decapitation, cardiac arrest, increased intracranial pressure and most commonly, vascular occlusion (with and without systemic hypotension) have all been employed to induce global cerebral ischaemia in rodents. Lowry *et al.*, (1964) induced global cerebral ischaemia in mice by decapitation to investigate the effects of ischaemia upon substrates and cofactors of the glycolytic pathway in the brain. More recently Woznicki and Walker (1980) investigated the utilisation of cyclocreatine phosphate during decapitation ischaemia in the mouse. Decapitation represents the simplest means of inducing global cerebral ischaemia. Xie *et al.*, (1995) induced global cerebral ischaemia by cardiac arrest without resuscitation to investigate the role of ion channels in the early phase of global ischaemia in the rat. Decapitation and cardiac arrest without resuscitation are limited however, as there is no facility to investigate post-ischaemic recirculation. Cardiac arrest with resuscitation has also been used to induce global cerebral ischaemia in the rat and mouse (De Garavilla *et al.*, 1984; Blomqvist *et al.*, 1985; Kawai *et al.*, 1992; Böttiger *et al.*, 1995, 1999). Cardiac arrest with resuscitation enables investigation of post-ischaemic recirculation and more closely resembles global cerebral ischaemia in the clinical setting. However, cardiac arrest also damages systemic organs (especially the heart) and disturbs arterial blood gas and electrolyte concentrations. The effects of myocardial damage and disturbances in systemic physiologic parameters, such as, arterial blood gases and electrolytes on ischaemic neuronal damage are unknown (Tamura *et al.*, 1995). Ljunggren *et al.*, (1974) produced global cerebral ischaemia in rats by raising intracranial pressure such that cerebral blood flow was almost zero.

Vascular occlusion is the most common means by which global cerebral ischaemia can be induced in rodent models. The first report of reversible global cerebral ischaemia induced by vascular occlusion in a rodent was reported five decades ago. Levine and Payan (1966) described ischaemic neuronal damage in gerbils following ligation of the common carotid

arteries. Levine and Sohn (1969) and Ito *et al.*, (1975) later correlated ischaemic neuronal damage in gerbils following BCCAo with hypoplasticity in the circle of Willis. A large number of gerbils subjected to BCCAo of 15 minutes or more have post-ischaemic seizures which, can greatly influence ischaemic neuronal damage (Kuroiwa *et al.*, 1990). The two classic models of global cerebral ischaemia in the rat were reported in the late 1970s and early 1980s. Pulsinelli and Brierly (1979) produced severe global cerebral ischaemia in rat by bilateral occlusion of the vertebral arteries (day 0) followed by BCCAo (day 1). Smith *et al.*, (1984) induced global cerebral ischaemia in rat by BCCAo with systemic hypotension (MABP circa 50mmHg). Production of global cerebral ischaemia in mouse by vascular occlusion dates from 1990. Himori *et al.*, (1990, 1991) investigated the effects of BCCAo in mouse on learning deficits and mortality rates. Histological analysis of ischaemic neuronal damage following BCCAo in mouse was first reported by Barone *et al.*, (1993). Since then several models of reversible global cerebral ischaemia (induced by vascular occlusion) have been reported in several strains of wild type mice (Panahian *et al.*, 1996, Fujii *et al.*, 1997; Yang *et al.*, 1997; Murakami *et al.*, 1998a; Sheng *et al.*, 1999; Section 3.1 in this thesis).

1.2.2 Rodent models of focal cerebral ischaemia

Rodent models of focal cerebral ischaemia, like rodent models of global cerebral ischaemia, can be induced permanently and transiently. The most commonly employed models of rodent focal cerebral ischaemia are based on occlusion of the middle cerebral artery (MCA). MCA occlusion (MCAo) in the rat has been in use since 1975 (Robinson *et al.*, 1975). Tamura *et al.*, (1981) induced permanent focal cerebral ischaemia in the rat by cauterising the MCA via a craniectomy. Zea Longa *et al.*, (1989) described the induction of focal cerebral ischaemia in rat without craniectomy. Zea Longa *et al.*, (1989) achieved permanent and transient focal cerebral ischaemia by advancing a suture (intraluminal thread) via the lumen of the carotid artery to the origin of the MCA, and either securing it

in place or withdrawing it after a given duration. The intraluminal thread model has also been adapted for use in mice (Hara *et al.*, 1996; Huang *et al.*, 1996). Macrae *et al.*, (1993) induced transient focal cerebral ischaemia by topical application of the vasoconstrictor peptide, endothelin 1. More recently, focal cerebral ischaemia has been induced in rat and mouse by embolic occlusion of the MCA (Zhang *et al.*, 1997; Zhang *et al.*, 1997).

1.3 Histopathology of cerebral ischaemia

1.3.1 Necrosis

Neuronal necrosis is commonly observed following cerebral ischaemia. The pathological hallmarks of necrosis are mitochondrial changes and increased influx of calcium across the cell membrane. Necrosis can essentially be regarded as a cytoplasmic event, as nuclear alterations are unclear. Briefly, the pathogenesis of ischaemic neuronal necrosis begins with ultrastructural changes in dendrites (Johansen *et al.*, 1984; Olney, 1969a, 1969b, 1971; Olney *et al.*, 1971; Yamamoto *et al.*, 1986, 1990). These dendritic abnormalities are thought to end in cell membrane breaks (Auer *et al.*, 1985; Simon *et al.*, 1985). Ultrastructural changes to ribosomes, cytoskeletal cell components and perturbation of cellular protein synthesis ensue (Kreutzberg *et al.*, 1997). Necrosis induced by ischaemia (or other stimuli such as excitatory amino acids or hypoglycaemia) can be identified using light microscopy. These observable alterations are referred to as ischaemic cell changes. Shrunken cell body and pyknotic, shrunken nucleus, signal Ischaemic cell change. Moreover, ischaemic cells often become triangular in shape and demonstrate increased affinity for acid dies such as eosin (Figure 2). If ischaemic neuronal damage is irreversible, cells further shrink and finally undergo homogenising cell change followed by ghost cell change, resulting in shrunken, pyknotic and fragmented nuclei without recognisable cytoplasm (Adams and Graham, 1989). It should be noted that the light microscopic characteristics of ischaemic cell change might also be observed in apoptosis.

Figure 2 Ischaemic cell change

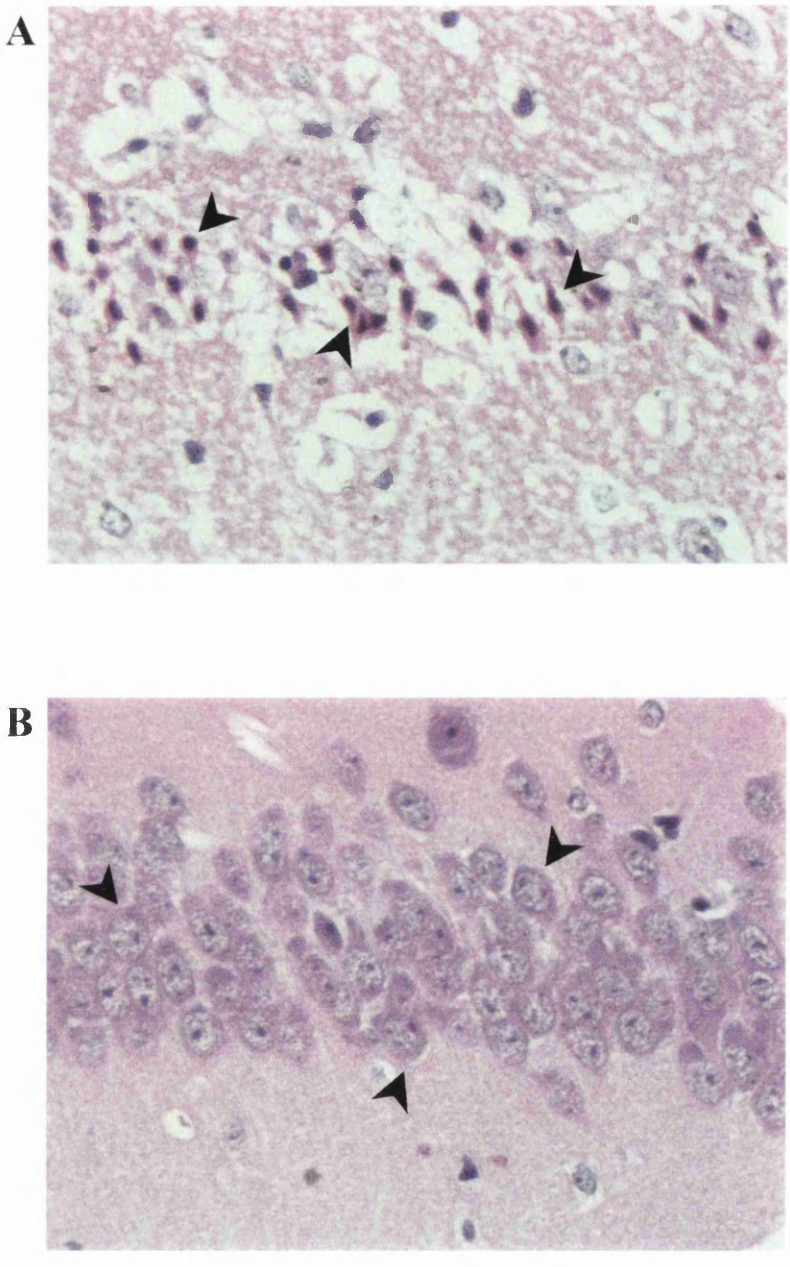

Haematoxylin and eosin histological staining to identify morphologically abnormal pyramidal neurones of hippocampus CA1 exhibiting features of ischaemic cell change (A) and morphologically normal pyramidal neurones of hippocampus CA1 exhibiting no features of ischaemic cell change (B). (Original magnification X200).

However, necrotic cells generally die in large clusters, whereas apoptotic cells tend to die singly (Kerr *et al.*, 1972; Majno *et al.*, 1995).

1.3.2 Apoptosis

Apoptosis refers to cell death which can occur spontaeneously as a physiological event during life (Kerr *et al.*, 1972; Wylie *et al.*, 1990; Cohen, 1991; Sen, 1992; Hockenbery, 1995; Majno *et al.*, 1995) and can be triggered by a variety of insults including ischaemia (McManus *et al.*, 1993). Apoptosis is essentially a nuclear event and can be divided into classic apoptotic cell death, autophagia and non-lysosomal vesiculate cell death (Clarke, 1990). The pathophysiological hallmark of apoptotic cell death is inter-nucleosomal DNA fragmentation (DNA laddering), into fragments of approximately 180-200 base pairs (Arends *et al.*, 1990). Apoptosis has a distinct morphology, which begins with changes to the outer membrane of the cell nucleus (Kerr *et al.*, 1972). Light microscopic identification of apoptotic cells was facilitated by the establishment of terminal transferase mediated nick-end labelling (TUNEL) (Gavrieli *et al.*, 1992). The TUNEL technique labels exposed DNA endings, on fragmented DNA, with labelled nucleotides. It should however be noted that DNA endbreaks are not specific to apoptosis, but may also occur during necrosis. Therefore, single-stranded DNA breaks require confirmation by ultrastructural identification.

1.3.3 Pan-necrosis

In pan-necrosis (infarction) all cellular elements of the CNS (neurones, glial cells and vascular components) die. Pan-necrosis is generally associated with focal, rather than global cerebral ischaemia, as cerebral blood flow to a specific territory is blocked permanently (or for a prolonged period). Several other conditions have also been reported to induce pan-necrosis including, lactic acidosis (Bogousslavsky *et al.*, 1982; Kuriyama *et*

al., 1984; Pavlakis *et al.*, 1984; Mukoyama *et al.*, 1986), status epilepticus (Nevander *et al.*, 1985) and hypoglycaemic ischaemia (Inamura *et al.*, 1987, 1988).

1.3.4 Selective vulnerability and delayed neuronal death

During global cerebral ischaemia the brain is deprived of blood flow. Blood represents the major source of oxygen and glucose, which are essential for brain function (see Section 1.5). Following transient cessation of blood flow to the brain, damage is restricted to specific brain regions (Adams and Graham, 1989; Auer and Beneviste, 1997). Six major brain regions are classically reported to be selectively vulnerable to global cerebral ischaemia (hippocampus, cortex, thalamus, basal ganglia, cerebellum and brainstem) (Auer, 1998). Within each of these brain regions, hierarchies of vulnerability exist. That is to say, some cell types are highly vulnerable while others may not be affected. Pyramidal neurones of the hippocampus CA1 sub-field have been shown to be more vulnerable than other hippocampal cell types to mild global cerebral ischaemia in gerbil (Kirino, 1982; Araki *et al.*, 1989) and rat (Smith *et al.*, 1984) and humans (Adams and Graham, 1989). Although other cell types of the hippocampal formation, such as, subiculum and CA4 have been reported to have minor damage after such mild global ischaemic insults, the remainder of the hippocampus is relatively unscathed. Where the duration (or severity) of global cerebral ischaemia is increased, ischaemic neuronal damage is not only observed in CA1 but is also observed more frequently in subiculum, CA4, CA3 and eventually in dentate gyrus (Smith *et al.*, 1984).

Global cerebral ischaemia in humans and experimental animals produces ischaemic neuronal damage in hippocampus CA1 pyramidal neurones which matures over a period of a few hours to a few days (Ito *et al.*, 1975; Pulsinelli and Brierly, 1979; Kirino, 1982; Kirino and Sano, 1984a; Smith *et al.*, 1984; Petito *et al.*, 1987; Bonnekoh *et al.*, 1990; Horn and Scholte, 1992). Pulsinelli *et al.*, (1982) investigated the relationship between

ischaemic neuronal damage and survival time in rats subjected to 30 minutes of global cerebral ischaemia. Pulsinelli and colleagues reported that at three-hour survival 65% of rats had no ischaemic neuronal damage in CA1; at six-hour survival 57% of rats had no ischaemic neuronal damage in CA1; at 24-hour survival 40% of rats had no ischaemic neuronal damage in CA1; and at 72-hour survival 0% of rats had no ischaemic neuronal damage in CA1. This phenomenon is known as delayed neuronal death and occurs despite rapid restoration of hydrogen, sodium, potassium and water in cells and fairly rapid recovery of high energy phosphate levels following restoration of cerebral blood flow (Siesjö *et al.*, 1995).

1.3.5 Delayed neuronal death: necrosis versus apoptosis

The time course with which delayed neuronal death occurs in hippocampus CA1 pyramidal neurones following global cerebral ischaemia (typically 24-72 hours post-ischaemia, Ito *et al.*, 1975; Pulsinelli and Brierly, 1979; Kirino, 1982; Kirino and Sano, 1984; Smith *et al.*, 1984; Petito *et al.*, 1987; Bonnekoh *et al.*, 1990; Horn and Scholte, 1992) could be consistent with apoptosis (Colbourne *et al.*, 1999). Neurochemical analysis suggests delayed neuronal death in hippocampus CA1 pyramidal neurones is apoptotic (McManus *et al.*, 1993, 1995; Okamoto *et al.*, 1993; Kihara *et al.*, 1994; Iwai *et al.*, 1995; Honkaniemi *et al.*, 1996; MacManus and Linnick, 1997; McManus *et al.*, 1999). Ultrastructurally, necrosis and apoptosis have distinct morphologies, with necrosis being considered predominantly a cytomplasmic event (Colbourne *et al.*, 1999). Electron microscopy of hippocampus CA1 pyramidal neurones which displayed delayed neuronal death following global cerebral ischaemia predominantly highlights features of necrotic cell death (Kirino and Sano, 1984b; Johansen *et al.*, 1984; Yamamoto *et al.*, 1990; Desphande *et al.*, 1992; Tomimoto *et al.*, 1993; Colbourne *et al.*, 1999). Nitatori *et al.*, (1995) however, describe features of apoptotic cell death in hippocampus CA1 pyramidal neurones following global cerebral ischaemia. The conclusions of Nitatori *et al.*, (1995) have been questioned by

Colbourne *et al.*, (1999) who claim to observe similar results which they say are markers of necrotic cell death. On balance, the compelling evidence from ultrastructural studies strongly suggests necrosis as a mechanism leading to delayed neuronal death in hippocampus CA1 pyramidal neurones following global cerebral ischaemia. However, the substantial neurochemical evidence and the ultrastructural evidence of Nitatori *et al.*, (1995) also imply apoptosis, as a process leading to delayed neuronal death in hippocampus CA1 neurones following global cerebral ischaemia. It is likely that both necrotic and apoptotic mechanisms contribute to cellular death following global cerebral ischaemia. While both necrosis and apoptosis are recognised to contribute to CNS pathology following global cerebral ischaemia, this thesis studied necrotic ischaemic neuronal damage using haematoxylin and eosin histochemical staining (as described in Sections 1.3.1 and 2.6.3).

1.3.6 Cerebral vasculature

Theoretically, BCCAo in normal, healthy rodents should not be sufficient to induce widespread ischaemic cell change, because of increased collateral blood flow to the brain via the basilar artery. BCCAo alone however, is commonly employed as a model of global cerebral ischaemia in gerbils and mice whereas BCCAo in rats, is only employed as a model of global cerebral ischaemia when accompanied by haemorrhagic hypotension (Smith *et al.*, 1984). However, BCCAo in gerbil and mouse is sufficient to induce considerable ischaemic damage in several forebrain structures. The reason for this is poor communication between anterior and posterior cerebral circulation. In gerbil, ischaemic neuronal damage following BCCAo was first correlated with hypoplasticity of the circle of Willis by Levine and Sohn (1969) and Ito *et al.*, (1975). Since then BCCAo in the gerbil has been used extensively as a model of global cerebral ischaemia. In mouse, ischaemic neuronal damage following BCCAo was first correlated with hypoplasticity of the circle of Willis by Barone *et al.*, (1993). Due largely to a growing availability of genetically

modified mice, a succession of studies have reported similar vascular anomalies in several mouse strains (Fujii *et al.*, 1997; Yang *et al.*, 1997; Murakami *et al.*, 1998; Section 3.1 of this thesis).

1.3.7 Temperature

Brain temperature can influence the degree of neuronal damage induced by global cerebral ischaemia. Hypothermia has been shown to delay neuronal necrosis in experimental models of global cerebral ischaemia (Dietrich *et al.*, 1993). Hypothermia has also been shown, in experimental models of global cerebral ischaemia, to reduce ischaemic damage (Busto *et al.*, 1987; Colbourne *et al.*, 1994, 1995). Furthermore, hypothermia has been employed in neurosurgical and cardiac procedures requiring interruption of the cerebral circulation with some success (Ginsberg *et al.*, 1992). In contrast, hyperthermia during global cerebral ischaemia has been shown to exacerbate ischaemic neuronal damage (Dietrich *et al.*, 1990). However, prolonged periods of hyperthermia before induction of global cerebral ischaemia, have been shown to reduce ischaemic neuronal damage (Kitagawa *et al.*, 1992). These reductions in ischaemic neuronal damage following global cerebral ischaemia after hyperthermic pre-conditioning have been associated with expression of hsps (see Section 1.7.3).

1.3.8 Global cerebral ischaemia

Global cerebral ischaemia (as opposed to focal cerebral ischaemia) was chosen to investigate the influence of hsp 70i in ischaemia in this thesis for two reasons. First, and most importantly, hsp 70i transgene expression in the transgenic mice used was driven by the rhombotin-1 promoter (also known as promoter 1 of the LMO-1 gene, Greenburg *et al.*, 1990) meaning hsp 70i was over-expressed in several brain regions known to be selectively vulnerable to global cerebral ischaemia (see Section 2.9 for details). Second,

global cerebral ischaemia enabled inter-hemispheric comparison of ischaemic neuronal damage in mice unilaterally injected with adenovirus (ad) hsp 70i.

1.4 Mechanisms of ischaemic cell death

Following global cerebral ischaemia in a number of species, hippocampus CA1 pyramidal neurones display delayed neuronal death (Ito *et al.*, 1975; Pulsinelli and Brierly, 1979; Kirino, 1982; Kirino and Sano, 1984a; Smith *et al.*, 1984; Petito *et al.*, 1987; Bonnekoh *et al.*, 1990; Horn and Scholte, 1992) while death in other structures, such as the striatum, is more rapid (Pulsinelli *et al.*, 1982; Crain *et al.*, 1988). The mechanisms leading to ischaemic cell death, be it delayed or rapid, are not yet fully elucidated. One major theory involves the release of neurotransmitters (notably glutamate) which leads to neuronal calcium overload. Calcium overload is thought to mediate activation of second messenger systems, inflammatory genes, production of free radicals, lipases and proteases, and induction of genes regulating apoptosis.

1.4.1 Glutamate excitotoxicity and calcium overload

The role of glutamate as a brain neurotransmitter was accepted in the 1980s (Watkins & Evans, 1981; Wroblewski & Danysz, 1989). Glutamate is the major fast excitatory neurotransmitter in the brain (McCulloch, 1994). However, the action of glutamate upon its receptors has been implicated as one of the leading theories contributing to ischaemic brain injury. Dialysis studies have indicated that background extracellular concentrations of glutamate are maintained between 1 and 5μM, while intracellular concentrations are maintained between 5 and 10mM. The differences in extracellular and intracellular glutamate are maintained by transmembrane sodium, potassium and charge gradients driving glutamate uptake (Attwell *et al.*, 1993). In ischaemic neurones deprived of oxygen and glucose high-energy phosphates are lost and the cells depolarise. Depolarisation leads to synaptic release of glutamate and reversal of electrogenic transport of glutamate from

astrocytes (Nicholls & Attwell, 1990). Extracellular glutamate increases and stimulates α-amino-2, 3-dihydro-5-methyl-3-oxo-4-isoxalepropanoic acid (AMPA), kainate and *N*-methyl-D-aspartate (NMDA) receptors which leads to an influx of sodium and calcium through the channels gated by these receptors. Excessive calcium influx is mediated directly and predominantly by NMDA receptors. Calcium influx however, can also be effected secondarily by sodium influx through AMPA; kainate and NMDA gated channels via activation of voltage gated calcium channels and reverse operation of the sodium/calcium exchanger. Sustained, excessive calcium concentrations are thought to trigger lethal metabolic derangements (Choi, 1988, Kristian and Siesjö, 1998). Excessive concentrations of intracellular calcium mediate cellular injury and death via several pathways, including activation of proteases, lipases and endonuleases and the production of cytokines and other factors, which directly or indirectly cause cell injury or death (Figure 3). Another divalent cation, zinc, has also been postulated to play a role in ischaemic cell death (Johansen *et al.*, 1993; Choi and Koh, 1998; Tonder *et al.*, 1998).

1.5 Energy generation in the brain

In an adult human the brain constitutes around 2% of body mass. Despite its relatively small size it receives 15% of cardiac output, consumes 20% of total body oxygen and is responsible for 25% of total body glucose utilisation (Edvinsson *et al.*, 1993). Glucose utilisation in the adult human brain is 30μmole / 100g / minute. Under normal, non-fasting conditions, the brain depends almost exclusively upon glucose as its source of energy (Kety, 1948; Sokoloff, 1977; Siesjö, 1978). Brain glucose concentration varies directly with plasma glucose concentration, tissue glucose is characteristically 10-15% lower than plasma glucose. Glucose is transported into brain cells rapidly by carrier mechanisms with greater affinity than those in cerebral endothelium. As much as 90% of brain glucose is aerobically catabolised. Hexokinase is responsible for the phosphorylation of glucose in the brain. The rate of glucose phosphorylation in the brain is governed only by the product

Figure 3 **Proposed mechanisms of glutamate excitotoxicity and calcium overload following cerebral ischaemia**

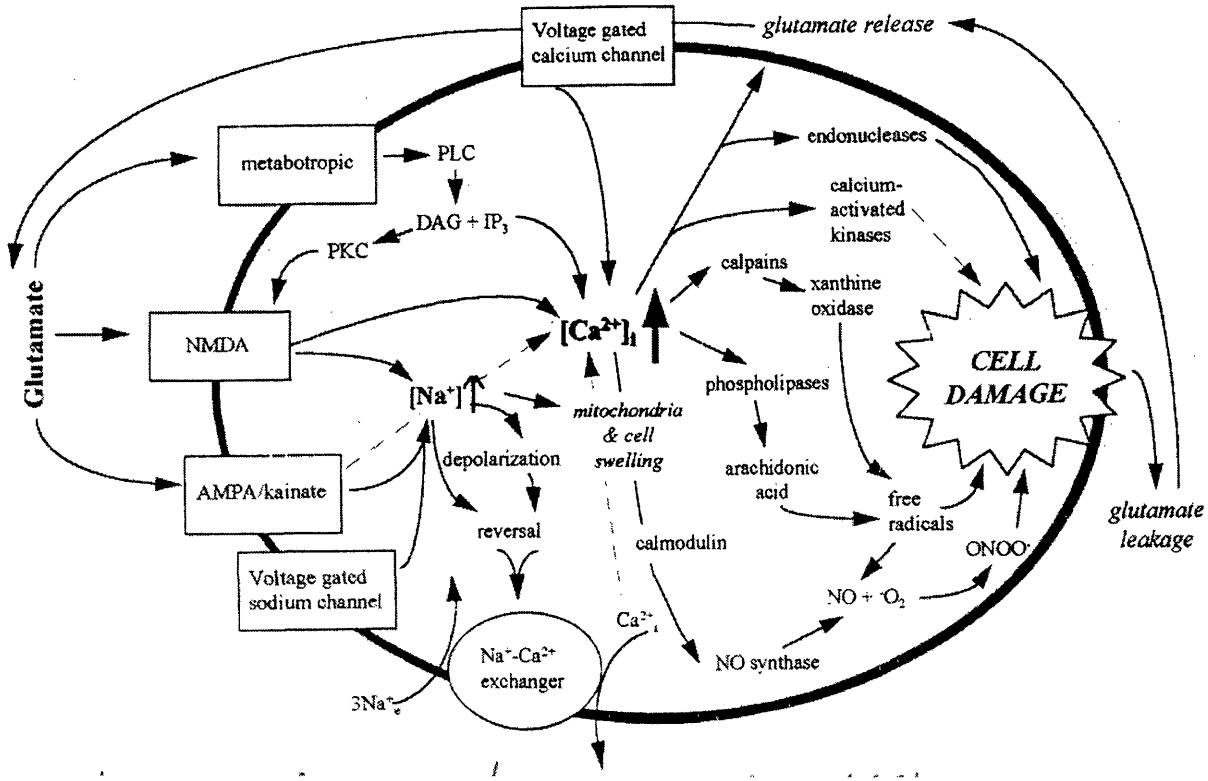

Adapted from Gill and Lodge, 1997.

of hexokinase, glucose-6-phosphate i.e., negative feedback. Glucose-6-phosphate is in turn converted to fructose-6-phosphate by phosphohexose isomerase, which is further metabolised by the glycolytic and tricarboxylic acid pathways. Each molecule of glucose metabolised in this manner yields 33 high energy phosphates. The remainder of the brain glucose fulfils several other important roles within the brain. For instance, glucose represents the principle source of carbon in cerebral lipids and is a precursor for neurotransmitters such as, γ-aminobuteric acid (GABA), glutamate and acetylcholine. Only 2% and 0.3% of all cerebral glucose utilisation is used for lipid and protein synthesis, respectively. The pentose phosphate pathway is responsible for catabolising a small portion of cerebral glucose, estimated at ~3% in the rat and ~6% in non-human primates (Siesjö, 1978; Gaitmonde *et al.*, 1983; Clarke *et al.*, 1989). The only other energy generating substrates within the brain, besides glucose, is glucose stored in the tissues as glycogen and ketone bodies. The levels of both are minimal under normal circumstances. The requirement of three grams of water for every gram of glycogen limits the glycogen levels in the brain (Cahill & Aoki, 1980). In the absence of glucose, these levels of glycogen could only support metabolic activity for a few minutes (Siesjö, 1978). Oxidation of ketone bodies in the brain in well-nourished animals is negligible. However, after 24 hours of starvation the contribution of ketone bodies to overall oxygen consumption rises from less than 1% to 20% (Siesjö, 1978).

1.6 Mapping brain function with ^{14}C-2-deoxyglucose autoradiography

The ^{14}C-2-deoxyglucose autoradiography technique developed by Sokoloff *et al.*, (1977) is an excellent tool with which neuroscientists can map brain function *in vivo*. The neurophysiological and neuropharmacological applications of ^{14}C-2-deoxyglucose autoradiography are widespread. This is largely due to its ability to enable determination of local cerebral glucose utilisation (LCGU) in discrete and functionally diverse brain regions in conscious, freely moving animals. The conceptual basis for ^{14}C-2-deoxyglucose

autoradiography stems from two simple premises: (1) under normal, non-fasting conditions the energy requirements of the adult brain are derived almost exclusively from the aerobic catabolism of glucose (Kety, 1948; Sokoloff, 1977; Siesjö, 1978), and (2) functional activity and energy metabolism within any region of the brain is associated intimately and directly (Sokoloff, 1977).

1.6.1 Concept

Tower (1958) reported glucose uptake and phosphorylation in brain slices to be inhibited by 2-deoxyglucose, an analogue of glucose (Figure 4). This was accompanied by an accumulation of 2-deoxyglucose-6-phosphate in the tissue. Bachelard (1971) and Oldendorf (1971) reported that the entry of glucose and 2-deoxyglucose into the brain was mediated via the same carrier mechanism. Once in the brain tissue, the hexokinase enzyme phosphorylates both glucose and 2-deoxyglucose. Glucose becomes glucose-6-phosphate, while 2-deoxyglucose becomes 2-deoxyglucose-6-phosphate. At this point glucose-6-phosphate is further metabolised via the glycolytic and tricarboxylic acid pathways and / or the pentose phosphate pathway (Bachelard, 1971). 2-deoxyglucose-6-phosphate is not a substrate for the primary enzymes of the above pathways, instead it is metabolised by glucose-6-phosphatase. Glucose-6-phosphatase hydrolyses 2-deoxyglucose-6-phosphate into deoxyglucose. In brain tissue glucose-6-phosphatase activity is also extremely low (Sokoloff *et al.*, 1977; Sokoloff, 1979). The limited glucose-6-phosphatase concentration present within the brain is associated with the cerebral capillaries rather than the tissue itself (Goldstein *et al.*, 1975). Accordingly, glucose-6-phosphatase activity is not a major concern in the use of 2-deoxyglucose in the brain, except when the measurement period is much greater than 45 minutes (Sokoloff, 1979).

By radiolabelling 2-deoxyglucose with ^{14}C, Sokoloff *et al.*, (1977) capitalised on the inability of the brains biochemical processes to metabolise 2-deoxyglucose by developing

Figure 4 Diagrammatic representation of glucose and 2-deoxyglucose

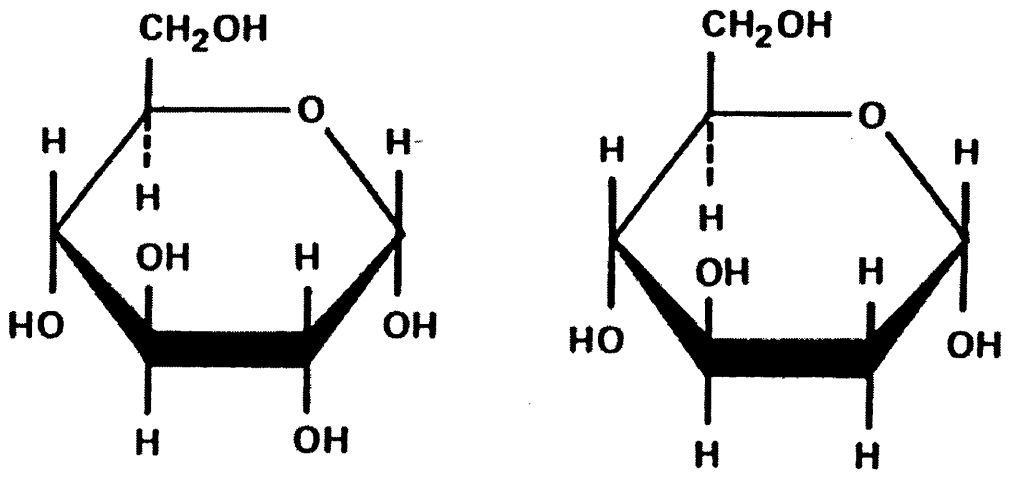

2-deoxyglucose differs from glucose in that it lacks a hydroxyl group on the 2-carbon position. Adapted from McCulloch, 1982.

a theoretical model (Figure 5). This model enabled the rate of glucose utilisation to be described mathematically by a single equation (Figure 6). The equation, known as the 'operational equation' (Sokoloff *et al.*, 1977) permits the rate of LCGU to be calculated from (1) the levels of plasma glucose and ^{14}C throughout the experimental period, and (2) the regional tissue concentration of ^{14}C at the end of the experiment (as derived using pre-calibrated standards).

1.6.2 Operational equation

The operational equation describes the rate of cerebral glucose utilisation (R_i) in terms of the concentration of plasma ^{14}C-2-deoxyglucose (C_p*) and plasma glucose levels (C_p) over the experimental time (T) and the concentration of ^{14}C found within the brain tissue (C_i*). The distribution ^{14}C-2-deoxyglucose between plasma and brain tissue is governed by the rate constants k_1*, k_2* and its phosphorylation to 2-deoxyglucose-6-phosphate k_3*. These rate constants are not measured for each experiment. Instead the original values determined by Sokoloff *et al.*, (1977) in the original description of the method are used.

1.6.3 Constraints

The ^{14}C-2-deoxyglucose autoradiographic technique is subject to several constraints: (1) the composite, lumped constant and the kinetic constants must be known for the region and condition being investigated, (2) the rate of glucose utilisation must remain constant over the period of measurement, (3) plasma glucose must remain constant over the experimental period, and (4) plasma ^{14}C-2-deoxyglucose and glucose must be representative of those in the cerebral capillaries. Variation of the lumped constant, which is a major determinant of the amount of ^{14}C retained in the brain, is not often altered under normal physiologic conditions. The lumped constant is not affected by marked changes in glucose utilisation (Sokoloff *et al.*, 1977), changes in cerebral blood flow (Sokoloff, 1979) or by moderate hypo or hyperglycaemia (McCulloch, 1982). The lumped constant can

Figure 5 Theoretical model of ^{14}C-2-deoxyglucose autoradiography

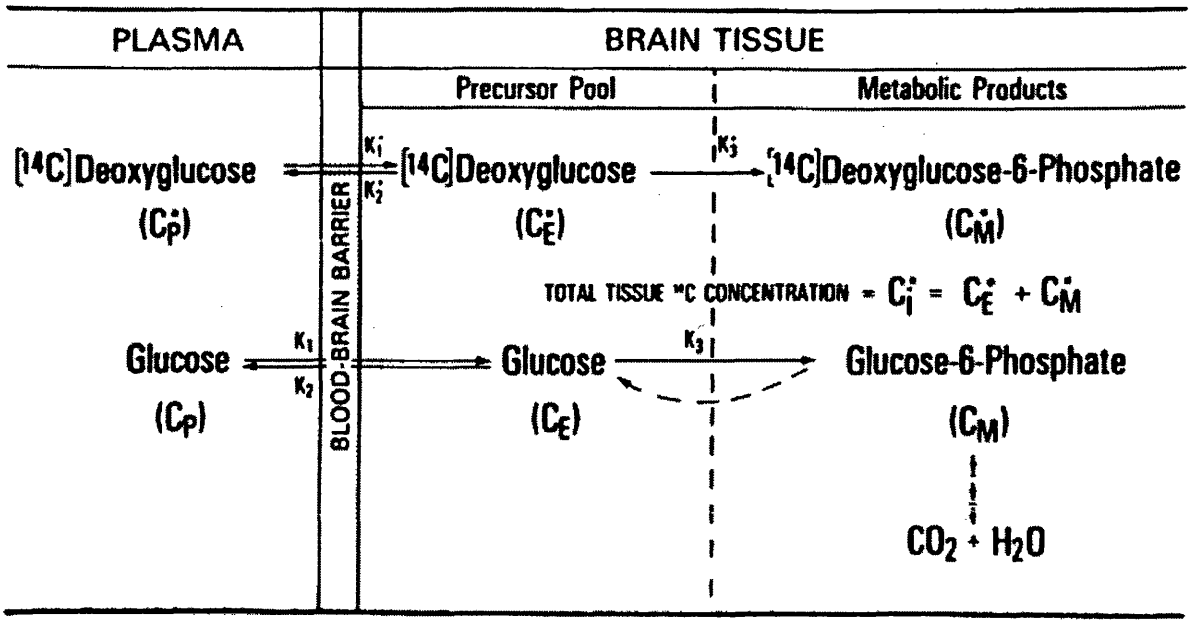

C_p* and C_p represent the concentrations of ^{14}C-2-deoxyglucose and glucose in arterial plasma, respectively; C_E* and C_E represent their respective concentrations in the tissue pools that serve as substrates for hexokinase. C_M* represents the concentration of ^{14}C-2-deoxyglucose in brain tissue. K_1*, K_2* and K_3* are the glucose rate constants. Adapted from Sokoloff *et al.*, 1977.

Figure 6 **^{14}C-2-deoxyglucose operational equation**

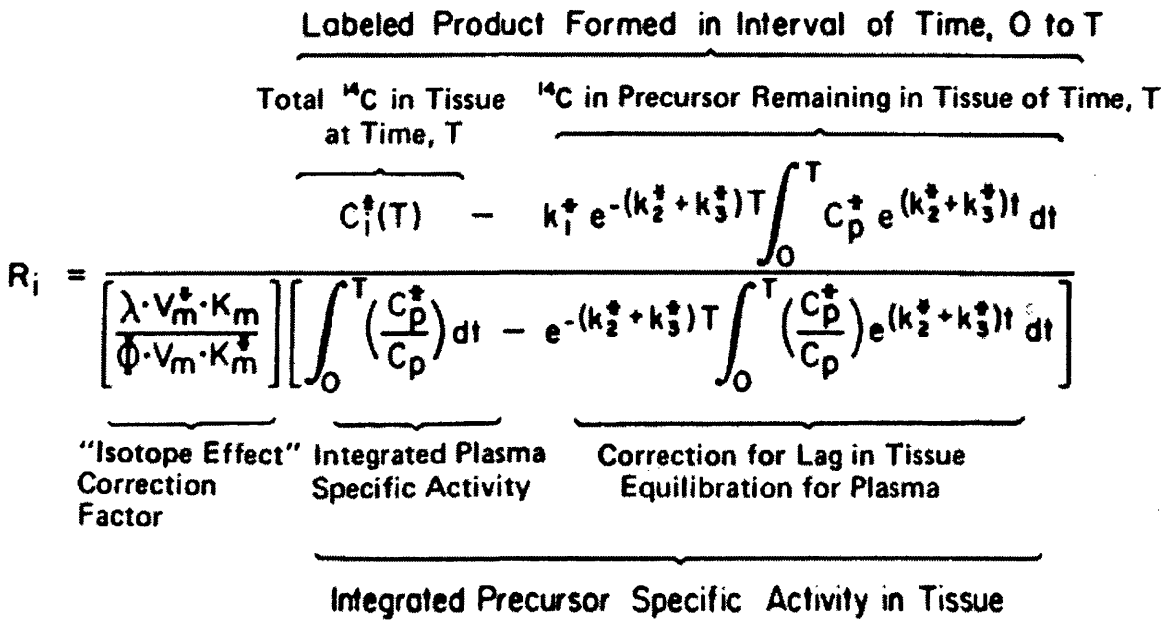

Figure shows the operational equation of the ^{14}c-2-deoxyglucose method. *T* represents the time at termination of the experimental period; λ equals the ratio of the distribution space of deoxyglucose in the tissue to that of glucose; Φ equals the fraction of glucose. K_M*, V_M* and K_M, V_M represents the familiar Michaelis-Menten kinetic constants of hexokinase for deoxyglucose and glucose, respectively. The other symbols are the same as those defined in Figure 5. Adapted from Sokoloff, 1978.

however, be altered by severe hypoglycaemia and hyperglycaemia (McCulloch, 1982), and structural alteration in brain tissue (Ginsberg & Reivich, 1979). The lumped constant displays differences between species (Sokoloff, 1979). The constancy of plasma glucose and the rate of glucose utilisation during the period of measurement impose only minor restrictions on experimental design (McCulloch, 1982).

1.6.4 Utility

LCGU, as measured by the ^{14}C-2-deoxyglucose autoradiography technique, predominantly reflects electrical activity in nerve terminals (Schwartz *et al.*, 1979). As alterations in glucose utilisation correspond to the activity in axonal pathways, changes in glucose use will not be restricted to receptor localisation, but also to the neuronal pathways connected to these regions. In consequence the ^{14}C-2-deoxyglucose autoradiography technique is ideal for mapping cerebral function in neuronal circuits. ^{14}C-2-deoxyglucose autoradiography has been used extensively to investigate the functional effects of several neuropharmacologic and neurophysiologic stimuli (McCulloch, 1982). Many of these studies were carried out in the rat, however Nowacyk and Des Rosier (1981) adapted the original ^{14}C-2-deoxyglucose technique of Sokoloff *et al.*, (1977) for use in the mouse. Browne *et al.*, (1999) employed the fully quantitative ^{14}C-2-deoxyglucose method of Nowacyk and Des Rosier (1981) to investigate the consequences of endothelial and neuronal nitric oxide deficiency in knockout mice. Fully quantitative ^{14}C-2-deoxyglucose autoradiography in mice is technically demanding and very invasive. In this thesis a modification of the original ^{14}C-2-deoxyglucose technique of Sokoloff *et al.*, (1977) was established in the mouse (see Sections 2.7.3 and 2.7.5). The semi-quantitative approach implemented only required intraperitoneal injection of ^{14}C-2-deoxyglucose and collection of a terminal blood sample, meaning it was not technically demanding or overly invasive. Using this approach the first reports of LCGU in transgenic mice over-expressing hsp 70i (Section 3.4) and ad egfp transfection in the mouse brain (Section 3.5) have been reported.

1.7 Heat shock proteins

Heat shock proteins (hsps) have been the subject of extensive investigation over the past four decades. Approximately 12,500 publications relating to these proteins are cited in the Medline database since 1962. The major eukaryotic hsps form a super-family consisting of several sub-families (Table 1). Subfamilies are identified by molecular weight and are further sub-divided according to cellular localisation, expression pattern and function. The 70-kilo Dalton family (hsp 70s) are the most abundant and conserved of these sub-families. Hsps may be expressed constitutively (e.g., heat shock cognate protein 70, hsc 70) or be induced (e.g., heat shock protein 70, hsp 70i). Constitutive proteins can also be induced, while some highly inducible proteins can be expressed basally at very low levels. Both constitutively expressed and inducible hsps are essential for development and cellular function (no hsp 70i null mice have been produced). Hsps can be induced by an array of stimuli including ischaemia (Currie and White, 1981; Nowak, 1985; Dienel *et al.*, 1986; Jacewizc *et al.*, 1986; Vass *et al.*, 1988; Gonzalez *et al.*, 1989), hyperthermia (Ritossa, 1962; Heikkila *et al.*, 1979; Heikkila and Brown, 1979a, 1979b; Freedman *et al.*, 1981; Cosgrove *et al.*, 1982), heavy metals (Wagner *et al.*, 1990; Lee *et al.*, 2000) and pharmacologic agents (Sharp *et al.*, 1991; Planas *et al.*, 1994; Armstrong *et al.*, 1996; Kondo *et al.*, 1997) (Figure 7). The balance between constitutively expressed and inducible hsps has been hypothesised to play a critical role in cellular homeostasis (Latchman, 1998). Hsps are thought to direct repair, refolding and trafficking of abnormal intracellular proteins by acting as molecular chaperones (Massa *et al.*, 1995; Morimoto 1998; Sharp *et al.*, 1999). In view of these activities it has been hypothesised the heat shock response may act as some kind of primeval mechanism facilitating cell survival after insult.

Table 1 Major eukaryotic stress proteins

sub-family	members	functional role	comments
hsp 27	hsp 27, hsp 26	protein folding; actin binding proteins	size ranges from 12-40 k Da
hsp 47	hsp 47	protein folding of collagen and possibly some others	has homology to protease inhibitors
hsp 56	hsp 56	protein folding, associated with hsp 90 and hsp 70 in steroid receptor complex	have peptidyl prolyl isomerase activity, target of immunosuppresive drugs
hsp 60	hsp 60	protein folding and mycobacterial unfolding, organelle translocation	major antigen of many bacteria and parasites which infect man
hsp 70	hsp 70, hsc 70, hsx 70, grp 78	protein folding and unfolding, assembly of multi-protein complexes	hsx 70 only in primates
hsp 90	hsp 90, grp 94	maintainence of proteins such as steroid receptors in an inactive form until appropriate	mutational analysis in yeast has demonstrated an absolute requirement for cell survival
hsp100	hsp 104, hsp 100	protein turnover	appear to be involved in tolerance to extreme temperature , have ATPase activity

hsp = heat shock protein; grp = glucose regulating protein; hsc = heat shock cognate protein

Figure 7 **Stimuli for hsp 70i induction**

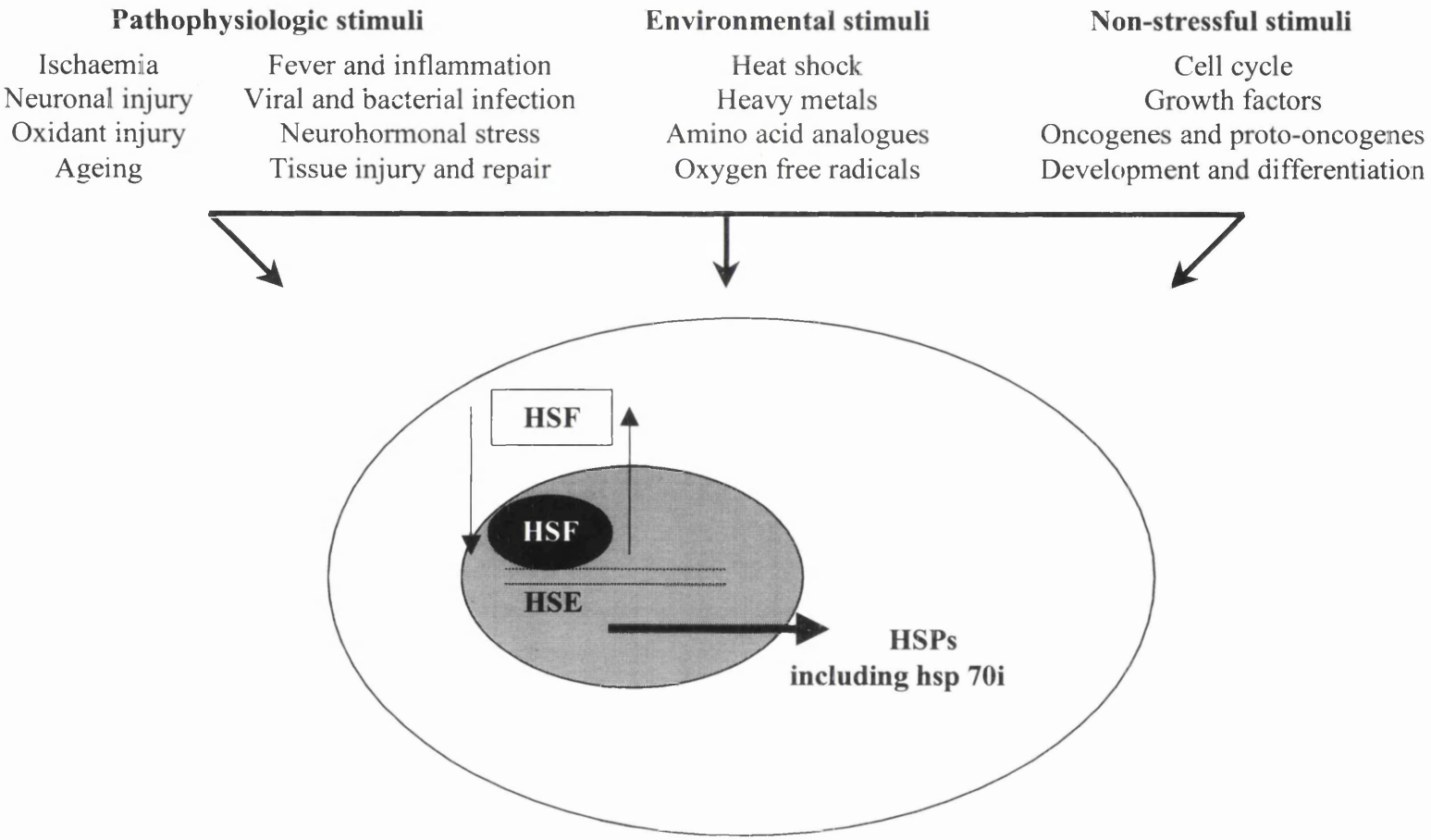

Expression of hsps (including hsp 70i) can be induced by numerous pathophysiologic, environmental and non-stressful stimuli. Figure shows hsp expression represented by activation of HSF (heat shock factor) binding to HSE (heat shock element) leading to elevated expression of hsps. Large white sphere = neuron cytoplasm, small grey sphere = nucleus.

1.7.1 The heat shock response: discovery and description

Since the 1950s puffing patterns in diptera polytene chromosomes were known to change in a very regular manner during larval development (see Ashburner, 1982). Beerman suggested that chromosome puffs represent actively transcribed genes and were sites of active gene loci (Beerman, 1956). Throughout the 1950s there was a great deal of interest in the type of nucleic acid synthesised in puffs of the salivary gland chromosomes of *Drosophila.* Clever and Karlson (1960) reported that ecdysteroid hormones mediated alterations in chromosome puffing patterns. Ritossa (1962) reported the first description of a heat shock response. Ritossa discovered a new puffing pattern in salivary gland polytene chromosomes of *Drosophila busckii* induced by elevated temperature and 2-4 dinitrophenol treatment. Serendipity had played a part in these discoveries as Ritossa identified this new cellular response only after a colleague had mistakenly increased the temperature of his incubator. This was the first description that puffing patterns could be manipulated by external stimuli. The work of Ritossa (1962, 1964) was complemented and extended by Berendes and Holt (1964), Berendes (1965a and 1965b) and Ashburner (1970). These groups investigated the effects of heat shock and other stresses in *Drosophila hydei* and *Drosophila melanogaster.* By the 1970s the heat shock response in diptera had been extensively characterised. First, the heat shock response was transient, with puffs reaching maximal size at about 30 minutes post heat shock. Second, heat shock puffs occurred in isolated organ preparations, i.e., an intact organism was not required for an heat shock response. Third, the heat shock response was not specific to tissue type or a particular stage of development.

Tissieres *et al.*, (1974) initiated investigation into the functional relevance of heat shock puffs using sodium dodecyl sulphate gel electrophoresis and radiolabelled amino acids. Tissieres *et al.*, (1974) reported that heat shock induced synthesis of a small number of proteins, but reduced synthesis of most other proteins in *Drosophila melanogaster* salivary

glands, brain and malphigian tubules. Lewis *et al.*, (1975) confirmed that these newly induced proteins were synthesised by heat shock puffs. McKenzie *et al.*, (1975) and Spralding *et al.*, (1975) reported identical heat shock responses in cultured *Drosophila* cells. McKenzie *et al.*, (1977) and Mirault *et al.*, (1978) provided strong *in vitro* evidence that hsps were coded for by the induced puffs. They achieved this by isolating heat shock messenger RNA, hybridising it back into polytene chromosomes and observing its translation *in vitro* into hsps. It was not long before the heat shock response was realised to be far more complex than originally envisaged. Lis *et al.*, (1978) cloned the first heat shock induced transcripts. These transcripts did not however bear the hallmarks of messenger RNA. The confusion was heightened by the first genetic correlation experiments into heat shock puffs and hsps. Ish-Horowitz *et al.*, (1977, 1979) reported that hsps were synthesised in *Drosophila melanogaster* embryos that had been modified to lack sites known to code hsp synthesis. These findings were explained when certain puffs were discovered at duplicate loci, both containing multiple hsp coding sequences (see Ashburner, 1982).

In 1978 mammalian and avian hsps were discovered (Kelley & Schlesinger, 1978; Hightower & Smith, 1978). The same proteins had been synthesised following heat shock and amino acid analogue (canavanine) treatment. Also in the same year, analogous heat shock (stress) responses were reported in bacteria (Lemeaux *et al.*, 1978; Yamamori *et al.*, 1978), and Tetrahymena (Fink & Zeuthen, 1978). By 1980 hsps had been reported in hamster cells (Bouche *et al.*, 1979), yeast (Miller *et al.*, 1979; McAlister *et al.*, 1979), Naegleria (Walsh *et al.*, 1980) plants (Barnett *et al.*, 1980) and rat (White, 1980b). It was now apparent that the so-called heat shock response, was not species dependant and could be evoked by a variety of stimuli (stresses) and not increased temperature alone. Hightower and White (1981) reported that the two proteins they had been working on independently in different species, in different systems, were the same protein. They also

reported the discovery of a constitutive protein they called P73 (now known as hsc 70). The same publication was responsible for the introduction of the terms 'cellular stress response' and 'stress proteins' into the literature.

1.7.2 Hsps and the CNS

Hsps in the *Drosophila* nervous system were discovered by Tissieres *et al.*, (1974). White (1980a; 1980b; and 1981) reported hsps in the mammalian CNS. In these publications White described a variety of proteins expressed in explanted rat brain slices. He did not immediately refer to them as hsps as they had not been classically induced following a heat shock. Instead White suggested these proteins were induced by the trauma of brain slicing and explantation. White had set about establishing an amenable means of studying normal brain protein synthesis in the CNS. The fact that these 'trauma induced' proteins in brain slices were not observed *in vivo* meant that this system might be flawed. White however, continued his studies of brain protein synthesis by investigating the proteins he had uncovered. Currie and White (1981, 1983) described induction of the same protein induced by brain slicing (known then as SP71) *in vivo* after heat shock. Throughout this period Browns laboratory in Canada had been investigating the effect of D-lysergic acid diethylamide (LSD) and bacterial pyrogen induced hyperthermia in the rabbit CNS (Hekkila *et al.*, 1979; Hekkila and Brown, 1979a, 1979b). These studies concluded that whole body hyperthermia caused dissagregation of brain polysomes. Freedman *et al.*, (1981) and Cosgrove *et al.*, (1982) went on to show that LSD induced messenger RNA which coded for a 74 kilo Dalton protein. Brown and co-workers continued throughout the early 1980's to report similar increases in such proteins in the rabbit CNS following hyperthermia.

1.7.3 Hsp 70i and cerebral ischaemia

In the ischaemic brain, protein synthesis is markedly decreased (Dienel *et al.*, 1980; Kleihues & Hossman, 1981; Kirino & Sano, 1984; Thilman *et al.*, 1986). While protein synthesis decreases there is considerable evidence that mRNA synthesis is less affected (Yanagihara, 1976, 1978). Currie & White (1981) first reported induction of hsp 70i in the ischaemic brain. This description was somewhat non-comprehensive as they reported induction of hsp 70i (known then as P_{71}) in the 'brain' in a single animal following 30-minute occlusion of one common carotid artery. Nowak (1985) provided a comprehensive description that transient global cerebral ischaemia in the gerbil (BCCAo) resulted in hsp 70i expression. Dienel *et al.*, (1986) reported expression of hsp 70i following global cerebral ischaemia in the rat soon after (four vessel model, bilateral carotid and vertebral artery occlusion). Jacewizc *et al.*, (1986) demonstrated expression of hsp 70i following a focal cerebral ischaemic insult (all of these studies employed protein synthesis assays). Although this approach adequately determined the protein content in a defined sample of brain tissue, it could not delineate the localisation of hsp 70i. Welch & Suhan (1986) developed a monoclonal antibody to hsp 70i. Vass *et al.*, (1988) and Gonzalez *et al.*, (1989) were the first to employ this antibody in studies of cerebral ischaemia. The cellular distribution of hsp could now be related to ischaemic cell damage following ischaemic insult. Vass *et al.*, (1988) employed the BCCAo model of global cerebral ischaemia in gerbils. They studied the distribution and time course of hsp 70i and related that to the distribution and time course of ischaemic neuronal damage. Vass and colleagues concluded that hsp 70i expression was most prevalent in neurons in brain regions which survived ischaemic challenge (i.e., the hippocampus CA3, dentate gyrus and entorhinal cortex). Brain regions in which cell death was evident (such as the hippocampus CA1) expressed only minimal hsp 70i expression. The time course of hsp 70i expression was maximal in hippocampus CA3 at 48 hours post insult. Gonzalez *et al.*, (1989) described the pattern of hsp 70i following focal cerebral ischaemia. Hsp 70i was located in cells

within the tissue margin surrounding the infarct core (i.e., in the penumbra). Extensive characterisation of the distribution and time course of hsp 70i expression following ischaemic insult ensued (see Massa *et al.*, 1996 for review).

In 1990 Nowak reported, in a BCCAo model of global cerebral ischaemia in gerbil, that hsp 70i mRNA was strongly expressed in hippocampus CA1 neurones. A new series of studies investigating the distribution and time course of hsp 70i mRNA expression following various ischaemic insults began (Abe *et al.*, 1991, 1992, 1993; Kawagoe *et al.*, 1993; Aoki *et al.*, 1993a, 1993b, 1993c). These studies led to the belief that hsp 70i and hsp 70i mRNA could be used as markers of neuronal damage. There was however, growing evidence that stress induced proteins (including hsp 70i) could function to protect neurones and other cell types from ischaemic injury. Efforts to resolve the dichotomy utilised two distinct lines of investigation, conditioning studies and cell culture studies. The classic conditioning studies of Chopp *et al.*, (1989) and Kirino *et al.*, (1991) took advantage of the fact hsp 70i was induced by transient hyperthermia and ischaemia, respectively. Chopp *et al.*, (1989) subjected rats to global cerebral ischaemia (BCCAo with hypotension) 24 hours after elevating the body temperature of rats to 41.5°C. A significant reduction in ischaemic neuronal damage compared with that of non-heat treated animals was observed. Kirino *et al.*, (1991) pre-treated gerbils with two-minutes of BCCAo; one day later the same animals were subjected to five minutes of BCCAo. Kirino and colleagues, like Chopp *et al.*, (1989), reported a significant decrease in the subsequent ischaemic neuronal damage, compared with untreated animals. This phenomenon, known as ischaemic tolerance, may involve hsp 70i as it is detected after such pre-treatments. However, many other stress-related proteins can also be detected *in vivo* following such interventions. Where cells in culture were manipulated to study the remedial effects of hsp 70i on simulated ischaemia, this doubt was less evident. In many of these studies neurones and other cell types were expressing hsp 70i and so were protected from ischaemic insult

(Lowenstein *et al.*, 1991; Dwyer & Nishimura, 1994; Mailhos *et al.*, 1994; Amin *et al.*, 1996; Xu & Giffard, 1997).

1.7.4 Regulation of hsp 70i

As hsps play important roles in normal and stressed cells, a complex regulatory process is required to ensure the correct expression patterns are maintained. These processes must also be operative in early development since hsp 70i and hsp 90 have both been shown to be amongst the first genes transcribed from the embryonic genome (Latchman, 1998). Heat shock factors (hsfs) essentially regulate the heat shock response. Lower organisms such as yeast and drosophila display only one hsf (Sorger & Pelham, 1988; Gallo *et al.*, 1993), while higher organisms such as plants, mice, chickens and humans exhibit multiple hsfs (Sorger *et al.*, 1991; Schuetz *et al.*, 1991; Nakai & Morimoto, 1993; Treuter *et al.*, 1993; Czarnecka-Verner *et al.*, 1995; Nakai *et al.*, 1997). Vertebrates ubiquitously exhibit hsf-1, hsf-2 and hsf-3 with hsf-4 found only in avian species (Morimoto, 1998). Following suitable stress in eukaryotic cells, hsf-1 binds to highly conserved regulatory sequences known as heat shock elements (hses). Hses are found on the heat shock gene. Once bound hsf-1 controls the expression of hsps (Wu, 1984; Sarge *et al.*, 1987; Zimarino &Wu, 1987; Larson *et al.*, 1988; Abrayava *et al.*, 1992; Mivechi *et al.*, 1992). Stress causes hsf-1 to trimerize enabling it to bind to DNA (i.e., the hses) and phosphorylate (Sarge *et al.*, 1987; Kim *et al.*, 1997). In mice and humans this hsf-1 trimerisation, binding and phosphorylation can activate the transcription of several hsps following heat shock and other stresses (Sarge *et al.*, 1991; Schuetz *et al.*, 1991; Mivechi *et al* 1992). Hsf-1 is readily activated in response to an array of stimuli (generally speaking the same ones as hsps, as hsf activation leads to hsp production, Figure 7) (Morimoto *et al.*, 1990, 1994, 1996; Wu, 1995). In stressed cells nascent protein synthesis is inhibited; these conditions lead to hsf-1 activation, which promotes hsp transcription. Hsps then act as molecular chaperones repairing, refolding and trafficking damaged proteins. A great deal has yet to

be established about the regulation of hsf-1. In some organisms hsf-1 is actively repressed and exists in the cell nucleus or cytosol in monomeric state. The precise mechanisms by which this repression is achieved are unknown. However, there is some evidence that hsp 90 may have a role in maintaining hsf-1 in this inert state (Ali *et al.*, 1998; Zou *et al.*, 1998). Moreover, following a heat shock response the subsequently high levels of hsp 70i suppress hsf-1 (Mosser *et al.*, 1993). The combined actions of all hsps, hsp 70 and hsp 90 included, are not sufficient to completely suppress hsf-1 trimerisation (Morimoto, 1998). Due to the ease with which hsf-1 is activated, there has been speculation that complex systems are in operation, which monitor and control hsf-1 in the activated state (see Morimoto, 1998 for details.).

1.8 Genetically modified mice

Around 100 different genes expressed in the CNS have been targeted and phenotyped in genetically modified mice (Crawley, 1999). More than 100 studies investigating the pathophysiology of ischaemic brain injury employing such mice were reported by mid 1999 (Ginsberg, 1999). Mice genetically modified to over-express or be deficient of certain genes or gene products have been used to investigate their roles in ischaemic brain injury. These include hsp 70i (this thesis Section 3.2; Plumier *et al.*, 1997; Radjev *et al.*, 1999; Yenari *et al.*, 1999), apolipoprotein E (Bart *et al.*, 1998; Sheng *et al.*, 1998; Horsburgh *et al.*, 1999), the nitric oxide synthases (Hara *et al.*, 1996; Huang *et al.*, 1994, 1996; Iadecola *et al.*, 1997; Nagayama *et al.*, 1999), superoxide dismutase (Chan *et al.*, 1993; Fujimura *et al.*, 1999; Keller *et al.*, 1998; Kinouchi *et al.*, 1991; Murakami *et al.*, 1998b), adhesion molecules (Connolly *et al.*, 1996, 1997; Kitagawa *et al.*, 1998a; Prestigiacomo *et al.*, 1999; Soriano *et al.*, 1998, 1999), apoptosis, cell damage and survival mediating gene products (Eliason *et al.*, 1997; Hara *et al.*, 1997; Kitagawa *et al.*,1998b), early response genes (Panahian *et al.*, 1997), transcription factors (Hata *et al.*, 1998;

Iadecola *et al.*, 1999; Schneider *et al.*, 1999) and cytokines (Bruce *et al.*, 1996; Schielke *et al.*, 1998).

1.8.1 Evolution and production of genetically modified mice

Mother Nature achieved the first successful introduction of foreign genetic material into host genomes in the early days of life on this planet, i.e., viruses, bacteria and spermatozoa. In the late twentieth century the tailored invention of genetically modified organisms started with the explosion of recombinant DNA technologies and the subsequent ability to isolate individual genes in the 1970s. Introduction of foreign genetic material into host cells and genomes was viewed as an excellent means by which an understanding of organism development and growth could be investigated. Pivotal to all advances in the synthesis of genetically modified organisms was the work of mammalian embryologists (see Brinster, 1972). For it was the development of techniques such as embryo removal, cultivation of embryos *in vitro* and returning of embryos to mothers for development, which enabled many early gene transfer studies.

1.8.2 Adding genetic information to mice

The infectivity of viruses meant these organisms were used extensively to transfer genetic information from one organism to another. Graham *et al.*, (1973) introduced ad 5 DNA into human KB cell monolayers. Viruses were again utilised, this time to introduce foreign DNA into intact organisms, by injection and infection of pre-implantation blastocysts and embryos (Jaenisch & Mintz, 1974; Jaenisch). The virus theme continued throughout the 1970s where successful introduction of exogenous DNA into cultured cells was becoming commonplace (Bachetti & Graham, 1977; Wigler *et al.*, 1977; Maitland & McDougall, 1977; Minson *et al.*, 1978). Gordon *et al.*, (1980) pioneered the technique of pronuclear injection to introduce foreign genetic information into intact mice (Figure 8). The pronuclear injection technique was complemented and extended by Gordon & Ruddle

Figure 8 Pronuclear injection technique of transgenic mouse production

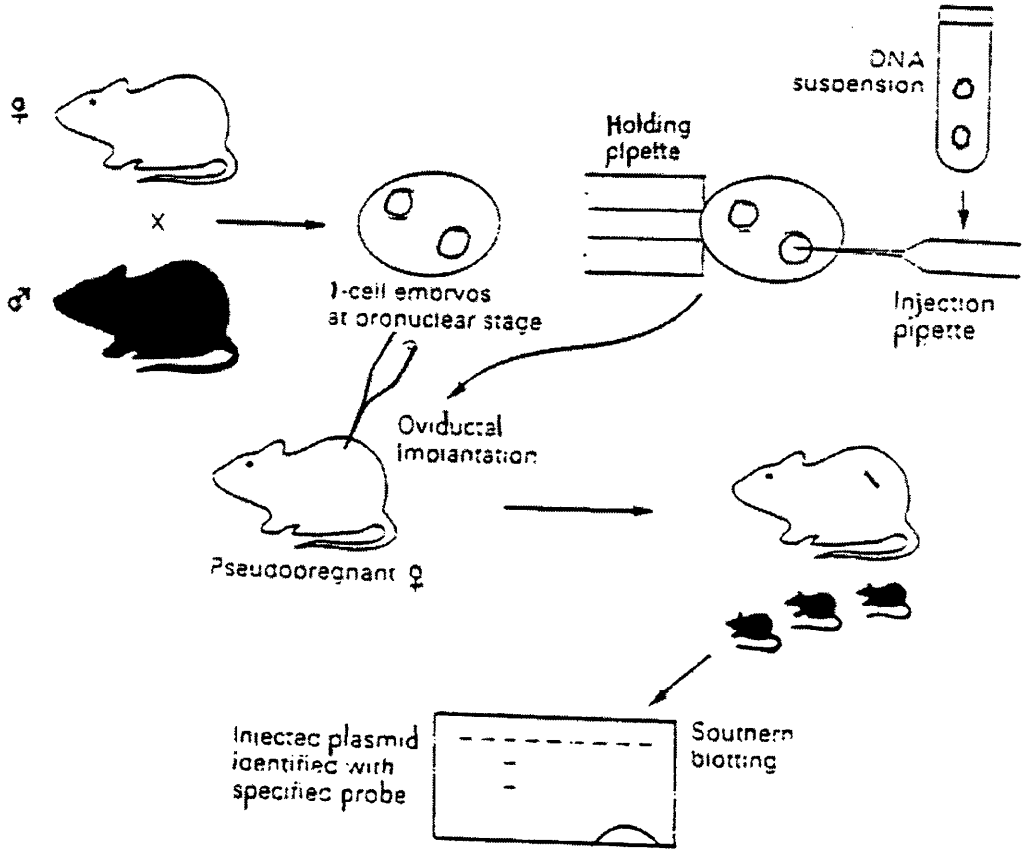

Single-celled fertilised eggs are extracted from superovulated female mice. Cloned DNA (in the case of this thesis human hsp 70i) is then injected into a pronucleus using a microneedle. Surviving embryos are then reimplanted into the oviduct of a pseudopregnant female. Offspring are screened using Southern blotting for DNA incorporation with an appropriate labelled probe. Positive mice are then back-crossed to homozygocity. Adapted from Reventos and Gordon, 1990.

(1981) who introduced the term 'transgenic' (to define: animals which have integrated foreign DNA in their germ line as a consequence of the experimental introduction of DNA) Brinster *et al.*, (1981); Constantini & Lacy, (1981) and notably, Palmiter *et al.*, (1982). Pronuclear injection is the most commonly used technique to produce transgenic animals and precipitated a logarithmic growth of transgenic science. During this time Mann *et al.*, (1983), Joyner & Bernstein (1983) and Miller *et al.*, (1983) produced recombinant retroviruses carrying heterologous genes, meaning the previous technique of Jaenisch *et al.*, (1976) could now be used to produce transgenic animals.

Embryonic stem cell lines were derived from pre-implantation embryos (Evans & Kaufman, 1981; Martin, 1981). These cells could be maintained in culture for extensive periods and could be subjected to various manipulations (Reventos & Gordon, 1990). Re-implantation of such blastocysts leads to animals with embryonic stem derived cells in all lineages (including the germ line) known as chimaeras (Figure 9). Chimaeras occur naturally in many species of mammals, including man (Gardner, 1968). Early experimental work to produce chimaeras focused primarily on the processes involved in mammalian differentiation during development. The first experimental attempt to produce a chimaeric animal was made by Nicholas and Hall (1942). Nicholas and Hall fused two 1-cell rat embryos together and reported that the product went to term. However, the results were inconclusive. Nineteen years later Tarkowski (1961) developed experimental chimaeras by fusing two embryos together. Tarkowski's method and that of Mintz (1962) were the forerunners to a technique of producing chimaeras, established by Gardner (1968, 1972). Gardner produced chimaeras by injecting foreign cells into the blastocoleic cavity of mouse blastocysts. Mosaicism was verified using genetic markers. Gardner's work bears many similarities to the techniques adopted to make modern day transgenic animals. In fact, Gardner and his peers were effectively producing transgenic animals as defined by Gordon & Ruddle (1981).

Figure 9 Production of chimaeric mice

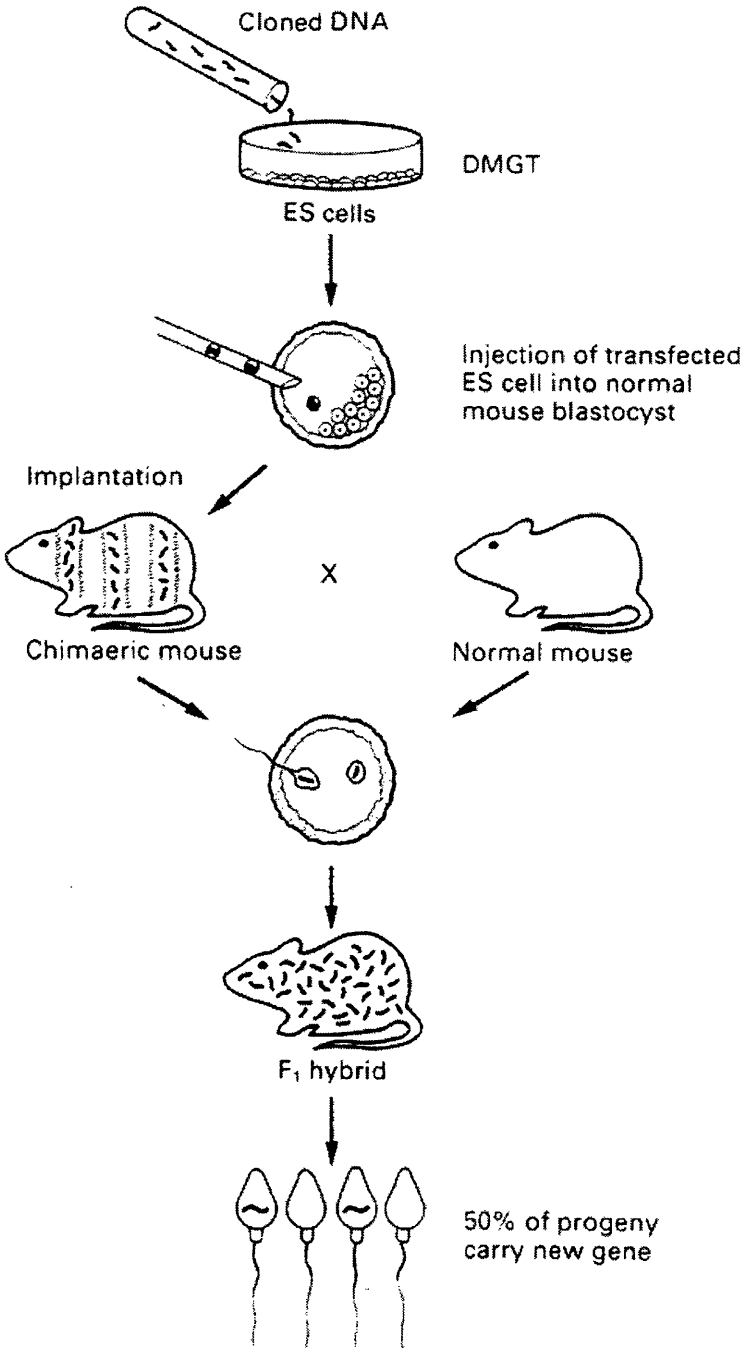

Chimaeric mice are produced by embryonic stem (ES) cell-mediated gene transfer. ES cells can be transfected by DNA-mediated gene transfer (DMTG). Transfected cells are then injected into the cavity of a blastocyst. Sperm of chimaeric mice, derived from ES cells, which contributes to the germ line produces transgenic mice. Adapted from Reventos and Gordon, 1990.

Brinster (1974) and Mintz & Illmensee (1975) published work investigating the transmission of genetic markers from adult mice to offspring. Transmission of genetic markers was achieved, in part, by placing malignant pluripotent teratocarcinoma cells into blastocysts and injecting these into the mother. Genetic markers highlighted that these tumour cells were spread throughout the offspring genome. Furthermore, these cells were functioning properly in their new surroundings, e.g., producing immunoglobulins, haemaglobin, etc. Evans and Kaufman (1981) and Martin (1981) further developed these observations with the characterisation of the mouse embryonic stem cell that could still enter the germ line after genetic manipulation *in vitro* (Gossler *et al.*, 1986; Robertson *et al.*, 1986). In 1985 Smithies *et al.*, unlocked the true potential of genetic manipulation of embryonic stem cells. Smithies group reported stable insertion of defined DNA sequences into the human β-globulin locus in a predictable fashion. This phenomenon was known as homologous recombination. Homologous recombination occurs very rarely in all species to produce DNA mutations. Smithies and his co-workers had been able to identify this process and detect it at a specific locus. Essentially, homologous recombination could be used to target specific genes on a chromosome. In the study conducted by Smithies *et* al., correctly targeted cells were obtained at a frequency of one event per 10 million treated cells. Despite this apparently low rate of targeted transformation several other groups reported encouraging findings. Constantini *et al.*, (1986) used this technology to correct murine β-thalassemia by transferring cloned β-globin genes into the mouse germ line. The mice in question had spontaneously developed a deletion of the β^{maj}-globulin gene, probably due to exhaustive inbreeding. Having cured β-thalassemia inside a generation, Constantini *et al.*, echoed the statements of Williamson (1982), Anderson (1984) and Walters (1986) in condemning the transfer of genes into the germ line as 'not a feasible strategy for human gene therapy'.

Targeted introduction of DNA largely evolved from the generation and use of hypoxanthine guanine phosphorybosil transferase (HPRT)-deficient mice. Two British groups had established mice deficient in HPRT and coined them animal models for the neurological and behavioural disorder Lesch-Nyhan syndrome. Hooper *et al.*, (1987) identified and selected variant embryonic stem cells deficient in HPRT and used these cells to produce germ line chimaeras. This led to female offspring heterozygous for HPRT-deficiency and the generation of HPRT-deficient pre-implantation embryos from these females. While Kuehn *et al.*, (1987) mutagenized embryonic stem cells by retroviral insertion and selected for loss of HPRT activity to manufacture chimaeric mice, Doetshman *et al.*, (1987) corrected the HPRT-deficiency in mice produced by Hooper *et al.*, (1987) by homologous recombination *in vitro*. Several studies of this nature ensued and new targeting vectors were investigated. Most of the early studies employed a targeting vector containing the bacterial neomycin resistance gene (*neo*^{r}) as a selectable marker gene facilitating the isolation of targeted clones (Thomas & Capecchi, 1987; Johnson *et al.*, 1989). Mansour *et al.*, (1988) included the herpes simplex virus (hsv) thymidine kinase gene (*tk*). This strategy was employed to select against non-homologous integration. Zimmer & Gruss (1989) used microinjection of a maternal gene fragment to disrupt the *Hox1.1* gene in embryonic stem cells.

1.8.3 Removing genetic information from mice

Thompson *et al.*, (1989) first described the combination of gene targeting with germ line transfer. They produced male mouse chimaeras, which transmitted HPRT corrected genes to their progeny. This however, was associated with an unanticipated deletion, which occurred during or after the targeting event. Later that year Koller *et al.*, (1989) reported high frequency germ-line transmission of a planned alteration to the HPRT gene by homologous recombination in embryonic stem cells. Zijlstra *et al.*, (1989) followed suit a couple of months later, reporting germ line transmission of a disrupted β_2-microglobulin

gene produced by homologous recombination in embryonic stem cells. In both cases, there were no dramatic pathologies observed in these mice carrying homozygous deletions in their genes (Figure 10i).

The classic approach of generating null mutants i.e., introducing a null mutation into embryonic stem cells from which homozygous mutant mice can be derived (described above), is somewhat indiscriminate. That is to say, the gene disruption or deletion is carried in the germ line. This means it is inserted in all embryonic stem cell lineages and is apparent from the onset of development. The characterisation and application of a system, known as the Cre-mediated *loxP* specific recombination system, from the *E. coli* bacteriophage P1 (Sternberg & Hamilton, 1981; Austin *et al.*, 1981; Abremski & Hoess, 1984; Sauer & Henderson 1988, 1989) enabled the inactivation of genes in a conditional manner. Cre is a 38-kilo Dalton recombinase protein, encoded by the *E. coli* bacteriophage P1. *loxP* is a 34 base pair sequence which consists of two 13 base pair inverted repeats, separated by an eight base pair spacer. Together these form two binding sites for the Cre recombinase (Figure 10i). Cre recombinase was shown to be capable of mediating *loxP* site-specific recombination in embryonic stem cells by Gu *et al.*, (1993) and in transgenic animals (Lasko *et al.*, 1992; Orban *et al.*, 1992). Cre-mediated recombination at site-specific *loxP* sites, to create exon specific gene knockouts (Figure 10ii), allowed scientists to investigate specific gene functions *in vivo* throughout development and maturity.

Conditional or tissue-specific gene deletions can also be engineered using the Cre-*loxP* system (Gu *et al.*, 1994; Di Santo *et al.*, 1995). This approach enables sequence specific removal of genetic information in specific tissue types or cell sub-populations. The general strategy of this approach is considered in some detail in van der Neut, (1997). Briefly, a *neo*^{r}-*tk* cassette flanked by two *loxP* sites is placed on one side of the sequence

Figure 10 Cre *loxP* recombinase and exon specific gene knockout

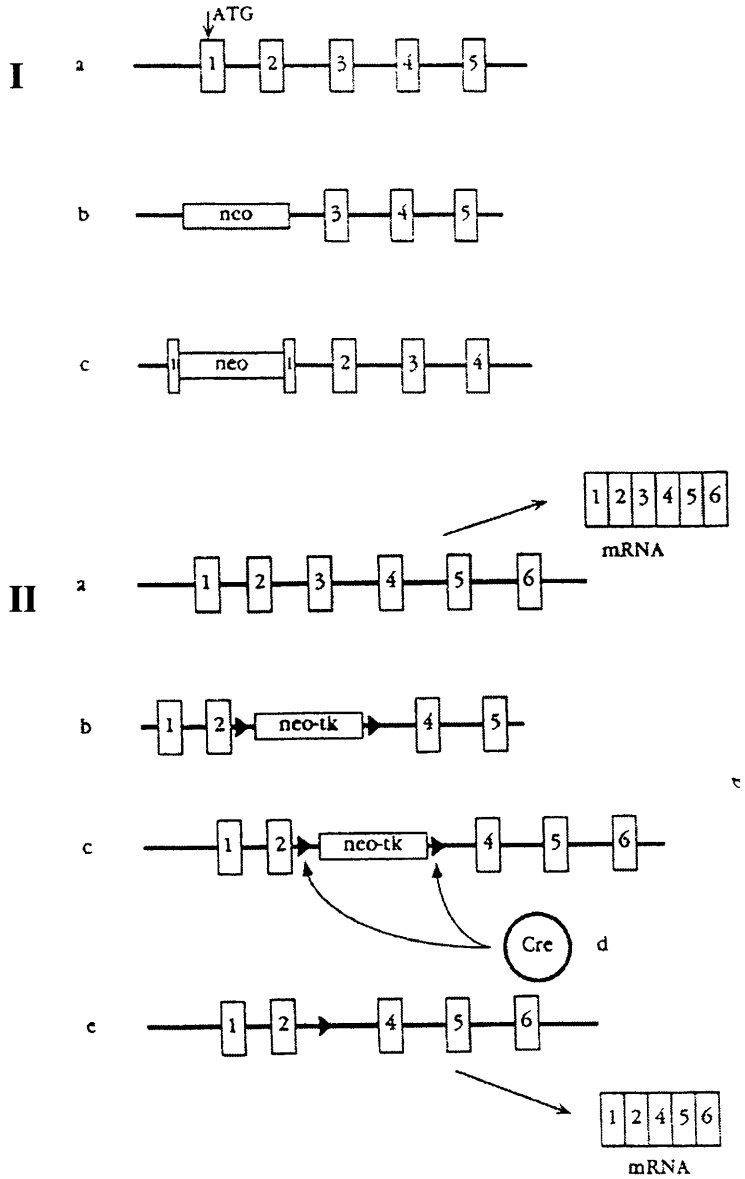

Inactivation of a gene (Ia) using two different targeting vectors. (Ib) crucial exon(s) can be replaced with the targeting vector (neo). (Ic) transcription of the gene is prevented by a targeting vector (neo) splitting a crucial exon. Alternative splicing in this way can however lead to partially functioning gene products. Exon-specific knockout (IIa) a gene contains 6 exons (1-6). Exon 3 has to be removed. (IIb) exon 3 is removed by insertion of a targeting vector (neo-tk) flanked by *loxP* (triangles). (IIc, IId) homologous recombination leads to embryonic stem (ES) cells with one allele (i.e., exon 3 is replaced by the neo-tk cassette), transient expression of a plasmid encoding Cre recombinase leads to recombination at the *loxP* sites, removing the neo-tk cassette. (IIe) ES cells containing recombined alleles produced. These can then be injected into blastocysts and introduced into pseudopregnant female mice, to produce gene deleted (knockout) mice. Adapted from van der Neut, 1997.

being deleted, with another *loxP* site positioned before said sequence. These clones are then transiently transfected with a Cre encoding plasmid, and selected using selective growth media. The Cre expression leads to three types of site-specific recombination: (1) the *neo*^{r}*-tk* cassette is preserved (these clones do not survive in the selection media) (2) only the *neo*^{r}*-tk* cassette is removed (this produces viable cells with one mutated allele flanked by two *loxP* sites), and (3) the whole insert is removed, i.e., the two extreme *loxP* sites are excised, these cells also survive the selection media. The cells with one mutated allele are separated by southern blotting and are injected into blastocysts. The resulting chimaeric mice are backcrossed until mice with one *loxP* flanked mutated allele are obtained. The mice are then crossed with transgenic mice containing Cre recombinase driven by tissue specific promoters. This results in mice homozygous for the *loxP* flanked mutated allele and the Cre transgene. Cre-mediated recombination ensues, resulting in tissue-specific null mice. Several variations of this technique that utilise tissue-specific and inducible promoters and also reporter constructs are now in use. These can be utilised to further tailor the excision of desired DNA sequences from specific cell subtypes at different stages of development and to express marker gene products to locate and identify regions of mutation.

In short, genetically modified mice can now be produced to over-express or be deficient of genes of interest. Moreover, this over-expression or deletion can be directed at specific cell subtypes and can be induced at different stages of development. These developments have led to the widespread, almost ubiquitous, use of such mice in most areas of animal based biomedical research, including the neurosciences.

1.8.4 Concerns over genetically modified and inbred mice

The use of transgenic and targeted deletion (knockout) mice, particularly in the past five years, has undoubtedly led to greater scientific understanding of the processes involved in

many research fields, including the neurosciences. However, while this field continues to grow and prosper, it should be noted that concerns about the field exist. The concerns voiced are primarily directed toward animals with gene deletions and abhorrent behaviours observed in inbred mouse strains (Choi, 1997; Crawley, 1996, 1999; Crawley *et al.*, 1997; Crusio, 1996; Gerlai, 1996a, 1996b; Lathe, 1996; Routtenberg, 1996; Wehner & Silva, 1996; Zimmer, 1996). This belt of publications led to the convening of a special workshop entitled 'Mutant Mice and Neuroscience' at Cold Spring Harbor laboratory in December of 1996 (Banbury conference of genetic background in mice, 1997). This meeting produced a series of recommendations and guidelines, which, if adhered to, would improve the power of studies employing such mice. Beyond gene deletion, complications stem from the spectrum of unique characteristics displayed by individual mouse strains. As far as brain function is concerned, inbred strains vary in their responses to many stimuli, including pharmacologic agents (Cooper & Francis, 1979; Holsztynska *et al.*, 1991; Seale *et al.*, 1984; Tolliver & Carney, 1994) and alcohol (Church & Feller, 1979). Major differences in brain anatomical structures are also reported in several mouse strains (Crusio *et al.*, 1990; Livy & Wahlsten, 1991; Schopke *et al.*, 1991; Wahlsten & Schalomon, 1994; Wainwright & Deeks, 1984). These anatomical differences are prevalent in SV129 strain mice. SV129 strain mice show absence of corpus callosum (Livy & Wahlsten, 1991) and perform poorly on memory tasks and stress-related paradigms (Crawley, 1996). During the development of reliable systems of embryonic stem cell gene transfer in the 1980's. The embryonic stem cells, which were most efficiently derived and manipulated, were those of SV129 strain mice (Lathe, 1996). Consequently, most knockout mice are derived from the SV129 lineage. Attempts to overcome the risk of neurological deficits in such knockout mice involved crossing these mice into and injecting SV129 embryonic stem cells into a C57bl/6 mouse strain background, however, this did not solve the problems (Choi, 1997; Crawley, 1996, 1999; Crawley *et al.*, 1997; Crusio, 1996; Gerlai, 1996a, 1996b; Lathe, 1996; Routtenberg, 1996; Wehner & Silva, 1996; Zimmer, 1996). Moreover, C57bl/6

strain mice display poor performance on passive avoidance and low levels of anxiety-like behaviours (Crawley & Davis, 1982; Mathis *et al.*, 1994, 1995). Added to this uncertainty is the argument that deleting a gene does not necessarily delete the function it would have performed (Crawley, 1996; Gerlai, 1996a). Crusio (1996) equates this strategy with brain lesioning. Crusio suggests that the common assumption in both situations is that the 'lesion' (of the brain or the chromosome) leads to the dysfunction observed in the residual organism. Although evidence supporting neurogenesis following brain lesions is now reported, (Lui *et al.*, 1998; Zupanc, 1999) 'genegenesis' is highly unlikely. Instead a process or processes akin to the re-routing principles of synaptic plasticity in the brain may well occur at the molecular genetic level i.e., other genes may effect some of the deleted genes properties. To further confound these complications, Lathe (1996) reports the observations of Wehner, who observed distinct behaviour and learning disabilities between the SV129J and SV129ev sub-strains of the SV129 strain.

In summary, the use of genetically modified mice is not without its problems. However, many of these problems are primarily peculiar to gene deletion mice, largely because of their strain derivation. Other cautionary points pertain mainly to the differences between strains and sub-strains in response to a host of different stimuli. In terms of scientific rigour the above points must be considered, understood and incorporated as integral sources of error in any given experimental paradigm. Furthermore, the recommendations of the Banbury conference (1997) should be heeded, and most importantly adequate scientific controls applied. A positive note, which can be extracted from strain and sub-strain differences in response to various stimuli, is the fact mice are not clones of each other i.e., they exhibit individual responses. This fact, if considered properly, may well add weight to scientific investigation of the human condition, as we too exhibit individual responses.

1.9 Viral vectors

Viruses are sub-microscopic biological entities (ranging from a few to a few hundred nanometers), capable of infecting and destroying host organisms. In the twentieth century alone smallpox killed an estimated 300 million people, about three-fold as many people as all the wars in the twentieth century combined (Oldstone, 1998). Today widespread vaccination programs have almost eradicated viral infections such as smallpox and polio in the Western world. However, human immunodeficiency virus, for which there is presently no vaccine or known cure, is reported to have infected somewhere in the region of 100 million people. Similarly, the common influenza virus continues to claim the lives of people in the United Kingdom, despite extensive vaccination programs.

Although small quantities of virus are used to prevent subsequent viral infections i.e., vaccination, until recently it was difficult to envisage the use of these particles in the therapy of any other disease states. One man, with what appears to be tremendous foresight on this matter, was Frank Herbert (1969). In his novel *Dune* Herbert wrote of a distant future in which physicians would harness deadly viruses and use them to therapeutically alter the genetic makeup of humans. His prediction came true in the early 1990's when viruses containing desirable gene products were injected into humans, a technique commonly known as gene therapy.

1.9.1 Vectors for gene therapy

By definition gene therapy is the introduction of therapeutic nucleic acids into cells with the aim of ameliorating or curing disease. There are two targets for gene therapy: (1) the germ line, and (2) somatic cells. Gene therapy of the germ line is often the starting point for the creation of transgenic and knockout mice (see Sections 1.8.2 and 1.8.3). Gene therapy of somatic cells involves the transfer of genetic information into mature cells as therapy for disease. In order that desired DNA can be introduced into target cells, a vector

is required. The most commonly used vectors are naked DNA (usually as a plasmid), cationic liposomes, viruses or a combination of the above. The choice of vector depends largely upon the target and the modality employed to transfer the genes into said target. There are two major approaches for transferring therapeutic genes into cells using the aforementioned vectors: (1) transplantation of autologous cells which have been genetically modified *ex vivo*, and (2) direct delivery into target tissue *in vivo* (Figure 11). The latter of these approaches has become the most widely used (Marcel & Grausz, 1997).

1.9.2 Viruses as vectors for gene therapy

The optimal vector that performs safe and efficient gene transfer to widespread areas of tissue has yet to be discovered. Viruses offer the greatest potential of the several candidate vectors presently being investigated. Five viruses in particular have been employed extensively in basic and clinical research to evaluate gene therapy, ad, adeno-associated virus, hsv, lentivirus and retrovirus. The three principle reasons why viruses are popular vectors for gene therapy are: (1) the relevant ease with which viruses can be engineered to contain genetic information of interest; (2) their natural propensity to infect; and (3) their ability to introduce foreign genetic material into host cells using the indigenous cell machinery for survival and replication. A major pre-requisite of all viral vectors is that they must be rendered replication defective. Strategies of rendering viruses replication defective involve the removal of the viral genes responsible for replication. Another measure which, is often required, is to reduce the cytopathogenicity of the virus. This is achieved by selective removal of viral genes responsible for eliciting these responses (see Hermens and Verhaagen, 1998 for an extensive review of virus recombination). The potential of any given virus as a modicum of therapeutic genetic information is very much dependant upon its own characteristics, the target tissue and the therapeutic gene. The characteristics of individual viruses vary considerably (Table 2). In terms of being used as a vector, the primary features are infectivity, immunocytopathogenicty and insert size.

Figure 11 ***In vivo* and *ex vivo* gene transfer with virus vectors**

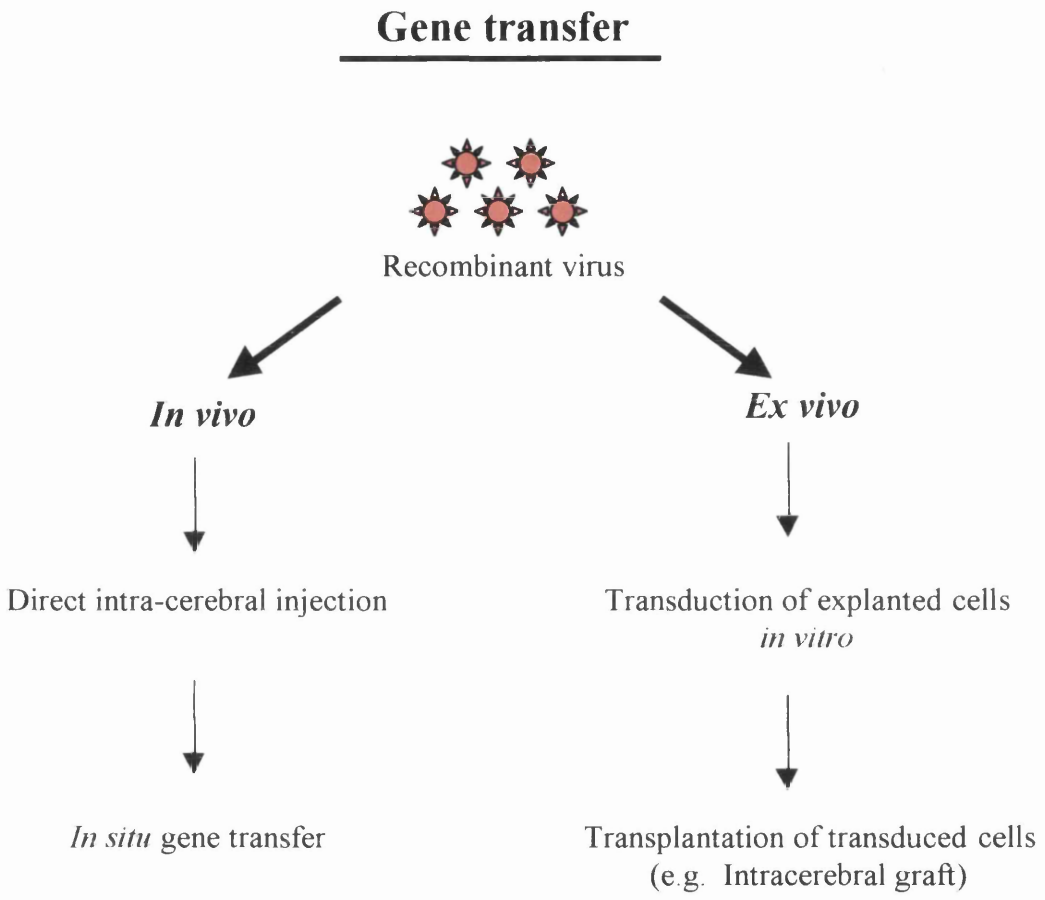

Table 2 **Characteristics of gene transfer viral vectors**

property	adenovirus	adeno-associated virus	herpes simplex virus	lentivirus	retrovirus
maximum insert size (kb)	~30	3.5-4.0	~35	7-7.5	7-7.5
viral particles per millilitre	~10^{12}	~10^{12}	~10^{8}	~10^{8}	~10^{8}
infectivity	broad	broad	broad	dividing cells	dividing cells
integration	episomal	chromosomal	episomal	chromosomal	chromosomal
stability	good	good	good	good	good
immune response	extensive	not known	medium	low	low
pre-existing immune-response	yes	yes	yes	unlikely	unlikely
latency in host	no	no	yes	no	no
safety	inflammation, toxicity	inflammation, toxicity	inflammation, toxicity	insertional mutagenesis	insertional mutagenesis

kb = kilobases

Much of the recent work on viral vectors has investigated the effect of the balance of these three features. For instance, the substantial immune response elicited in response to early (E1 deleted) ad vectors (Yang *et al.*, 1994a) led researchers to delete more genes, E2 (Englehardt *et al.*, 1994; Yang *et al.*, 1994b) and E4 genes (Dedieu *et al.*, 1997). These vectors produced increased duration of transgene expression due to a reduction in the severity of the immune response (Dedieu *et al.*, 1997). Unfortunately the stability of transgene expression was affected by E4 deletion (Armentano *et al.*, 1997). The latest generation of ad vectors known as 'minimal' or 'gutless' vectors have also been developed (Fisher *et al.*, 1996; Kochanek *et al.*, 1996). These vectors are devoid of almost all viral genes. Subsequently, they can house much larger DNA inserts and elicit diminished immune responses. Initial work with these vectors has been fruitful, with stable, long-term transgene expression reported (Burcin *et al.*, 1999; Schiedner *et al.*, 1998). Moreover, the tetracycline (Tet)-Off system (Gossen & Bujard, 1992), which effectively enables the switching on and off of transgene expression, has been successfully applied to ad (Harding *et al.*, 1997, 1998), gutless ad (Burcin *et al.*, 1999), hsv (Fotaki *et al.*, 1997; Ho *et al.*, 1996) and adeno-associated viral vector systems (Rendahl *et al.*, 1998).

1.9.3 Gene therapy for the brain

The classical retroviral vectors, which are widely used to transfer genetic information into tissues with a high degree of cell division, cannot be used to transduce non-dividing cells such as neurones (Fritsch & Temin, 1977; Miller *et al.*, 1990). Although this discounts their use in direct *in vivo* gene transfer to the brain, retroviruses have been used to modify cells *ex vivo*, and are then transplanted into the nervous system (Gage *et al.*, 1987, 1991; Gage and Fisher, 1991; Fisher, 1995; Lisovoski *et al.*, 1997). This approach has however, been overtaken by direct *in vivo* gene transfer to the brain using other viruses. The first viral vectors to be directly introduced into the brain were based on the hsv (Andersen *et al.*, 1992; Fink *et al.*, 1992; Huang *et al.*, 1992). Soon after ad vectors were directly

introduced into the brain (Akli *et al.*, 1993; Bajocchi *et al.*, 1993; Davidson *et al.*, 1993; le Gal le Salle *et al.*, 1993). Similar progress was reported with adeno-associated virus (Kaplitt *et al.*, 1994) and lentivirus (Naldini *et al.*, 1996) in subsequent years. The utility of each of these viral vectors for gene therapy in the brain has been extensively researched over the past seven years or so. The main areas of brain dysfunction that have been foremost in these researches are; cerebrovascular disease (such as ischaemia and hypotension), neurodegenerative disorders (such as Parkinson's chorea and Alzheimer's disease), neuroendocrine disorders (such as hypothalamic diabetes insipidus) and brain cancers (predominantly gliomas). As the focus of this thesis revolves around ischaemic insult, only this category will be discussed in this introductory section.

1.9.4 Gene therapy for cerebrovascular disease

There are two primary targets for gene therapy in cerebrovascular disease. These are the cells of the grey and white matter (especially neurones) and cerebral blood vessels. Whether the object of gene therapy is to prevent ischaemia (i.e., modulating hypotension) or trying to prevent cell loss after ischaemia, the general principles are the same: (1) the vector must be delivered to the site of damage, (2) the vector must transfect a suitable number of cells at the target site, (3) the expression of the delivered transgene and the duration of that expression must be appropriate, and (4) the immune response must be minimal. An overview of the use of viruses as vectors of therapeutic genetic information toward the therapy of ishaemic brain cells is offered below.

1.9.5 Gene therapy and cerebral ischaemia

Current strategies of viral vector gene therapy for cerebral ischaemia are threefold (1) to enhance energy metabolism, (2) to reduce necrotic cell death, and (3) to antagonise apoptotic cell death. The pathophysiology and mechanisms of cell death in cerebral ischaemia are complex and not completely understood (see Sections 1.3 and 1.4). In brief,

the major processes occurring in the ischaemic brain are; loss of ion homeostasis, loss of high-energy phosphates (i.e., energy failure), increased intracellular calcium, excitotoxicity and free radical production. The factors above invariably lead to either necrotic or apoptotic cell death.

As energy availability influences excitatory amino acid secretion and calcium mobilisation, one of the early attempts of gene therapy in cerebral ischaemia was to deliver the glucose transporter (Glut-1). The logic in delivering more glucose transporters was simply that more glucose could be transported. Lawrence *et al.*, (1996b) reported that virally mediated Glut-1 transporter protected striatal neurons from focal cerebral ischaemia. Several other studies *in vitro* produced similar results (Lawrence *et al.*, 1995; Ho *et al.*, 1995a, 1995b; Dash *et al.*, 1996). Kindy *et al.*, (1996) were the forerunners to investigate the viral vector gene transfer of a protein called calbindin D28K (a calcium binding protein). The principle of delivering calbindin D28K was that it would help overcome the calcium overload associated with ischaemic insults. After ad gene transfer Kindy and colleagues reported an increase in the number of neurones expressing calbindin D28K surviving following global cerebral ischaemia. Yenari *et al.*, (1999) have also recently used virus transfection of calbindin D28K to attenuate striatal neuronal death following focal cerebral ischaemia. These findings are supported by several other *in vivo* and *in vitro* studies exploring features of ischaemic cell change, including excitotoxicity and metabolic challenges (Meier *et al.*, 1997, 1998; Phillips *et al.*, 1999).

One of the peculiarities of cerebral ischaemia is that, due largely to the related calcium overload, normal intracellular protein synthesis is ceased. Associated with this reduction in nascent protein synthesis are incorrect intracellular targeting of proteins, protein malfolding and aggregation. These conditions propagate the induction and synthesis of a group of special proteins, the hsps (most notably hsp 70i, the major interest of this thesis).

The activities of hsp 70i are widely regarded to be of therapeutic value following insults such as ischaemia (see Section 1.7). At the outset of this thesis, no investigators had studied the *in vivo* effects of gene transfer of hsp 70i with viral vectors or in transgenic mice over-expressing hsp 70i, following cerebral ischaemia. One recent report emphasises that viral vector gene transfer of hsp 70i can protect neurones from focal ischaemic and excitotoxic insults *in vivo* (Yenari *et al.*, 1998). Others report virus mediated gene transfer of hsp 70i to protect cultured neurones from an array of excitotoxic anoxic and glycaemic insults (Papadopoulos *et al.*, 1996; Xu & Giffard, 1997).

Further virus mediated gene transfer approaches of protecting / salvaging neurones from ischaemic insult investigate the use of anti-apoptotic genes and cytokine receptor antagonists. The models investigated include excitotoxic insults, global and focal cerebral ischaemia, hypoxia / glycaemia and reactive oxygen species generation in whole animals and in cultured cells. For the most part the results were favourable. Viral vector mediated gene transfer of anti-apoptotic genes such as *Bcl-2* inferred protection of neurones and increased resistance to several ischaemic insults (Jia *et al.*, 1996; Lawrence *et al.*, 1996a; Linnik *et al.*, 1995). While other anti-apoptotic genes such as neuronal apoptosis inhibitory protein (Xu & Crocker, 1997) and crmA (Roy & Sapolsky, 1999) produced similar results. Viral vector mediated gene transfer of interleukin-1 receptor antagonist has also been shown to protect neurones following focal cerebral ischaemia (Betz *et al.*, 1995; Yang *et al.*, 1997) and excitotoxic seizures (Hagan *et al.*, 1996).

1.9.6 Concerns over viral vectors and gene therapy

In the autumn of 1999, Jesse Gilsenger (an 18-year old man from Arizona) was infused with one of the largest doses of ad ever given to a human. He developed influenza-like symptoms with a high fever one day after treatment. On the second day he developed liver injury (the organ infused) and inappropriate blood clotting. By day three he developed

trouble breathing and his vital organs were failing. On the fourth day he was taken off life support, and died. This chilling reminder of what viruses are capable of created a shockwave in the field of gene therapy, and importantly, out with the field of gene therapy. A meeting of the recombinant DNA advisory committee was called to discuss this case and concluded that death had resulted as a consequence of the ad infusion. It also advised gene therapy researchers to increase their safety measures, such as checking sequence integrity and closer monitoring of cytokines pre and post vector administration. Moreover, this case is now subject to federal investigation. This death and the findings of the committee led to the publication of a clutch of editorials and viewpoints on this topic (Fox, 1999, 2000; Smaglik, 1999; Ciment, 2000; Commander, 2000; Hollon, 2000). One of the major points of conjecture in gene therapy is the lack of standard approaches for measuring and comparing the strength and potential toxicity of vectors (Smaglik, 1999). This statement is consolidated by the report of Nyberg-Hoffman & Aguiler-Cordova (1999) who report instability of viral vectors during shipping in dry ice. These findings suggest that the user cannot be sure of the titre at the point of administration. Furthermore, when this is combined with variations in different virus production systems, in terms of purity and titre, then a significant source of error exists. In the aftermath of the first, and hopefully only death resulting solely from gene therapy, these issues are being considered far more intensely on the bench and at the bedside.

1.10 Aims of thesis

This body of work was designed to fulfil three main aims:

(1) To investigate the pathologic and physiologic consequences of global cerebral ischaemia on MF1 strain mice. In order to achieve this a mouse model of BCCAo was established.

(2) To investigate the influence of hsp 70i over-expression on ischaemic outcome following BCCAo. Hsp 70i over-expression was explored in two systems, (a) MF1 strain hsp 70i over-expressing transgenic mice, and (b) C57bl/6 strain mice intrastriatally injected with ad hsp 70i.

(3) To investigate the functional consequences of transgenic over-expression of hsp 70i (in the basal state and following metabolic activation with dizocilpine, 1mg/kg) and ad-mediated over-expression of egfp. In order to achieve this a modification of the ^{14}C-2-deoxyglucose autoradiography technique of Sokoloff *et al.*, (1977) was established in the mouse.

CHAPTER TWO: METHODS AND MATERIALS

2.1 Mice

MF1 and C57bl/6 strain mice used in this thesis were supplied by Harlan Olac Limited. Transgenic mice over-expressing hsp 70i and their wild type littermates (MF1 background, see Section 2.9 for detail) were bred and supplied by Dr James Uney from the University of Bristol (the original source of founder mice was Harlan Olac Limited). All mice were maintained on a 12 hour light / dark cycle and allowed free access to food and water. Male mice were used in all studies within this thesis. Female mice were not used in order that hormonal fluctuations peculiar to menstruation could be eliminated.

2.2 Global cerebral ischaemia

2.2.1 Experimental groups

Global cerebral ischaemia (BCCAo) was used in four separate studies in this thesis. In the first, to investigate the impact of BCCAo on MF1 and C57bl/6 strain mice. Adult male MF1 and C57bl/6 strain mice weighing between 30-40 grams were subjected to 10 minutes (n=6 MF1; n=6 C57bl/6); 15 minutes (n=6 MF1; n=6 C57bl/6); and 20 minutes (n=6 MF1; n=6 C57bl/6) of BCCAo. Sham procedures were also carried out for 10 minutes (n=3 MF1; n=2 C57bl/6); 15 minutes (n=2 MF1; n=2 C57bl/6); and 20 minutes (n=2 MF1; n=3 C57bl/6). In the second study, the impact of prolonging the duration of BCCAo on MF1 strain mice was investigated. Adult male MF1 strain mice weighing between 30-40 grams were subjected to 25 minutes (n=6), 30 minutes (n=6), 35 minutes (n=8), 40 minutes (n=6) and 45 minutes (n=6) of BCCAo. Sham procedures were also carried out for 25 minutes (n=5), 30 minutes (n=5), 35 minutes (n=6), 40 minutes (n=5) and 45 minutes (n=5). In the third study, the effect of transgenic over-expression of hsp 70i on pathologic outcome following BCCAo investigated. Adult male MF1 strain transgenic mice over-expressing hsp 70i (n=10) and their wild type littermates (n=9) weighing between 30-40 grams were subjected to 25 minutes of BCCAo. Sham procedures were also carried out in hsp 70i transgenic (n=10) and wild type littermate (n=9) mice. In the fourth study, the effect of

intrastriatally injected ad vectors containing hsp 70i or egfp (reporter gene) were investigated. Adult male C57bl/6 strain mice weighing between 30-40 grams were subjected to 10 or 20 minutes of BCCAo. These mice had been intrastriatally injected with recombinant ad vectors containing hsp 70i or enhanced egfp insert 14-days prior to induction of ischaemia. Mice intrastriatally injected with ad vector containing hsp 70i were subjected to 20 minutes (n=8) or 10 minutes (n=7) of BCCAo. Mice intrastriatally injected with ad vector containing egfp were also subjected to 20 minutes (n=8) or 10 minutes (n=6) of BCCAo.

2.2.2 Statistical power calculations

In any study when the challenge fails to reveal a significant change, the possibility of a type 2 error (i.e., a false negative) needs to be considered. In this thesis post hoc power calculations were employed to predict the differences in neuronal damage following BCCAo which could be detected. In all studies a difference of approximately 30% could be detected with the groups sizes employed:

1. 20-minute BCCAo in MF1 strain mice. Ischaemic neuronal damage in caudate nucleus was 1.5 ± 0.4 (mean ± standard deviation, SD) group size was 6. For 80 power, predicted detectable difference was 28%.

2. 20-minute BCCAo in C57bl/6 strain mice. Ischaemic neuronal damage in caudate nucleus was 2.3 ± 0.6 (mean ± SD) group size was 7. For 80% power, predicted detectable difference was 24%.

3. 45-minute BCCAo in MF1 strain mice. Ischaemic neuronal damage in caudate nucleus was 14 ± 4.6% (mean ± SD) group size was 6. For 80% power, predicted detectable difference was 33%.

4. 25-minute BCCAo in wild type littermate mice. Ischaemic neuronal damage in caudate nucleus was 21 ± 5.8% (mean ± SD) group size was 9. For 80% power, predicted detectable difference was 28%.

5. 20-minute BCCAo in ad egfp gene transfer C57bl/6 strain mice. Ischaemic neuronal damage in caudate nucleus was 33 ± 10% group size was 8. For 80% power, predicted detectable difference was 31%.

2.2.3 Surgical procedure

Global cerebral ischaemia was induced in the mouse by BCCAo. Surgical anaesthesia was induced in a perspex chamber with halothane (3%) in a mixture of nitrous oxide and oxygen (70:30) for 2.5 minutes. Anaesthesia was maintained throughout the procedure with halothane (1.2-1.7%) delivered via a facemask. Core body temperature was recorded using a rectal temperature probe and maintained around 37°C using a heating lamp throughout the procedure. Via a small skin incision in the neck, the common carotid arteries were freed from connecting tissues by blunt dissection. Lengths of surgical silk (4-0) were placed around both common carotid arteries. Carotid arteries were occluded by applying tension to these silks and placing an aneurysm clip (50-80 gram closing pressure) on each vessel. Complete vessel occlusion was observed and the incision site irrigated with sterile saline throughout the course of the occlusion. Sham operated mice had surgical silks (4-0) placed around both common carotid arteries and the incision site irrigated with sterile saline; no tension was applied to the silks. Clips were removed from occluded animals according to occlusion duration. Vessel patency was checked and the incision site sutured using surgical silk (6-0). Anaesthesia was discontinued. Each mouse injected subcutaeneously with sterile saline (0.5ml), was ventilated with 100% oxygen until recovery from anaesthesia and returned to its cage. The animals were placed in an incubator at 29°C for two hours post-operatively. Thereafter mice were housed in a

temperature-controlled facility for the remainder of the 72-hour survival period. A 72-hour (3-day) survival period was chosen to investigate ischaemic neuronal damage based on observations in a pilot study (which indicated that ischaemic neuronal damage at three and seven days post-BCCAo was similar).

2.3 Visualisation of circle of Willis anatomy

2.3.1 Experimental groups

The anatomy of the circle of Willis was analysed and recorded in two separate studies within this thesis. First, adult male MF1 strain mice (n=16) and C57bl/6 strain mice (n=8) weighing between 30-45 grams were investigated. Second, transgenic adult male MF1 strain mice over-expressing hsp 70i (n=9) and their wild type littermates (n=9) weighing between 30-40 grams were investigated.

2.3.2 Surgical procedure

Surgical anaesthesia was induced in a perspex chamber with halothane (3%) in a mixture of nitrous oxide and oxygen (70:30) for 2.5 minutes. Anaesthetic was maintained throughout the procedure with halothane (1.5%) delivered via a facemask. The heart was exposed by making a small incision at the base of the chest, cutting across the diaphragm and then through the ribcage bilaterally. A 20 gauge venous catheter connected to a 20ml pipette filled with heparinised saline (0.5%) was inserted into the left ventricle and clamped in place, the right atrium cut and the heparinised saline perfused through the mouse at 3.33ml/min using an infusion pump. After blood had been flushed from the animal a syringe containing carbon black ink was connected to the catheter and the ink perfused through the mouse at 3.33ml/min using an infusion pump. Carbon black infusion was discontinued upon observation of darkened (ink-filled) extremities, including nose, ears and mouth. The brains were removed carefully and the anatomy of the circle of Willis

visualised using a dissecting microscope (magnification X10). The gross structure of the circle of Willis and its major arterial branches were recorded diagrammatically.

2.4 Measurement of key physiologic variables

2.4.1 Experimental groups

MABP in mice was measured before, during and following BCCAo in mice in three separate studies in this thesis. Arterial pH, carbon dioxide and oxygen tensions were measured following BCCAo in these studies. First, key physiologic variables were measured in adult, male MF1 (n=8) and C57bl/6 (n=8) strain mice weighing between 30-40 grams subjected, to 20 minutes of BCCAo. Second, key physiological variables were measured in adult, male MF1 (n=8) strain mice weighing between 35-45 grams, subjected to 45 minutes of BCCAo. Third, key physiologic variables were measured in adult, male MF1 strain transgenic mice over-expressing hsp 70i (n=9) and their wild type littermates (n=9) weighing between 30-40 grams, subjected to 25 minutes of BCCAo.

2.4.2 Surgical procedure

Surgical anaesthesia was induced in a perspex chamber with halothane (3%) in a mixture of nitrous oxide and oxygen (70:30) for 2.5 minutes. Anaesthesia was maintained throughout the procedure with halothane (1.2-1.7%) delivered via a facemask. Via a small skin incision at the junction of hind leg and body, the left femoral blood vessels were exposed. The femoral artery and vein were freed of connecting tissues by blunt dissection. Three lengths of surgical silk (6-0) were placed around the femoral vessels. The first of these silks was tied at the distal end of the exposed vessels and some tension applied. The second silk was positioned at the proximal end of the exposed vessels and tension applied such that blood flow in the exposed section of the femoral artery was stopped. A small, diagonal incision was made in the femoral artery and a polythene cannula (outside diameter = 0.61mm; internal diameter = 0.29mm) containing heparinised saline (0.5%)

was introduced into the lumen of the vessel. The third silk was tied around the vessel to hold the cannula in place. Tension was removed from the second silk, the cannula flushed and patency observed. The cannula was further secured in place with a small amount of general-purpose cyanocrylate glue. Arterial blood pressure was recorded and stored by connecting the cannula to a pre-calibrated small bore pressure transducer attached to a personal computer running Acknowledge 3.24 software. Blood gas tensions and pH were measured from arterial blood samples (circa 50µl) using a blood gas analyser. Core body temperature was recorded using a rectal temperature probe and maintained around 37°C using a heating lamp throughout the procedure.

2.5 Transcardiac perfusion fixation

Surgical anaesthesic was induced in a perspex chamber with halothane (3%) in a mixture of nitrous oxide and oxygen (70:30) for 2.5 minutes. Anaesthetic was maintained throughout the procedure with halothane (1.5%) delivered via a facemask. The heart was exposed via a small incision at the base of the chest, cutting across the diaphragm and then through the ribcage bilaterally. A 20 gauge venous catheter connected to a 20ml pipette filled with heparinised saline (0.5%) was inserted into the left ventricle and clamped in place, the right atrium cut and heparinised saline perfused through the mouse at 3.33ml/min using an infusion pump. After blood had been flushed from the animal a 20ml syringe containing 4% paraformaldehyde (Appendix A) was connected to the catheter and the fixative perfused through the animal at 3.33ml/min using an infusion pump. Mice were decapitated and their heads immersed in paraformaldehyde (4%) for 24 hours at 4°C. The brains were then removed and stored in phosphate buffer for 24 hours at 4°C before being processed.

2.6 Tissue processing and staining

2.6.1 Tissue processing

Paraformaldehyde fixed brains were cut into three coronal blocks (3mm thick) using a rodent brain matrix. Individual blocks were placed into labelled embedding cassettes. The cassettes were placed into a wide necked glass jar and processed for wax embedding as follows:

1.	Running water	30 min
2.	70% ethanol	2 x 30 min
3.	90% ethanol	2 x 30 min
4.	100% ethanol	2 x 30 min
5.	100% ethanol/xylene (1:1)	30 min
6.	Xylene	2 x 30 min
7.	Paraffin wax	60°C, 1 hour
8.	Paraffin wax	60°C, overnight

Stainless steel moulds were cleaned with xylene, placed on a hotplate and the inside surface coated with a thin film of glycerine. The moulds were then filled with liquid wax and returned to the hotplate. Individual brain blocks were put into the wax moulds and removed from the hotplate. The surface of the wax was allowed to form a skin and the embedding cassette attached to it. Dispensing more liquid wax on top of the cassette and allowing the wax to solidify securely connected this. Once hardened the moulds were stored at 4°C for an hour or so and the wax blocks popped out of the moulds. The paraffin blocks produced were sectioned at 6μm on a microtome. Sections were stretched by surface tension on a water bath at 40°C and collected on poly-*L*-lysine coated slides. Slides were allowed to dry slowly at room temperature and stored in dust tight slide boxes until required.

2.6.2 Histochemical staining

Steps 1-17 (below) describe haematoxylin and eosin staining of paraffin embedded 4% paraformaldehyde fixed sections, while steps 4-17 (below) describe haematoxylin and eosin staining of fresh frozen sections. Haematoxylin and eosin stained sections were employed to identify ischaemic neuronal damage and structural damage and inflammatory responses following ischaemia and intracerebral injection of ad vectors, respectively.

1.	Histoclear	2 x 10 min (to dewax tissue)
2.	Absolute ethanol	2 x 10 min (to dehydrate Sections)
3.	Methylated spirit	30 seconds
4.	Running tap water	1 min
5.	Haematoxylin	1-2 min
6.	Running tap water	1 min
7.	Hydrochloric acid & methanol	5 seconds
8.	Running tap water	1 min
9.	Scots tap water substitute	2 min
10.	Running tap water	1 min
11.	Aqueous eosin	3 min
12.	Running tap water	1 min
13.	70% ethanol	2 x 5 min
14.	90% ethanol	2 x 5 min
15.	100% ethanol	2 x 5 min
16.	Histoclear	5 min
17.	Mount coverslips using DPX	leave to dry for 24 hours

2.6.3 Identification and quantification of ischaemic neurones

Ischaemic neuronal damage following BCCAo was determined in 4% paraformaldehyde fixed, wax embedded coronal sections (6μm thick). Haematoxylin and eosin staining was employed to identify ischaemic neurones. Morphologically abnormal neurones exhibiting features of ischaemic cell change, including shrunken cell bodies, triangulated nuclei and intensely eosinophilic cytoplasm (Adams & Graham, 1988) were estimated in several brain regions. Two methods of quantifying ischaemic neurones were used in this thesis. First, ischaemic neurones in a defined region were scored using the scoring system below. Second, ischaemic neurones and non-ischaemic neurones in a defined region were counted and the percentage ischaemic neurones determined. My ability to identify ischaemic

neuronal change was validated by direct comparison with values recorded by an experienced investigator (see Appendix B). Furthermore, my ability to quantify ischaemic neuronal damage reproducibly was validated by double-blinded analysis of the same material (see Appendix C).

Score	% ischaemic neurones
0	0%
1	1-30%
2	31-65%
3	66-100%

2.6.4 Structural and inflammatory responses following intracerebral injection

Haematoxylin and eosin staining was employed to delineate the presence of structural deformation and inflammatory response following intrastriatal injection of recombinant ad vectors and saline (see Section 2.8). Structural deformation resulting from needle insertion through the cortex, subcortical white matter and into the caudate nucleus was clearly delineated by haematoxylin and eosin. Local infiltration of inflammatory cells to the site of intrastriatal injection was also clearly delineated by haematoxylin and eosin staining (see Figure 49).

2.6.5 Immunohistochemical localisation of hsp 70i

Established immunohistochemical detection techniques were employed to identify hsp 70i in brain sections prepared from mice. All brains were perfusion fixed with paraformaldehyde 4% and paraffin wax embedded. Brains were coronally sectioned at 6 microns using a microtome with sections collected onto poly-*L*-lysine coated glass slides. Immunohistochemical staining for hsp 70i was carried out using the standard avidin-biotin method (Figure 12).

Figure 12 Schema of avidin-biotin complex immunodetection method

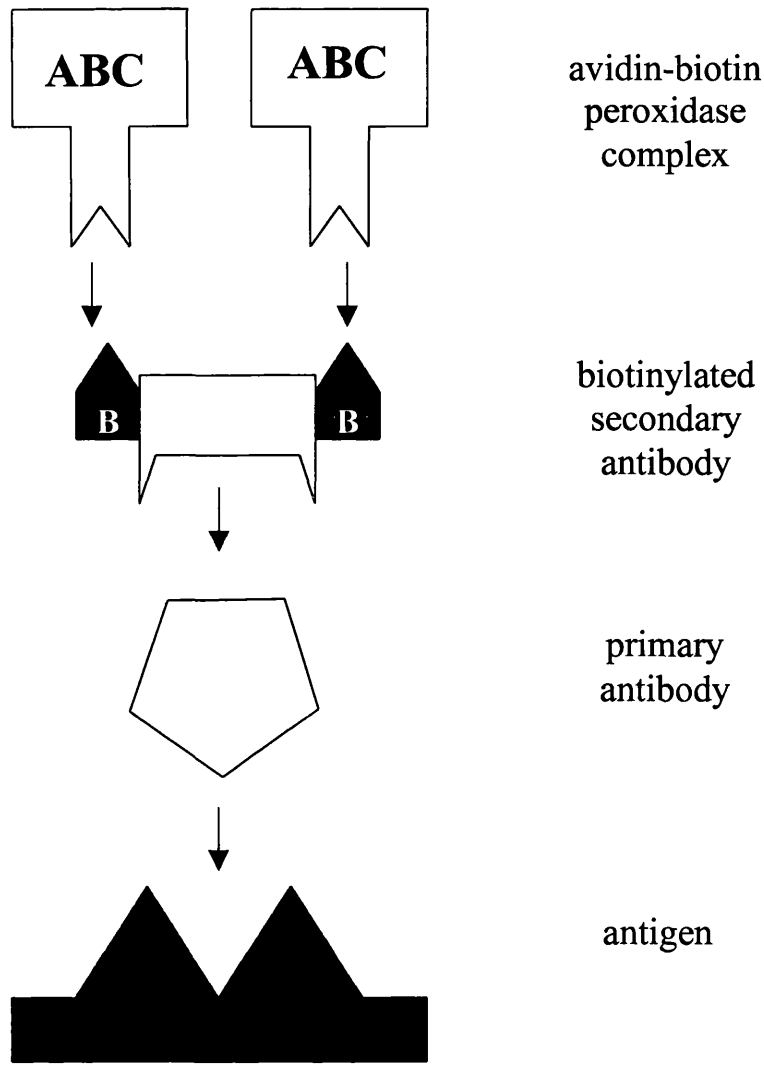

Adapted from Jackson and Blythe, 1993.

Day 1: Paraformaldehyde fixed, wax embedded sections were pre-treated with xylene to remove all wax from the tissue (2 x 15 minutes). Sections were then dehydrated in fresh absolute ethanol for 20 minutes (2 x 10 minutes). For optimal staining of hsp 70i antibody (Calbiochem Incorporated) antigenic site retrieval was employed at this stage. Retrieval of antigenic sites was achieved by immersing sections in citric acid buffer (0.01 mM, pH 6.0) and microwaving (650 watts) for five minutes on full power. The sections were left for one minute; additional citric acid buffer was added and the sections were then microwaved for a further five minutes. Thereafter, sections were left to cool for 30 minutes in citric acid buffer. Endogenous peroxidase activity was then quenched by immersing sections in hydrogen peroxide (3%) in methanol for 30 minutes. Slides were then rinsed in running tap water for 10 minutes before being rinsed in phosphate buffered saline (50mM) for a further 10 minutes. Using a hydrophobic pen, each section was circled in order to create a barrier to trap and minimise the volume of reagents required to incubate each section. Sections were then incubated with 200µl of blocker, which consisted of normal horse serum (10%) and bovine serum albumin (5%) in phosphate buffered saline for one hour at normal room temperature. This suppressed non-specific binding of the immunoglobulin. The blocker was removed and the sections incubated with 200µl of the optimal concentration of hsp 70i primary antibody made up in normal horse serum (1.5%) and bovine serum albumin (1%) in phosphate buffered saline (see Appendix D, for details of antibody optimisation procedure). Sections were incubated overnight at 4°C.

Day 2: Primary antibody solution was removed and sections were rinsed with phosphate buffered saline (2 x 10 minutes). Sections were then incubated with 200µl of secondary antibody (mouse anti-IgG) diluted 1:100 in phosphate buffered saline and incubated for one hour at room temperature. Sections were again rinsed with phosphate buffered saline (2 x 10 minutes) and then incubated with 200µl of avidin-biotin horseradish peroxidase complex for one hour. The avidin-biotin horseradish complex was prepared 40 minutes

before use from an Elite kit from Vector Laboratories (1 drop solution A and 1 drop solution B in 4.9ml phosphate buffered saline). Sections were then rinsed once more with phosphate buffered saline (2 x 10 minutes) and the peroxidase reaction developed using the diaminobenzidine chromogen. A standard diaminobenzidine chromogen kit (Vector Laboratories) was used where two drops of buffer, four drops of diaminobenzidine and two drops of hydrogen peroxide were added and mixed with five millimetres of distilled water in that order. Sections were incubated for four minutes with diaminobenzidine; the reaction being stopped by adding distilled water. Following incubation with this diaminobenzidine mixture cells labelled with primary antibody appeared brown. All hsp 70i stained sections were then lightly counterstained with haematoxylin and mounted as follows:

1.	Running tap water	10 minutes
2.	Haematoxylin	45 seconds
3.	Running tap water	1 minute
4.	Hydrochloric acid & methanol	5 seconds
5.	Running tap water	1 minute
6.	Scots tap water substitute	2 minute
7.	Running tap water	1 minute
8.	70% ethanol	2 x 5 minutes
9.	90% ethanol	2 x 5 minutes
10.	Absolute ethanol	2 x 5 minutes
11.	Histoclear	10 minutes
12.	Mount coverslips using DPX	leave to dry for 24 hours

2.7 *In* vivo ^{14}C-2-deoxyglucose autoradiography in mouse

2.7.1 Experimental groups

LCGU was estimated in conscious, freely moving mice by means of a modification of the ^{14}C-2-deoxyglucose technique originally described by Sokoloff *et al.*, (1977). Two studies within this thesis employed this technique. First, relative rates of LCGU were estimated in 36 brain regions of transgenic mice over-expressing hsp 70i and their wild type littermates. Twenty-eight adult, male MF1 strain mice (14 transgenic and 14 wild type littermates) weighing between 30-40 grams were used. The mice were divided into four groups (two hsp 70i transgenic and two wild type littermate, n=7 per group). Ten minutes prior to the

start of the ^{14}C-2-deoxyglucose procedure. One group of transgenic and one group of wild type mice were intraperitoneally injected with saline. The two remaining groups were intraperitoneally injected with dizocilpine (1mg/kg) dissolved in saline (0.4ml). Second relative rates of LCGU were estimated in nine brain regions of mice following intrastriatal injection with 1μl (0.1μl/minute) of recombinant ad egfp (1.57 x 10^{10} particle forming units/ml) or sterile saline. The impact of ad egfp transfection upon LCGU and the effect of delay in needle withdrawal after injection (i.e., 2 mins versus 10 mins) were investigated at seven and 28 days post injection. Thirty-two adult, male C57bl/6 strain mice weighing between 25-35 grams were used. The mice were divided into six groups: two groups (n=6) were injected with saline (2 minute delay in needle withdrawal); two groups (n=6) were injected with ad (2 minute delay in needle withdrawal); and two groups (n=5) were injected with ad (10 minute delay). In one of each treatment group LCGU was estimated at seven days and the other at 28 days post injection.

2.7.2 Statistical power calculations

Data from a pilot study using ^{14}C-2-deoxyglucose autoradiography was used to predict the differences in LCGU, which could be detected in the two ^{14}C-2-deoxyglucose autoradiography studies in this section. Statistical power calculations predicted that a difference of less than 10% would be detected. Post hoc power calculations confirmed this prediction:

1. Dizocilpine injected hsp 70i transgenic mice. LCGU in dorsal hippocampus CA1 stratum lacunosum moleculare was 2.7 ± 0.2 (mean ± SD) group size was 7. For 80% power, predicted detectable difference was 7%.

2. Ad egfp gene transfer of C57bl/6 strain mice. LCGU in caudate nucleus was 1.45 ± 0.1 (mean ± SD) group size was 6. For 80% power, predicted detectable difference was 8%.

2.7.3 Modified ^{14}C-2-deoxyglucose experimental procedure

Conscious mice were intraperitoneally injected with 5μCi of ^{14}C-2-deoxyglucose in 0.4ml saline over a ten second period. Mice were returned to their cages for 42.5 minutes and general behaviour observed. At the end of this period each animal was anaesthetised in a perspex chamber containing halothane (2.5%) in a mixture of nitrous oxide and oxygen (70:30) for a period of exactly 2.5 minutes. At 45 minutes after isotope injection the mice were decapitated and a terminal blood sample collected by torso inversion. Plasma was prepared by centrifugation and the concentrations of plasma glucose and ^{14}C determined by automated enzymatic assay and liquid scintillation counting, respectively. Brains were removed rapidly and frozen in chilled isopentane (-42°C) for 10 minutes. The brains were then coated in Lipshaw brain matrix, dipped into the chilled isopentane (to harden the Lipshaw matrix) and mounted onto cryostat chucks. Mounted brains were stored at –20°C for less than 24 hours. Serial coronal sections (20μm thick) were then prepared in a cryostat at –20°C sampled every 60μm through the cerebrum. Brain sections were collected onto coverslips (20mm x 40mm) and dried rapidly on a hotplate at 60°C. The coverslips were then mounted onto standard deoxyglucose cards sequentially. Autoradiograms of these sections were produced by exposing them with medical X-ray film in light tight X-ray cassettes for three days with pre-calibrated methacrylate standards. After three days the films were developed: developer five minutes; stop bath 45 seconds; fixer 10 minutes; followed by 30 minutes in cold, running tapwater; and placed in a fan-heated cupboard until dry.

2.7.4 Densitometric analysis of ^{14}C-2-deoxyglucose autoradiograms

Densitometric analysis was carried out using a computer based densitometer; micro computer imaging device. Briefly, densitometric measurements (in this case taken from the X-ray film autoradiogram) represent digital signal. This digital signal is initially expressed as grey levels which range from 0 (black) to 255 (white). Grey levels are then

Figure 13 Densitometric analysis of discrete brain regions

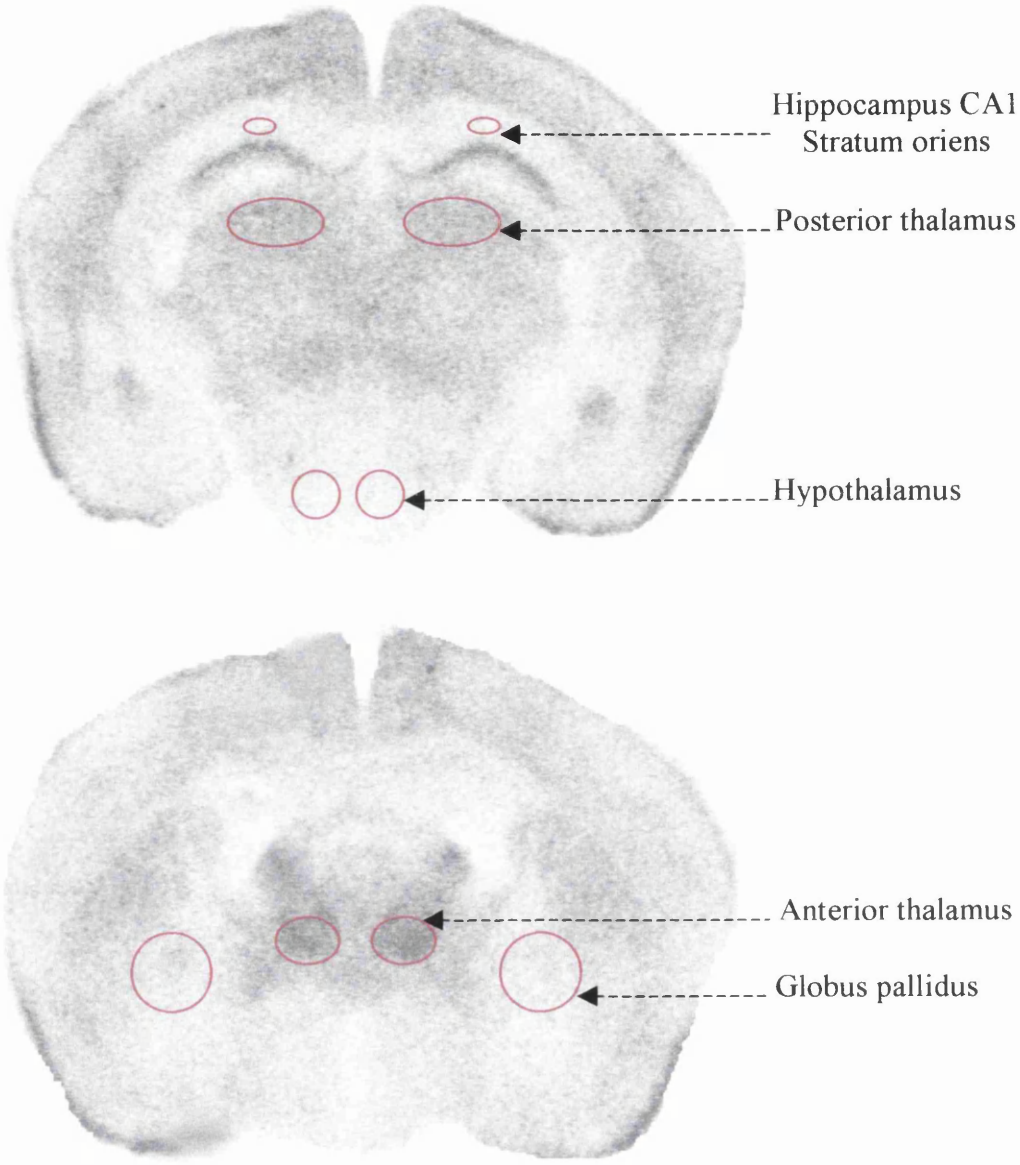

Densitometric analysis of discrete brain regions such as hippocampus CA1 stratum oriens, posterior thalamus, hypothalamus (top), anterior thalamus and globus pallidus (bottom). ^{14}C-2-deoxyglucose autoradiograms shown taken from dizocilpine (1mg/kg) treated mice.

converted into values of optical density ranging from 0 (white) to 2.4 (black), by the densitometer. After calibrating the densitometer to the pre-calibrated methacrylate standards of known radioactivity (ranging from 44-2500 nCi/g), ^{14}C concentrations in selected brain areas could be determined. Cerebral ^{14}C concentrations were measured in discrete brain regions by placing autoradiograms on a light box under a closed circuit camera (at the same magnification and light intensity used for calibration) and positioning a frame over each brain region of interest (see Figure 13). The size of the frame used to capture ^{14}C concentration varied with the size of the region or the point of interest. The mean ^{14}C was calculated from readings made in 3-6 (predominantly 6) sections per mouse bilaterally (maximum = 12). All anatomic brain structures were defined with reference to a stereotactic mouse brain atlas (Franklin & Paxinos, 1997).

2.7.5 Estimation of LCGU

In the original and definitive ^{14}C-2-deoxyglucose technique Sokoloff *et al.*, (1977) described the collection of 14 timed arterial blood samples over the 45-minute experimental period. These blood samples were assayed to determine plasma ^{14}C and glucose concentrations throughout the experimental period. The plasma integral required for the operational equation (Section 1.6.2, Figure 6) could then be employed to determine LCGU in μmol/100g/minute. In this thesis, only a terminal blood sample was collected from each mouse. LCGU was estimate as the ratio of ^{14}C concentration in regions of interest versus ^{14}C concentration in cerebellar cortical grey matter:

$$\frac{\text{Tissue } ^{14}C \text{ in region of interest}}{\text{Tissue } ^{14}C \text{ in cerebellar cortical grey matter}}$$

2.8 Stereotaxic intrastriatal injection of ad

2.8.1 Experimental groups

Intrastriatal injection into the right caudate nucleus of mice was carried out in two studies within this thesis. First, adult male C57bl/6 strain mice weighing between 25-35 grams were intrastriatally injected with recombinant ad hsp 70i (n=17) or ad egfp (n=16). Second, adult male C57bl/6 strain mice weighing between 25-35 grams were intrastriatally injected with recombinant ad egfp (n=22) or sterile saline (n=12).

2.8.2 Establishing injection coordinates

Stereotaxic coordinates for injection into the centre of the right caudate nucleus were derived from the mouse stereotaxic brain atlas (Franklin & Paxinos, 1997). Exact coordinates were established and determined by placement studies using indelible ink. The coordinates used in all mice were calculated with reference to bregma. The coordinates used in all mice were: 0.26mm posterior to bregma, 2.0mm lateral (right) of bregma; and 3.0mm ventral to the dorsal surface of the brain.

2.8.3 Surgical procedure

Surgical anaesthesia was induced in a perspex chamber with halothane (3%) in a mixture of nitrous oxide and oxygen (70:30) for 2.5 minutes. Animals were removed from the chamber and connected to a stereotaxic frame using a specially designed facemask. Halothane anaesthesia was delivered via the facemask using a small animal ventilator. Animals were mechanically ventilated at 110 breaths per minute, tidal volume was 0.15ml with 50:50 inspiration / expiration ratio. Via a rostro-caudal midline scalp incision the skull was exposed and the bregma landmark visualised. A small burrhole was drilled at stereotactic coordinates previously determined to enable injection into the centre of the right caudate nucleus (see above). All injectants were delivered via a 30 gauge dental needle connected to a 10μl Hamilton syringe by a 2cm piece of cannula. Injection rate was

controlled and maintained at 0.1μl per minute using a pre-calibrated microinfusion pump. Body temperature was maintained between 36.5 and 37.5°C throughout the procedure using a thermostatically controlled heating blanket and a rectal temperature probe. Post operatively the animals were housed in a temperature-controlled facility until required.

2.9 Transgenic mice over-expressing hsp 70i

Transgenic mice over-expressing hsp 70i used in this thesis were produced and supplied by Dr James Uney from the University of Bristol. MF1 strain mice were used to generate hsp 70i transgenic mice for three reasons: first, the large numbers of eggs they produce, second, the large litter sizes they produce, and third, MF1 strain mice are good mothers. The technique used to produce the hsp 70i transgenic mice used in this thesis was based on the generation of rhombotin-1 transgenic mice (Greenburg *et al.*, 1990). Briefly, hsp 70i was fused with the rhombotin-1 (also known as promoter-1 of the Lmo-1 gene, Hinks *et al.*, 1997) and microinjected into fertilised (MF1 X MF1) mouse eggs (see Figure 8). Transgenic animals were selected and bred to homozygosity in an MF1 background (Figure 14). Transgenic mice over-expressing the firefly luciferase reporter gene under the control of the rhombotin-1 promoter were produced at the same time. Immunohistochemical detection of the luciferase reporter gene confirmed the region specific nature of transgene expression (Figure 15).

2.10 Recombinant ad hsp 70i and ad egfp vectors

All ad vectors used in this thesis were produced and supplied by Dr James Uney from the University of Bristol. Recombinant (replication defective) ads containing hsp 70i and egfp driven by a cytomegalovirus (CMV) promoter were used. Production of recombinant ad hsp 70i and ad egfp can be found in Beaucamp *et al.*, (1998). A simplified schematic representation is provided in Figure 16. Transfection of E1-deleted ad egfp was visualised

Figure 14 Confirmation of transgenic hsp 70i expression

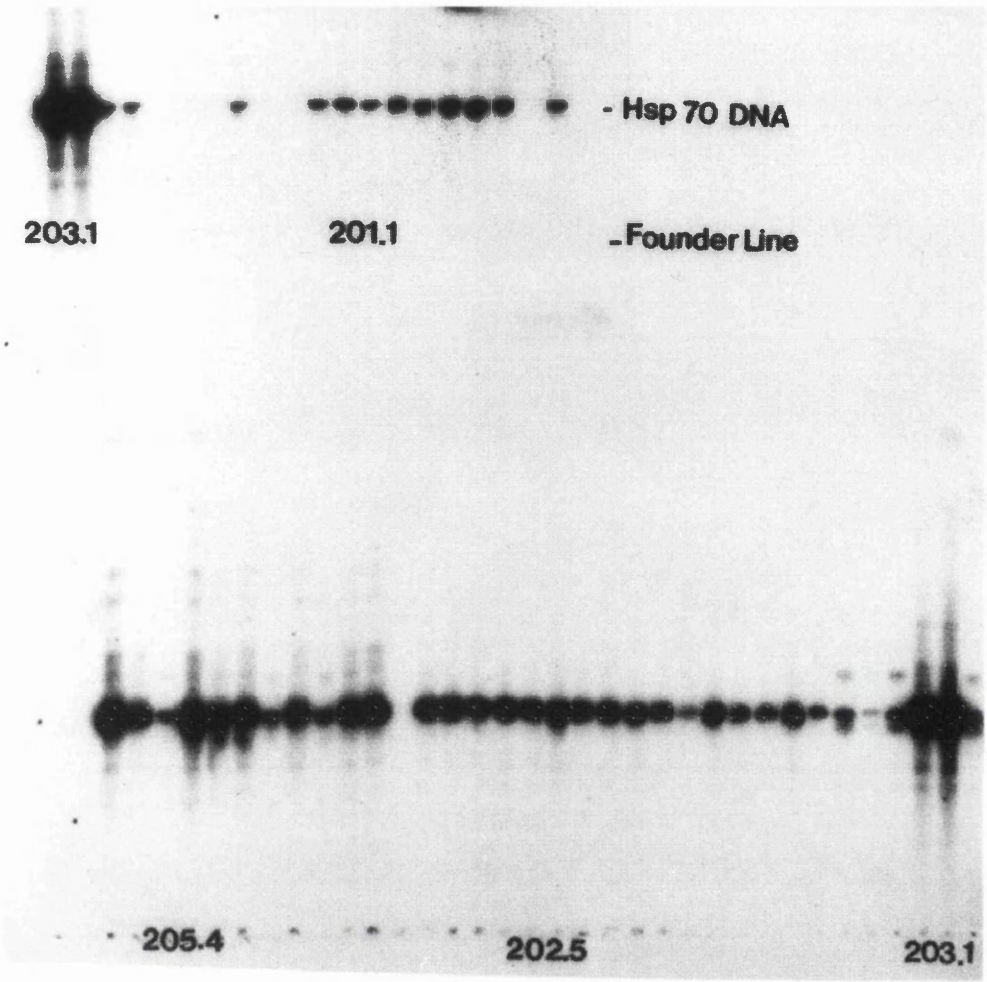

Southern blot analysis confirmed hsp 70i expression in transgenic mice.

(Courtesy of Dr James Uney)

Figure 15 Distribution of hsp 70i transgene expression

Immunohistochemical detection of the firefly luciferase reporter gene under control of the rhombotin-1 promoter delineated the region specific nature of hsp 70i transgene expression. Brown regions represent luciferase immunoreactive cells.

(Courtesy of Dr James Uney).

Figure 16 Production of recombinant ad hsp 70i and ad egfp vectors

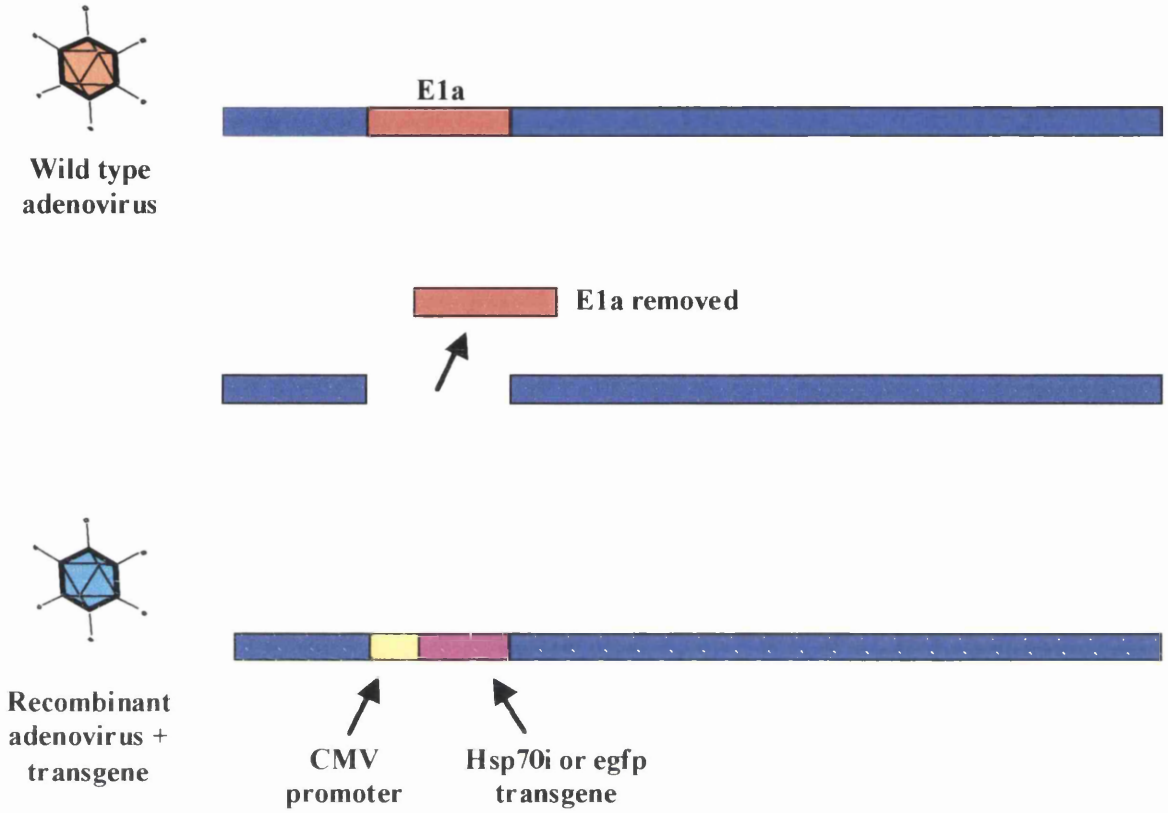

Schematic representation of recombinant ad hsp 70i and ad egfp production. Briefly, wild type ad particles were rendered replication defective by removal of the E1a region of their genome. The resultant void was filled with either hsp 70i or egfp transgene, which was driven by the cytomegalovirus (CMV) promoter.

using fluorescence light microscopy. Egfp transfection was analysed at 1 (not shown), 7, 17 and 28 days post ad injection.

2.11 Statistical analyses

All data in this thesis was collected and expressed using a scoring system or as continuous numeric data. Data expressed as a score was analysed using non-parametric statistical analyses. Mann-Whitney test was used where two unpaired groups were compared. Wilcoxon signed rank test was used where paired groups were compared. Spearman rank correlation was used where correlation between groups was investigated. Continuous numeric data was separated into normally (parametric) and non-normally (non-parametric) distributed groups using GraphPad Incorporated statistical software and analysed appropriately. Non-normally distributed continuous numeric data was analysed using non-parametric tests as described above. Normally distributed continuous numeric data was analysed using parametric statistical analysis. Student's *t*-test (paired or unpaired, according to source) was employed where two groups were compared. Analysis of variance, was used to compare three or more groups followed by Student's *t*-test with Bonferroni correction. Pearsons correlation was used where correlation between groups was investigated. All data throughout this thesis are expressed as mean ± the standard error of the mean, with *n* defined. Data that took the form of contingency table (i.e., PcomA data) was analysed using Fishers exact test.

CHAPTER THREE: RESULTS

3.1 BCCAo in MF1 and C57bl/6 strain mice

BCCAo was established as a model of global cerebral ischaemia in MF1 and C57bl/6 strain mice. Neuropathologic and physiologic consequences of BCCAo in MF1 strain mice were compared with those of C57bl/6 strain mice (as the effects of BCCAo in C57bl/6 strain mice had already been reported, Fujii *et al.*, 1997; Yang *et al.*, 1997).

3.1.1 Ischaemic neuronal damage in MF1 and C57bl/6 mice following BCCAo

10-20 minute BCCAo

Ischaemic neuronal damage in MF1 and C57bl/6 strain mice following 10, 15 and 20-minute BCCAo was scored using a semi-quantitative scoring system (see Section 2.6.3 for details). Following 10-minute BCCAo none of the seven brain regions analysed displayed any significant differences in ischaemic neuronal damage between MF1 and C57bl/6 strain mice (Table 3, Figure 17). Following 15-minute BCCAo MF1 strain mice displayed significantly less ischaemic neuronal damage than C57bl/6 strain mice in hippocampus CA2 (Table 3, Figure 17). Following 20-minute BCCAo MF1 strain mice displayed significantly less ischaemic neuronal damage than C57bl/6 strain mice in hippocampus CA1 and CA2 (Table 3, Figures 17, 18 and 19).

25-45 minute BCCAo

MF1 strain mice were subjected to extended durations (25, 30, 35, 40 and 45-minutes) of BCCAo. Extended BCCAo in MF1 strain mice was investigated to see if ischaemic neuronal damage in this strain could be increased to match the anatomically widespread and extensive damage observed in C57bl/6 strain mice (after 20-minute BCCAo). Furthermore, ischaemic neuronal damage was quantified as a percentage, as the semi-quantitative scoring system applied in the previous study was considered insensitive for low levels of ischaemic neuronal damage.

Ischaemic neuronal damage in 25-minute BCCAo mice did not differ significantly from that in sham-operated mice in any of the five brain regions analysed (Table 4, Figure 20). Ischaemic neuronal damage in 30 and 35-minute BCCAo mice was significantly increased in caudate nucleus compared to sham-operated mice (Table 4, Figure 20). Ischaemic neuronal damage in 40-minute BCCAo mice was significantly increased in hippocampus CA1, CA2 and caudate nucleus compared with sham-operated mice (Table 4, Figure 20). Ischaemic neuronal damage in 45-minute BCCAo mice was significantly increased in hippocampus CA1 and caudate nucleus compared with sham-operated mice (Table 4, Figure 20).

These data clearly indicated two important features of BCCAo in MF1 mice. First, BCCAo could induce ischaemic neuronal damage in this strain. Second, despite increasing BCCAo duration in this strain (to more than double that observed in C57bl/6 strain mice) ischaemic neuronal damage was not as extensive or anatomically widespread.

Table 3 **Ischaemic neuronal damage in MF1 and C57bl/6 strain mice: semi-quantitative assessment**

	Duration of BCCAo						
	10 mins		15 mins		20 mins		
	MF1 (n = 6)	C57bl/6 (n = 6)	MF1 (n = 6)	C57bl/6 (n = 6)	MF1 (n = 6)	C57bl/6 (n = 6)	
Hippocampus CA1	1 ± 0	1.2 ± 0.2	1 ± 0	1.2 ± 0.2	1.4 ± 0.2	2.1 ± 0.2	*
Hippocampus CA2	1 ± 0	1.9 ± 0.3	0.7 ± 0.2	2 ± 0.3 *	1.4 ± 0.2	2.5 ± 0.2	**
Hippocampus CA3	1 ± 0	1 ± 0	0.9 ± 0.1	1 ± 0	1.1 ± 0.1	1.7 ± 0.2	
Dentate gyrus	0.9 ± 0.1	1 ± 0	1 ± 0	0.9 ± 0.1	1 ± 0.2	1.4 ± 0.6	
Posterior thalamus	1.1 ± 0.2	1.5 ± 0.2	1.2 ± 0.1	1.6 ± .3	1.3 ± 0.1	1.8 ± 0.3	
Somatosensory cortex	1.2 ± 0.1	1.2 ± 0.1	1 ± 0	1.4 ± 0.2	1.3 ± 0.1	1.8 ± 0.3	
Caudate nucleus	1.1 ± 0.1	1.2 ± 0.2	1.1 ± 0.1	1.7 ± 0.4	1.5 ± 0.2	2.3 ± 0.3	

Data are expressed as mean ± standard error of the mean.

* $p < 0.05$; ** $p < 0.01$ Mann-Whitney test.

Figure 17 **Ischaemic neuronal damage in MF1 and C57bl/6 strain mice: semi-quantitative assessment**

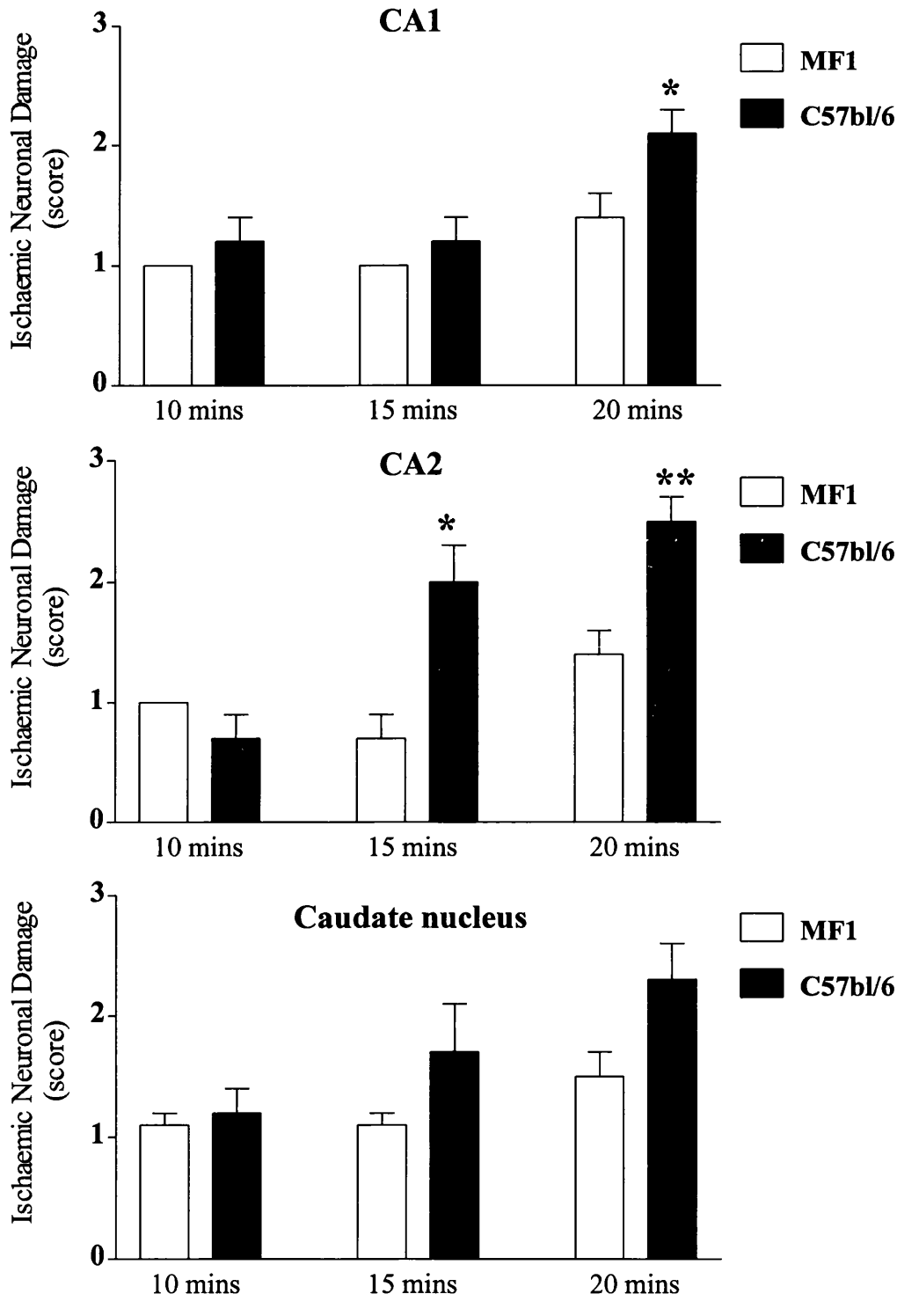

MF1 strain mice displayed significantly less ischaemic neuronal damage than C57bl/6 strain mice in hippocampus CA2 (following 15 and 20-minute BCCAo) and in hippocampus CA1 (following 20-minute BCCAo). Data are presented as mean ± standard error of the mean. *$p<0.05$; **$p<0.01$ Mann-Whitney test. ($n = 6$ per group).

Figure 18 Ischaemic neuronal damage in hippocampus CA1 of MF1 strain mice

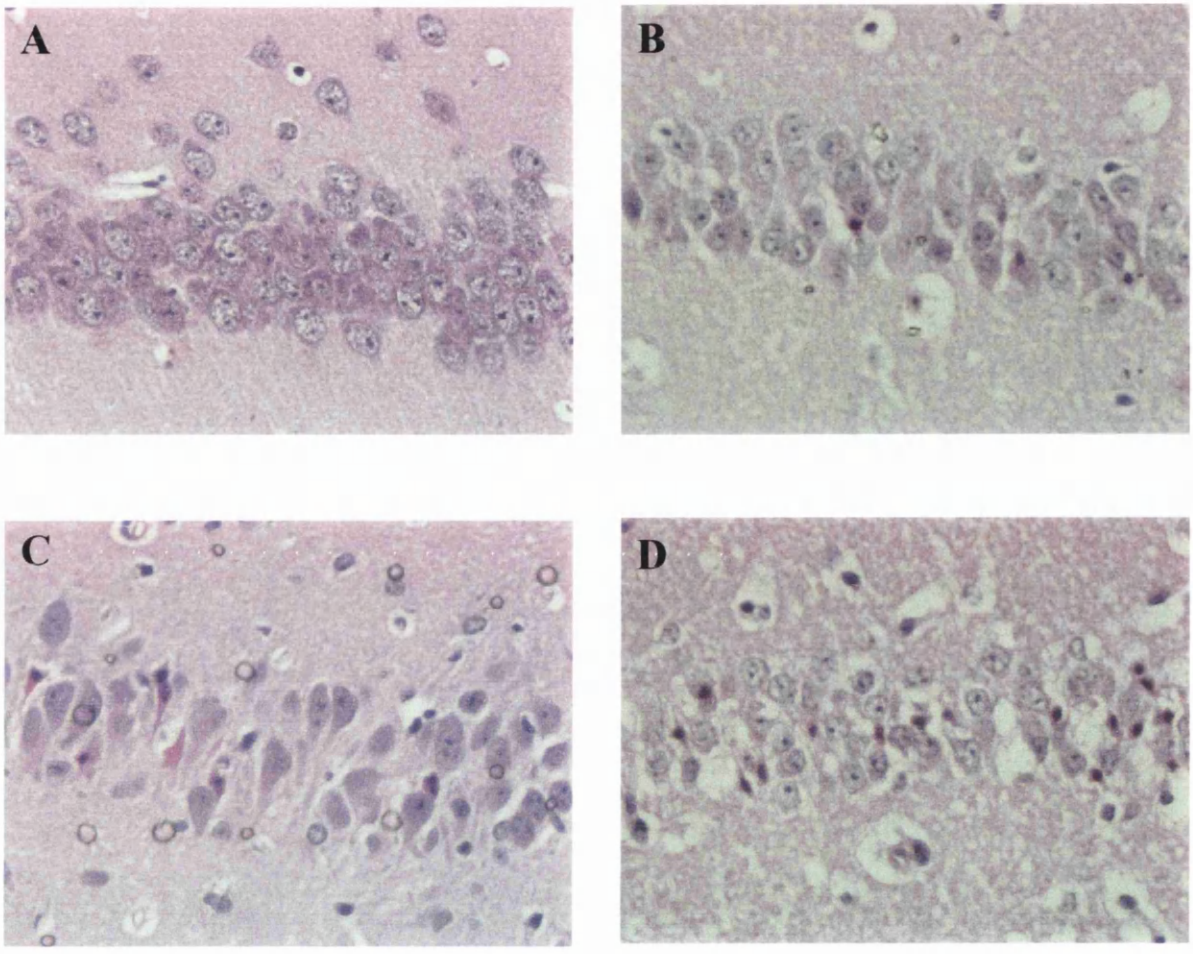

Ischaemic neuronal damage in hippocampus CA1 of MF1 strain mice, in sham-operated (A) and following 10-minute (B), 15-minute (C) and 20-minute (D) BCCAo. In sham-operated mice there were no neurones showing features of ischaemic cell change. Ten and 15-minute BCCAo induced ischaemic cell change in a few neurones, while 20-minute BCCAo induced ischaemic cell change in a dozen or so neurones.

(Original magnification X200).

Figure 19 Ischaemic neuronal damage in hippocampus CA1 of C57bl/6 strain mice

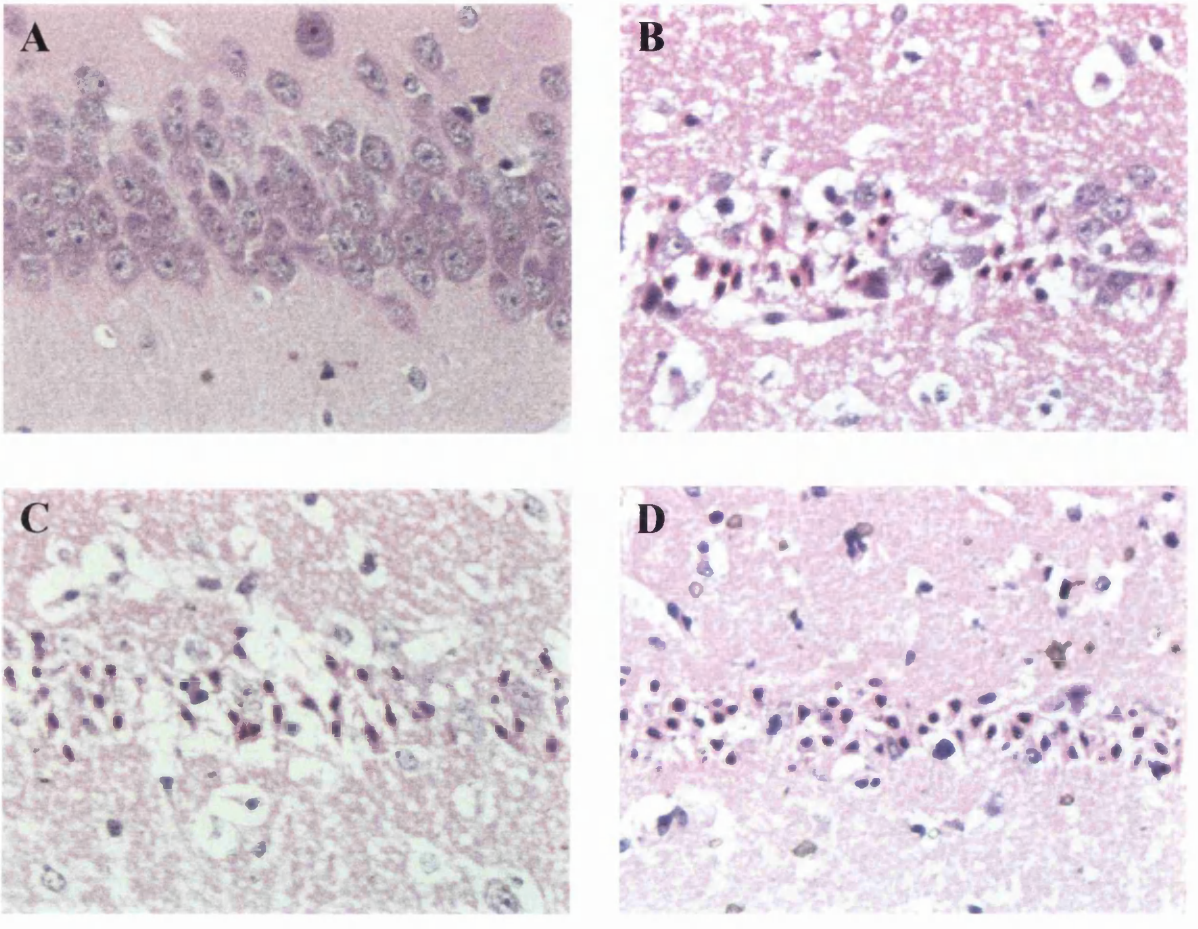

Ischaemic neuronal damage in hippocampus CA1 of C57bl/6 strain mice in sham-operated mice (A) and following 10-minute (B), 15-minute (C) and 20-minute (D) BCCAo. In sham operated mice no neurones exhibited features of ischaemic cell change, while 10, 15 and 20-minute BCCAo induced widespread ischaemic neuronal damage in pyramidal neurones. (Original magnification X200).

Table 4 **Ischaemic neuronal damage in MF1 strain mice with extended BCCAo: quantitative assessment**

SHAM-OPERATED

	Duration of sham-BCCAo				
	25 mins (n = 5)	**30 mins** (n = 5)	**35 mins** (n = 5)	**40 mins** (n = 5)	**45 mins** (n = 6)
Hippocampus CA1	1.5 ± 0.2	1.1 ± 0.1	0.8 ± 0.1	1.3 ± 0.4	1.2 ± 0.2
Hippocampus CA2	0.5 ± 0.3	0.5 ± 0.2	0.5 ± 0.5	0.3 ± 0.3	0.9 ± 0.4
Hippocampus CA3	0.1 ± 0.1	0.6 ± 0.3	0.1 ± 0.1	0.9 ± 0.3	0.5 ± 0.2
Dentate gyrus	0 ± 0	0 ± 0	0 ± 0	0.1 ± 0.1	0.4 ± 0.4
Caudate nucleus	4.6 ± 0.6	4.0 ± 0.4	3.0 ± 0.6	2.8 ± 0.5	4.0 ± 0.4

BCCAo

	Duration of BCCAo				
	25 mins (n = 6)	**30 mins** (n = 6)	**35 mins** (n = 6)	**40 mins** (n = 6)	**45 mins** (n = 6)
Hippocampus CA1	22.0 ± 10.7	4.5 ± 2.9	14.7 ± 6.4	27.3 ± 7.9 *	27.8 ± 8.4 *
Hippocampus CA2	9.5 ± 4.4	0.9 ± 0.3	3.7 ± 3.0	21.6 ± 7.2 *	14.3 ± 6.5
Hippocampus CA3	2.0 ± 1.5	0.4 ± 0.2	6.2 ± 4.7	10.9 ± 4.4	5.9 ± 2.4
Dentate gyrus	0.8 ± 0.4	0.8 ± 0.4	0 ± 0	3.3 ± 2.4	3.5 ± 3.0
Caudate nucleus	17.2 ± 6.2	9.8 ± 2.0 *	13.6 ± 3.9 *	17.6 ± 3.3 **	14.0 ± 1.9 **

Morphologically abnormal neurones exhibiting features of ischaemic cell change and morphologically normal neurones in a defined region were counted and the percentage ischaemic neurones determined. Ischaemic neurones in mice subjected to BCCAo of a given duration were compared with sham-operated mice of the same duration. Data are expressed as mean ± standard error of the mean. *$p<0.05$; **$p<0.01$ unpaired Student's *t*-test.

Figure 20 **Ischaemic neuronal damage in MF1 mice with extended BCCAo: quantitative assessment**

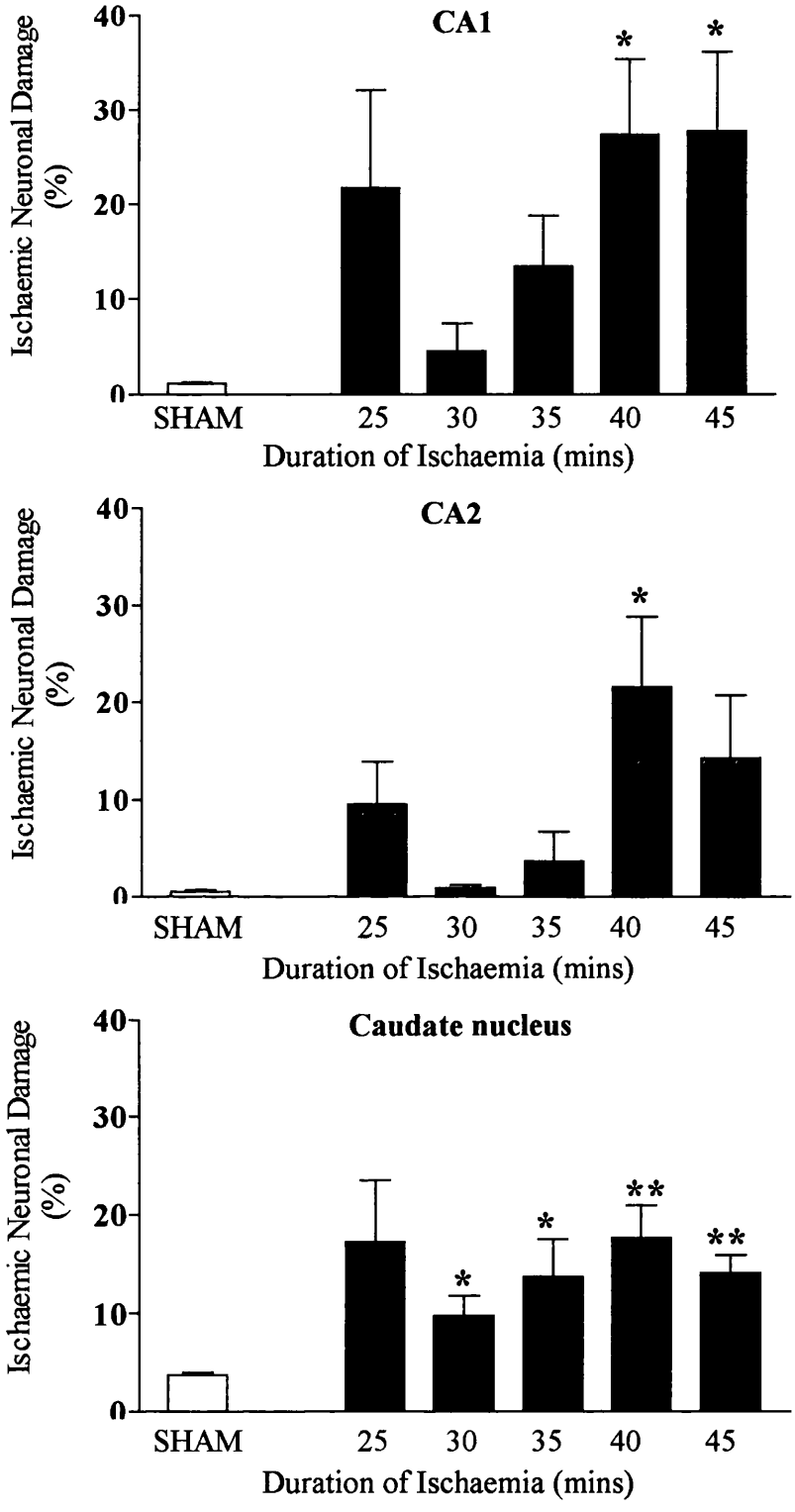

Ischaemic neuronal damage (percent) in mice subjected to BCCAo was significantly different from sham-operated mice in hippocampus CA1, hippocampus CA2 and caudate nucleus. Ischaemic neuronal damage in mice subjected to BCCAo of a given duration was compared with sham-operated mice of the same duration. Sham groups are consolidated in this figure. Data are presented as mean ± standard error of the mean. *$p<0.05$; **$p<0.01$ unpaired Student's *t*-test. (n=26 sham, n=6 20, 25, 30, 40, 45 mins; n=8 35 mins).

3.1.2 Circle of Willis anatomy in MF1 and C57bl/6 strain mice

Vascular anomalies of the circle of Willis have been directly linked with the degree of ischaemic neuronal damage following BCCAo (see Section 1.3.6). The most frequent anomaly reported in mice is posterior communicating artery (PcomA) hypoplasticity. In MF1 strain mice studied here (n=16) only one mouse was deficient of both PcomAs (Figure 21). In C57bl/6 strain mice studied (n=8) five mice were deficient of both PcomAs (Figure 22). Furthermore, 56% of MF1 strain mice investigated had both PcomAs, while no C57bl/6 strain mice had both PcomAs (Table 5). Forty-four percent of MF1 strain mice displayed an incomplete circle of Willis, while 100% of C57bl/6strain mice displayed an incomplete circle of Willis (Table 5). These data show that MF1 strain mice are significantly less likely to be deficient of both communicating arteries than C57bl/6 strain mice.

Figure 21 Circle of Willis anatomy in MF1 strain mice

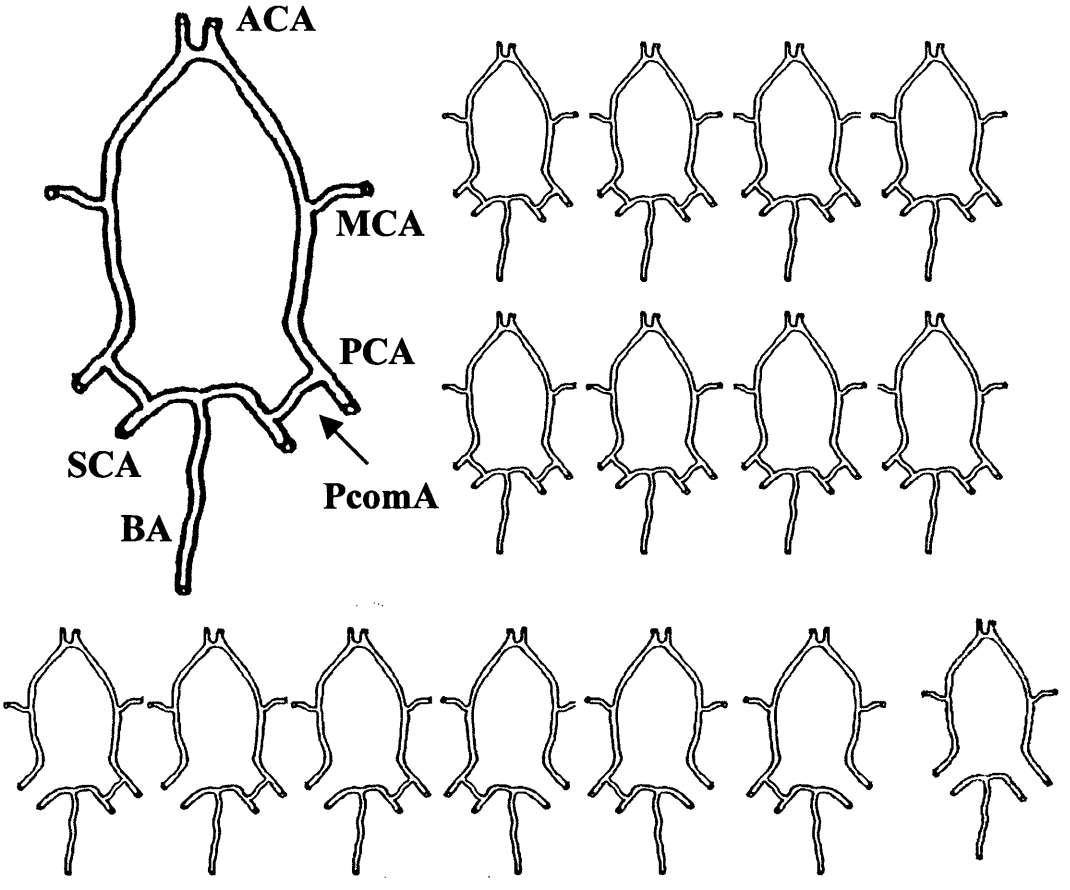

The presence of ACA (anterior cerebral arteries), MCA (middle cerebral arteries), PCA (posterior cerebral arteries), PcomA (posterior communicating arteries), BA (basilar artery) and SCA (superior cerebellar arteries) in individual MF1 mice (n=16) is summarised in this diagram. The top two rows and the large annotated section represent nine mice, which displayed a complete circle of Willis with two PcomAs. The second panel consists of six mice, which displayed only one PcomA, and one mouse displayed no PcomA.

Figure 22 Circle of Willis anatomy in C57bl/6 strain mice

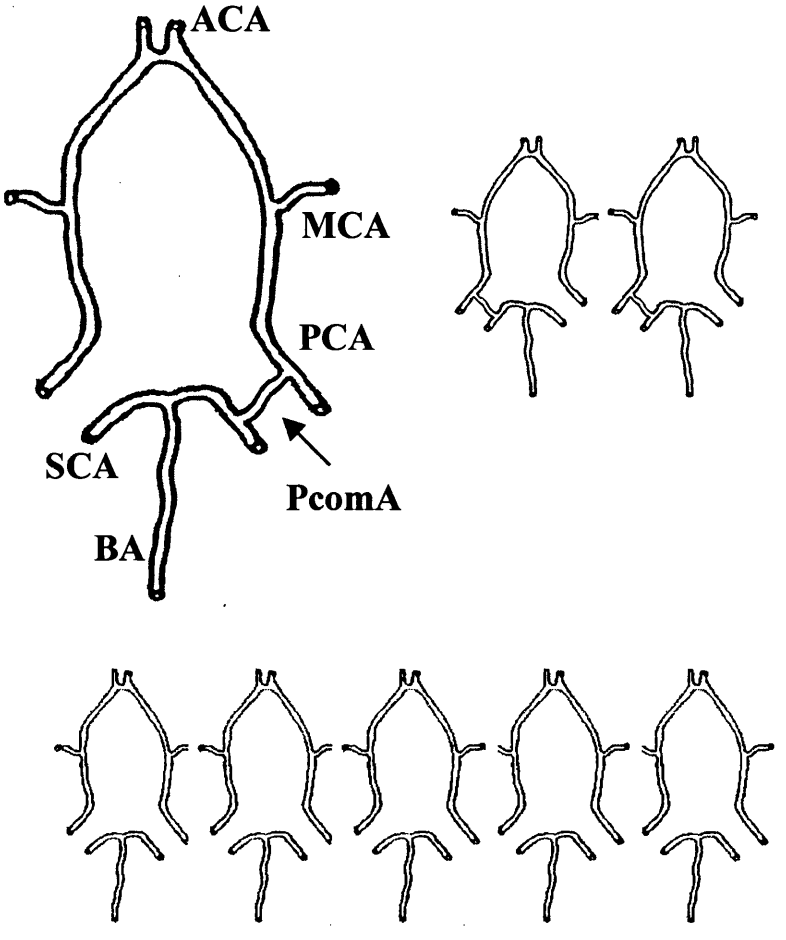

The presence of ACA (anterior cerebral arteries), MCA (middle cerebral arteries), PCA (posterior cerebral arteries), PcomA (posterior communicating arteries), BA (basilar artery) and SCA (superior cerebellar arteries) in individual C57bl/6 mice (n=8) is summarised in this diagram. None of the eight mice investigated had a complete circle of Willis. Three mice had only one PcomA (top panel), while the remaining five mice had no PcomAs.

Table 5 PcomAs in MF1 and C57bl/6 strain mice

Number of posterior communicating arteries	MF1 (n = 16)	C57bl/6 (n = 8)
Two (complete)	9	0
One or none (incomplete)	7	8
Incomplete circle of Willis (%)	44**	100

**p<0.01 Fishers exact test.

3.1.3 Physiologic variables in MF1 and C57bl/6 mice subjected to BCCAo

20-minute BCCAo

MABP and temperature have been directly linked with the degree of ischaemic neuronal outcome following BCCAo (see Sections 1.2.1 and 1.3.7). During 20-minute BCCAo MABP in MF1 strain mice was significantly increased compared to that in C57bl/6 strain mice (Table 6). Prior to and following BCCAo MABP in MF1 and C57bl/6 strain mice was similar (Table 6). A descriptive, temporal profile of MABP recorded every two minutes throughout the entire BCCAo procedure highlights the decrease in MABP in C57bl/6 strain mice (Figure 23). Upon BCCAo MABP in MF1 and C57bl/6 strain mice increased to similar levels (Figure 23). MF1 strain mice maintained MABP above baseline throughout the entire period of BCCAo. In C57bl/6 strain mice MABP decreased progressively, commencing at around eight minutes after BCCAo (Figure 23). Removal of the carotid clips produced sharp, transient decreases in MABP in both MF1 and C57bl/6 strain mice, which returned to baseline levels over the next 10 or so minutes (Figure 23). Core body temperature was controlled, in both strains of mice; to minimise any temperature related effect upon ischaemic outcome or other physiologic variables (Table 6). Arterial pH, carbon dioxide and oxygen tensions, measured 10 minutes post occlusion were similar in MF1 and C57bl/6 strain mice (Table 6).

45-minute BCCAo

MABP in MF1 strain mice prior to and following 45-minute of BCCAo were similar (Table 7). Upon BCCAo MABP was increased, and this increase maintained above baseline for the duration of the 45-minute occlusion period (Figure 24). This maintained increase in MABP throughout the 45-minute occlusion period was similar to the increase in MABP observed over a 20-minute occlusion period in a previous study (Figure 23). Together these data highlight the ability of MF1 strain mice to increase and maintain MABP during BCCAo. Core body temperature was controlled; to minimise any

temperature related effect upon ischaemic outcome or other physiologic variables. Arterial pH, carbon dioxide and oxygen tensions were similar to those observed in MF1 mice following 20-minute BCCAo (Table 7, although no direct comparisons were made).

Table 6 Physiologic variables in MF1 and C57bl/6 mice: 20-minute BCCAo

	MF1 (n = 8)	C57bl/6 (n = 8)	
Weight (g)	35 ± 1	30 ± 1	30 minutes before procedure
Temperature (^{o}C)	37 ± 0.04	37 ± 0.03	during entire procedure †
MABP (mmHg)	84 ± 1	89 ± 3	10 minutes before BCCAo ‡
	102 ± 5	87 ± 5*	during 20-minute BCCAo ‡
	86 ± 5	84 ± 2	10 minutes after BCCAo ‡
Arterial pH	7.25 ± 0.01	7.21 ± 0.04	10 minutes after BCCAo
Arterial pCO_2 (mmHg)	111 ± 9	115 ± 8	10 minutes after BCCAo
Arterial pO_2 (mmHg)	52 ± 4	49 ± 4	10 minutes after BCCAo

† Once stabilised (between 36.8 and 37.2°C) all changes in temperature were recorded throughout the entire experimental procedure. Data shown represent the mean temp throughout the experimental period. ‡ Following femoral artery cannulation, MABP was continuously recorded until ten minutes post-occlusion. Data shown represent the MABP measured in the ten-minute period preceding BCCAo, the period of BCCAo, and the ten-minute period post BCCAo. All other data are expressed as mean ± standard error of mean. * $p < 0.05$ unpaired Student's *t*-test.

Figure 23 Influence of 20-minute BCCAo on MABP

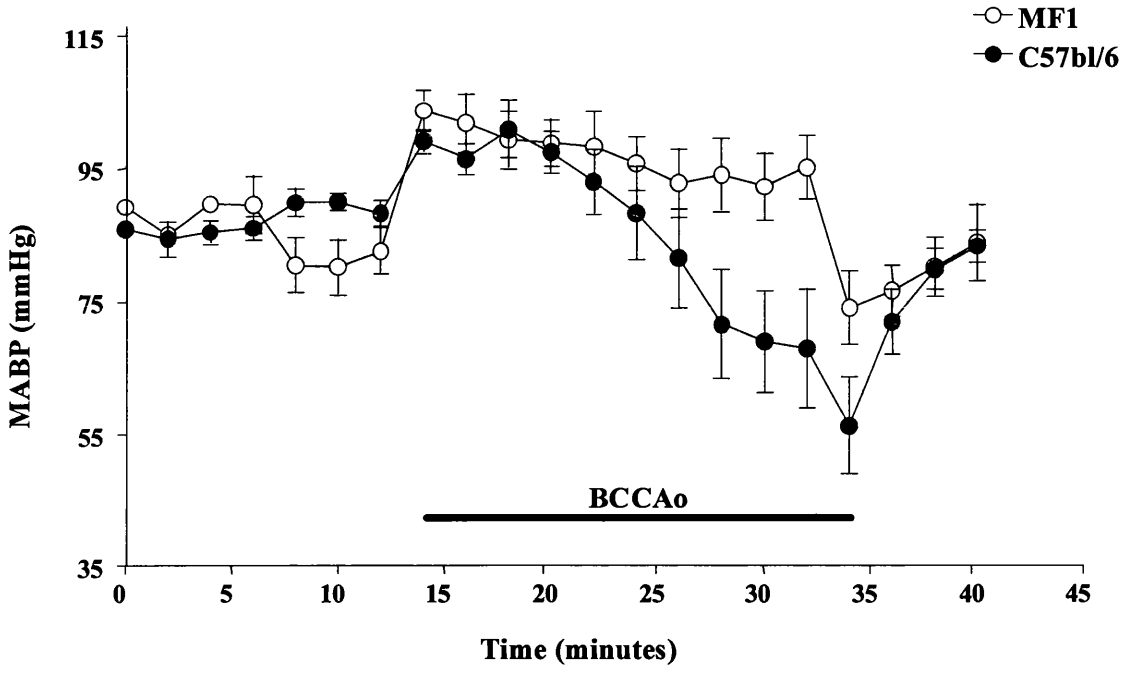

Data are expressed as mean ± standard error of the mean. Each point represents MABP recorded every two minutes throughout the 20-minute BCCAo procedure. (MF1 n=8; C57bl/6 n=8).

Table 7 Physiologic variables in MF1 mice: 45-minute BCCAo

	MF1 (n = 8)	
Weight (g)	42 ± 3	30 minutes before procedure
Temperature (°C)	37 ± 0.07	during entire procedure †
MABP (mmHg)	91 ± 6	10 minutes before BCCAo ‡
	103 ± 12	during 20-minute BCCAo ‡
	88 ± 8	10 minutes after BCCAo ‡
Arterial pH	7.28 ± 0.07	10 minutes after BCCAo
Arterial pCO_2 (mmHg)	121 ± 25	10 minutes after BCCAo
Arterial pO_2 (mmHg)	59 ± 10	10 minutes after BCCAo

† Once stabilised (between 36.8 and 37.2°C) all changes in temperature were recorded throughout the entire experimental procedure. Data shown represent the mean temp throughout the experimental period. ‡ Following femoral artery cannulation, MABP was continuously recorded until ten minutes post-occlusion. Data shown represent the MABP measured in the ten-minute period preceding BCCAo, the period of BCCAo, and the ten-minute period post BCCAo. All other data are expressed as mean ± standard error of mean.

Figure 24 Influence of 45-minute BCCAo on MABP

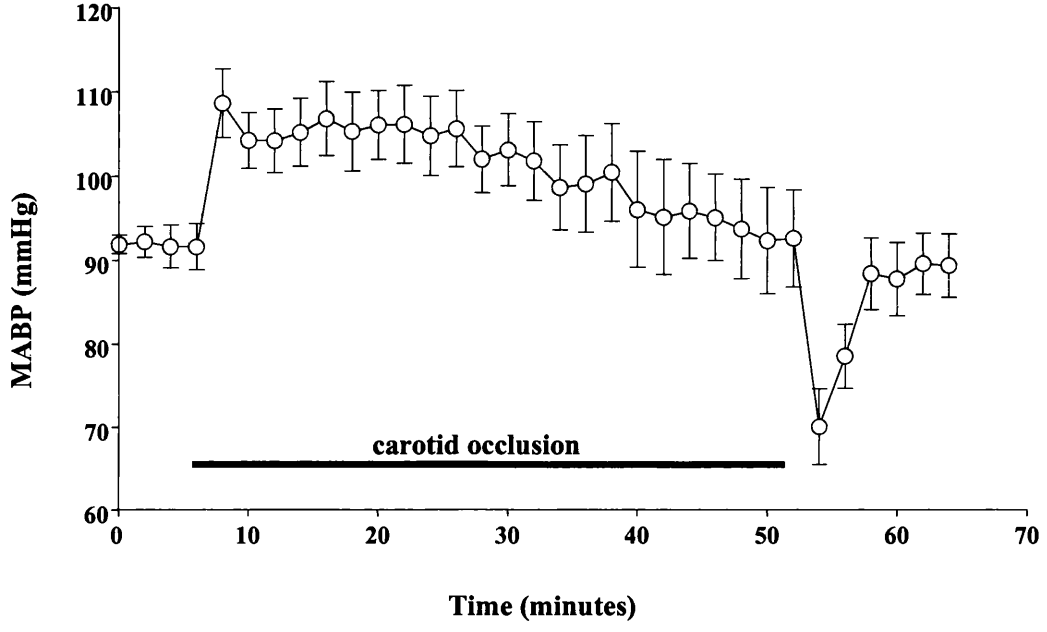

Data are expressed as mean ± standard error of the mean. Each point represents MABP in MF1 mice, recorded every two minutes throughout the 45-minute BCCAo procedure. (n=8).

3.1.4 Hsp 70i immunoreactivity in MF1 and C57bl/6 mice following BCCAo

Immunohistochemical localisation of hsp 70i following global cerebral ischaemia has been reported in several brain structures (including hippocampus, corpus striatum and cortex) in gerbil and rat (see Section 1.7.3). In mouse immunohistochemical localisation of hsp 70i following global cerebral ischaemia has not been shown. In this thesis immunohistochemical localisation of hsp 70i was observed in MF1 and C57bl/6 strain mice in several brain structures following BCCAo.

10-20 minute BCCAo

There were no hsp 70i immunoreactive neurones (or any other cell types) observed in any sham-operated mice (Figures 26 and 27). However, following BCCAo there was notable cellular immunoreactivity to hsp 70i particularly in neurones and processes. Hsp 70i immunoreactive neurones in MF1 and C57bl/6 strain mice following 10, 15 and 20-minute BCCAo were determined in five brain regions (Table 8). In three of these regions, namely hippocampus CA1, CA2 and CA3, MF1 strain mice displayed significantly fewer hsp 70i immunoreactive neurones (Table 8, Figures 25, 26 and 27). This trend was also evident in the caudate nucleus, although, the differences failed to achieve statistical significance. Neurones in the dentate gyrus displayed hsp 70i immunoreactivity only in a few C57bl/6 strain mice following 20-minute BCCAo (Table 8). The greatest number of hsp 70i immunoreactive neurones were observed in hippocampus CA1, followed by hippocampus CA3, caudate nucleus, hippocampus CA2 and dentate gyrus, respectively in both strains. Moreover, the number of hsp 70i immunoreactive neurones was not directly correlated with duration of occlusion (Table 8, Figure 25).

25-45 minute BCCAo

Hsp 70i immunoreactive neurones in MF1 strain mice following 25, 30, 35, 40 and 45 minutes BCCAo were determined in five brain regions. All five-brain regions analysed

displayed hsp 70i immunoreactive neurones following BCCAo (Table 9, Figure 28). The greatest number of hsp 70i immunoreactive neurones were observed in hippocampus CA1, followed by hippocampus CA3, hippocampus CA2, caudate nucleus and dentate gyrus (Table 9). The number of hsp 70i immunoreactive neurones was not directly correlated with the duration of ischaemia (Table 9, Figure 28). Although direct comparison could not be made, the number of hsp 70i immunoreactive neurones observed following 25-45 minutes of BCCAo was broadly similar to those observed following 10-20 minutes of BCCAo.

Table 8 **Hsp 70i immunoreactive neurones in MF1 and C57bl/6 mice**

	Duration of BCCAo					
	10 mins		15 mins		20 mins	
	MF1 (n = 6)	C57bl/6 (n = 5)	MF1 (n = 6)	C57bl/6 (n = 6)	MF1 (n = 7)	C57bl/6 (n = 5)
Hippocampus CA1	89 ± 47	411 ± 92 **	5 ± 5	227 ± 45 ***	90 ± 44	351 ± 62 **
Hippocampus CA2	2 ± 1	33 ± 9 **	1 ± 1	24 ± 12	7 ± 4	37 ± 13 *
Hippocampus CA3	12 ± 8	108 ± 23 **	2 ± 2	104 ± 19 ***	35 ± 13	159 ± 12 ***
Dentate Gyrus	0 ± 0	0 ± 0	0 ± 0	0 ± 0	0 ± 0	5 ± 3
Caudate nucleus	10 ± 8	96 ± 58	2 ± 2	1 ± 1	42 ± 38	82 ± 55

Data are expressed as mean ± standard error of the mean. *p=<0.05; **p<0.01; ***p<0.001 unpaired Student's *t*-test.

Sham groups are consolidated in this table; as there were no hsp 70i immunoreactive neurones observed in any sham-operated mice.

Figure 25 Hsp 70i immunoreactive neurones in MF1 and C57bl/6 mice

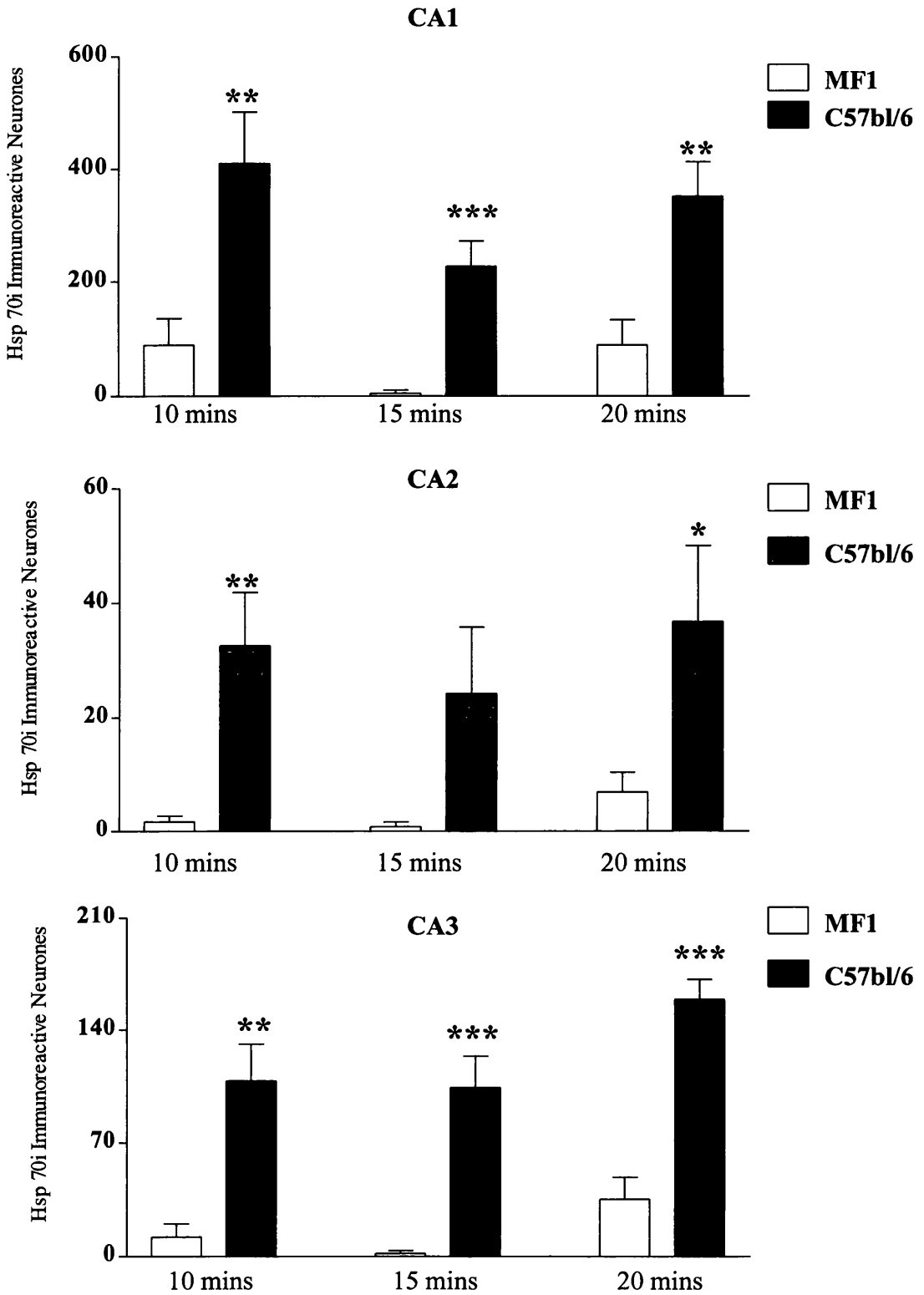

MF1 strain mice displayed significantly fewer hsp 70i immunoreactive neurones than C57bl/6 strain mice in hippocampus CA1 and CA3 (all BCCAo durations) and hippocampus CA2 (at 10 and 20-minute BCCAo). Data are presented as mean ± standard error of the mean. *$p<0.05$; **$p<0.01$; ***$p<0.001$ unpaired Student's *t*-test. (n = 5 C57bl/6 10, 20 mins; n = 6 MF1 10, 15 mins, C57bl/6 15 mins; n = 7 MF1 20 mins).

Figure 26 Hsp 70i immunoreactive neurones in hippocampus of MF1 mice

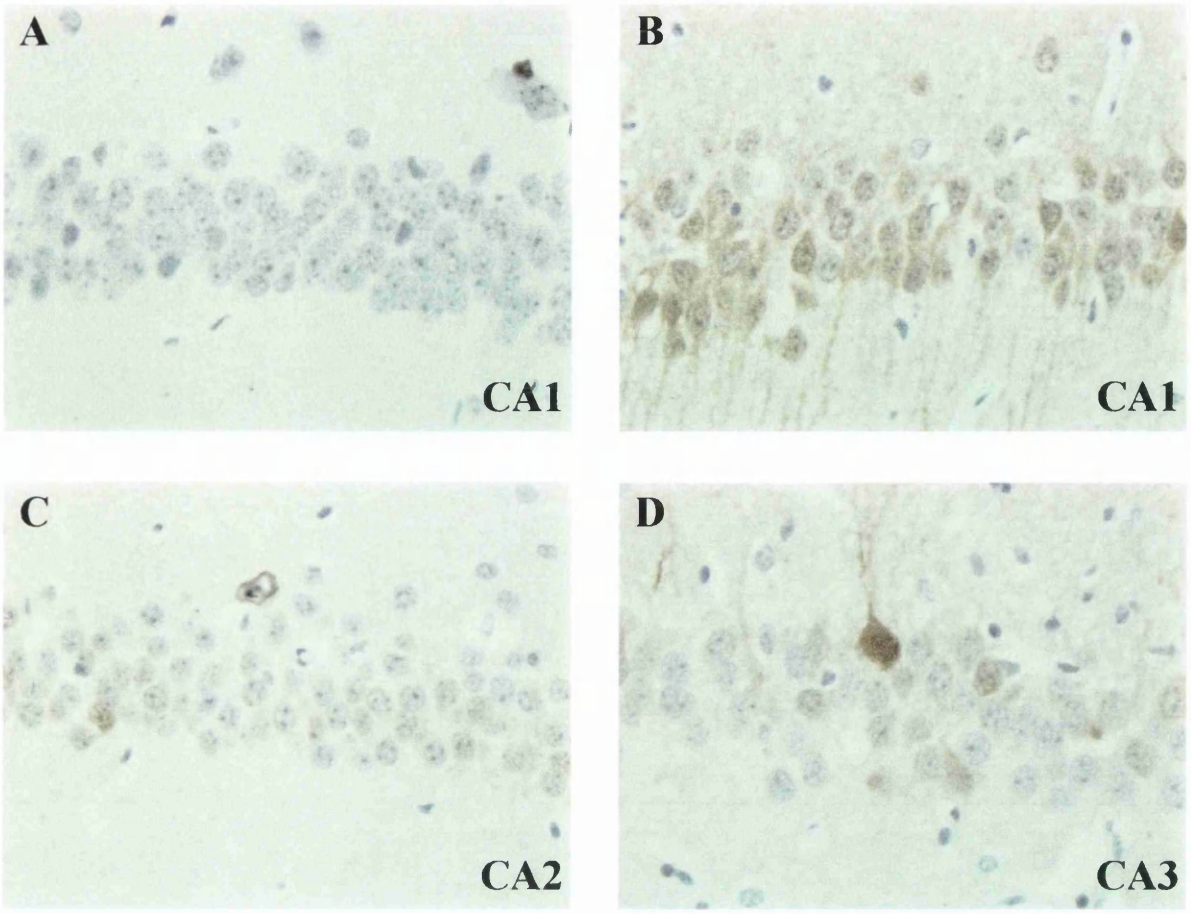

No hsp 70i immunoreactive neurones in hippocampus CA1 of sham-operated MF1 strain mice (A). Hsp 70i immunoreactive neurones in hippocampus CA1 (B), CA2 (C) and CA3 (D) of MF1 strain mice subjected to 20-minute BCCAo. (Original magnification X200).

Figure 27 Hsp 70i immunoreactive neurones in hippocampus of C57bl/6 mice

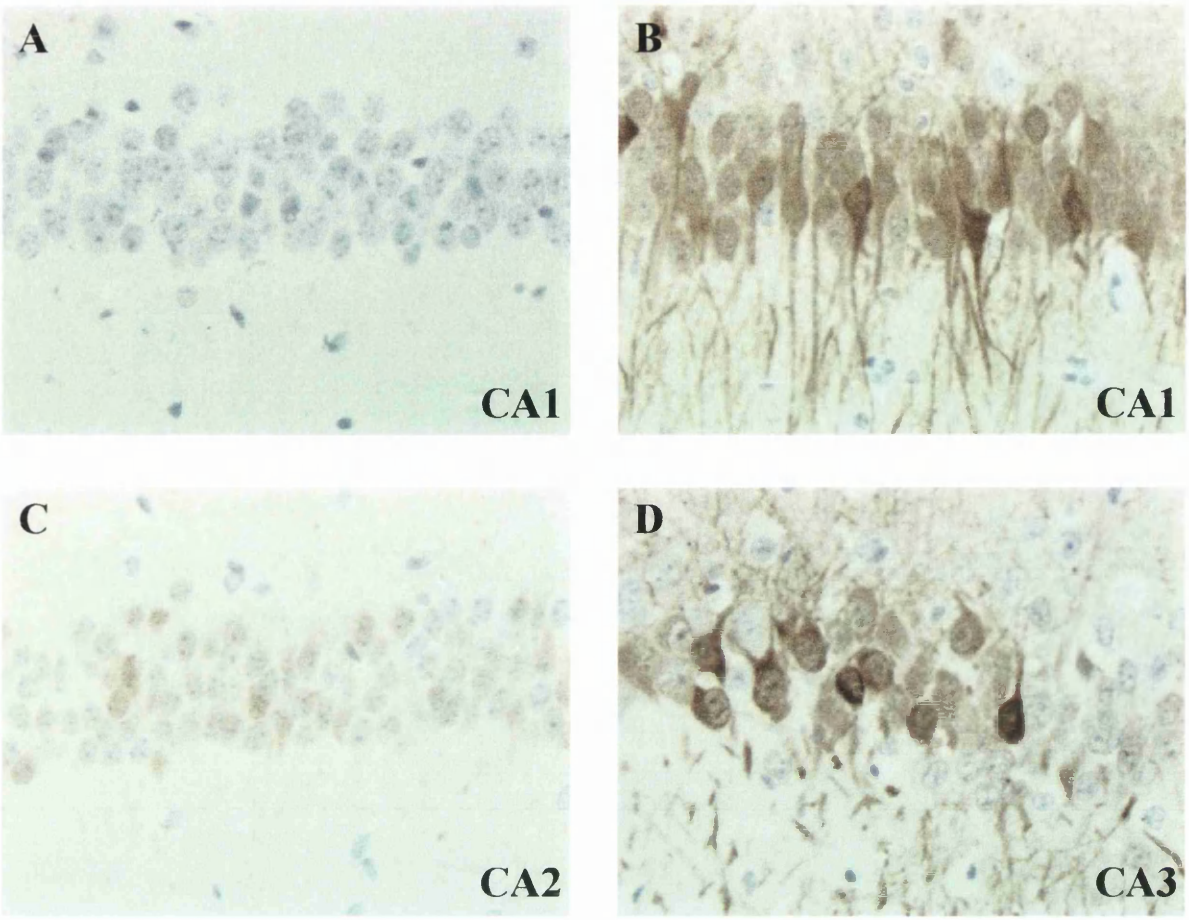

No hsp 70i immunoreactive neurones in hippocampus CA1 of sham-operated C57bl/6 strain mice (A). Hsp 70i immunoreactive neurones in hippocampus CA1 (B), CA2 (C) and CA3 (D) of C57bl/6 strain mice subjected to 20-minute BCCAo. (Original magnification X200).

Table 9 **Hsp 70i immunoreactive neurones in MF1 mice with extended BCCAo**

		Dnration of BCCAo				
	Sham (n = 26)	**25 mins** (n = 6)	**30 mins** (n = 6)	**35 mins** (n = 7)	**40 mins** (n = 6)	**45 mins** (n = 6)
Hippocampus CA1	0 ± 0	173 ± 19	50 ± 50	135 ± 53	127 ± 60	40 ± 13
Hippocampus CA2	0 ± 0	16 ± 12	9 ± 9	18 ± 11	21 ± 11	3 ± 2
Hippocampus CA3	0 ± 0	102 ± 47	25 ± 25	68 ± 36	118 ± 26	79 ± 38
Dentate Gyrus	0 ± 0	6 ± 4	0 ± 0	2 ± 1	7 ± 4	6 ± 4
Caudate nucleus	0 ± 0	28 ± 18	6 ± 5	5 ± 4	4 ± 2	6 ± 4

Data are expressed as mean ± standard error of the mean.

Sham groups are consolidated in this table; as there were no hsp 70i immunoreactive neurones observed in any sham-operated mice.

Figure 28 **Hsp 70i immunoreactive neurones in hippocampus MF1 mice with extended BCCAo**

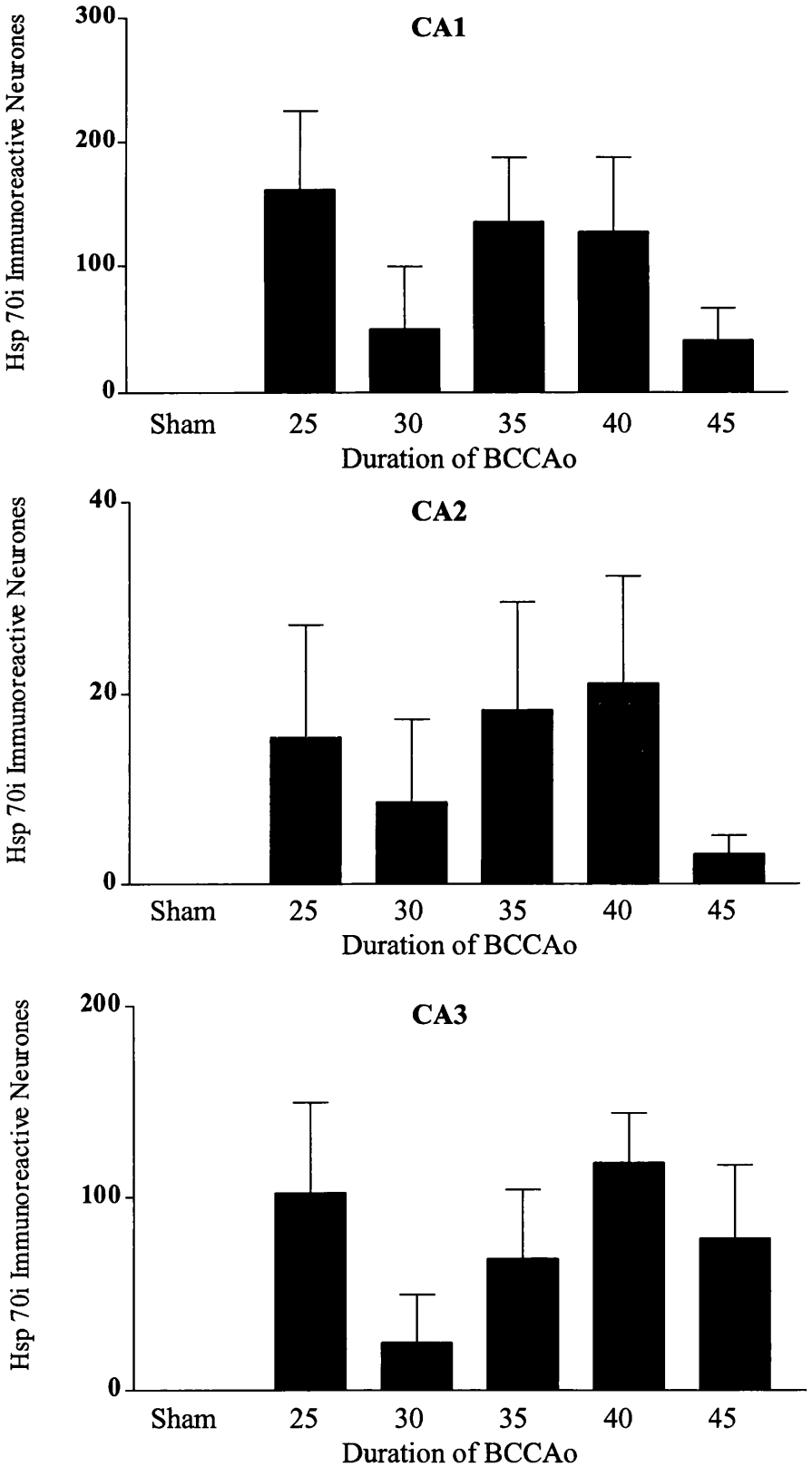

Hsp 70i immunoreactivity in MF1 strain mice did not increase with duration of BCCAo. Data are presented as mean ± standard error of the mean. (n = 6 25, 30, 40, 45 mins; n = 7 35 mins).

3.2 BCCAo in transgenic mice over-expressing hsp 70i

Neuropathologic and physiologic consequences of BCCAo in transgenic mice over-expressing hsp 70i were compared with those of their wild type littermates.

3.2.1 Ischaemic neuronal damage in hsp 70i transgenic mice following BCCAo

Ischaemic neuronal damage in hsp 70i transgenic and wild type littermate mice following 25-minute BCCAo and 25-minute sham-BCCAo was quantified as a percentage (see Section 2.6.3). Four comparisons were made (Tables 10, 11, 12 and 13) hence the Bonferroni correction factor four. Ischaemic neuronal damage in sham-operated hsp 70i transgenic and wild type littermate mice did not differ significantly in any of the eight brain regions analysed (Table 10, Figure 29). In hsp 70i transgenic mice 25-minute BCCAo produced significantly increased ischaemic neuronal damage in four of the eight brain regions analysed, compared with sham-operated hsp 70i transgenic mice (Table 11, Figure 29). In wild type littermate mice, 25-minute BCCAo produced significantly increased ischaemic neuronal damage in seven of the eight brain regions analysed, compared with sham-operated wild type littermate mice (Table 12, Figure 29). Twenty-five minute BCCAo produced significantly less ischaemic neuronal damage in hsp 70i transgenic mice in three of the eight brain regions analysed, compared with 25-minute BCCAo in wild type littermate mice (Table 13, Figure 29).

These data clearly indicated two important features. First, BCCAo could induce ischaemic neuronal damage in hsp 70i transgenic mice and their wild type littermates. Second, BCCAo produces significantly less ischaemic neuronal damage in hsp 70i transgenic, mice than in wild type littermate mice.

Figure 29 Ischaemic neuronal damage in hsp 70i transgenic mice

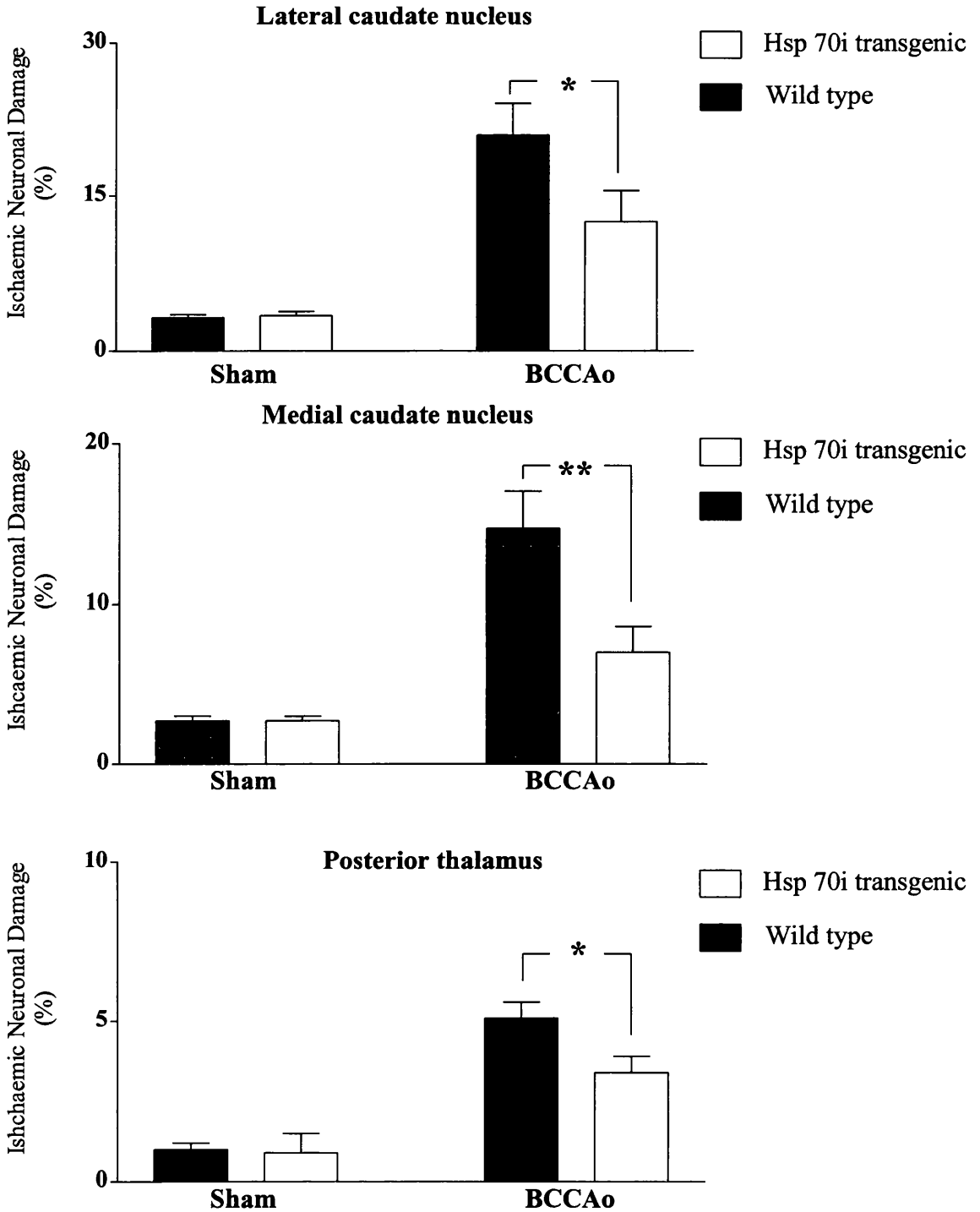

Hsp 70i transgenic mice displayed significantly less ischaemic neuronal damage than wild type littermate mice in lateral caudate nucleus, medial caudate nucleus and posterior thalamus following 25-minute BCCAo. Ischaemic neuronal damage in BCCAo mice was significantly increased compared to that in sham-operated mice (not highlighted on graph, see Tables 11 and 12 for detaials). Data are presented as mean ± standard error of the mean. *$p<0.05$; **$p<0.01$ One way analysis of variance followed by unpaired Student's *t*-test with Bonferroni correction factor of four. (n = 10 hsp 70i transgenic; n = 9 wild type littermate).

Table 10 **Ischaemic neuronal damage in hsp 70i transgenic and wild type littermate mice: sham-operated**

	hsp 70i transgenic SHAM (%)	wild type littermates SHAM (%)
Lateral caudate nucleus	3.4 ± 0.4	3.2 ± 0.3
Medial caudate nucleus	2.7 ± 0.3	2.7 ± 0.3
Hippocampus CA1	1.3 ± 0.3	1.9 ± 0.3
Posterior thalamus	1.0 ± 0.2	0.9 ± 0.6
Hippocampus CA3	0.2 ± 0.1	0.7 ± 0.2
Somatosensory cortex	0.8 ± 0.3	1.1 ± 0.2
Hippocampus CA2	1.0 ± 0.3	0.7 ± 0.2
Dentate gyrus	0.0 ± 0.0	0.03 ± 0.03

Data are expressed as mean ± standard error of the mean. $p>0.05$ One way analysis of variance followed by unpaired Student's *t*-test with Bonferroni correction factor of four. (n= 10 hsp 70i transgenic; n = 9 wild type littermates).

Table 11 **Ischaemic neuronal damage in hsp 70i transgenic mice: sham versus 20-minute BCCAo**

	hsp 70i transgenic SHAM (%)	hsp 70i transgenic BCCAo (%)	
Lateral caudate nucleus	3.4 ± 0.4	12.5 ± 3.0	*
Medial caudate nucleus	2.7 ± 0.3	7.0 ± 1.6	
Hippocampus CA1	1.3 ± 0.3	5.4 ± 1.1	
Posterior thalamus	1.0 ± 0.2	3.4 ± 0.5	***
Hippocampus CA3	0.2 ± 0.1	4.4 ± 1.1	**
Somatosensory cortex	0.8 ± 0.3	3.6 ± 0.5	***
Hippocampus CA2	1.0 ± 0.3	1.3 ± 0.3	
Dentate gyrus	0.0 ± 0.0	0.2 ± 0.1	

Data are expressed as mean ± standard error of the mean. *$p<0.05$; **$p<0.01$; ***$p<0.001$ One way analysis of variance followed by unpaired Student's *t*-test with Bonferroni correction factor of four. (n= 10 hsp 70i transgenic; n = 9 wild type littermates).

Table 12 **Ischaemic neuronal damage in wild type littermate mice: sham versus 20-minute BCCAo**

	wild type littermates SHAM (%)	wild type littermates BCCAo (%)	
Lateral caudate nucleus	3.2 ± 0.3	21.0 ± 3.1	***
Medial caudate nucleus	2.7 ± 0.3	14.7 ± 2.3	***
Hippocampus CA1	1.9 ± 0.3	6.8 ± 1.9	**
Posterior thalamus	0.9 ± 0.6	5.1 ± 0.5	***
Hippocampus CA3	0.7 ± 0.2	4.8 ± 1.2	***
Somatosensory cortex	1.1 ± 0.2	4.1 ± 0.3	***
Hippocampus CA2	0.7 ± 0.2	2.2 ± 0.4	*
Dentate gyrus	0.03 ± 0.03	0.1 ± 0.1	

Data are expressed as mean ± standard error of the mean. *p<0.05; **p<0.01; ***p<0.001 One way analysis of variance followed by unpaired Student's *t*-test with Bonferroni correction factor of four. (n= 10 hsp 70i transgenic; n = 9 wild type littermates).

Table 13 **Ischaemic neuronal damage in hsp 70i transgenic and wild type littermate mice: 20-minute BCCAo**

	hsp 70i transgenic BCCAo (%)	wild type littermates BCCAo (%)	
Lateral caudate nucleus	12.5 ± 3.0	21.0 ± 3.1	*
Medial caudate nucleus	7.0 ± 1.6	14.7 ± 2.3	**
Hippocampus CA1	5.4 ± 1.1	6.8 ± 1.9	
Posterior thalamus	3.4 ± 0.5	5.1 ± 0.5	*
Hippocampus CA3	4.4 ± 1.1	4.8 ± 1.2	
Somatosensory cortex	3.6 ± 0.5	4.1 ± 0.3	
Hippocampus CA2	1.3 ± 0.3	2.2 ± 0.4	
Dentate gyrus	0.2 ± 0.1	0.1 ± 0.1	

Data are expressed as mean ± standard error of the mean. *$p<0.05$; **$p<0.01$; One way analysis of variance followed by unpaired Student's *t*-test with Bonferroni correction factor of four. (n= 10 hsp 70i transgenic; n = 9 wild type littermates).

3.2.2 Circle of Willis anatomy in hsp 70i transgenic mice

In transgenic mice over-expressing hsp 70i (n=9) and their wild type littermates (n=9) no animals were deficient of both PcomAs (Figures 30 and 31). No hsp 70i or wild type littermate mice were deficient of both PcomAs. Sixty-seven percent of hsp 70i transgenic and wild type littermate mice had both PcomAs (Table 14). Thirty-three percent of hsp 70i transgenic and wild type littermate mice displayed an incomplete circle of Willis (Table 14). These results indicate that transgenic mice over-expressing hsp 70i and their wild type littermates are as likely as one another to have an incomplete circle of Willis.

Figure 30 Circle of Willis anatomy in transgenic hsp 70i mice

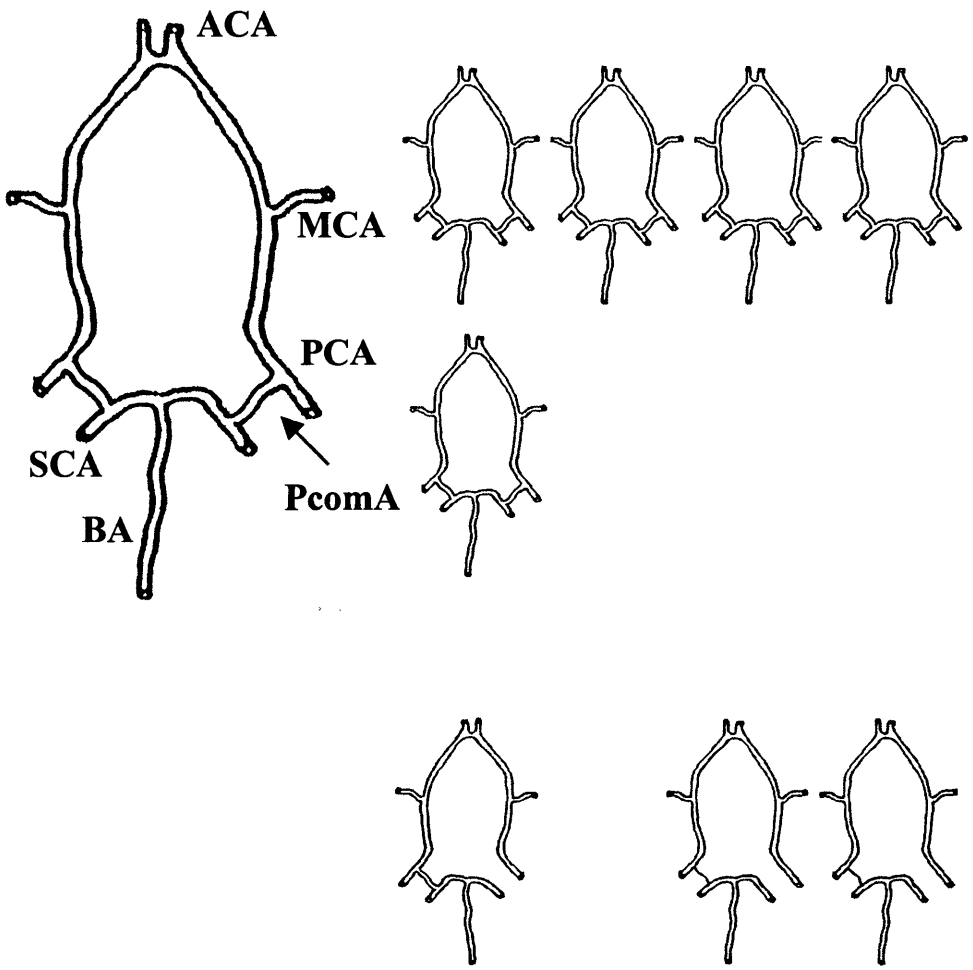

The presence of ACA (anterior cerebral arteries), MCA (middle cerebral arteries), PCA (posterior cerebral arteries), BA (basilar artery) and SCA (superior cerebellar arteries) in individual transgenic mice over-expressing hsp 70i (n=9) is summarised in this diagram. Six mice presented with both PcomAs (top panel and large annotated section) and three presented with only one PcomA (bottom panel). Of the three mice presenting with only one PcomA two mice displayed abnormally thin PcomA.

Figure 31 Circle of Willis anatomy in wild type littermate mice

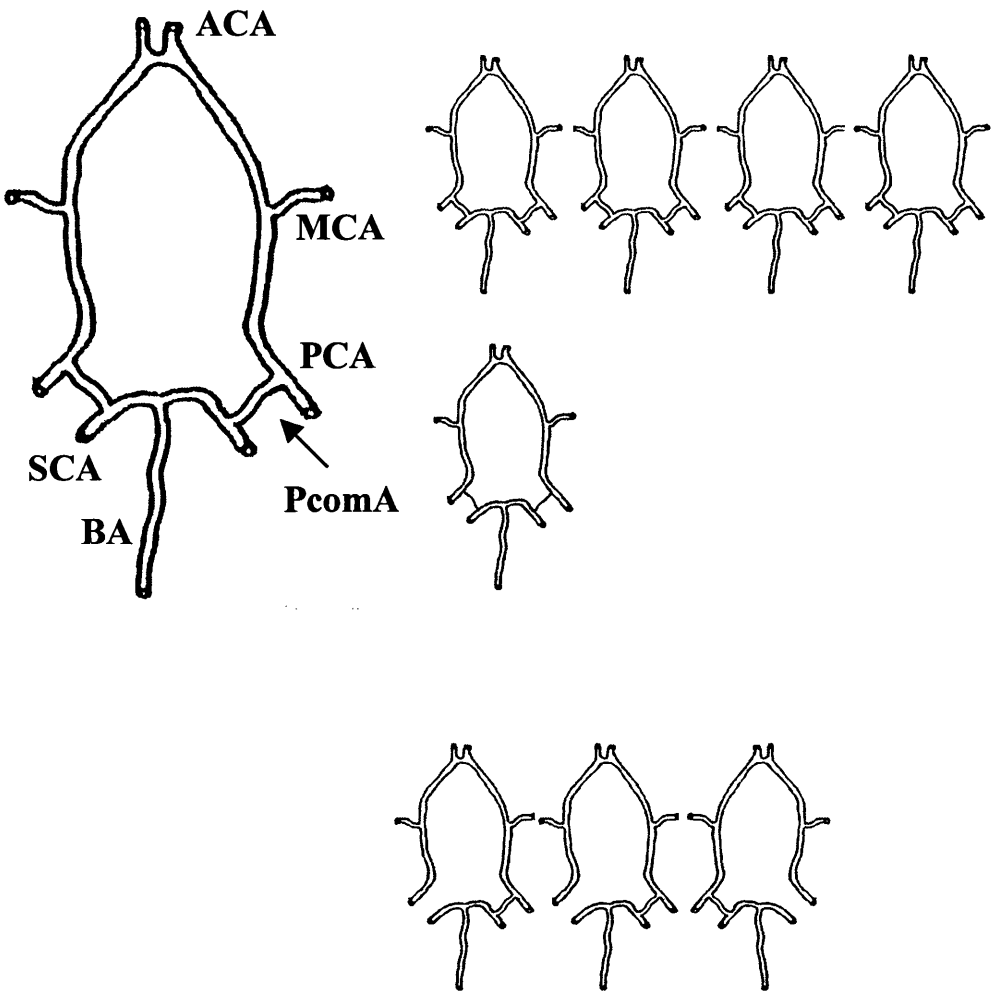

The presence of ACA (anterior cerebral arteries), MCA (middle cerebral arteries), PCA (posterior cerebral arteries), BA (basilar artery) and SCA (superior cerebellar arteries) in individual wild type mice (n=9) (littermates of hsp 70i transgenic mice) is summarised in this diagram. Six mice presented with both PcomAs (top panel and large annotated section) and three presented with only one PcomA (bottom panel). Of the six mice presenting with two PcomAs one mouse displayed abnormally thin vessels.

Table 14 PcomAs in hsp 70i transgenic mice

Number of posterior communicating arteries	hsp 70i transgenic (n = 9)	wild type littermates (n = 9)
Two (complete)	6	6
One or none (incomplete)	3	3
Incomplete circle of Willis (%)	33	33

3.2.3 Physiologic variables in hsp 70i transgenic mice: 25-minute BCCAo

Key physiologic variables in transgenic mice over-expressing hsp 70i and their wild type littermates with 25-minute BCCAo were investigated. MABP in hsp 70i transgenic and wild type littermate mice was broadly similar prior to, during and following BCCAo (Table 15). Upon BCCAo MABP in hsp 70i transgenic and wild type littermate mice increased to similar levels (Figure 32). In both hsp 70i transgenic and wild type littermate mice, increased MABP was maintained above baseline throughout the entire period of BCCAo (Figure 32). Removal of carotid clips produced sharp, transient decreases on MABP in both hsp 70i transgenic and wild type littermate mice, which returned to around baseline levels over the next 10 or so minutes (Figure 32). Core body temperature was controlled, in both groups, to minimise any temperature related effect upon ischaemic outcome or other physiologic variables. Arterial pH and carbon dioxide and oxygen tensions, measured 10 minutes after transient forebrain ischaemia, were broadly similar in hsp 70i transgenic and wild type littermate mice (Table 15).

Table 15 Physiologic variables in hsp 70i transgenic mice: 25-minute BCCAo

	hsp 70i transgenic (n = 9)	wild type littermates (n = 9)	
Weight (g)	36.5 ± 1	37.6 ± 1	30 minutes before procedure
Temperature (°C)	37.0 ± 0.02	37.0 ± 0.02	during entire procedure †
MABP (mmHg)	90 ± 3	94 ± 3	10 minutes before BCCAo ‡
	109 ± 4	115 ± 3	during 25-minute BCCAo ‡
	85 ± 2	92 ± 3	10 minutes after BCCAo ‡
Arterial pH	7.34 ± 0.02	7.33 ± 0.01	10 minutes after BCCAo
Arterial pCO_2 (mmHg)	47 ± 3.3	51 ± 2	10 minutes after BCCAo
Arterial pO_2 (mmHg)	112 ± 5	104 ± 4	10 minutes after BCCAo

† Once stabilised (between 36.8 and 37.2°C) all changes in temperature were recorded throughout the entire experimental procedure. Data shown represent the mean temp throughout the experimental period. ‡ Following femoral artery cannulation, MABP was continuously recorded until ten minutes post-occlusion. Data shown represent the MABP measured in the ten-minute period preceding BCCAo, the period of BCCAo, and the ten-minute period post BCCAo. All other data are expressed as mean ± standard error of mean. $p>0.05$ unpaired Student's *t*-test.

Figure 32 Influence of 25-minute BCCAo on MABP

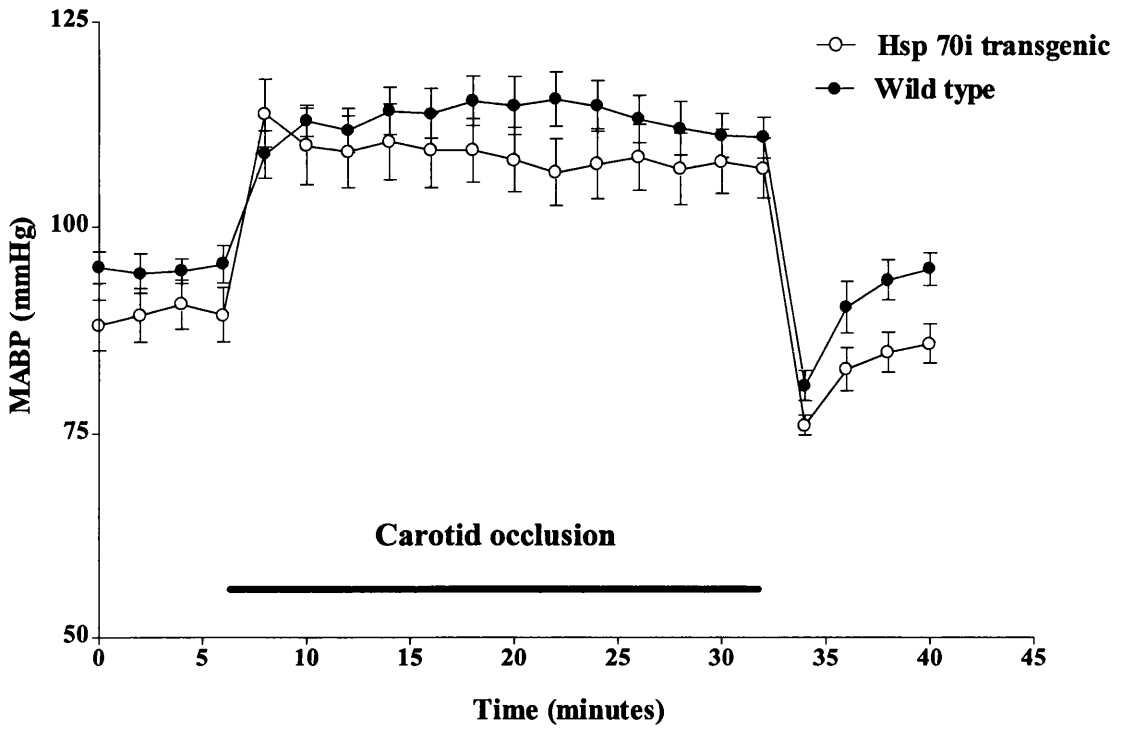

Data are expressed as mean ± standard error of the mean. Each point represents MABP recorded every two minutes throughout the 25-minute BCCAo procedure. (hsp 70i transgenic n=9; wild type littermates n=9).

3.2.4 Hsp 70i immunoreactivity in hsp 70i transgenic mice following BCCAo

There were no hsp 70i immunoreactive neurones (or any other cell types) observed in any sham-operated mice (Figures 34 and 35). However, following BCCAo there was notable cellular immunoreactivity to hsp 70i particularly in neurones and processes. Following 25-minute BCCAo there were no statistically significant differences in the number of hsp 70i immunoreactive neurones in hsp 70i transgenic mice compared with their wild type littermates, in any of the eight brain regions analysed (Table 16, Figure 33). The greatest number of hsp 70i immunoreactive neurones, in both hsp 70i transgenic and wild type mice, were observed in hippocampus CA1, followed by hippocampus CA3 and CA2 (Table 16, Figures 33, 34 and 35).

Table 16 Hsp 70i immunoreactive neurones in hsp 70i transgenic and wild type mice

	hsp 70i transgenic SHAM (n=9)	wild type littermates SHAM (n=9)	hsp 70i transgenic BCCAo (n=10)	wild type littermates BCCAo (n=10)
Hippocampus CA1	0 ± 0	0 ± 0	291 ± 87	334 ± 65
Hippocampus CA3	0 ± 0	0 ± 0	44 ± 11	109 ± 35
Hippocampus CA2	0 ± 0	0 ± 0	30 ± 11	25 ± 7
Medial caudate nucleus	0 ± 0	0 ± 0	14 ± 6	7 ± 4
Posterior thalamus	0 ± 0	0 ± 0	14 ± 9	6 ± 3
Lateral caudate nucelus	0 ± 0	0 ± 0	13 ± 8	3 ± 1
Somatosensory cortex	0 ± 0	0 ± 0	8 ± 4	6 ± 3
Dentate gyrus	0 ± 0	0 ± 0	0.5 ± 0.2	0.2 ± 0.2

Data are expressed as mean ± standard error of the mean. $p>0.05$ unpaired Student's *t*-test (hsp 70i transgenic versus wild type littermate with BCCAo only, as sham-operated mice had no hsp 70i immunoreactive neurones).

Figure 33 Hsp 70i immunoreactive neurones in hippocampus CA1, CA2 and CA3

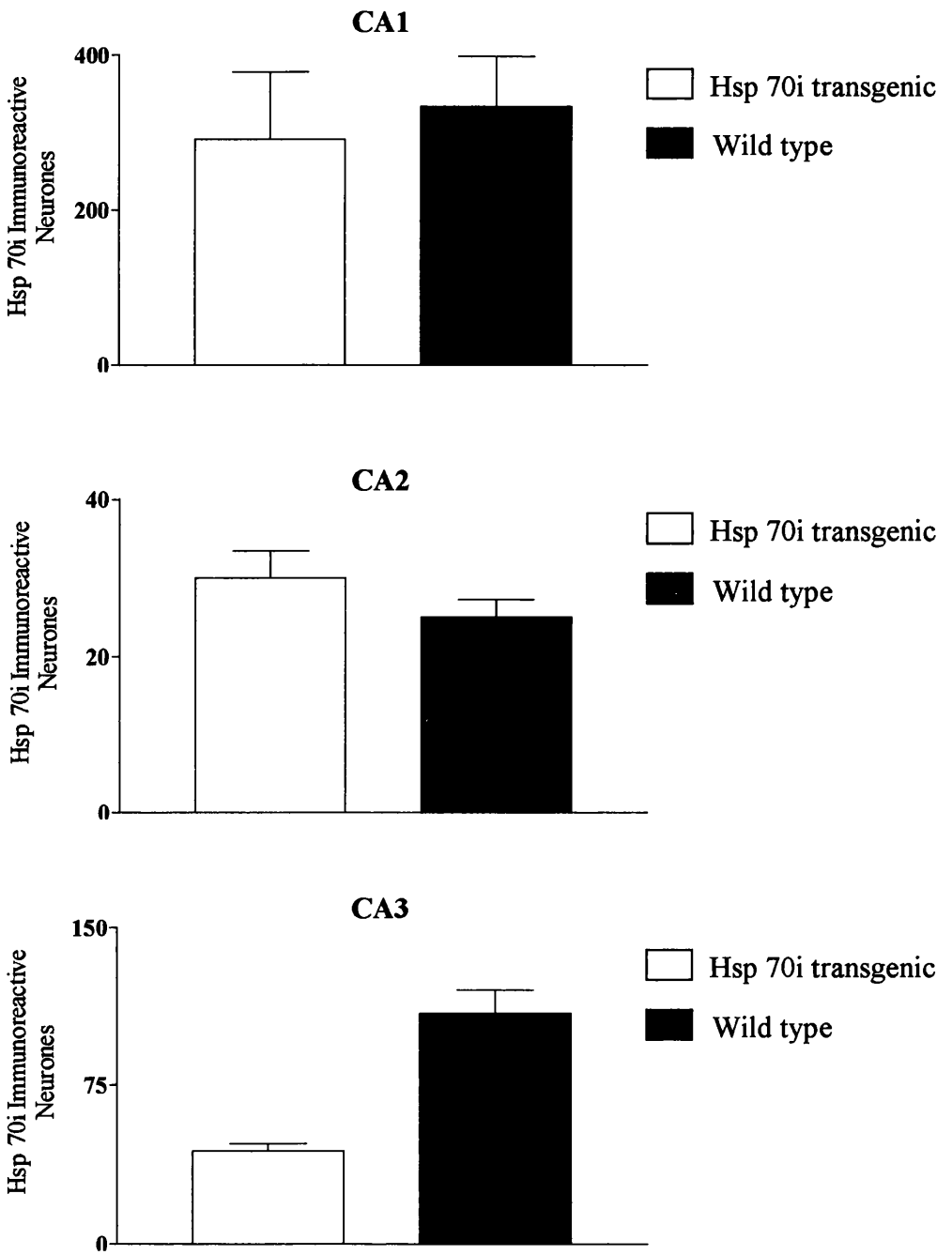

The number of hsp 70i immunoreactive neurones in hsp 70i transgenic mice did not differ significantly compared with wild type littermate mice following 25 minutes of transient forebrain ischaemia. Data are presented as mean ± standard error of the mean. (n = 10 hsp 70i transgenic; n = 9 wild type littermate).

Figure 34 **Hsp 70i immunoreactive neurones in hippocampus of hsp 70i transgenic mice**

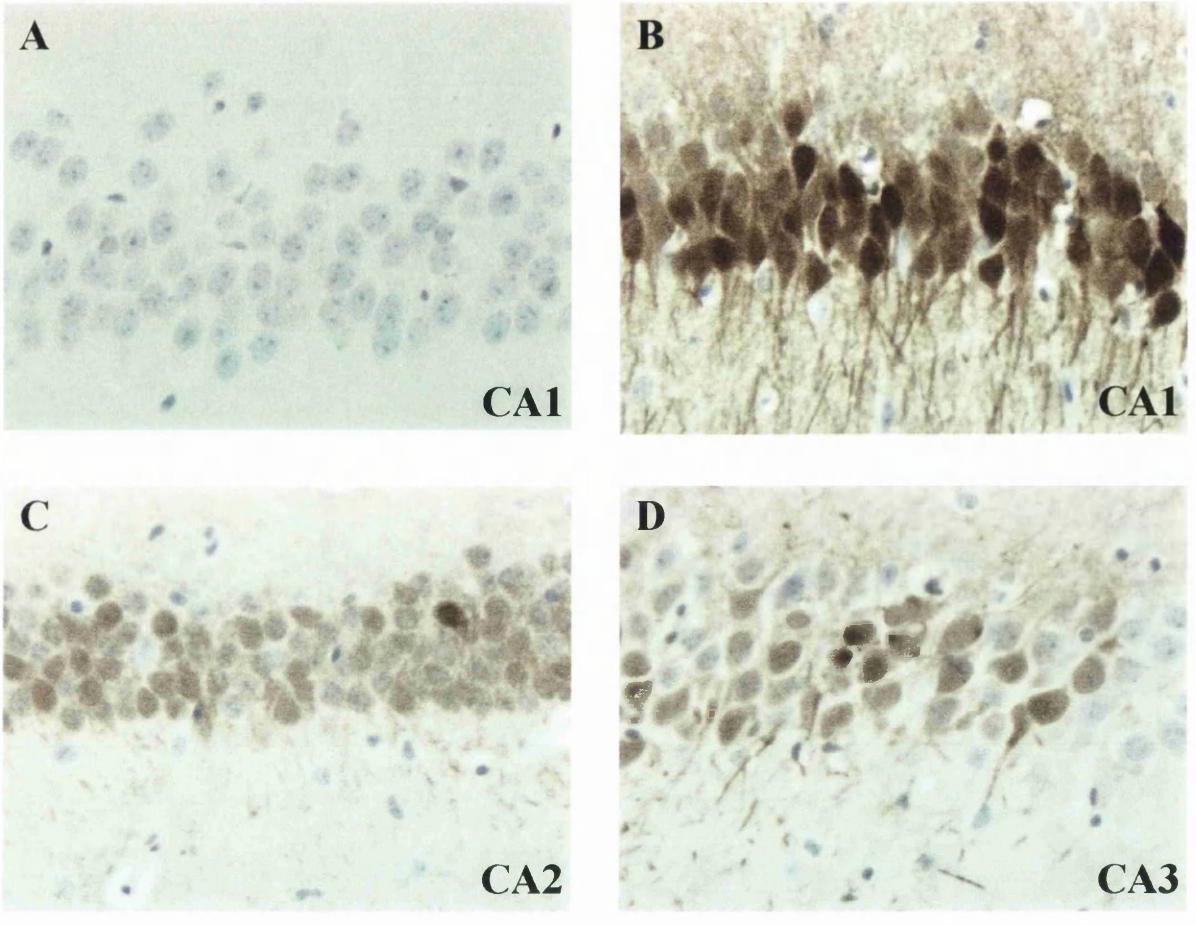

No hsp 70i immunoreactive neurones in hippocampus CA1 of sham-operated hsp 70i transgenic mice (A). Hsp 70i immunoreactive neurones in hippocampus CA1 (B), CA2 (C) and CA3 (D) of hsp 70i transgenic mice subjected to 25-minute of BCCAo. (Original magnification X200).

Figure 35 Hsp 70i immunoreactive neurones in hippocampus of wild type mice

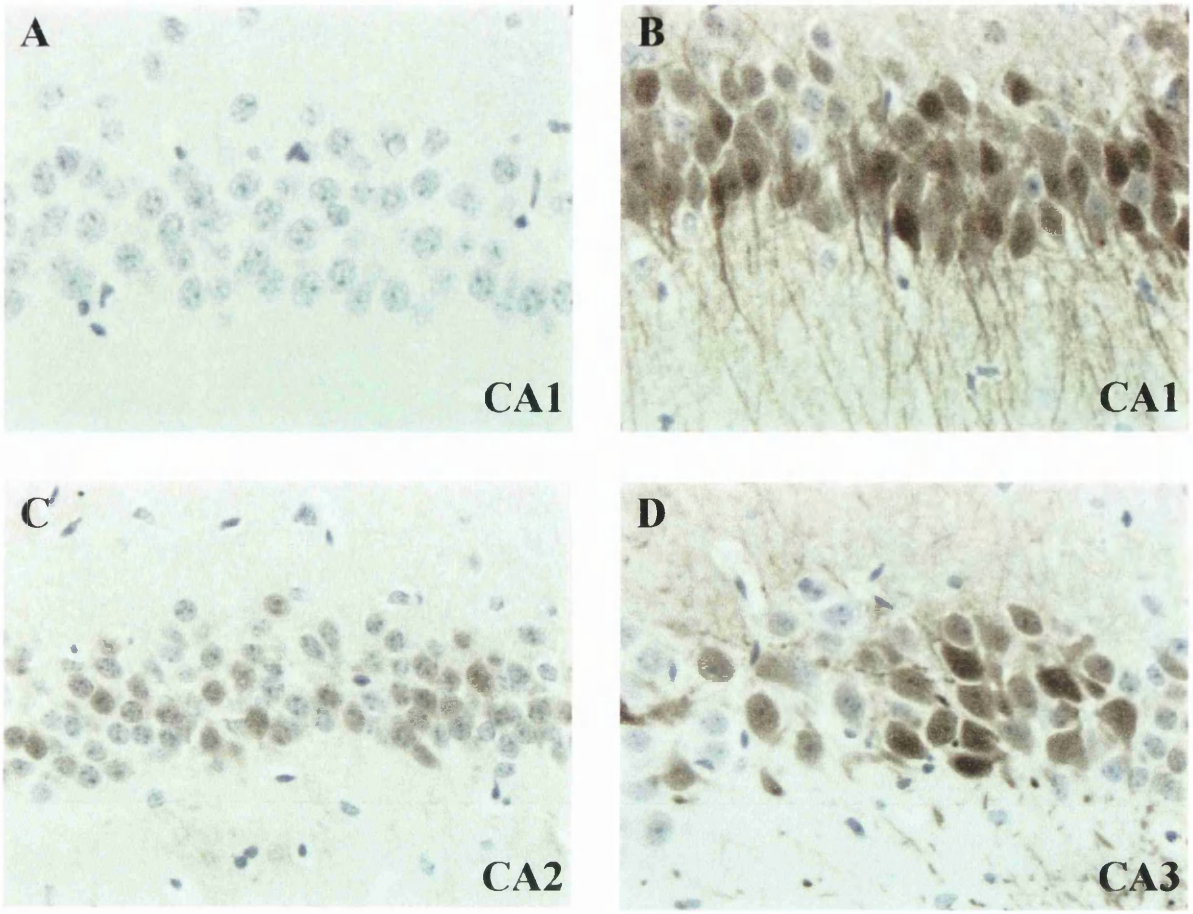

No hsp 70i immunoreactive neurones in hippocampus CA1 of sham-operated wild type littermate mice (A). Hsp 70i immunoreactive neurones in hippocampus CA1 (B), CA2 (C) and CA3 (D) of wild type littermate mice subjected to 25-minute. (Original magnification X200).

3.3 BCCAo in ad hsp70i and ad egfp transfected mice

Neuropathologic consequences of BCCAo in C57bl/6 strain mice intrastriatally injected with one microlitre (over ten minutes) of ad hsp 70i and ad egfp were investigated. C57bl/6 strain mice were used in this study for two reasons. First, previous studies within this thesis had shown them to be more susceptible to BCCAo than MF1 strain mice. Second, inter-hemispheric association of ischaemic neuronal damage in C57bl/6 strain mice was much stronger than that of MF1 strain mice (particularly in the caudate nucleus, Appendix E).

3.3.1 Behaviour following intrastriatal injection of ad hsp 70i and ad egfp

Overt behaviour of mice which received intrastriatal injection of ad hsp 70i (0.75×10^{10} plaque forming units/ml) was indistinguishable from mice that received intrastriatal injection of ad egfp (0.75×10^{10} plaque forming units/ml).

3.3.2 Ad hsp 70i and ad egfp transfection

Direct localisation of hsp 70i transfection following intrastriatal injection in mice was not possible in this study as all mice injected were also subjected to BCCAo, which induces hsp 70i. Notwithstanding this, hsp 70i immunoreactivity was significantly increased in the ad hsp 70i injected hemisphere compared to the contralateral hemisphere, following 10 and 20-minute BCCAo (see Section 3.3.4). The transfection capacity of ad could however be analysed where mice were intrastriatally injected with ad egfp. The extent of ad egfp transfection and the cell types transfected can be assumed to correlate well to areas of ad hsp 70i transfection. Moreover, a 100% transfection rate of ad egfp in this study (n=16 mice) and in a previous study (n=22, see Section 3.5) suggested that ad hsp 70i transfection did occur. Ad egfp transfection was observed in the caudate nucleus in all mice (Figure 36). Ad egfp transfection was also frequently observed in fibres of the subcortical white matter and white matter bundles within the caudate nucleus (Figures 37 and 38). Several

cell types were transfected with ad egfp including, neurones (Figure 39), astrocytes (Figure 40) and ependymal cells of the right ventricle (Figure 41).

Figure 36 Ad egfp transfection in caudate nucleus

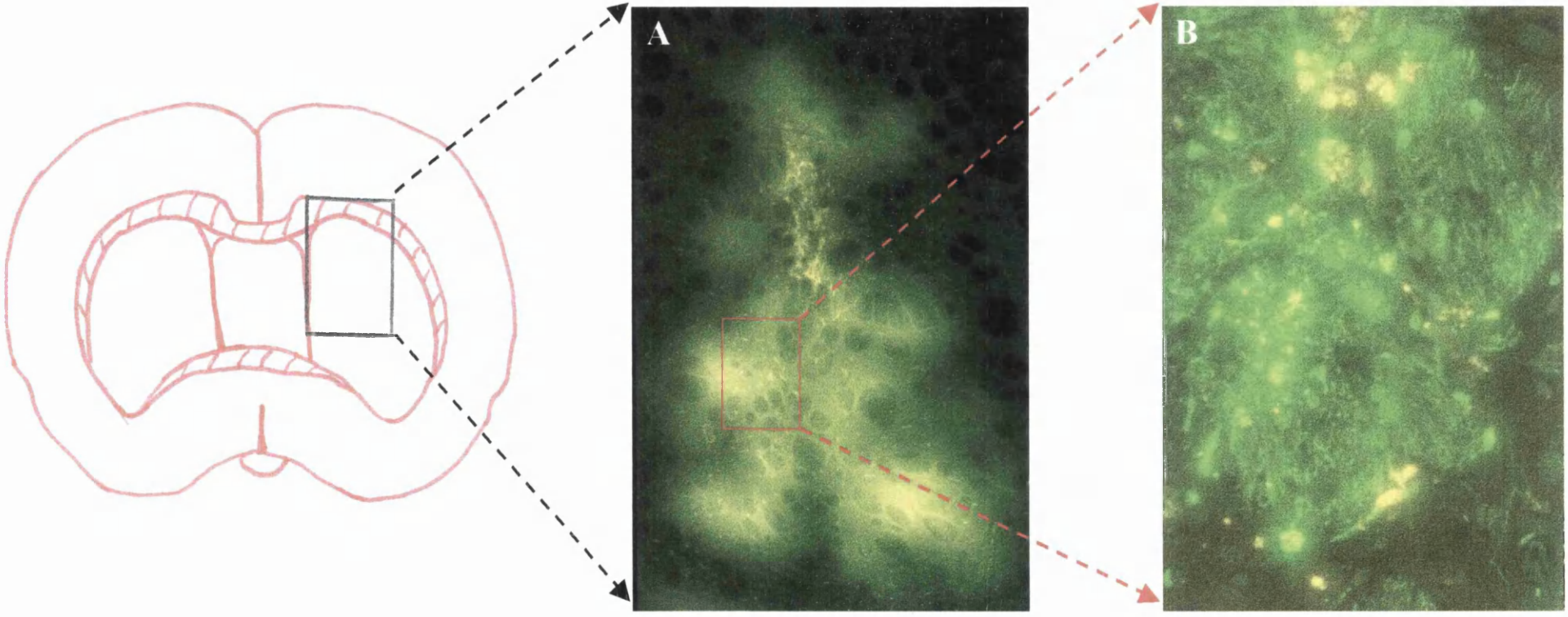

Intrastriatal injection of ad egfp resulted in widespread transfection of the caudate nucleus (A, original magnification X100). Several cell types and fibres were all transfected (B, original magnification X200). (Green = egfp).

Figure 37 Ad egfp transfection in subcortical white matter

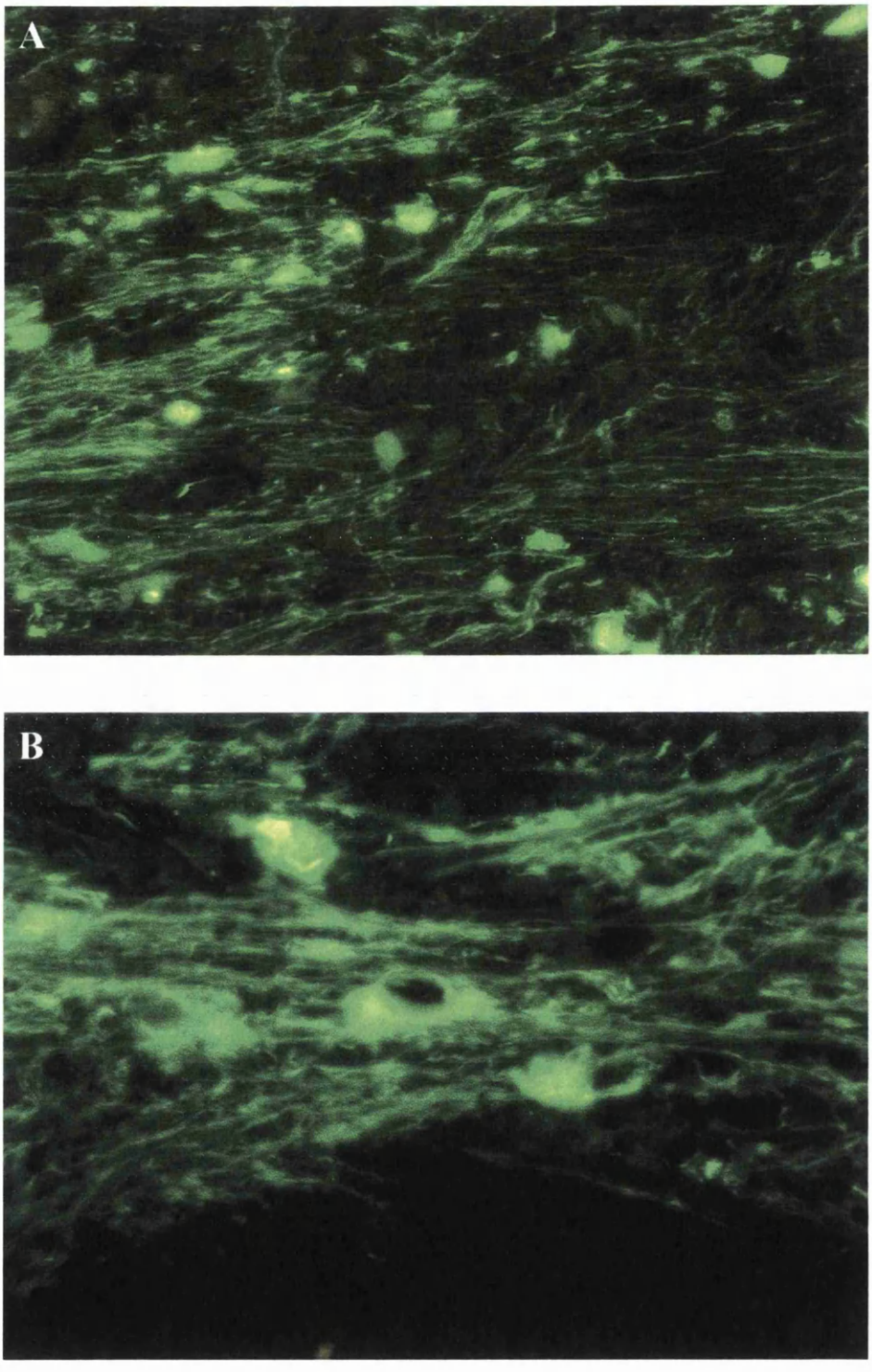

Intrastriatal injection of ad egfp resulted in extensive transfection of cells and axons within ipsilateral subcortical white matter. (Green = egfp). (A, original magnification X200; B, original magnification X400).

Figure 38 Ad egfp transfection of white matter bundles in caudate nucleus

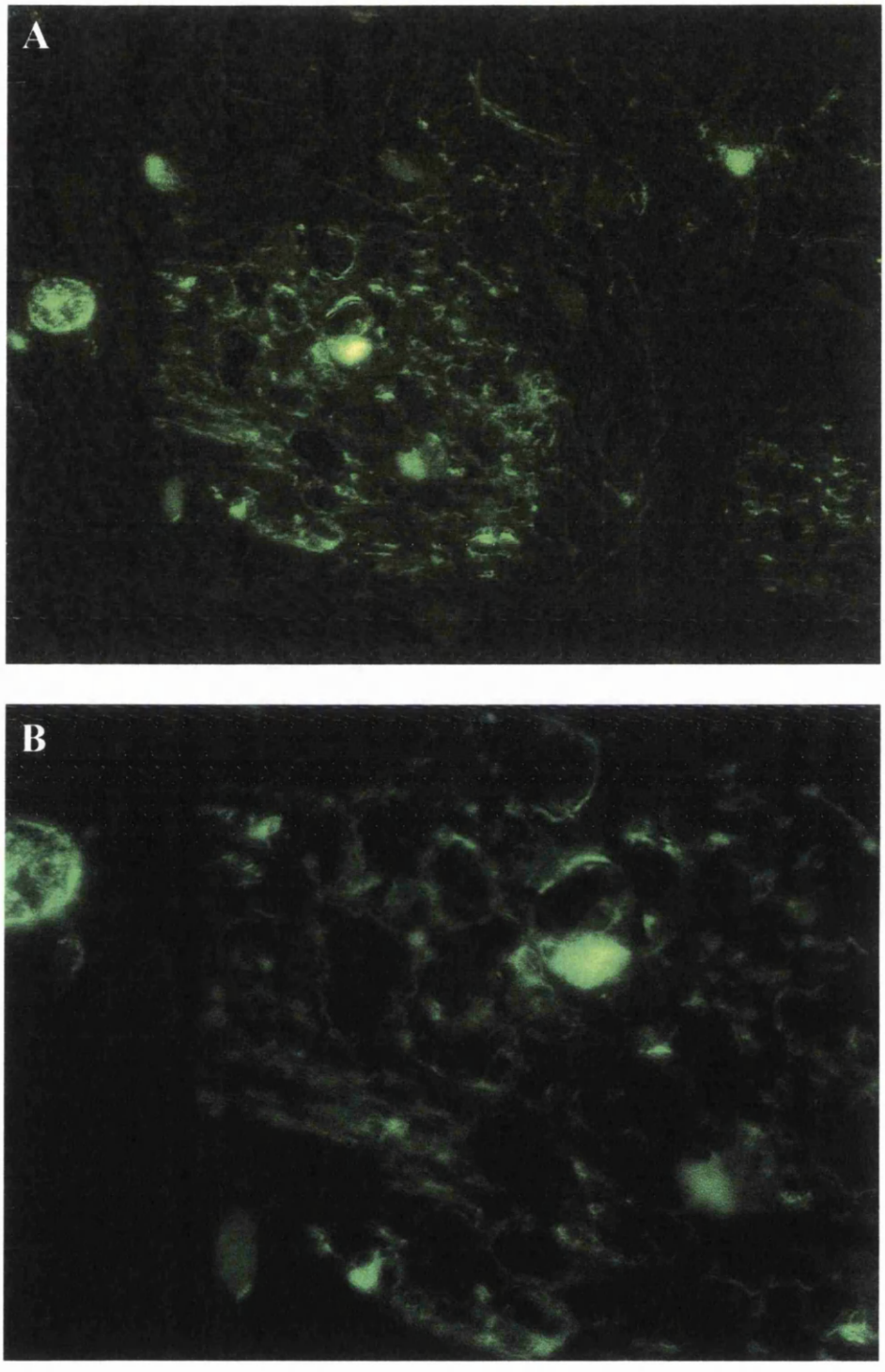

Ad mediated egfp transfection of white matter bundles in the caudate nucleus was a common feature of mice intrastriatally injected with ad egfp. (Green = egfp). (A, original magnification X200; B, original magnification X400).

Figure 39 Ad egfp transfection of neurones

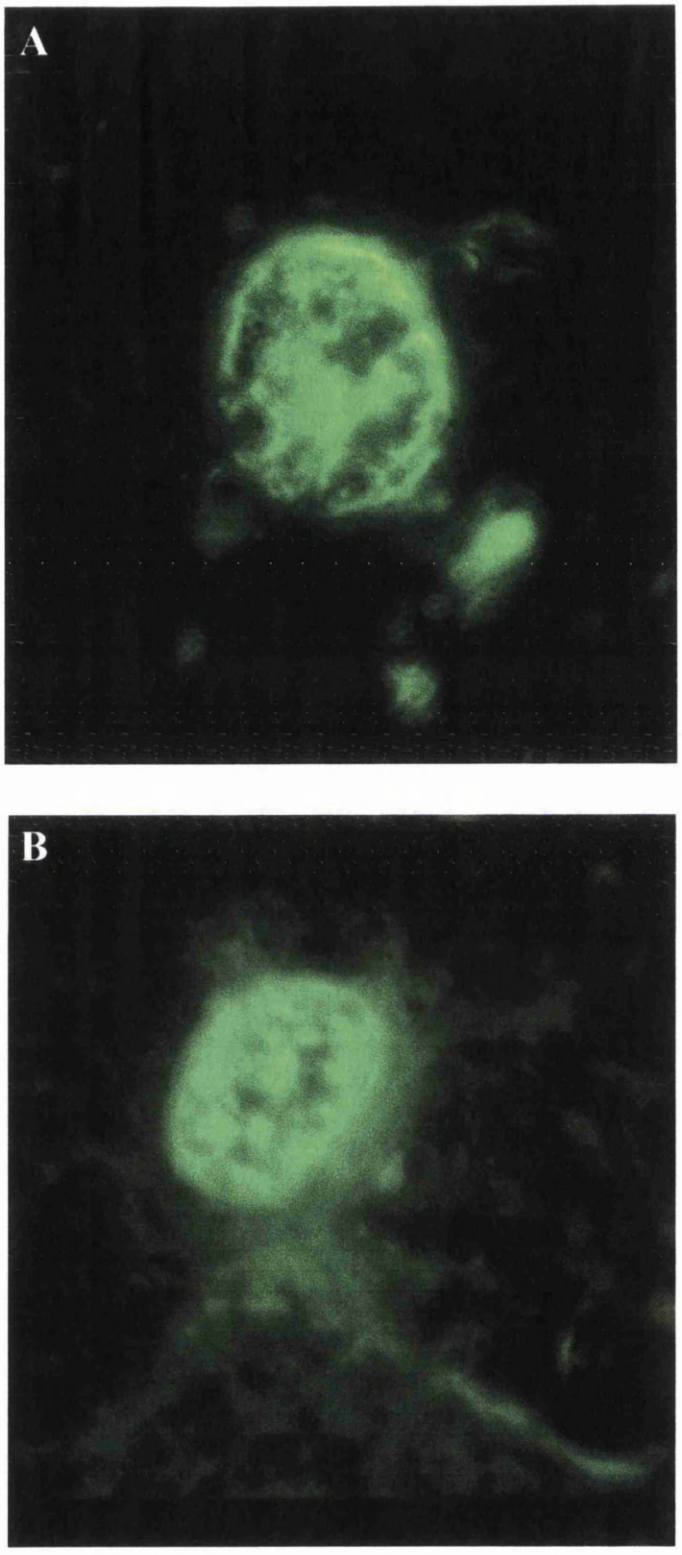

Ad egfp transfection of a large neuron (A) and a small neuron (B) in the caudate nucleus. (Original magnification X400). (Green = egfp).

Figure 40 **Association of ad egfp transfection with astrocytes and activated neurofilaments in subcortical white matter and caudate nucleus**

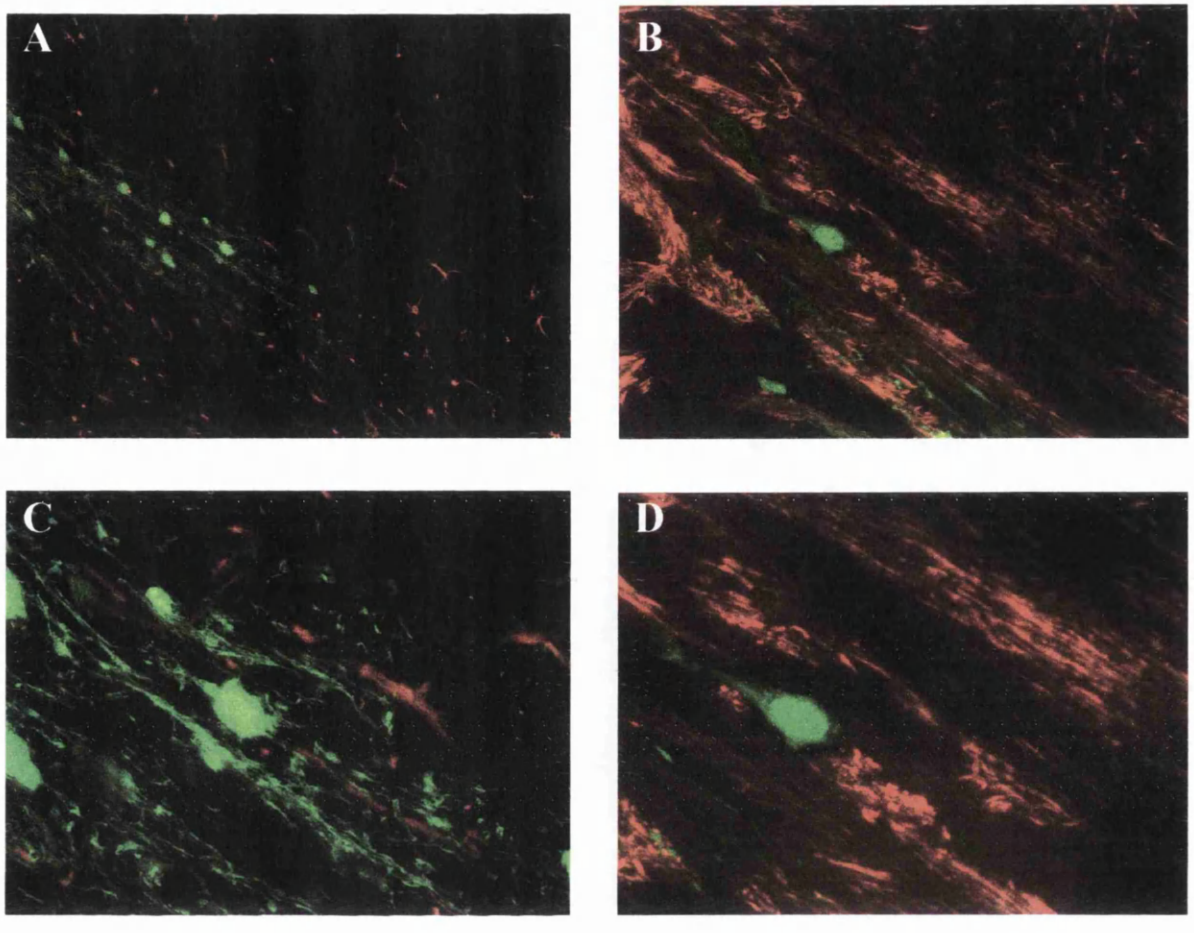

Ad egfp transfection was intimately associated with astrocytes (A, original magnification X100 and C, original magnification X400) and activated neurofilaments (A, original magnification X200 and D, original magnification X400). Standard immunohistochemical detection techniques were employed to detect astrocytes with anti-glial astrocytic fibrillary protein antibody and activated neurofilaments H and M with anti-SMI-31 antibody (Dr Julia Edgar). The secondary antibody used was labelled with rodamine, which produced the red fluorescence. (Green = egfp).

Figure 41 Ad egfp transfection in ependymal cells

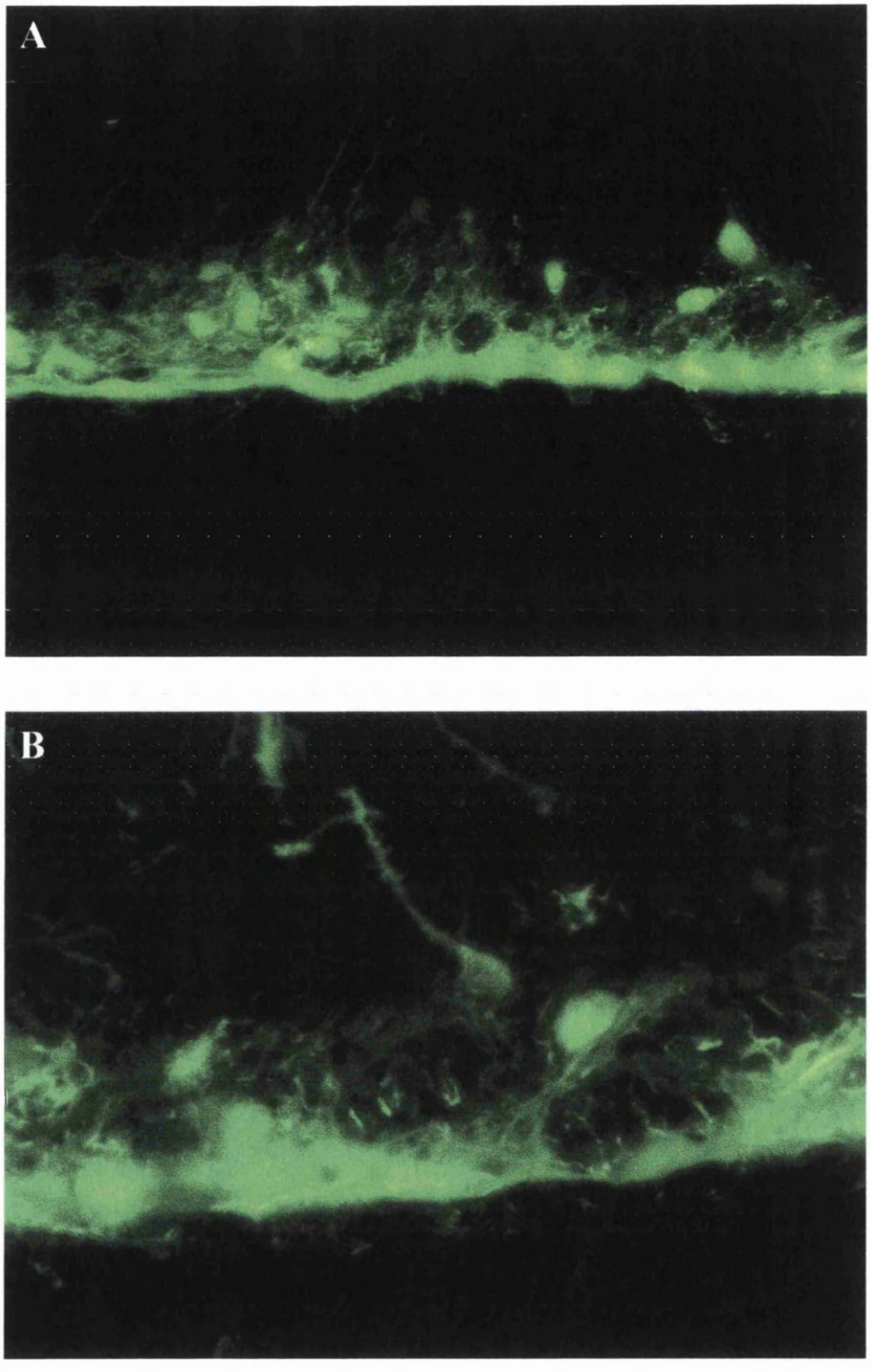

Intrastriatal injection of ad egfp occasionally resulted in transfection of ependymal cells of the ipsilateral lateral ventricle. (Green = egfp). (A, original magnification X200; B, original magnification X400).

3.3.3 Ischaemic neuronal damage in ad hsp 70i and ad egfp transfected mice following BCCAo

20-minute BCCAo

In ad hsp 70i transfected mice, ischaemic neuronal damage in the injected caudate nucleus was significantly reduced compared to ischaemic neuronal damage in the contralateral caudate nucleus (Figures 42 and 43). Ischaemic neuronal damage did not differ significantly between hemispheres in any of the four other brain regions analysed, irrespective of ad hsp 70i injection (Table 17). In ad egfp transfected mice, ischaemic neuronal damage in the injected caudate nucleus was significantly reduced compared to ischaemic neuronal damage in the contralateral caudate nucleus (Figures 42 and 43). Ischaemic neuronal damage did not differ significantly between hemispheres in any of the four other brain regions analysed, irrespective of ad egfp injection (Table 17).

10-minutes BCCAo

In ad hsp 70i transfected mice, ischaemic neuronal damage in the injected hemisphere did not differ significantly compared with ischaemic neuronal damage in the contralateral hemisphere in any of the five brain regions analysed (Table 18). In ad egfp transfected mice, ischaemic neuronal damage in the injected hemisphere did not differ significantly compared with ischaemic neuronal damage in the contralateral hemisphere in any of the five brain regions analysed (Table 18).

Figure 42 **Ischaemic neuronal damage in caudate nucleus of ad hsp 70i and ad egfp transfected mice: 20-minute BCCAo**

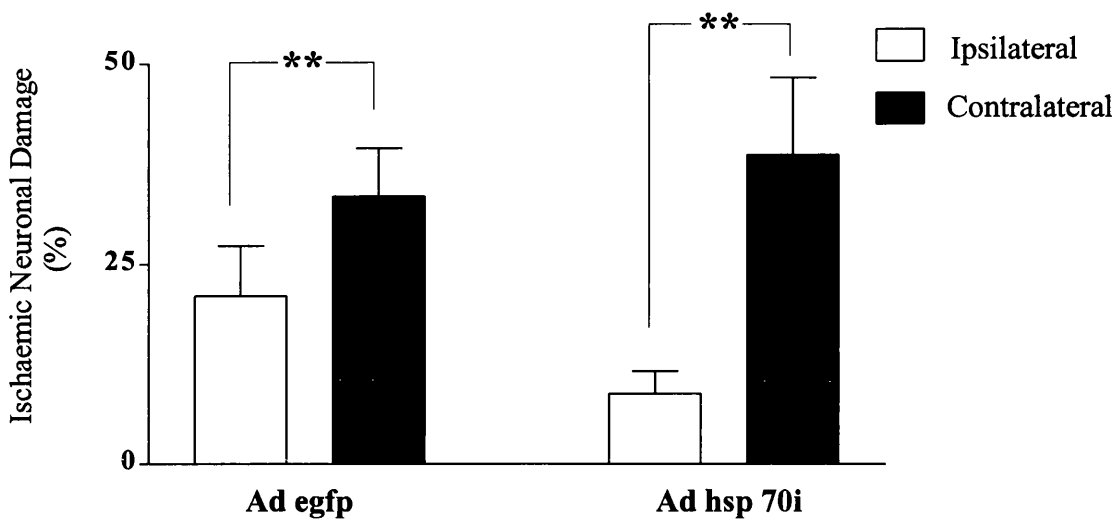

Intrastriatal injection of ad hsp 70i and ad egfp significantly reduced ischaemic neuronal damage in ipsilateral caudate nucleus (compared with contralateral caudate nucleus) produced by 20-minute BCCAo. Data are presented as mean ± standard error of the mean. **$p<0.01$ paired Student's *t*-test. (n = 9 ad hsp 70i; n = 8 ad egfp).

Figure 43 **Ischaemic neurones in caudate nucleus of ad hsp 70i and ad egfp transfected mice: 20-minute BCCAo**

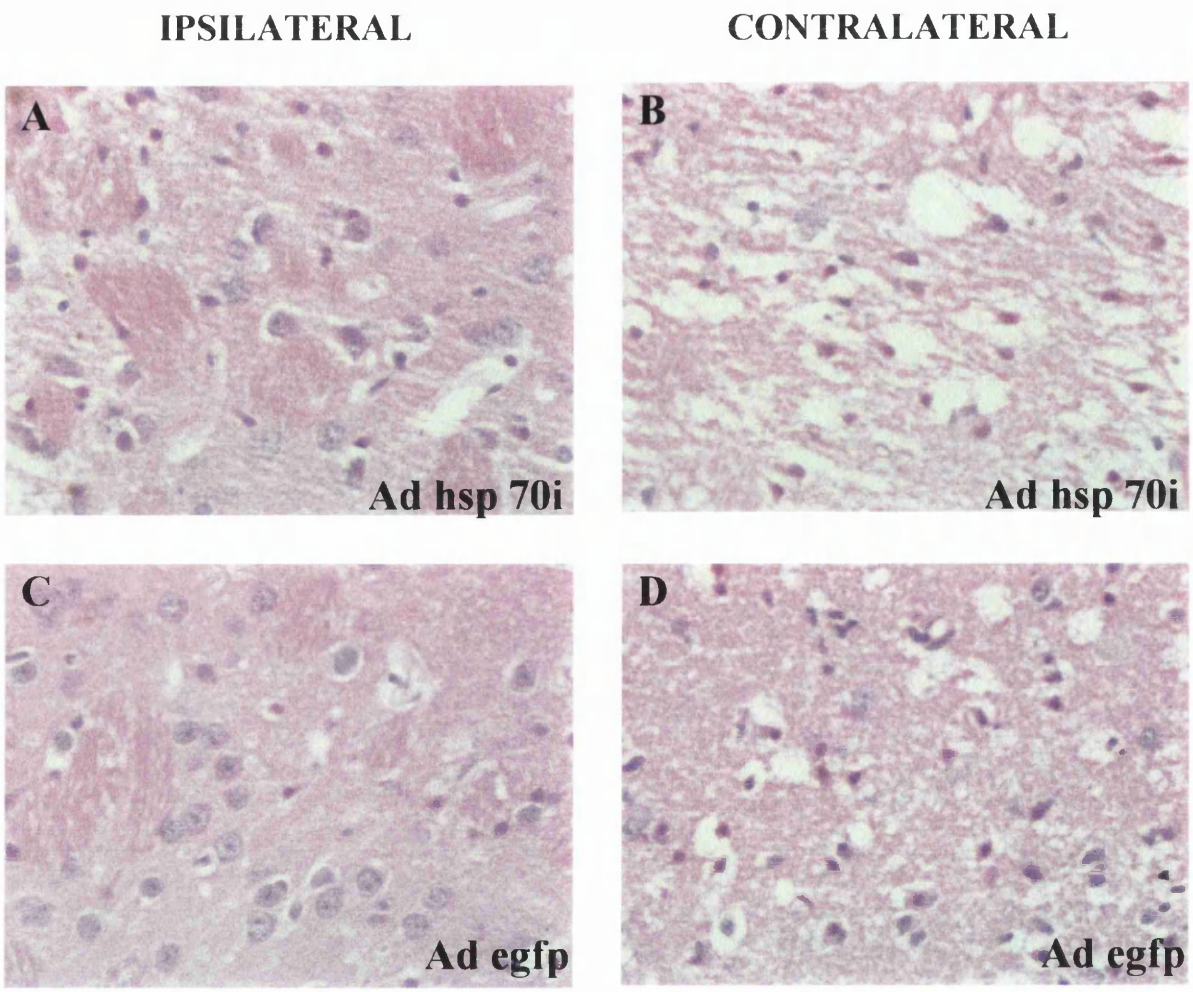

Ischaemic neuronal damage in ipsilateral caudate nucleus of ad hsp 70i (A) and ad egfp (C) transfected mice was significantly less than that in contralateral caudate nucleus (B and D, respectively). (Original magnification X200).

Table 17 **Ischaemic neuronal damage in ad hsp 70i and ad egfp transfected mice: 20-minute BCCAo**

	20-minute BCCAo			
	ADENOVIRUS HSP 70i (n=9)		ADENOVIRUS EGFP (n=8)	
	IPSI (%)	CONTRA (%)	IPSI (%)	CONTRA (%)
Hippocampus CA1	18.4 ± 8.5	15.5 ± 9.6	19.1 ± 9.8	20.7 ± 11.3
Hippocampus CA2	26.8 ± 11.0	20.9 ± 9.3	19.0 ± 10.6	11.1 ± 7.0
Hippocampus CA3	12.5 ± 7.1	5.6 ± 2.3	7.7 ± 2.3	4.7 ± 2.7
Dentate gyrus	3.7 ± 3.2	2.8 ± 2.7	0.8 ± 0.3	0.5 ± 0.3

Data are expressed as mean ± standard error of the mean. $p>0.05$ paired Student's *t*-test (ipsi versus contra). (IPSI = ipsilateral; CONTRA = contralateral).

Table 18 **Ischaemic neuronal damage in ad hsp 70i and ad egfp transfected mice: 10 minutes ischaemia**

	10-minute BCCAo			
	ADENOVIRUS HSP 70i (n=7)		ADENOVIRUS EGFP (n=6)	
	IPSI (%)	CONTRA (%)	IPSI (%)	CONTRA (%)
Caudate nucleus	3.4 ± 0.9	5.0 ± 1.2	2.8 ± 0.7	3.2 ± 1.1
Hippocampus CA1	4.7 ± 3.0	1.8 ± 0.4	13.3 ± 9.7	4.2 ± 0.8
Hippocampus CA2	3.6 ± 2.4	4.7 ± 3.4	11.7 ± 7.0	14.2 ± 7.7
Hippocampus CA3	4.6 ± 3.4	12.9 ± 8.3	5.1 ± 1.9	5.1 ± 1.2
Dentate gyrus	0.2 ± 0.2	0 ± 0	2.6 ± 2.4	0.2 ± 0.1

Data are expressed as mean ± standard error of the mean. $p>0.05$ paired Student's *t*-test (ipsi versus contra). (IPSI = ipsilateral; CONTRA = contralateral).

3.3.4 Hsp 70i immunoreactivity in ad hsp 70i and ad egfp transfected mice following BCCAo

20-minute BCCAo

In ad hsp 70i transfected mice, hsp 70i immunoreactivity in the injected caudate nucleus was significantly increased compared with hsp 70i immunoreactivity in the contralateral caudate nucleus (Figures 44 and 45). Hsp 70i immunoreactivity did not differ significantly between hemispheres in any of the four other brain regions analysed, irrespective of ad hsp 70i injection (Table 19, Appendix F). In ad egfp transfected mice, hsp 70i immunoreactivity in the injected caudate nucleus did not differ significantly from hsp 70i immunoreactivity in the contralateral caudate nucleus (Figure 44 and 46). Hsp 70i immunoreactivity did not differ significantly between hemispheres in any of the four other brain regions analysed, irrespective of ad egfp injection (Table 19).

10-minute BCCAo

In ad hsp 70i transfected mice, hsp 70i immunoreactivity in the injected caudate nucleus was significantly increased compared with hsp 70i immunoreactivity in the contralateral caudate nucleus (Figures 47 and 48). Hsp 70i immunoreactivity did not differ significantly between hemispheres in any of the four other brain regions analysed, irrespective of ad hsp 70i injection (Table 20). In ad egfp transfected mice, hsp 70i immunoreactivity in the injected caudate nucleus did not differ significantly from hsp 70i immunoreactivity in the contralateral caudate nucleus (Figure 47 and 48). Hsp 70i immunoreactivity did not differ significantly between hemispheres in any of the four other brain regions analysed, irrespective of ad egfp injection (Table 20).

Figure 44 **Hsp 70i immunoreactive neurones in caudate nucleus of ad hsp 70i and ad egfp transfected mice: 20-minute BCCAo**

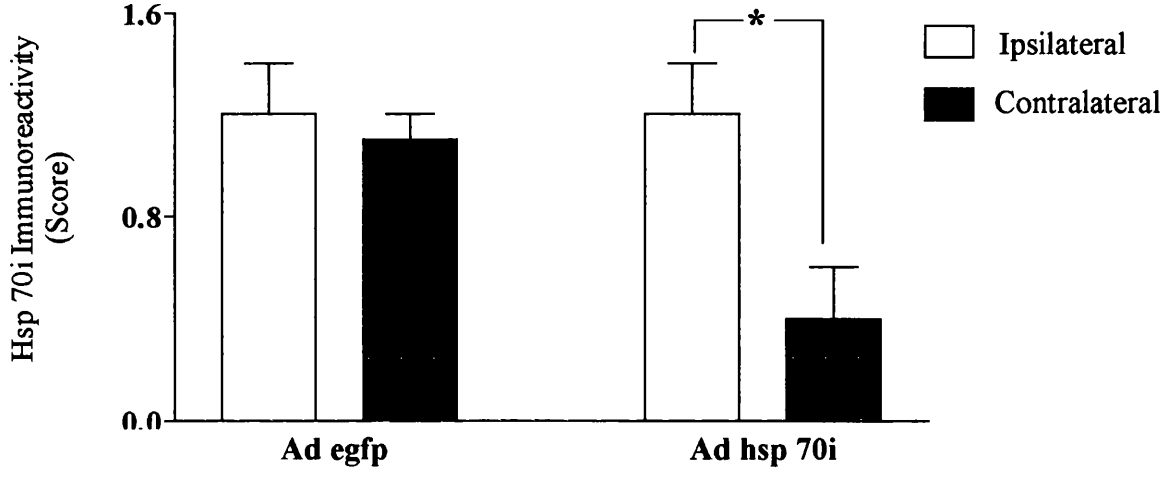

Intrastriatal injection of ad hsp 70i displayed significantly increased numbers of hsp 70i immunoreactive neurones in ipsilateral caudate nucleus (compared with contralateral caudate nucleus) following 20-minute BCCAo. Hsp 70i immunoreactive neurones in ipsilateral and contralateral caudate nucleus of ad egfp transfected mice were similar. Data are presented as mean ± standard error of the mean. *$p<0.05$ paired Student's *t*-test. (n = 9 ad hsp 70i; n = 8 ad egfp).

Figure 45 **Hsp 70i immunoreactive neurones in caudate nucleus of ad hsp 70i transfected mice: 20-minute BCCAo**

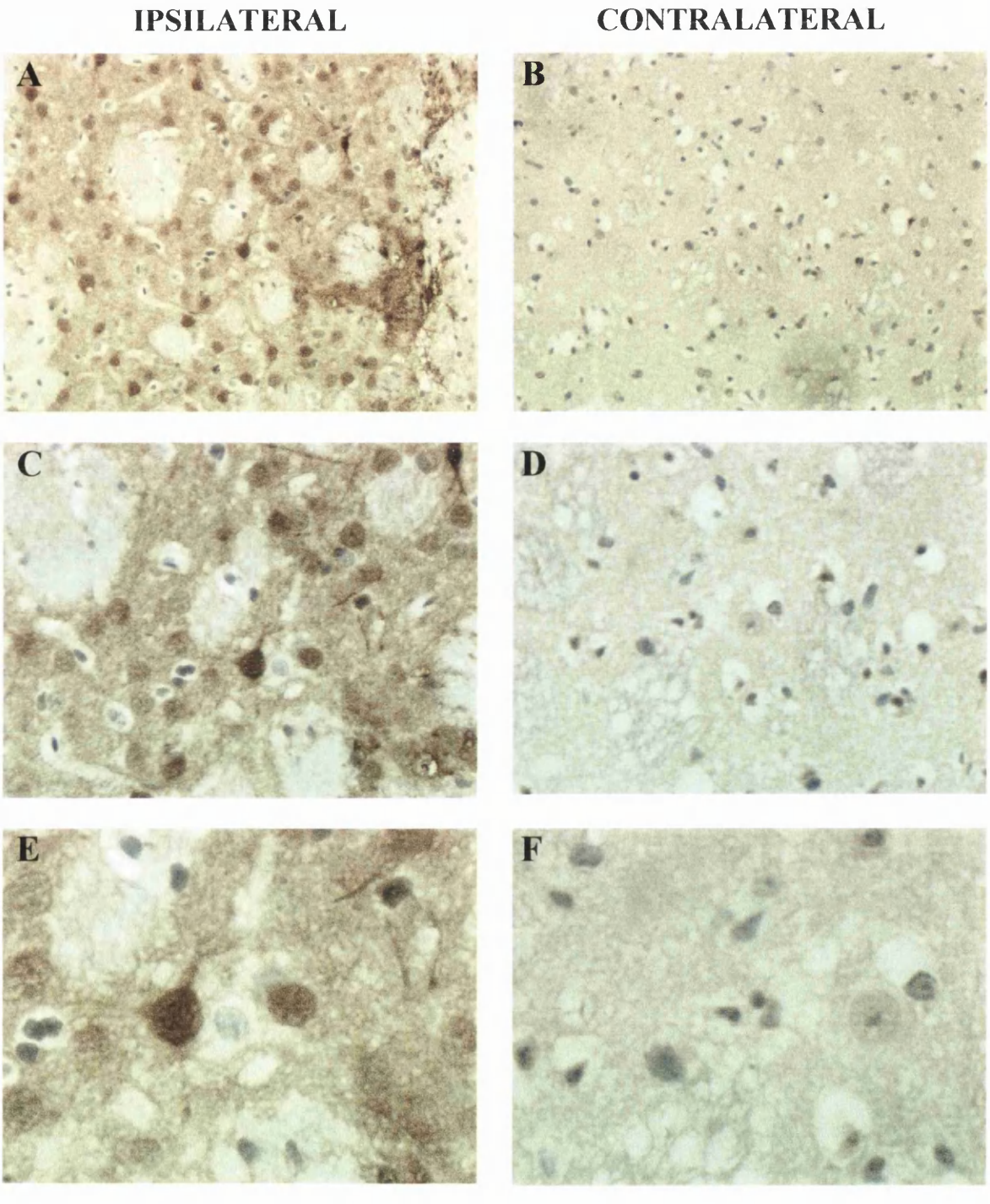

Significantly more hsp 70i immunoreactive neurones in ipsilateral caudate nucleus of ad hsp 70i transfected mice subjected to 20-minute BCCAo. (A and B, original magnification X100; C and D, original magnification X200; E and F, original magnification X400).

Figure 46 **Hsp 70i immunoreactive neurones in caudate nucleus of ad egfp transfected mice: 20-minute BCCAo**

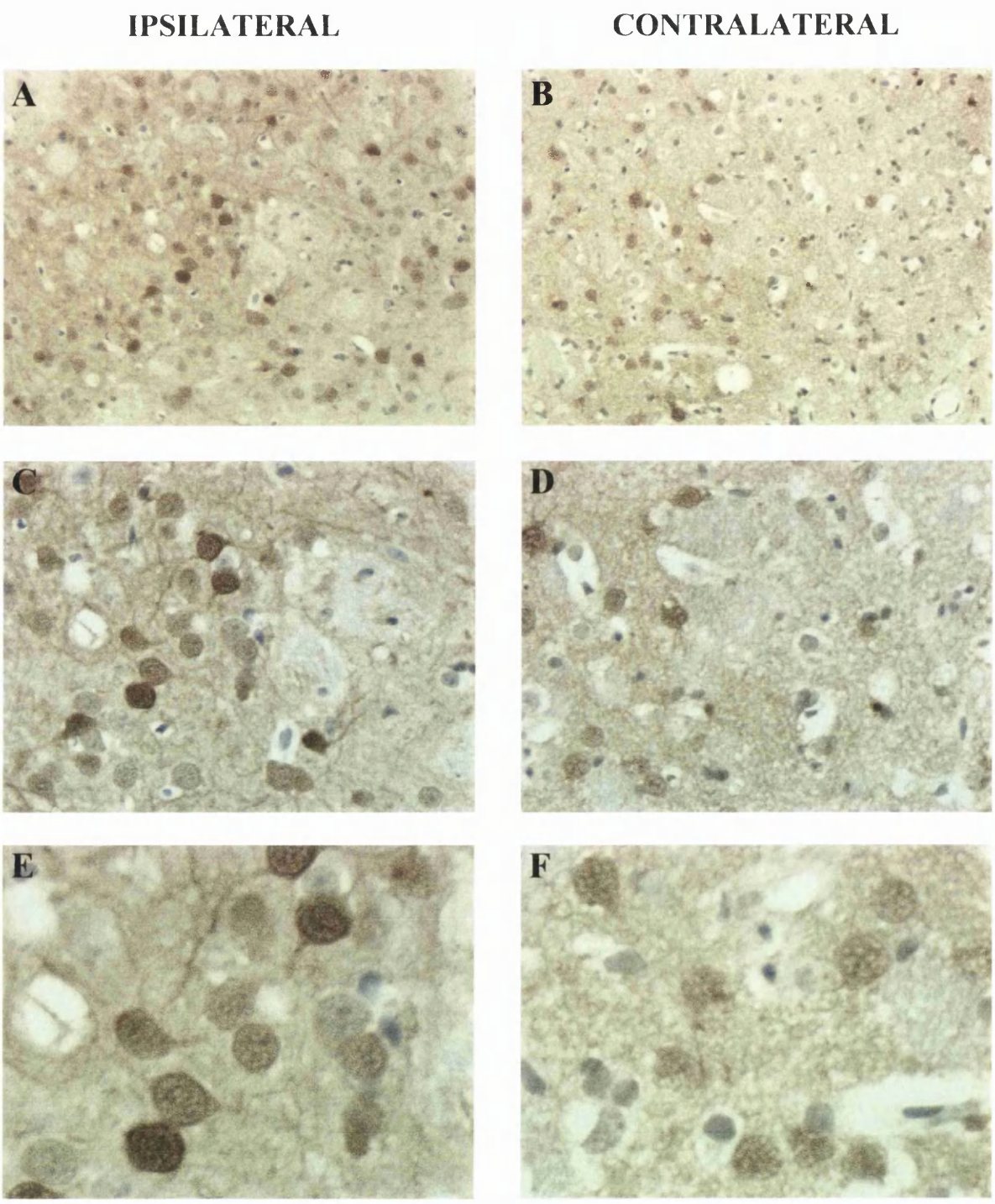

Hsp 70i immunoreactive neurones in ipsilateral and contralateral caudate nucleus of ad egfp transfected mice subjected to 20-minute BCCAo were similar in number. (A and B, original magnification X100; C and D, original magnification X200; E and F, original magnification X400).

Table 19 **Hsp 70i immunoreactive neurones in ad hsp 70i and ad egfp transfected mice: 20-minute BCCAo**

	20-minute BCCAo			
	ADENOVIRUS HSP 70i (n=9)		ADENOVIRUS EGFP (n=8)	
	IPSI	CONTRA	IPSI	CONTRA
Hippocampus CA1	0.6 ± 0.3	0.3 ± 0.2	0.2 ± 0.2	0.5 ± 0.4
Hippocampus CA2	0.6 ± 0.3	0.3 ± 0.2	0 ± 0	0.1 ± 0.1
Hippocampus CA3	0.6 ± 0.3	0.3 ± 0.2	0.2 ± 0.2	0.5 ± 0.2
Dentate gyrus	0.2 ± 0.2	0 ± 0	0 ± 0	0.1 ± 0.1

Semi-quantitative assessment of immunoreactive neurones 0 = no hsp70i immunoreactive neurones; 1 = a few hsp 70i immunoreactive neurones; 2 = many hsp 70i immunoreactive neurones; and 3 = very many of hsp 70i immunoreactive neurones. Data are expressed as mean ± standard error of the mean. $p>0.05$ paired Student's *t*-test (ipsi versus contra). (IPSI = ipsilateral; CONTRA = contralateral).

Figure 47 **Hsp 70i immunoreactive neurones in caudate nucleus of ad hsp 70i and ad egfp transfected mice: 10-minute BCCAo**

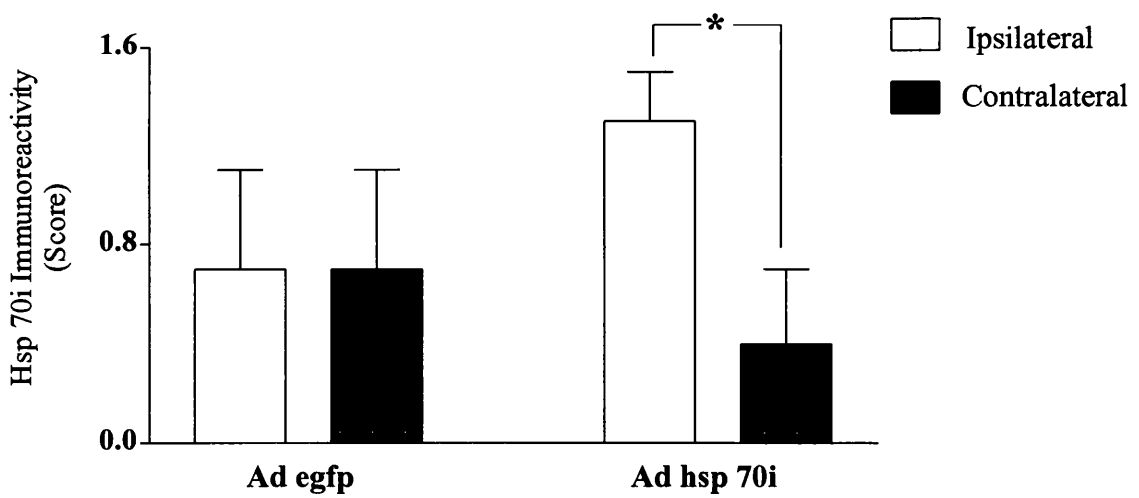

Mice intrastriatally injected with ad hsp 70i displayed significantly increased numbers of hsp 70i immunoreactive neurones in ipsilateral caudate nucleus (compared with contralateral caudate nucleus) following 10-minute BCCAo. Hsp 70i immunoreactive neurones in ipsilateral and contralateral caudate nucleus ad egfp transfected mice were similar. Data are presented as mean ± standard error of the mean. *$p<0.05$ paired Student's *t*-test. (n = 7 ad hsp 70i; n = 6 ad egfp).

Figure 48 **Hsp 70i immunoreactive neurones in caudate nucleus of ad hsp 70i and ad egfp transfected mice: 10-minute BCCAo**

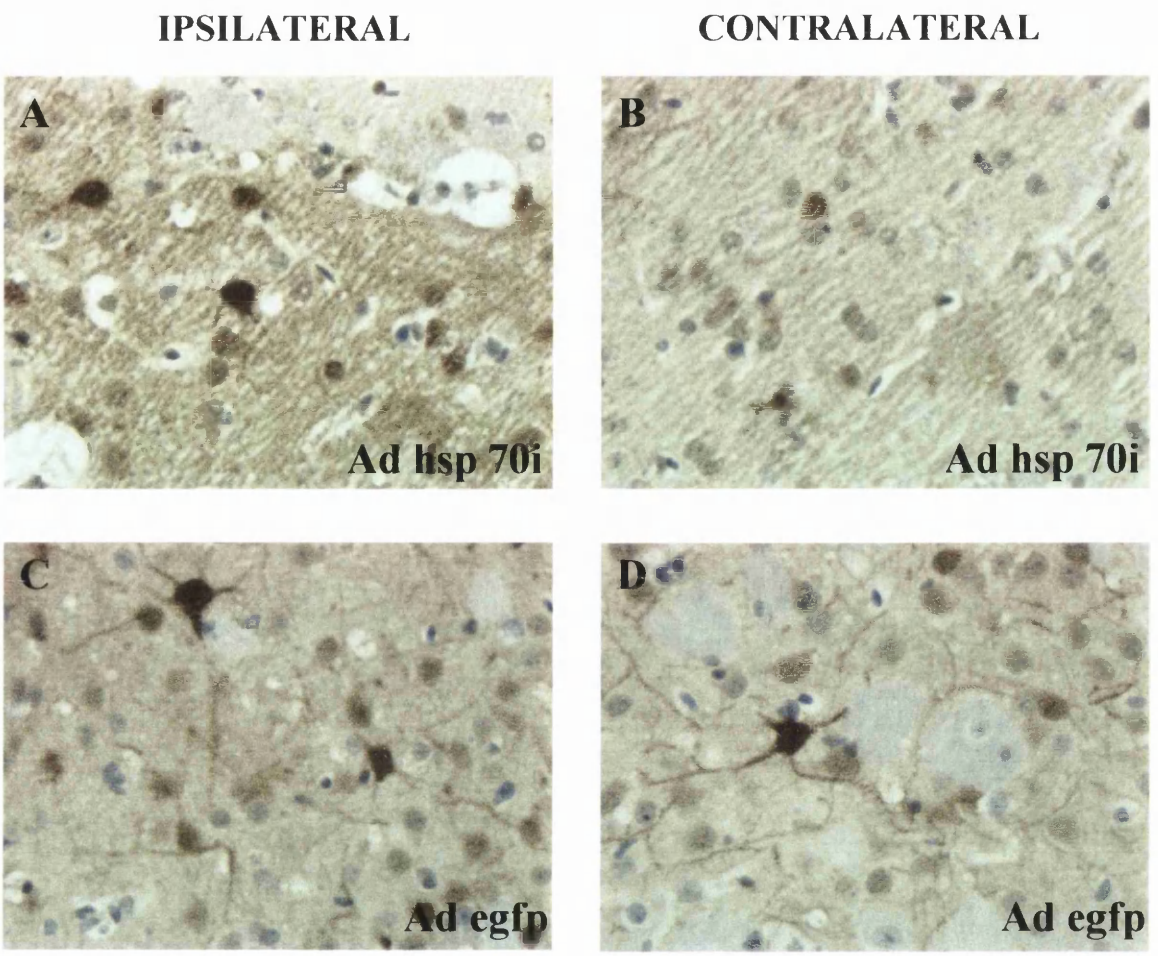

Significantly more hsp 70i immunoreactive neurones in ipsilateral caudate nucleus of ad hsp 70i transfected mice subjected to 10-minute BCCAo (A and B, original magnification X200). Hsp 70i immunoreactive neurones in ipsilateral and contralateral caudate nucleus of ad egfp transfected mice were similar in number. (C and D, original magnification X400).

Table 20 **Hsp 70i immunoreactive neurones in ad hsp 70i and ad egfp transfected mice: 10-minute BCCAo**

	10-minute BCCAo			
	ADENOVIRUS HSP 70i (n=7)		ADENOVIRUS EGFP (n=6)	
	IPSI	CONTRA	IPSI	CONTRA
Hippocampus CA1	0.3 ± 0.3	0.4 ± 0.2	0.7 ± 0.2	0.5 ± 0.2
Hippocampus CA2	0 ± 0	0 ± 0	0.2 ± 0.2	0 ± 0
Hippocampus CA3	0.4 ± 0.2	0.6 ± 0.2	0.7 ± 0.2	0.5 ± 0.2
Dentate gyrus	0 ± 0	0 ± 0	0 ± 0	0 ± 0

Semi-quantitative assessment of immunoreactive neurones 0 = no hsp70i immunoreactive neurones; 1 = a few hsp 70i immunoreactive neurones; 2 = many hsp 70i immunoreactive neurones; and 3 = very many of hsp 70i immunoreactive neurones. Data are expressed as mean ± standard error of the mean. $p>0.05$ paired Student's *t*-test (ipsi versus contra). (IPSI = ipsilateral; CONTRA = contralateral).

3.3.5 Structural and inflammatory response following ad injection

Intrastriatal injection of ad hsp 70i and ad egfp produced localised damage in the caudate nucleus (Figure 49), cortex and subcortical white matter. Furthermore, intrastriatal injection of ad hsp 70i and ad egfp resulted in infiltration of inflammatory cells (Figure 49). Structural deformation and inflammatory response in ad hsp 70i and ad egfp injected mice were similar (Figure 49).

Figure 49 Needle damage and inflammatory cells after ad injection

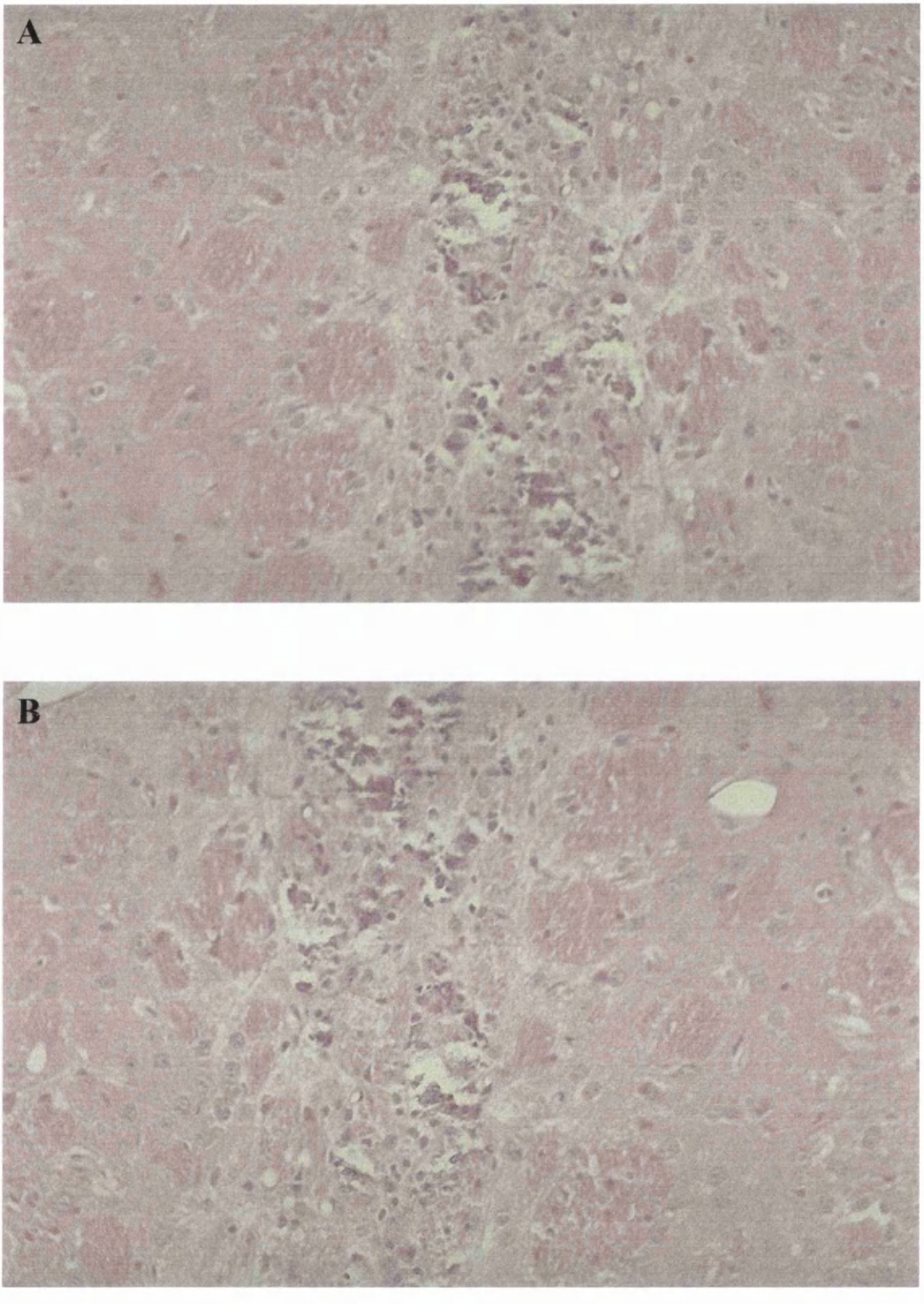

Intrastriatal injection of ad hsp 70i (A) and ad egfp (B) resulted in localised structural deformation and infiltration of inflammatory cells of the caudate nucleus. (Original magnification X50).

3.4 Mapping brain function in transgenic mice over-expressing hsp 70i

LCGU was estimated in transgenic mice over-expressing hsp 70i and their wild type littermates using ^{14}C-2-deoxyglucose autoradiography (see Section 2.7 for details). LCGU was measured in the basal state (following intraperitoneal injection with sterile saline, 0.4ml) and following metabolic activation (intraperitoneal injection with dizocilpine 1mg/kg dissolved in 0.4ml sterile saline).

3.4.1 Behaviour following intraperitoneal injection with dizocilpine

All mice intraperitoneally injected with dizocilpine displayed overt behavioural changes. These changes were predominantly increases in motor activity (typically repetitive movement of the head) and elevated excitability. The magnitude of these responses was broadly similar in all mice, irrespective of genotype. None of the mice intraperitoneally injected with saline displayed abnormal or overt changes in behaviour, irrespective of genotype.

3.4.2 Plasma ^{14}C and glucose concentrations

Plasma ^{14}C and glucose concentrations in transgenic mice over-expressing hsp 70i did not differ significantly from plasma ^{14}C and glucose concentrations in wild type littermate mice, irrespective of dizocilpine or saline injection (Table 21). Moreover, terminal plasma ^{14}C / glucose ratio correlated well with tissue ^{14}C (cerebellar cortical grey matter), irrespective of treatment or genotype (Figure 50).

Table 21 Plasma ^{14}C and glucose concentrations in hsp 70i transgenic mice

	hsp 70i transgenic		wild type littermates	
	SALINE (n=7)	**DIZOCILPINE** (n=7)	**SALINE** (n=7)	**DIZOCILPINE** (n=7)
Plasma ^{14}C (nCi/g)	35.8 ± 4.4	41.1 ± 3.7	28.9 ± 4.4	41.4 ± 4.0
Plasma glucose (mM)	10.1 ± 0.5	9.7 ± 0.6	8.7 ± 0.8	9.0 ± 0.4

Data are expressed as mean ± standard error of the mean. $p>0.05$ One way analysis of variance followed by unpaired Student's *t*-test with Bonferroni correction factor of four.

Figure 50 Relationship between tissue ^{14}C and terminal plasma ^{14}C / glucose ratio

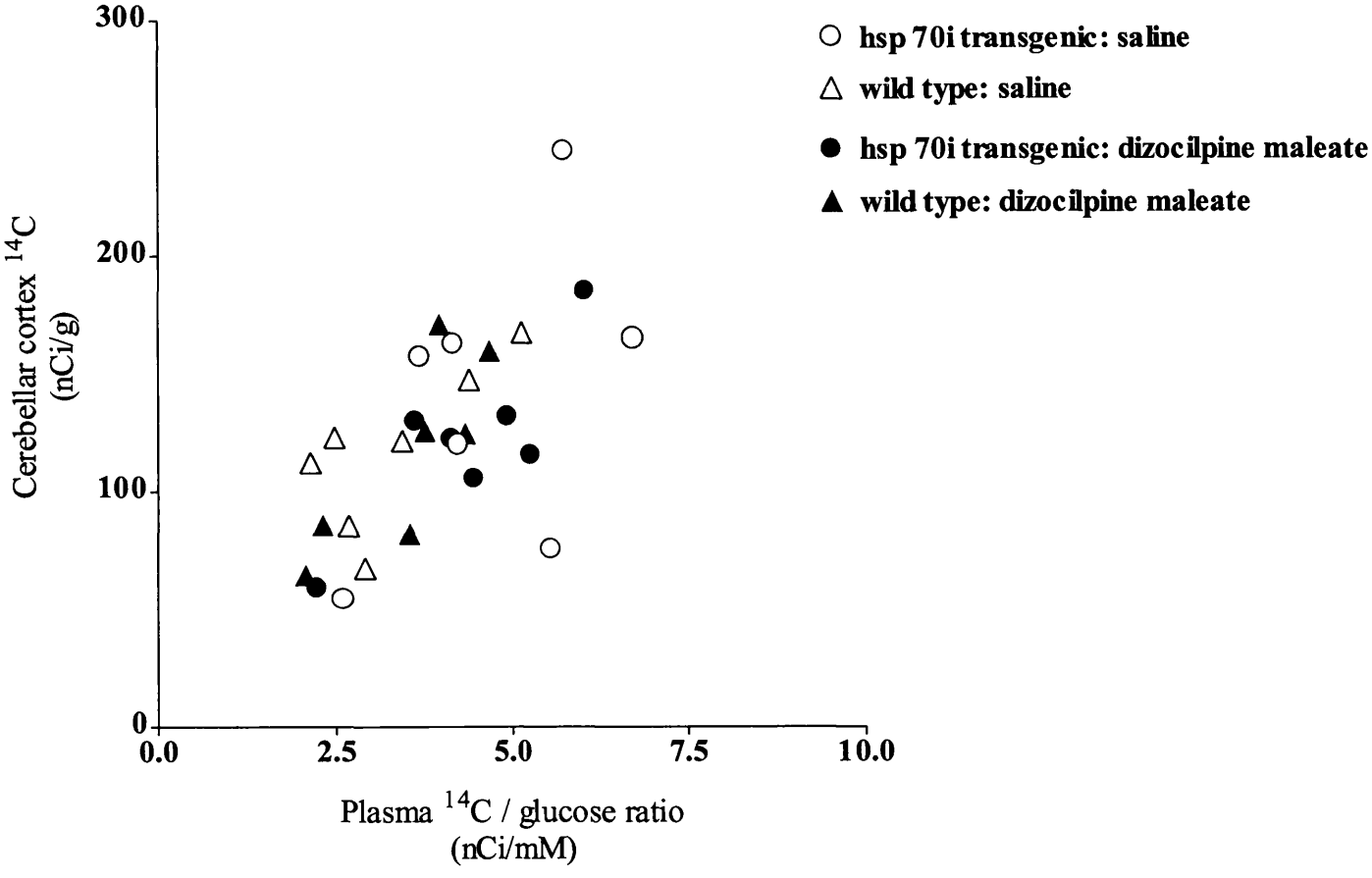

The relationship between cerebellar cortical ^{14}C concentration and plasma ^{14}C / glucose was similar between groups, irrespective of treatment and genotype. (n=7 per group).

3.4.3 LCGU in hsp 70i transgenic and wild type littermate mice

Following intraperitoneal injection of saline

LCGU in transgenic mice over-expressing hsp 70i did not differ significantly from LCGU in wild type littermate mice in any of the 35 brain regions analysed, following saline injection (Table 22, Figures 51, 52, 53 and 54). This was true even of brain regions known to over-express the hsp 70i transgene, such as, hippocampus CA1, caudate nucleus and anterior thalamus.

Following intraperitoneal injection with dizocilpine

In hsp 70i transgenic mice, intraperitoneal injection of dizocilpine evoked widespread, heterogeneous alterations in LCGU compared with intra-peritoneal injection with saline (Table 23, Figure 51, 52, 53 and 54). LCGU was markedly increased in 22 brain regions, including several regions of the limbic system. LCGU was significantly decreased in two brain regions, sensory motor cortex and inferior colliculus. There were no significant alterations in LCGU in any of the remaining 11 brain regions analysed (Table 23).

In wild type littermate mice, intraperitoneal injection of dizocilpine evoked widespread, heterogeneous alterations in LCGU compared with intraperitoneal injection of saline (Table 24, Figures 51, 52, 53 and 54). LCGU was markedly increased in 20 brain regions, including several regions of the limbic system. LCGU was significantly decreased in two brain regions, sensory motor cortex and inferior colliculus. There were no significant alterations in LCGU in any of the remaining brain regions analysed (Table 24).

Intraperitoneal injection of dizocilpine evoked significant alterations in LCGU in five brain regions between transgenic mice over-expressing hsp 70i and their wild type littermates (Table 25, Figures 51, 52, 53 and 54). LCGU in hsp 70i transgenic mice was significantly greater in three brain regions (anterior thalamic nucleus, Hippocampus CA1 stratum oriens

and hippocampus CA1 stratum lacunosum moleculare, Figures 51, 52 and 53) than in wild type littermate mice. LCGU in hsp 70i transgenic mice was markedly lower in two brain regions (superior olivary body and nucleus of the lateral lemniscus, Figure 54) than in wild type littermate mice. There were no significant differences in LCGU in any of the remaining 30 brain regions analysed between hsp 70i transgenic and wild type littermate mice following intraperitoneal injection of dizocilpine (Table 25).

Figure 51 Increased LCGU in hsp 70i transgenic mice: dizocilpine injected

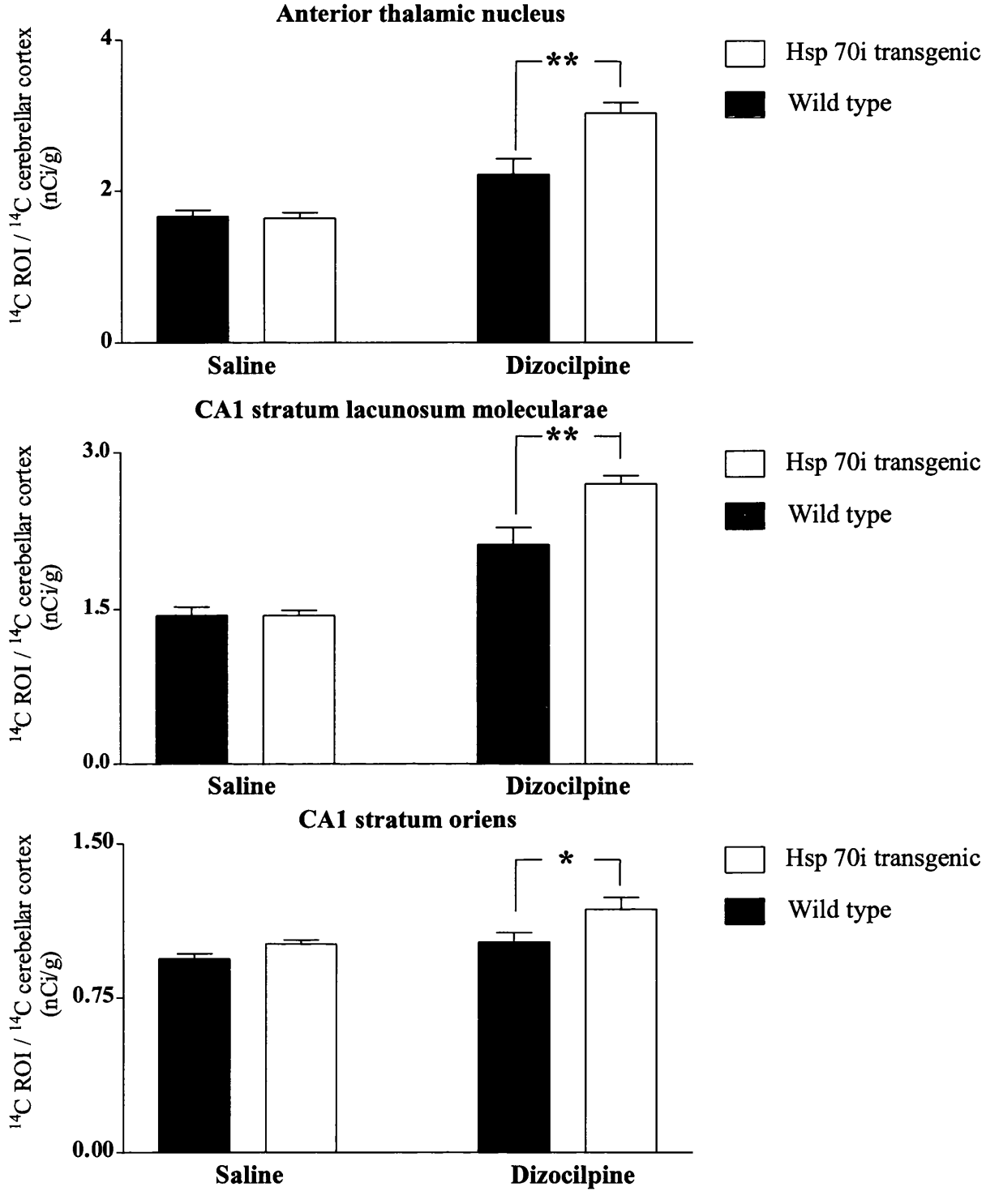

Following intraperitoneal injection with dizocilpine LCGU in hsp 70i transgenic mice was significantly increased in anterior thalamic nucleus, hippocampus CA1 stratum laucunosum moleculare and CA1 stratum oriens compared with wild type littermate mice. LCGU in dizocilpine injected mice was significantly increased compared to that in saline injected mice (not highlighted on graph, see Tables 22 and 23). Data are presented as mean ± standard error of the mean. *$p<0.05$; **$p<0.01$ One way analysis of variance followed by unpaired Student's *t*-test with Bonferroni correction factor of four. (n = 7 per group; ROI = region of interest)

Figure 52 Representative ^{14}C-2-deoxyglucose autoradiograms of dorsal hippocampus

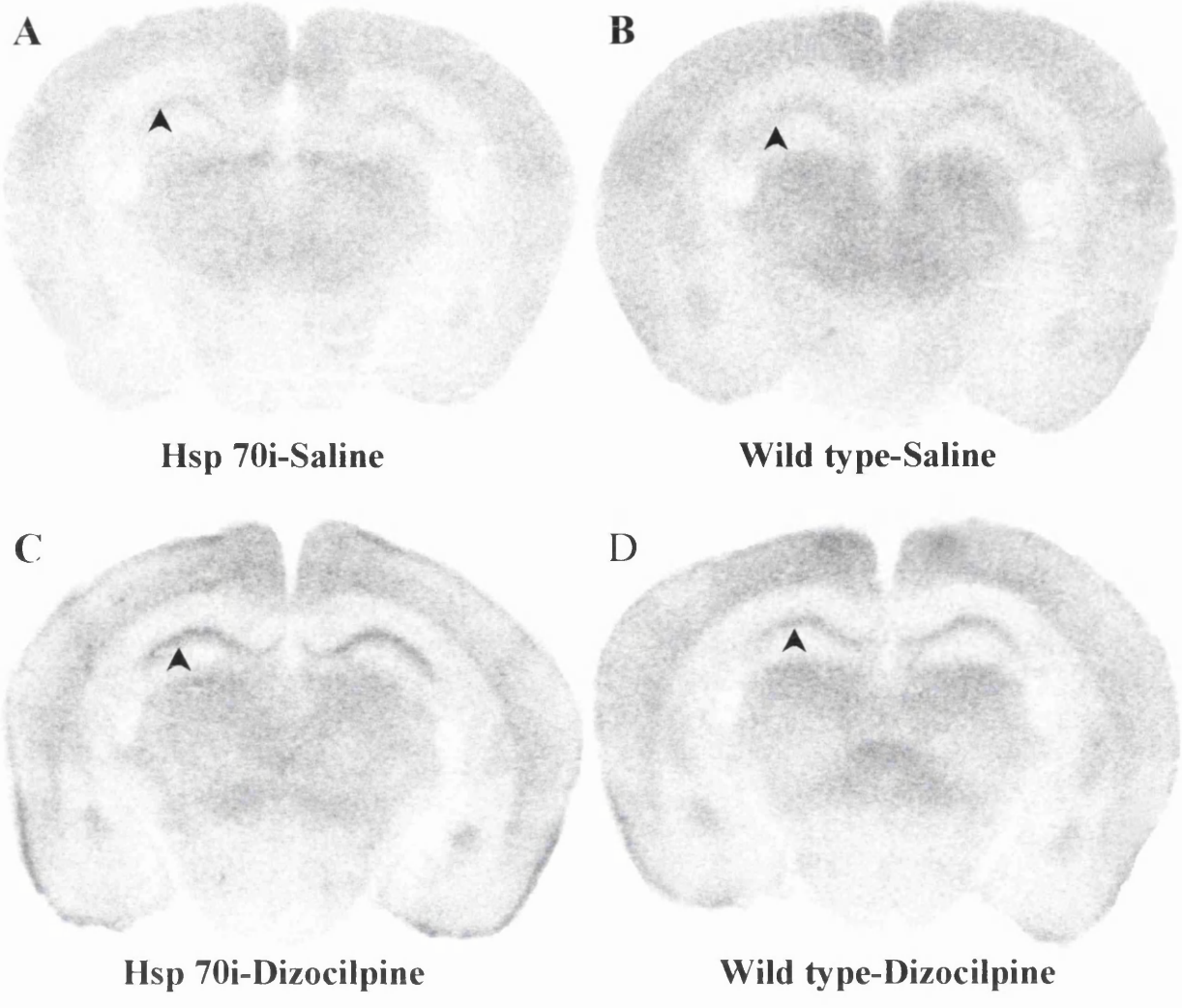

Representative examples of ^{14}C-2-deoxyglucose autoradiograms at the level of the dorsal hippocampus from hsp 70i transgenic saline injected mice (A), wild type littermate saline injected mice (B), hsp 70i transgenic dizocilpine injected mice (C), and wild type littermate dizocilpine injected mice (D). Dorsal hippocampus CA1 stratum lacunosum (CA1 slm, arrows) in dizocilpine injected mice (C and D) exhibit increased LCGU compared to saline injected mice (A and B, respectively). Furthermore, LCGU in CA1 slm in dizocilpine injected hsp 70i transgenic mice (C) is increased compared to CA1 slm in dizocilpine injected wild type littermate mice (D).

Figure 53 Representative ^{14}C-2-deoxyglucose autoradiograms of anterior thalamic nuclei

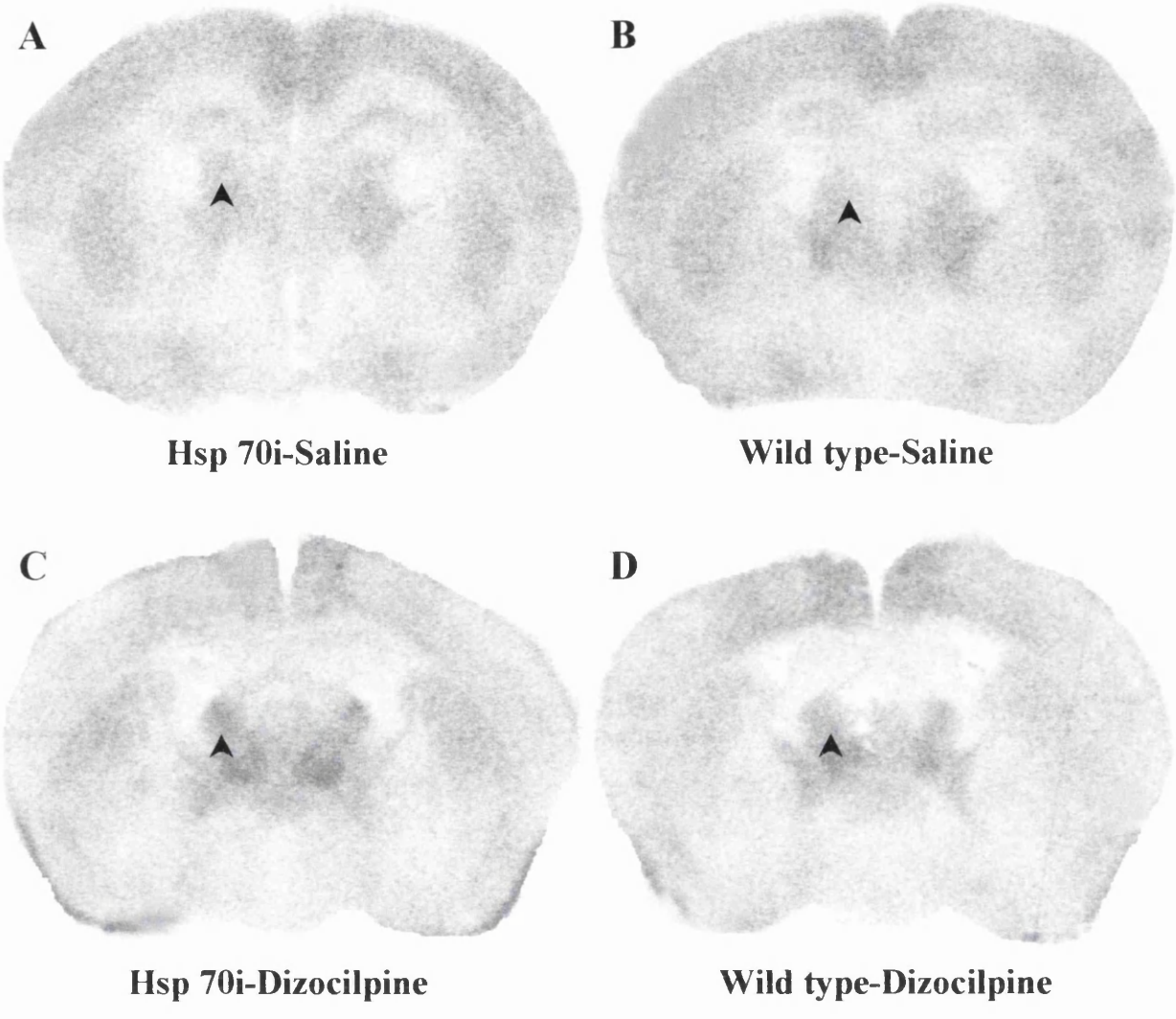

Representative examples of ^{14}C-2-deoxyglucose autoradiograms at the level of the anterior thalamic nucleus from hsp 70i transgenic saline injected mice (A), wild type littermate saline injected mice (B), hsp 70i transgenic dizocilpine injected mice (C), and wild type littermate dizocilpine injected mice (D). Anterior thalamic nucleus (ATN, arrows) in dizocilpine injected mice (C and D) exhibit increased LCGU compared to saline injected mice (A and B, respectively). Furthermore, LCGU in ATN in dizocilpine injected hsp 70i transgenic mice (C) is increased compared to ATN in dizocilpine injected wild type littermate mice (D).

Figure 54 Decreased LCGU in hsp 70i transgenic mice: dizocilpine injected

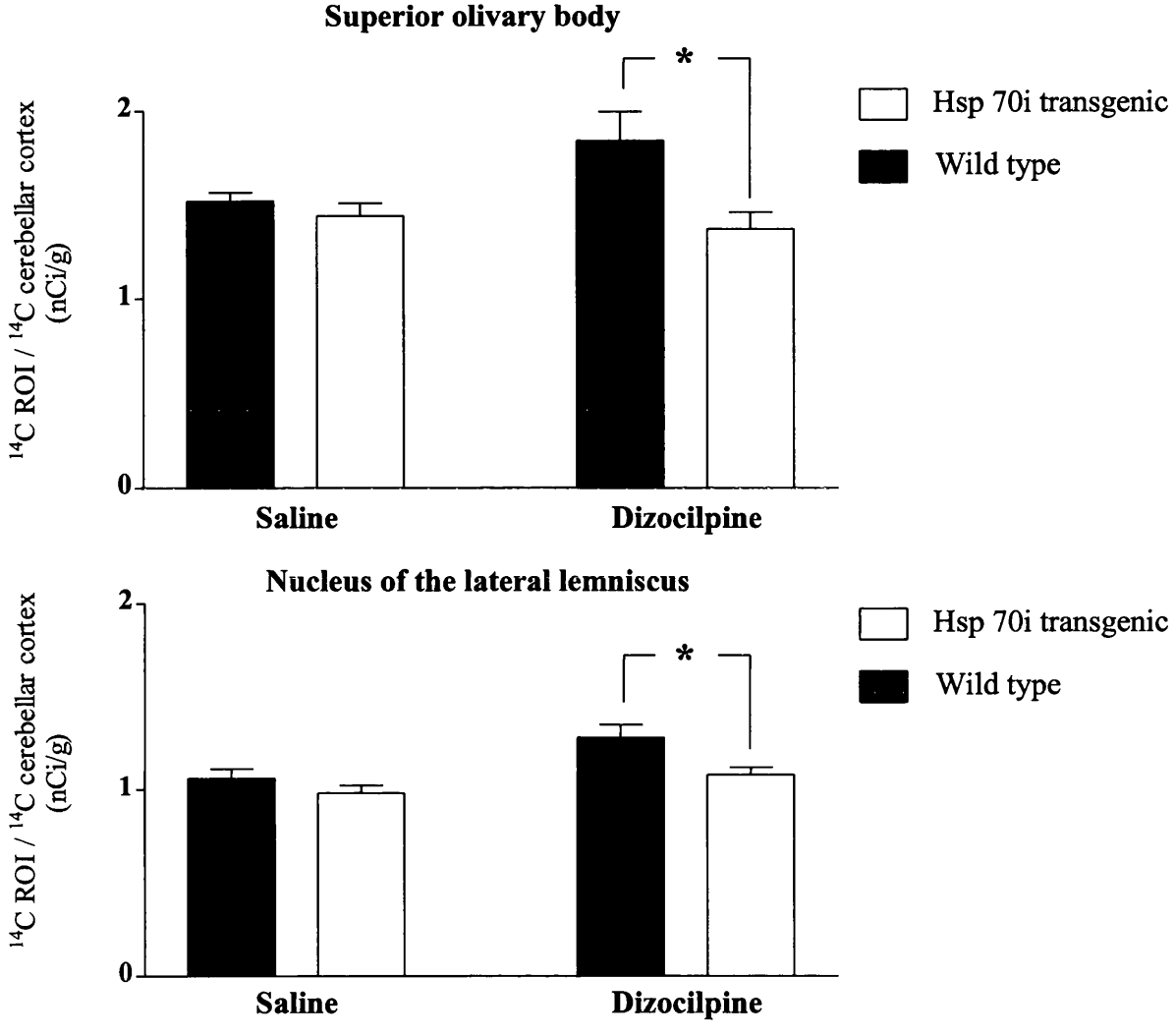

Following intraperitoneal injection with dizocilpine LCGU in hsp 70i transgenic mice was significantly decreased in superior olivary body and nucleus of the lateral lemniscus compared with wild type littermate mice. Data are presented as mean ± standard error of the mean. *$p<0.05$ One way analysis of variance followed by unpaired Student's *t*-test with Bonferroni correction factor of four.

(n = 7 per group; ROI = region of interest)

Table 22 LCGU in hsp 70i transgenic and wild type littermate mice: saline injected

	hsp 70i transgenic SALINE (n=7)	wild type littermates SALINE (n=7)
Anterior thalamic nucleus	1.64 ± 0.072	1.66 ± 0.083
Dorsal CA 1 stratum lacunosum moleculare	1.44 ± 0.049	1.44 ± 0.083
Superior olivary body	1.44 ± 0.068	1.52 ± 0.045
Dorsal hippocampus CA 1 stratum oriens	1.01 ± 0.019	0.94 ± 0.023
Nucleus of the lateral lemniscus	0.98 ± 0.042	1.16 ± 0.053
Lateral caudate nucleus	1.54 ± 0.053	1.34 ± 0.034
Hippocampus CA 1 stratum lacunosum moleculare	1.26 ± 0.042	1.24 ± 0.057
Vestibular nucleus	1.77 ± 0.034	1.80 ± 0.045
Superior colliculus	1.40 ± 0.045	1.38 ± 0.049
Lateral ventro dorsal thalamus	1.61 ± 0.06	1.69 ± 0.087
Medial beniculate body	1.25 ± 0.049	1.32 ± 0.053
Sensory motor cortex	1.59 ± 0.057	1.51 ± 0.045
Hypothalamus	0.75 ± 0.038	0.69 ± 0.060
Inferior colliculus	2.25 ± 0.260	2.77 ± 0.068
Lateral septal nuclei	0.94 ± 0.038	0.83 ± 0.038
Amygdala	1.15 ± 0.026	1.15 ± 0.030
Substantia nigra pars compacta	1.05 ± 0.030	1.17 ± 0.049
Anterior pyriform cortex	1.73 ± 0.083	1.59 ± 0.068
Dentate gyrus	0.86 ± 0.026	0.79 ± 0.026
Anterior commisure	0.96 ± 0.049	0.91 ± 0.026
Medial caudate nucleus	1.55 ± 0.042	1.31 ± 0.049
Ventromedial thalamus	1.53 ± 0.049	1.57 ± 0.026
Medial mammillary body	1.94 ± 0.064	1.79 ± 0.052
Anterior cingulate cortex	1.62 ± 0.298	1.51 ± 0.057
Anteromedial thalamic nuclei	1.50 ± 0.053	1.53 ± 0.098
Subthalamic nucleus	1.27 ± 0.049	1.32 ± 0.068
Globus pallidus	0.86 ± 0.038	0.85 ± 0.053
Posterior entorhinal cortex	1.05 ± 0.049	1.07 ± 0.049
Lateral habenular nuclei	1.06 ± 0.019	1.04 ± 0.049
Lateral geniculate body	1.21 ± 0.026	1.27 ± 0.068
Mediolateral posterior thalamus	1.62 ± 0.053	1.62 ± 0.042
Substantia nigra pars reticulata	0.81 ± 0.026	0.79 ± 0.034
Nucleus accumbens	0.79 ± 0.042	0.68 ± 0.038
Posterior cingulate cortex	1.86 ± 0.042	1.75 ± 0.049
Pontine reticular formation	1.03 ± 0.026	1.08 ± 0.026

Data are expressed as mean ratio of ^{14}C in region of interest / ^{14}C in cerebellar cortex (nCi/g) ± standard error of the mean. $p>0.05$ One way analysis of variance followed by unpaired Student's *t*-test with Bonferroni correction factor of four.

Table 23 LCGU in hsp 70i transgenic mice: saline versus dizocilpine injected

	hsp 70i transgenic SALINE (n=7)	hsp 70i transgenic DIZOCILPINE (n=7)
Anterior thalamic nucleus	1.64 ± 0.072	3.04 ± 0.136 ***
Dorsal CA 1 stratum lacunosum moleculare	1.44 ± 0.049	2.70 ± 0.079 ***
Superior olivary body	1.24 ± 0.068	1.37 ± 0.090
Dorsal hippocampus CA 1 stratum oriens	1.01 ± 0.019	1.18 ± 0.057 *
Nucleus of the lateral lemniscus	0.98 ± 0.042	1.08 ± 0.410
Lateral caudate nucleus	1.54 ± 0.053	2.56 ± 0.120 ***
Hippocampus CA 1 stratum lacunosum moleculare	1.26 ± 0.042	2.36 ± 0.128 ***
Vestibular nucleus	1.77 ± 0.034	1.66 ± 0.052
Superior colliculus	1.40 ± 0.045	1.39 ± 0.071
Lateral ventro dorsal thalamus	1.61 ± 0.06	3.08 ± 0.177 ***
Medial beniculate body	1.25 ± 0.049	1.54 ± 0.079 **
Sensory motor cortex	1.59 ± 0.057	1.33 ± 0.053 *
Hypothalamus	0.75 ± 0.038	0.91 ± 0.034 *
Inferior colliculus	2.25 ± 0.260	1.62 ± 0.120 *
Lateral septal nuclei	0.94 ± 0.038	1.43 ± 0.034 ***
Amygdala	1.15 ± 0.026	1.75 ± 0.083 ***
Substantia nigra pars compacta	1.05 ± 0.030	1.36 ± 0.034 *
Anterior pyriform cortex	1.73 ± 0.083	3.50 ± 0.306 ***
Dentate gyrus	0.86 ± 0.026	1.12 ± 0.015 ***
Anterior commisure	0.96 ± 0.049	1.29 ± 0.049 **
Medial caudate nucleus	1.55 ± 0.042	1.79 ± 0.083
Ventromedial thalamus	1.53 ± 0.049	1.95 ± 0.090 **
Medial mammillary body	1.94 ± 0.064	2.24 ± 0.143
Anterior cingulate cortex	1.62 ± 0.298	1.91 ± 0.068
Anteromedial thalamic nuclei	1.50 ± 0.053	1.99 ± 0.060 ***
Subthalamic nucleus	1.27 ± 0.049	1.40 ± 0.019
Globus pallidus	0.86 ± 0.038	1.10 ± 0.034 **
Posterior entorhinal cortex	1.05 ± 0.049	2.22 ± 0.139 ***
Lateral habenular nuclei	1.06 ± 0.019	1.22 ± 0.034
Lateral geniculate body	1.21 ± 0.026	1.45 ± 0.068 *
Mediolateral posterior thalamus	1.62 ± 0.053	2.05 ± 0.087 **
Substantia nigra pars reticulata	0.81 ± 0.026	0.99 ± 0.037 *
Nucleus accumbens	0.79 ± 0.042	0.94 ± 0.038
Posterior cingulate cortex	1.86 ± 0.042	2.15 ± 0.049
Pontine reticular formation	1.03 ± 0.026	1.28 ± 0.037 **

Data are expressed as mean ratio of ^{14}C in region of interest / ^{14}C in cerebellar cortex (nCi/g) ± standard error of the mean. *p<0.05; **p<0.01; ***p<0.001 One way analysis of variance followed by unpaired Student's *t*-test with Bonferroni correction factor of four.

Table 24 LCGU in wild type littermate mice: saline versus dizocilpine injected

	wild type littermates SALINE (n=7)	wild type littermates DIZOCILPINE (n=7)
Anterior thalamic nucleus	1.66 ± 0.083	2.22 ± 0.211 *
Dorsal CA 1 stratum lacunosum moleculare	1.44 ± 0.083	2.12 ± 0.162 ***
Superior olivary body	1.52 ± 0.045	1.84 ± 0.155
Dorsal hippocampus CA 1 stratum oriens	0.94 ± 0.023	1.02 ± 0.045
Nucleus of the lateral lemniscus	1.16 ± 0.053	1.28 ± 0.068
Lateral caudate nucleus	1.34 ± 0.034	2.24 ± 0.143 ***
Hippocampus CA 1 stratum lacunosum moleculare	1.24 ± 0.057	2.06 ± 0.124 ***
Vestibular nucleus	1.80 ± 0.045	1.82 ± 0.079
Superior colliculus	1.38 ± 0.049	1.58 ± 0.098
Lateral ventro dorsal thalamus	1.69 ± 0.087	2.69 ± 0.226 ***
Medial beniculate body	1.32 ± 0.053	1.40 ± 0.049
Sensory motor cortex	1.51 ± 0.045	1.19 ± 0.071 **
Hypothalamus	0.69 ± 0.060	0.82 ± 0.049
Inferior colliculus	2.77 ± 0.068	1.95 ±0.117 **
Lateral septal nuclei	0.83 ± 0.038	1.33 ± 0.094 ***
Amygdala	1.15 ± 0.030	1.91 ± 0.158 ***
Substantia nigra pars compacta	1.17 ± 0.049	1.44 ± 0.090 **
Anterior pyriform cortex	1.59 ± 0.068	3.26 ± 0.215 ***
Dentate gyrus	0.79 ± 0.026	1.08 ± 0.052 ***
Anterior commisure	0.91 ± 0.026	1.35 ± 0.090 ***
Medial caudate nucleus	1.31 ± 0.049	1.72 ± 0.094 **
Ventromedial thalamus	1.57 ± 0.026	2.03 ± 0.125 **
Medial mammillary body	1.79 ± 0.052	2.13 ± 0.177
Anterior cingulate cortex	1.51 ± 0.057	2.03 ± 0.094
Anteromedial thalamic nuclei	1.53 ± 0.098	1.93 ± 0.109 *
Subthalamic nucleus	1.32 ± 0.068	1.44 ± 0.109
Globus pallidus	0.85 ± 0.053	1.08 ± 0.030 **
Posterior entorhinal cortex	1.07 ± 0.049	2.18 ± 0.117 ***
Lateral habenular nuclei	1.04 ± 0.049	1.20 ± 0.087
Lateral geniculate body	1.27 ± 0.068	1.43 ± 0.086
Mediolateral posterior thalamus	1.62 ± 0.042	2.03 ± 0.120 **
Substantia nigra pars reticulata	0.79 ± 0.034	1.00 ± 0.064 **
Nucleus accumbens	0.68 ± 0.038	0.93 ± 0.038 **
Posterior cingulate cortex	1.75 ± 0.049	2.30 ± 0.102
Pontine reticular formation	1.08 ± 0.026	1.28 ± 0.056 *

Data are expressed as mean ratio of ^{14}C in region of interest / ^{14}C in cerebellar cortex (nCi/g) ± standard error of the mean. *p<0.05; **p<0.01; ***p<0.001 One way analysis of variance followed by unpaired Student's *t*-test with Bonferroni correction factor of four.

Table 25 LCGU in hsp 70i transgenic and wild type littermates: dizocilpine injected

	hsp 70i transgenic	wild type littermates
	DIZOCILPINE (n=7)	DIZOCILPINE (n=7)
Anterior thalamic nucleus	3.04 ± 0.136	2.22 ± 0.211 **
Dorsal CA 1 stratum lacunosum moleculare	2.70 ± 0.079	2.12 ± 0.162 **
Superior olivary body	1.37 ± 0.090	1.84 ± 0.155 *
Dorsal hippocampus CA 1 stratum oriens	1.18 ± 0.057	1.02 ± 0.045 *
Nucleus of the lateral lemniscus	1.08 ± 0.041	1.28 ± 0.068 *
Lateral caudate nucleus	2.56 ± 0.120	2.24 ± 0.143
Hippocampus CA 1 stratum lacunosum moleculare	2.36 ± 0.128	2.06 ± 0.124
Vestibular nucleus	1.66 ± 0.052	1.82 ± 0.079
Superior colliculus	1.39 ± 0.071	1.58 ± 0.098
Lateral ventro dorsal thalamus	3.08 ± 0.177	2.69 ± 0.226
Medial beniculate body	1.54 ± 0.079	1.40 ± 0.049
Sensory motor cortex	1.33 ± 0.053	1.19 ± 0.071
Hypothalamus	0.91 ± 0.034	0.82 ± 0.049
Inferior colliculus	1.62 ± 0.120	1.95 ±0.117
Lateral septal nuclei	1.43 ± 0.034	1.33 ± 0.094
Amygdala	1.75 ± 0.083	1.91 ± 0.158
Substantia nigra pars compacta	1.36 ± 0.034	1.44 ± 0.090
Anterior pyriform cortex	3.50 ± 0.306	3.26 ± 0.215
Dentate gyrus	1.12 ± 0.015	1.08 ± 0.052
Anterior commisure	1.29 ± 0.049	1.35 ± 0.090
Medial caudate nucleus	1.79 ± 0.083	1.72 ± 0.094
Ventromedial thalamus	1.95 ± 0.090	2.03 ± 0.125
Medial mammillary body	2.24 ± 0.143	2.13 ± 0.177
Anterior cingulate cortex	1.91 ± 0.068	2.03 ± 0.094
Anteromedial thalamic nuclei	1.99 ± 0.060	1.93 ± 0.109
Subthalamic nucleus	1.40 ± 0.019	1.44 ± 0.109
Globus pallidus	1.10 ± 0.034	1.08 ± 0.030
Posterior entorhinal cortex	2.22 ± 0.139	2.18 ± 0.117
Lateral habenular nuclei	1.22 ± 0.034	1.20 ± 0.087
Lateral geniculate body	1.45 ± 0.068	1.43 ± 0.086
Mediolateral posterior thalamus	2.05 ± 0.087	2.03 ± 0.120
Substantia nigra pars reticulata	0.99 ± 0.037	1.00 ± 0.064
Nucleus accumbens	0.94 ± 0.038	0.93 ± 0.038
Posterior cingulate cortex	2.15 ± 0.049	2.30 ± 0.102
Pontine reticular formation	1.28 ± 0.037	1.28 ± 0.056

Data are expressed as mean ratio of ^{14}C in region of interest / ^{14}C in cerebellar cortex (nCi/g) ± standard error of the mean. *p<0.05; **p<0.01; ***p<0.001 One way analysis of variance followed by unpaired Student's *t*-test with Bonferroni correction factor of four.

3.5 Mapping brain function following ad egfp gene transfer

LCGU was estimated in C57bl/6 strain mice seven and 28-days after intrasrtriatal injection with ad egfp or saline (one microlitre over a 10-minute period). The impact of two versus ten-minute delay in post-injection needle extraction upon egfp transfection and LCGU was also investigated. Two densitometric analysis strategies were employed. First, LCGU in the entire caudate nucleus was measured. Second, LCGU in circumscribed areas of the caudate nucleus was measured (this enabled analysis of ad egfp transfected areas and needle damage, see Appendix G for more detail). The remaining eight brain regions were analysed using standard densitometric analysis techniques (see Section 2.7.4).

3.5.1 Behaviour following intrastriatal injection with ad

Overt behaviour of mice which received intrastriatal injection of 1 microlitre (0.1μl/minute) of ad egfp (1.57×10^{10} plaque forming units/ml) was indistinguishable from mice that received intrastriatal injection of sterile saline.

3.5.2 Ad egfp transfection

All of the 22 mice intrastriatally injected with ad egfp displayed transfection. Ad egfp transfection was prevalent in three structures in all mice, the caudate nucleus, subcortical white matter and white matter bundles within the caudate nucleus. The extent of ad egfp transfection was not noticeably different at seven and 28-days post injection (Figure 55). Moreover, the delay in post-injection needle extraction did not noticeably affect the extent of ad egfp transfection (Figure 56). In some mice, ad egfp transfection was observed in ependymal cells of the right ventricle (Figure 56).

Figure 55 Ad egfp transfection: 7 and 28 days post-injection

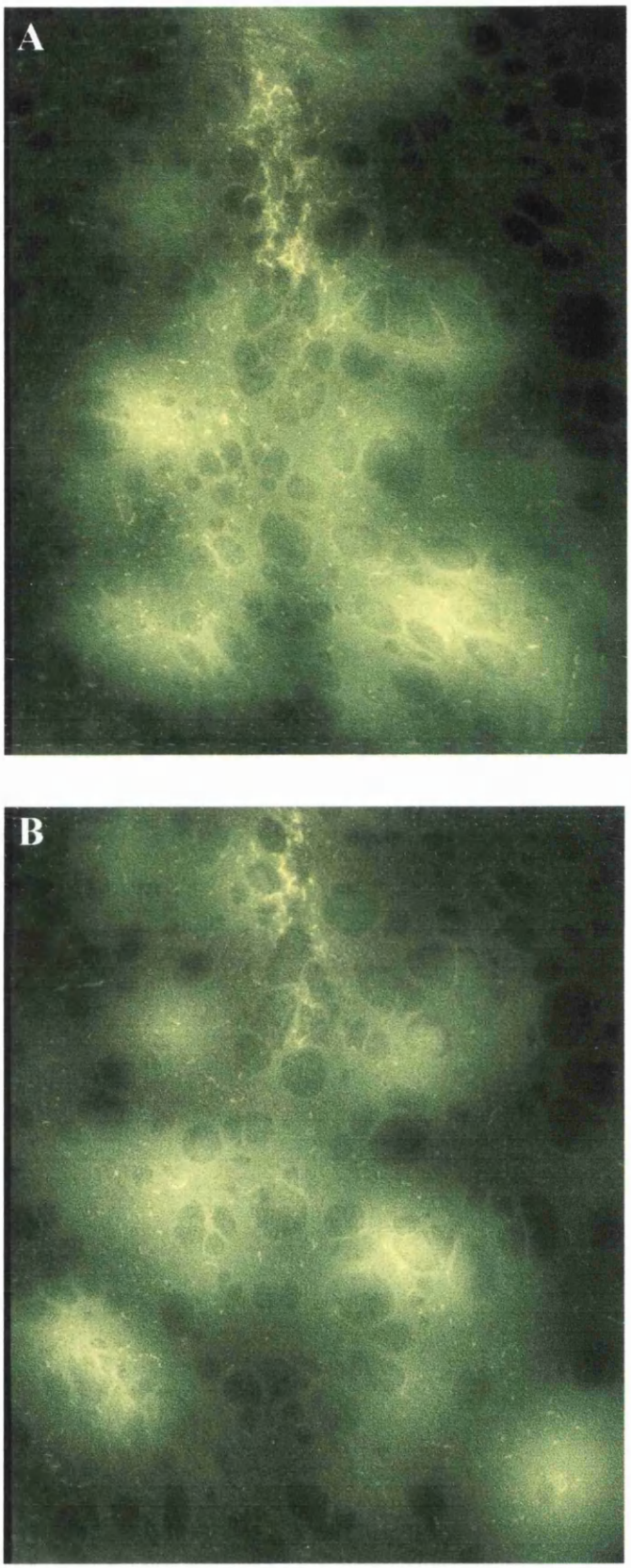

Ad egfp transfection in caudate nucleus at seven days post-injection (A) was similar to that observed at 28 days post-injection (B). (Original magnification X100).

Figure 56 Ad egfp transfection: 2 versus 10-minute delay in needle extraction

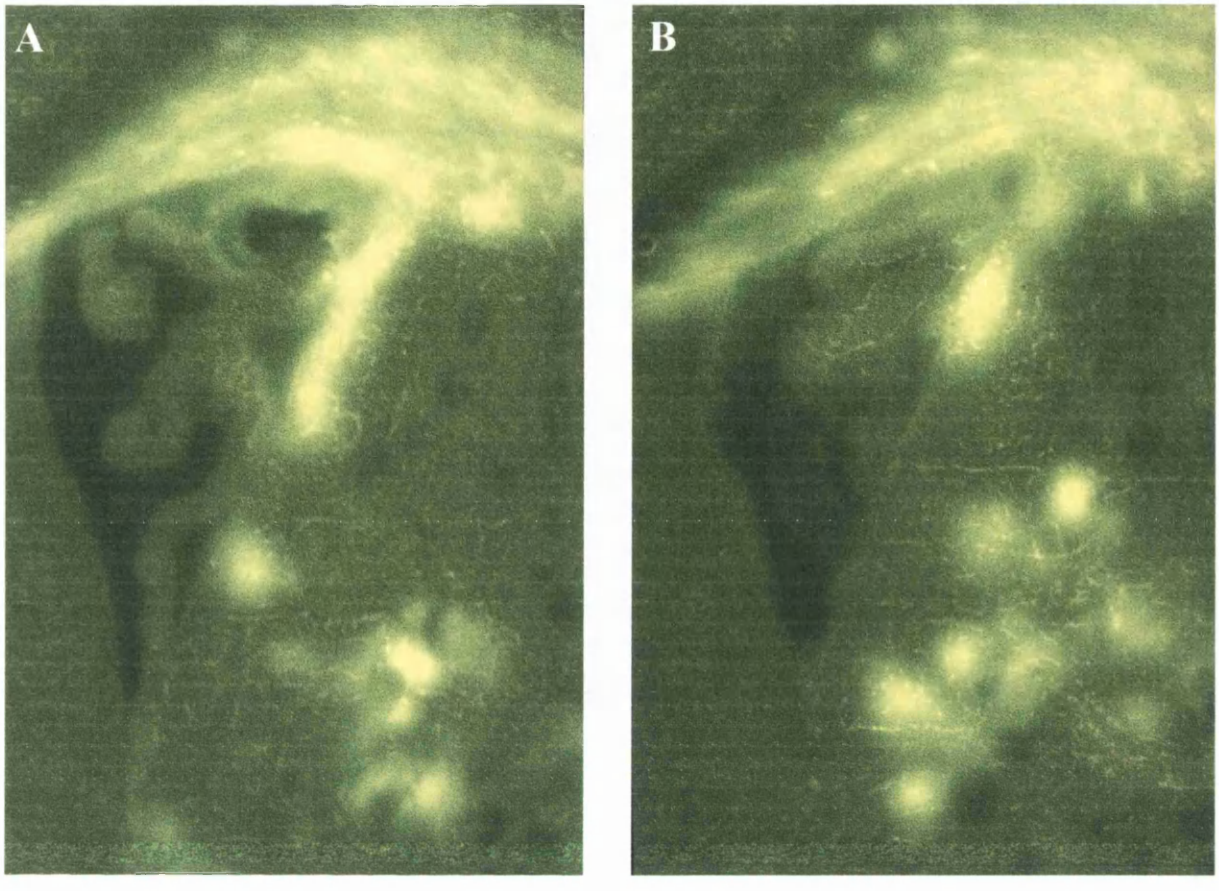

Ad egfp transfection in the caudate nucleus, subcortical white matter and ependymal cells (of the lateral ventricle) was similar in mice where the needle was extracted two (A) and 10 (B) minutes after injection. (Original magnification X100).

3.5.3 Plasma ^{14}C and glucose concentrations

Plasma ^{14}C and glucose concentrations in seven and 28-day ad egfp transfected and saline injected mice did not differ significantly (Table 26). Moreover, terminal plasma ^{14}C / glucose correlated well with tissue ^{14}C (cerebellar cortical grey matter), irrespective of treatment (Figure 57).

3.5.4 LCGU in ad egfp transfected mice

LCGU in entire caudate nucleus

There were no significant inter-hemispheric differences in LCGU where the entire caudate nucleus was analysed (Figure 58 and 59). Moreover, there were no significant inter-group differences in hemispheric LCGU. LCGU in the entire caudate nucleus was similar in all groups irrespective of treatment or survival duration.

LCGU in areas of ad egfp transfection in caudate nucleus

LCGU was analysed in areas of ad egfp transfection and areas of needle damage on autoradiograms (see Appendix F for details on delineation of these areas). In areas of ad egfp transfection LCGU was significantly decreased compared to LCGU in the contralateral hemisphere at seven and 28-days post-injection (Figures 60 and 61). In saline injected mice, there was a significant difference in LCGU between ipsilateral and contralateral hemispheres at seven days, but not at 28-days post-injection (Figure 60). LCGU in areas of ad egfp transfection was similar in all groups irrespective of treatment or survival duration.

LCGU in areas of needle damage in caudate nucleus

In areas of injection damage, ad egfp transfected mice displayed no significant differences in LCGU between hemispheres at seven days post-injection (Figure 61). Ad egfp transfected mice did however display significant decreases in LCGU at 28-days in the

transfected hemisphere compared to the contralateral hemisphere (Figure 61). In saline injected mice, the opposite was observed. LCGU in the saline injected hemisphere was significantly increased compared to LCGU in the contralateral hemisphere at seven days post-injection (Figure 61). At 28-days post saline injection there were no significant differences in LCGU between hemispheres (Figure 61).

LCGU in other brain regions analysed

There were no significant inter-hemispheric differences in LCGU in any of the other eight brain regions analysed at seven or 28-days post-injection (Tables 27 and 28).

Table 26 Plasma ^{14}C and glucose concentrations in ad egfp transfected mice

	7 Day survival			28 Day survival		
	Saline 2 mins (n=6)	**Ad egfp 2 mins** (n=6)	**Ad egfp 10 mins** (n=5)	**Saline 2 mins** (n=6)	**Ad egfp 2 mins** (n=6)	**Ad egfp 10 mins** (n=5)
Plasma ^{14}C (nCi/g)	63.3 ± 6.2	72.8 ± 7.6	53.7 ± 4.3	55.1 ± 5.1	69.4 ± 9.3	66.7 ± 7.7
Plasma glucose (mM)	11.8 ± 0.5	13.0 ± 0.5	11.1 ± 0.5	11.4 ± 0.4	11.5 ± 0.4	11.2 ± 0.4

Data are expressed as mean ± standard error of the mean. $p>0.05$ One way analysis of variance followed by unpaired Student's *t*-test with Bonferroni correction factor of four.

Figure 57 Relationship between tissue ^{14}C and terminal plasma ^{14}C / glucose ratio

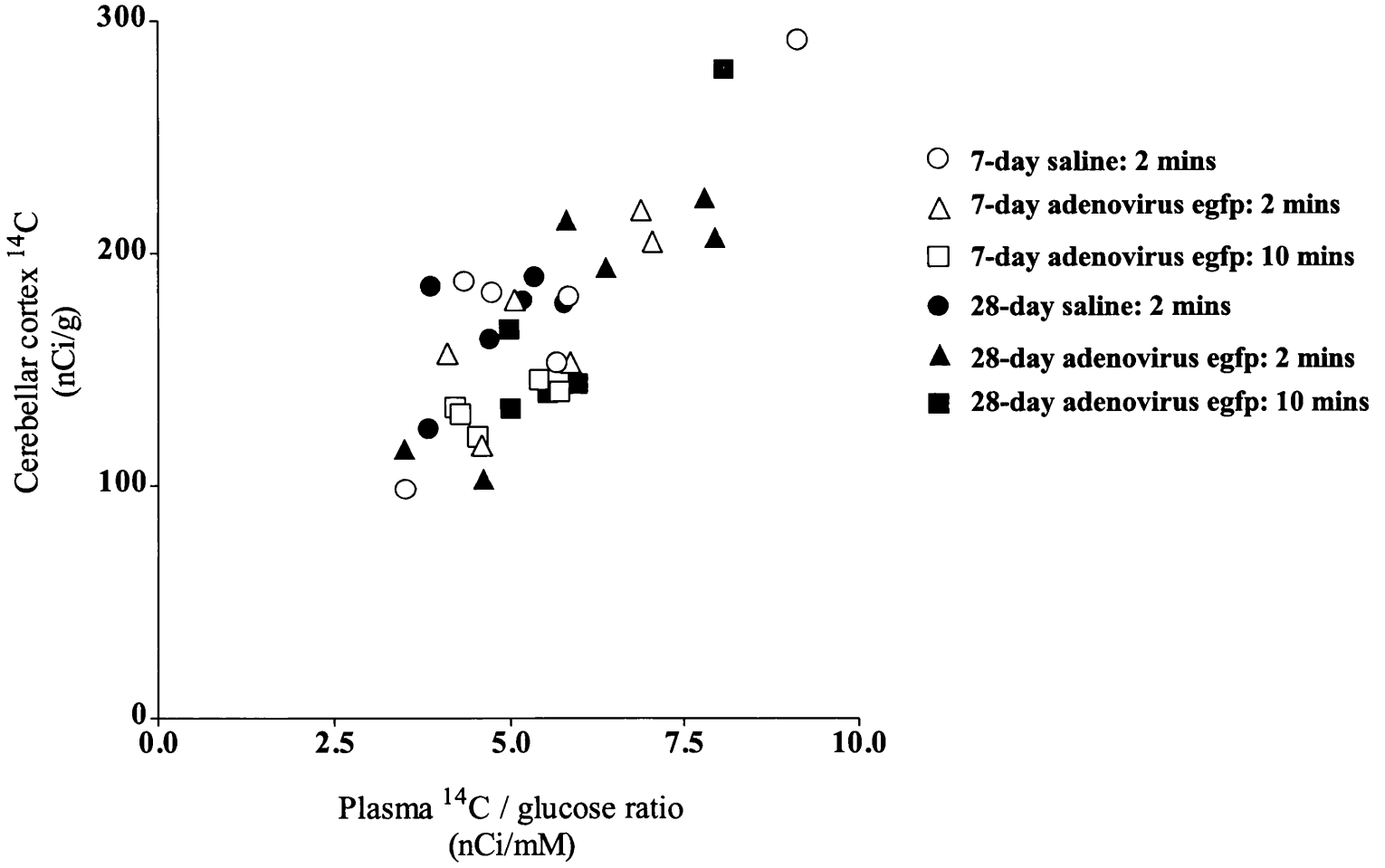

The relationship between cerebellar cortical ^{14}C concentration and plasma ^{14}C / glucose was similar between groups, irrespective of treatment. (n=6 7 and 28-day saline, 7 and 28-day adenovirus egfp: 2 mins; n=5 per group 7 and 28-day adenovirus egfp: 10 mins).

Figure 58 LCGU in entire caudate nucleus of ad egfp transfected mice

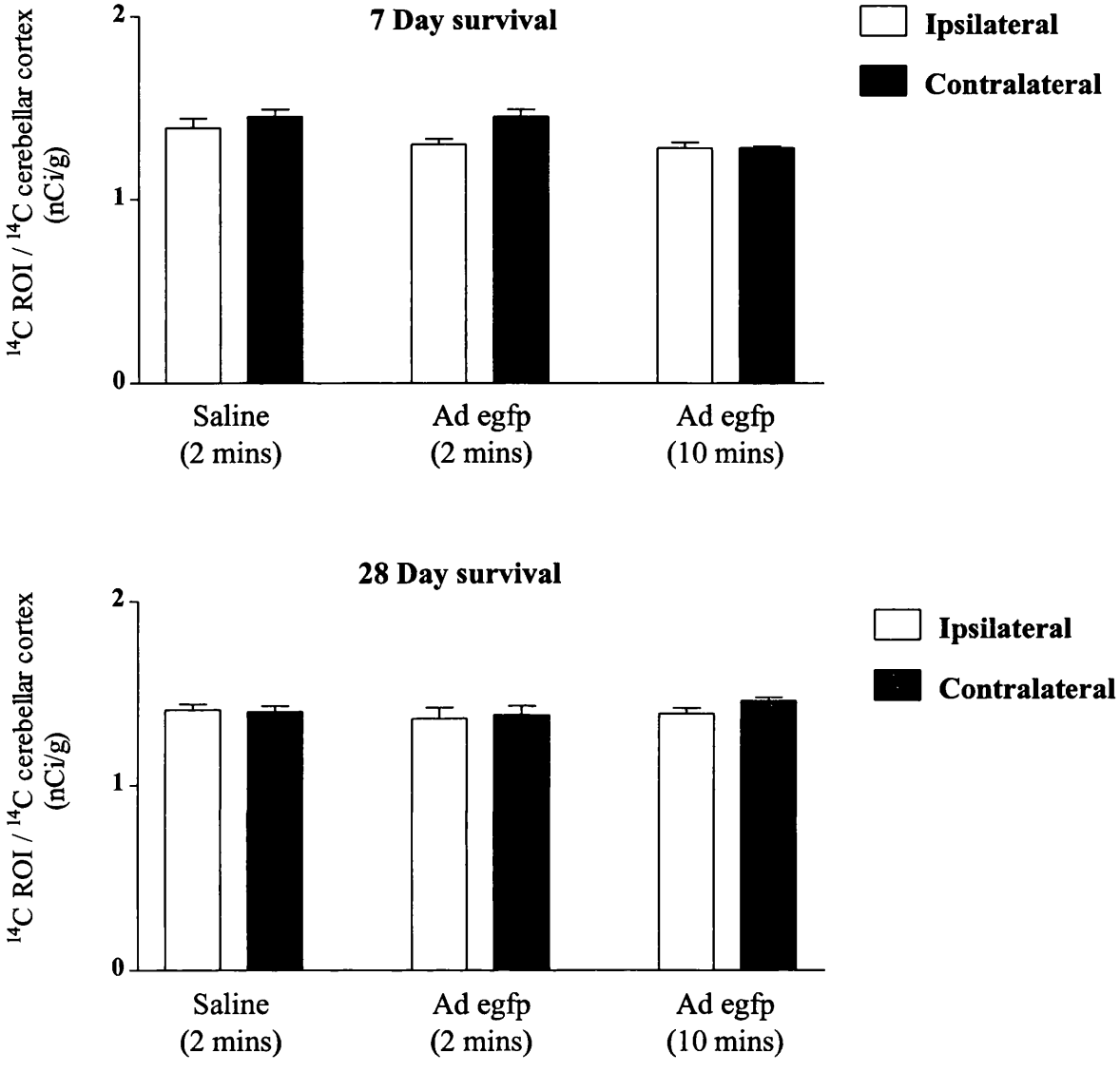

LCGU measured in entire ipsilateral and contralateral caudate nucleus was similar at seven and 28 days post-injection. Data are presented as mean ± standard error of the mean. P>0.05 Paired Student's *t*-test. (n=6 7 and 28-day saline, 7 and 28-day adenovirus egfp: 2 mins; n=5 per group 7 and 28-day adenovirus egfp: 10 mins). (ROI = region of interest).

Figure 59 **Representative ^{14}C-2-deoxyglucose autoradiograms of injected caudate nucleus**

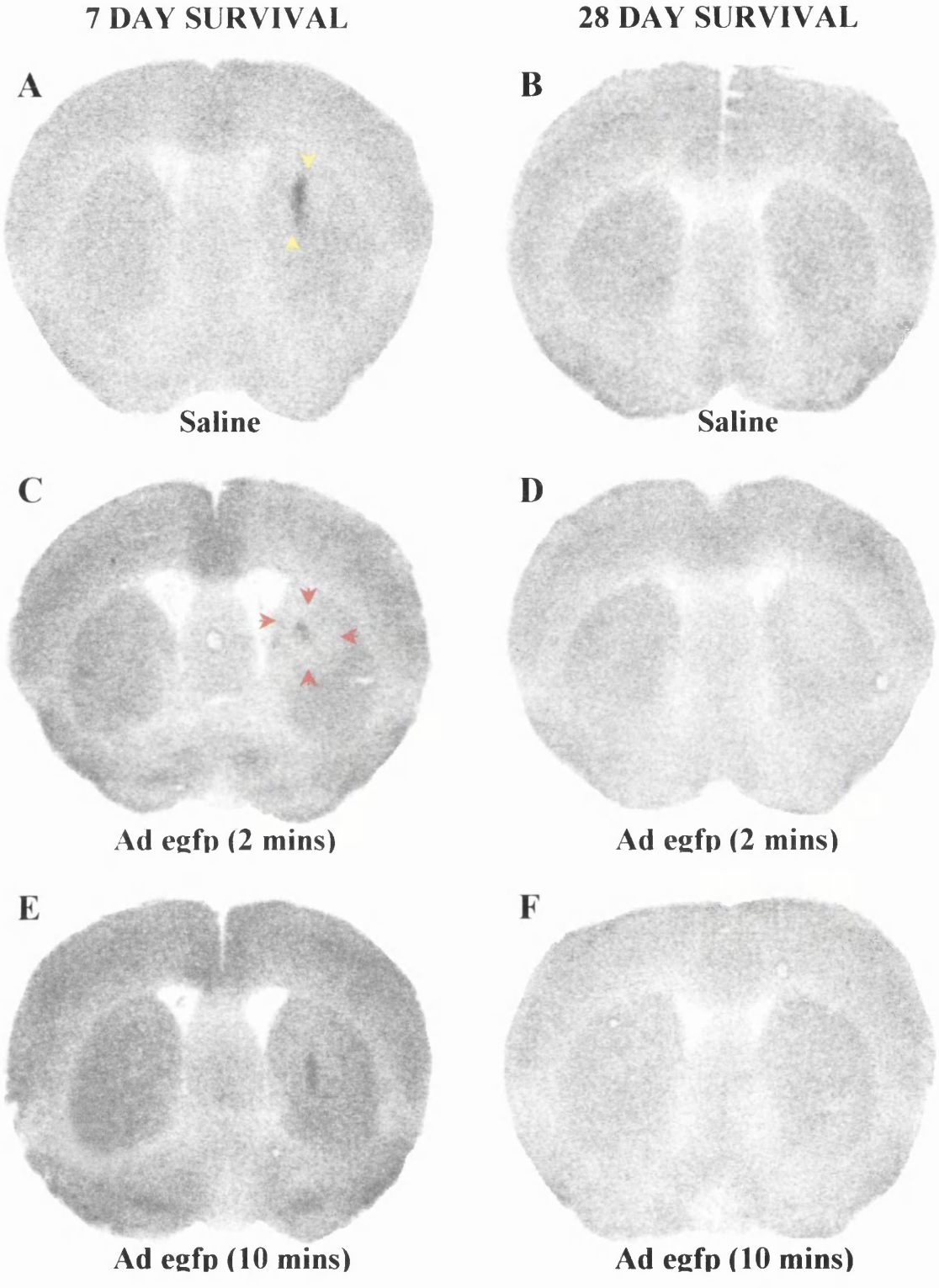

Representative examples of ^{14}C-2-deoxyglucose autoradiograms of the site of injection in the caudate nucleus of saline injected (A and C), ad egfp with 2 minutes needle extraction (C and D) and ad egfp with 10 minutes needle extraction (E and F). Areas of ad egfp transfection (red arrows) and areas of needle damage (yellow arrows) are highlighted.

Figure 60 LCGU in areas of ad egfp transfection in caudate nucleus

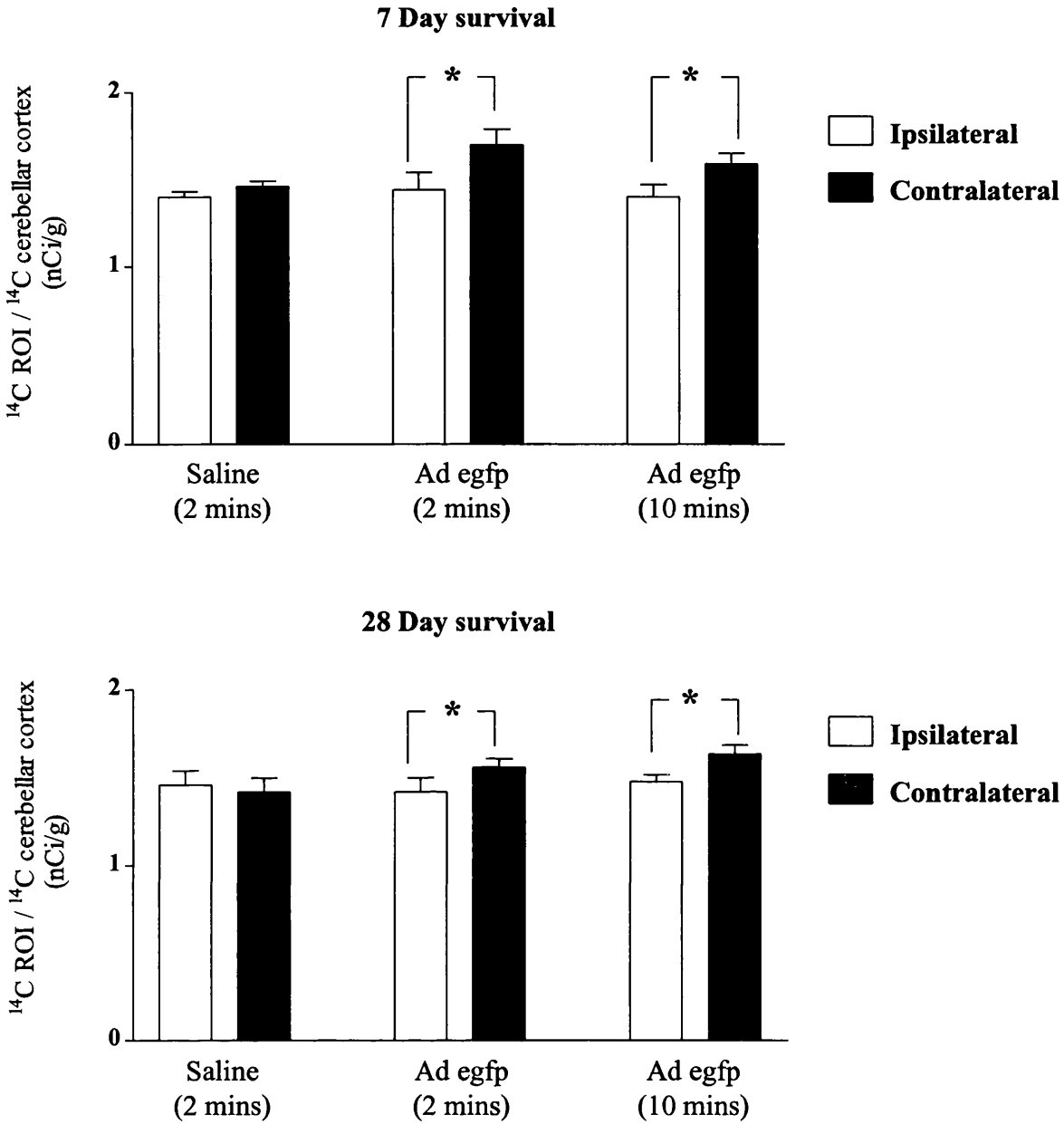

LCGU in areas of ad egfp transfection was significantly decreased compared with contralateral hemisphere at seven and 28 days post injection (irrespective of 2 or 10-minute needle extraction delay). LCGU was similar in saline injected and contralateral hemisphere at seven and 28 days post injection. Data are presented as mean ± standard error of the mean. *$p<0.05$ paired Student's *t*-test. (n=6 7 and 28-day saline, 7 and 28-day adenovirus egfp: 2 mins; n=5 per group 7 and 28-day adenovirus egfp: 10 mins). (ROI = region of interest).

Figure 61 LCGU in areas of needle damage in caudate nucleus

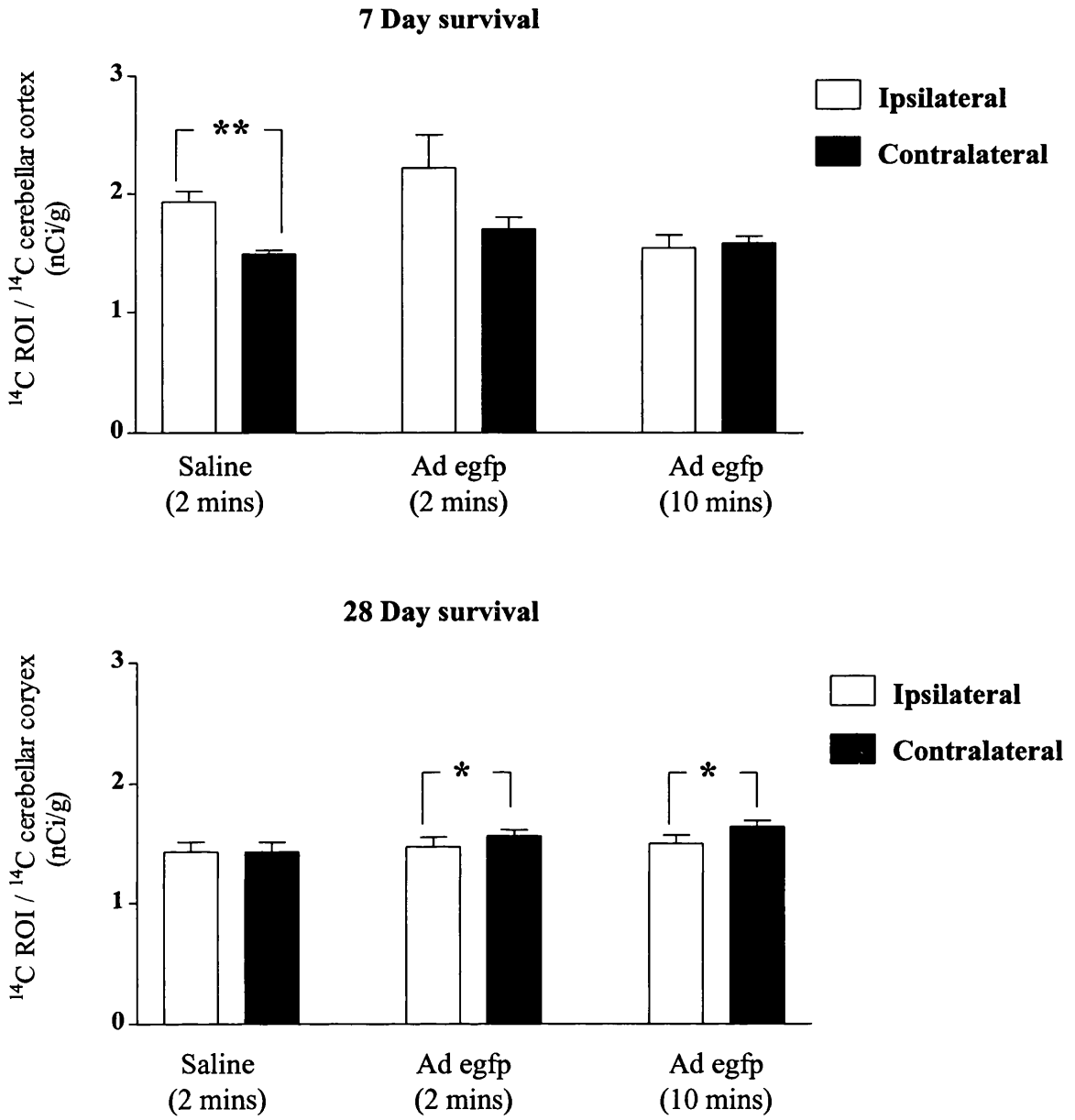

LCGU in areas of needle damage in intrastriatally injected mice was significantly decreased compared with contralateral hemisphere at 28 days post injection (at both 2 and 10-minute needle extraction delay). LCGU was increased in areas of needle damage in saline injected mice at 7 days. LCGU in ad egfp transfected mice at 7 days post-injection and saline injected mice at 28 days was similar to that in contralateral hemisphere. Data are presented as mean ± standard error of the mean. *$p<0.05$; **$p<0.01$ paired Student's *t*-test. (n=6 7 and 28-day saline, 7 and 28-day adenovirus egfp: 2 mins; n=5 per group 7 and 28-day adenovirus egfp: 10 mins). (ROI = region of interest).

Table 27 LCGU in ad egfp transfected mice: 7 day survival

	7 Day survival					
	Saline 2 mins (n=6)		Ad egfp 2 mins (n=6)		ad egfp 10 mins (n=5)	
	IPSI	**CONTRA**	**IPSI**	**CONTRA**	**IPSI**	**CONTRA**
Cingulate cortex	1.59 ± 0.06	1.62 ± 0.07	1.66 ± 0.06	1.64 ± 0.06	1.55 ± 0.06	1.55 ± 0.06
Corpus callosum	0.74 ± 0.04	0.74 ± 0.04	0.74 ± 0.04	0.74 ± 0.04	0.74 ± 0.04	0.74 ± 0.03
Globus pallidus	1.05 ± 0.02	1.05 ± 0.02	1.03 ± 0.03	1.08 ± 0.03	1.03 ± 0.04	1.05 ± 0.03
Anterior thalamus	1.77 ± 0.06	1.75 ± 0.06	1.80 ± 0.03	1.83 ± 0.06	1.73 ± 0.04	1.74 ± 0.06
Retrosplenial cortex	1.74 ± 0.05	1.76 ± 0.06	1.74 ± 0.05	1.74 ± 0.04	1.68 ± 0.07	1.66 ± 0.05
Hypothalamus	0.70 ± 0.02	0.70 ± 0.02	0.80 ± 0.03	0.81 ± 0.04	0.75 ± 0.03	0.76 ± 0.04
Internal capsule	0.79 ± 0.03	0.83 ± 0.04	0.80 ± 0.05	0.82 ± 0.06	0.89 ± 0.01	0.90 ± 0.02
Hippocampus CA1	1.62 ± 0.11	1.58 ± 0.09	1.73 ± 0.08	1.71 ± 0.08	1.58 ± 0.03	1.57 ± 0.04

Data are expressed as mean ratio of ^{14}C in region of interest / ^{14}C in cerebellar cortex ± standard error of the mean (nCi/g). $p>0.05$ One way analysis of variance followed by unpaired Student's *t*-test with Bonferroni correction factor of four (ipsi versus contra) (IPSI = ipsilateral; CONTRA = contralateral).

Table 28 LCGU in ad egfp transfected mice: 28 day survival

	28 Day survival					
	Saline 2 mins (n=6)		Ad egfp 2 mins (n=6)		Ad egfp 10 mins (n=5)	
	IPSI	CONTRA	IPSI	CONTRA	IPSI	CONTRA
Cingulate cortex	1.63 ± 0.08	1.62 ± 0.07	1.56 ± 0.08	1.56 ± 0.08	1.57 ± 0.04	1.57 ± 0.06
Corpus callosum	0.83 ± 0.05	0.82 ± 0.05	0.73 ± 0.04	0.75 ± 0.04	0.69 ± 0.04	0.70 ± 0.04
Globus pallidus	1.12 ± 0.03	1.12 ± 0.04	1.07 ± 0.06	1.08 ± 0.06	1.09 ± 0.04	1.12 ± 0.06
Anterior thalamus	1.88 ± 0.08	1.93 ± 0.09	1.90 ± 0.08	1.90 ± 0.10	1.90 ± 0.08	1.98 ± 0.09
Retrosplenial cortex	1.70 ± 0.8	1.70 ± 0.07	1.74 ± 0.09	1.72 ± 0.08	1.74 ± 0.09	1.76 ± 0.09
Hypothalamus	0.75 ± 0.02	0.76 ± 0.02	0.77 ± 0.03	0.80 ± 0.04	0.74 ± 0.04	0.72 ± 0.03
Internal capsule	0.82 ± 0.04	0.84 ± 0.04	0.84 ± 0.05	0.86 ± 0.04	0.88 ± 0.09	0.84 ± 0.07
Hippocampus CA1	1.67 ± 0.06	1.63 ± 0.04	1.62 ± 0.03	1.64 ± 0.02	1.70 ± 0.04	1.72 ± 0.05

Data are expressed as mean ratio of ^{14}C in region of interest / ^{14}C in cerebellar cortex ± standard error of the mean (nCi/g). $p>0.05$ One way analysis of variance followed by unpaired Student's *t*-test with Bonferroni correction factor of four (ipsi versus contra) (IPSI = ipsilateral; CONTRA = contralateral).

CHAPTER FOUR: DISCUSSION

Recent research has shown that hsp 70i may ameliorate ischaemic neuronal damage induced by cerebral ischaemia. Moreover, genetically modified mice and viral vectors are increasingly being employed as research tools to gain insight into the processes and mechanisms involved in cerebral ischaemia. The studies of this thesis were designed to address two major themes. First, the influence of hsp 70i upon ischaemic outcome following global cerebral ischaemia (BCCAo) was investigated using transgenic mice over-expressing hsp 70i and ad hsp 70i gene transfer in the caudate nucleus. Second, the functional consequences of transgene over-expression in the brain were investigated, in transgenic mice over-expressing hsp 70i and following ad egfp gene transfer in the caudate nucleus.

4.1 BCCAo in mice

To investigate the influence of hsp 70i in cerebral ischaemia a murine model of cerebral ischaemia had to be established. Global cerebral ischaemia was chosen on the basis of the over-expression pattern of hsp 70i in the transgenic mice available. In these transgenic mice, hsp 70i over-expression was driven by the rhombotin 1 promoter (see Section 2.9 for details), meaning hsp 70i was over-expressed in several brain regions selectively vulnerable to global cerebral ischaemia (including, hippocampus and striatum). However, the background strain of the hsp 70i transgenic mice (MF1) had not been described in any ischaemic paradigm. Furthermore, no mouse ischaemia models had been established in my laboratory. The first aim of this thesis was therefore, to establish a mouse model of global cerebral ischaemia and describe its effects on MF1 strain mice. Global cerebral ischaemia was induced by BCCAo. BCCAo had been reported to induce ischaemic neuronal damage in several other mouse strains, including C57bl/6 and SV129 (the most commonly employed strains for producing genetically modified mice) by Yang *et al.*, (1997) and Fujii *et al.* (1997). Employing different occlusion durations and anaesthesia paradigms, Yang *et al.*, (1997) and Fujii *et al.*, (1997) both observed C57bl/6 strain mice to be the most

susceptible to BCCAo. C57bl/6 strain mice were employed in this thesis to compare the effects of BCCAo on MF1 mice and to ensure BCCAo could induce ischaemic neuronal damage with the methodology used.

4.1.1 Susceptibility of mouse strain to BCCAo

Ischaemic neuronal damage in seven brain regions was determined histologically following BCCAo of 10, 15 and 20 minutes duration in MF1 and C57bl/6 strain mice, and compared (see Table 3, Figure 17). MF1 strain mice were observed to display significantly less ischaemic neuronal damage than C57bl/6 strain mice following 15 and 20-minute BCCAo. These data corroborated the previous findings of Yang *et al.*, (1997) and Fujii *et al.*, (1997) in that BCCAo (of short duration, 10-20 minutes) produced widespread ischaemic neuronal damage in C57bl/6 strain mice. In MF1 mice however, BCCAo of short duration (10-20 minutes) did not produce widespread ischaemic neuronal damage. Instead only minimal to moderate ischaemic neuronal damage was observed in brain areas selectively vulnerable to global cerebral ischaemia. In an attempt to increase the ischaemic neuronal damage in MF1 mice, BCCAo duration was extended (25-45 minutes). A similar ploy had been adopted by Fujii *et al.*, (1997) who reported only minimal ischaemic neuronal damage in SV129 strain mice following short durations of BCCAo, compared to C57bl/6 strain mice. In this thesis however, ischaemic neuronal damage in MF1 strain mice was investigated at several durations of extended BCCAo and was assessed quantitatively (as percentage ischaemic neurones, not as a semi-quantitative score). By investigating several durations of extended BCCAo and assessing ischaemic neuronal damage quantitatively, an accurate profile of the effect of increasing BCCAo duration was obtained (see Table 4, Figure 20). There was a trend of increased ischaemic neuronal damage with increased BCCAo duration versus sham-operated mice (see Figure 20). However, ischaemic neuronal damage in 25-minute BCCAo mice was similar to 45-minute BCCAo mice in all five-brain regions analysed (see Table 4). Moreover, the ischaemic neuronal damage observed in

MF1 mice following extended duration BCCAo was similar to that in MF1 mice following 10-20 minute BCCAo (see Table 3) and was not as extensive or widespread as that observed in C57bl/6 strain mice following 10-20 minute BCCAo (see Table 3). In short, BCCAo induced ischaemic neuronal damage in MF1 strain mice, but the degree of ischaemic neuronal damage was moderate in comparison to that induced in C57bl/6 strain mice.

4.1.2 Hierarchy of ischaemic neuronal damage in MF1 and C57bl/6 mice

Differences in the rank order of ischaemic neuronal vulnerability following global cerebral ischaemia in gerbil and rat have been well documented (Kirino, 1982; Kirino and Sano, 1984a; Pulsinelli *et al.*, 1982; Smith *et al.*, 1984). In mice, the rank order of ischaemic neuronal vulnerability has been shown to be quite different from that in gerbil and rat (Yang *et al.*, 1997; Fujii *et al.*, 1997; Murakami *et al.*, 1998). In gerbil and rat models ischaemic neuronal damage was predominantly observed in hippocampus CA1, CA4 and subiculum. The major differences in mouse relate to the incidence of ischaemic neuronal damage in hippocampus CA2, caudate nucleus and cerebral cortex as well as hippocampus CA1. In this thesis, BCCAo produced ischaemic neuronal damage of varying degrees throughout the hippocampus, caudate nucleus, cortex and thalamus in MF1 and C57bl/6 strain mice (see Tables 3 and 4). The regional hierarchy of ischaemic neuronal vulnerability in MF1 strain mice was different to that of C57bl/6 strain mice (Table 29).

Table 29 Hierarchy of ischaemic neuronal damage in MF1 and C57bl/6 mice

	MF1	C57bl/6
Most damaged area	Caudate nucleus	Hippocampus CA2
	Somatosensory cortex	Caudate nucleus
	Posterior thalamus	Posterior thalamus
	Hippocampus CA1	Somatosensory cortex
	Hippocampus CA2	Hippocampus CA1
	Hippocampus CA3	Hippocampus CA3
Least damaged area	Dentate gyrus	Dentate gyrus

4.1.3 Factors influencing ischaemic neuronal damage following BCCAo

The increased susceptibility of C57bl/6 strain mice to BCCAo has been suggested to be due to their increased likelihood of circle of Willis hypoplasticity. Yang *et al.*, (1997) and Fujii *et al.*, (1997) both reported a high incidence of PcomA hypoplasticity in C57bl/6 strain mice. The first report of PcomA hypoplasticity in any mouse strain was Barone *et al.*, (1993). Barone and colleagues (1993) suggested that PcomA hypoplasticity in balb-c strain mice might render this strain susceptible to BCCAo as a murine model of global cerebral ischaemia. BCCAo in the Mongolian gerbil had been (and remains) widely employed as a model of global cerebral ischaemia, as they lack anastomoses between anterior and posterior cerebral circulations (Levine and Sohn, 1969; Ito *et al.*, 1975). Murakami *et al.*, (1998) have also correlated increased ischaemic neuronal damage in CD-1 strain mice with PcomA hypoplasticity. In this thesis, hypoplasticity of the PcomAs in C57bl/6 and MF1 strain mice were significantly different (see Figures 21 and 22, Table 5). No C57bl/6 strain mouse investigated displayed a complete circle of Willis (i.e., no C57bl/6 mice had two PcomAs). In contrast, more than half of MF1 strain mice investigated displayed a complete circle of Willis (i.e., nine MF1 mice from 16 had two PcomAs). Moreover, five of eight C57bl/6 strain mice had no PcomAs, whereas only one from 16 MF1 strain mice had no PcomAs. Therefore, a lack of PcomA hypoplasticity in MF1 strain mice could be a major factor why only minimal to moderate ischaemic neuronal damage was observed following BCCAo thus, reducing ischaemic neuronal damage. That is to say, collateral blood flow via the vertebro-basilar arterial branches may help overcome reduced blood flow to the forebrain during BCCAo in MF1 strain mice. In C57bl/6 mice increased PcomA hypoplasticity, and therefore reduced collateral blood flow, is most likely a major factor why BCCAo produces extensive and widespread ischaemic neuronal damage in this study and others (Yang *et al.*, 1997; Fujii *et al.*, 1997). Another feature of ischaemic neuronal damage, particularly in MF1 strain mice, was its unilateral distribution. That is to say, only one brain hemisphere displayed ischaemic

neuronal damage in many of the MF1 mice subjected to BCCAo (see Appendix E). A likely cause of unilateral ischaemic neuronal damage could be unilateral PcomA hypoplasticity. Of MF1 strain mice investigated, six had one PcomA compared with only three C57bl/6 strain mice displaying unilateral PcomA hypoplasticity.

The influence of systemic hypotension upon ischaemic neuronal damage during BCCAo was elegantly illustrated in the rat by Smith *et al*, (1984). Smith and colleagues employed BCCAo in rat with systemic hypotension (circa 60mmHg) to induce global cerebral ischaemia. Without accompanying hypotension, BCCAo alone in rat does not induce global cerebral ischaemia. This is not the case in gerbils (Levine and Payan, 1966) or mice (Barone *et al.*, 1993). In this thesis however, MABP in C57bl/6 strain mice was observed to decrease progressively (after a transient increase) during 20-minute BCCAo to around 55mmHg (see Figure 23). In contrast, MABP in MF1 strain mice during 20 and 45-minute BCCAo was maintained above baseline (after a transient increase) throughout the entire occlusion durations (see Figures 23 and 24). It is entirely likely that the maintained increase in MABP in MF1 strain mice during BCCAo coupled with the increased presence of PcomAs promotes collateral blood flow to the forebrain thus, reducing the neuropathologic impact of BCCAo. In C57bl/6 strain mice, the progressive decrease in MABP during BCCAo coupled with the decreased presence of PcomAs does not promote collateral blood flow to the forebrain thus, increasing the neuropathologic impact of BCCAo.

4.1.4 Hsp 70i and cerebral ischaemia

In normal (unstressed brain), hsp 70i is expressed only in minuscule amounts (Latchman, 1998). Cerebral ischaemia however can induce hsp 70i such that it is expressed in several brain regions. Global cerebral ischaemia has been shown to induce hsp 70i in gerbil (Nowak, 1985; Vass *et al.*, 1988; Aoki *et al.*, 1993a, 1993b; Soriano *et al.*, 1994; Ferrer *et*

al., 1995) and rat (Dienel *et al.*, 1986; Gaspary *et al.*, 1995). Hsp 70i induction and expression varies with the severity of the ischaemic insult. In gerbils BCCAo induces significant hsp 70i expression in CA3, but not hippocampus CA1 (Vass *et al.*, 1988; Aoki *et al.*, 1993a). Nowak *et al.*, (1990) however, reported significant hsp 70i mRNA expression in hippocampus CA1 neurones following BCCAo in the gerbil. Similar results have been reported in rat models of global cerebral ischaemia (Kawagoe *et al.*, 1993). Moreover, in focal cerebral ischaemia in rat, hsp 70i immunoreactive neurones are located within the margin of viable tissue surrounding the infarct core (penumbra) and not within the infarcted core (Gonzalez *et al.*, 1989). These data imply that while hsp 70i is induced by ischaemia, hsp 70i protein transcription can also be disrupted by ischaemia if severe enough. In mice, hsp 70i expression following ischaemia has only been detected by Southern and Western blot analysis (Plumier *et al.*, 1997; Radjev *et al.*, 1999). In this thesis, hsp 70i expression following BCCAo was immunohistochemically detected in neurones in several brain regions (notably hippocampus CA1 and CA3) in MF1 and C57bl/6 strain mice. MF1 strain mice displayed significantly fewer hsp 70i immunoreactive neurones than C57bl/6 strain mice following BCCAo (see Tables 8 and 9). That is to say, C57bl/6 strain mice displayed greater numbers of hsp 70i immunoreactive neurones and more extensive ischaemic neuronal damage than MF1 strain mice. These findings suggest that the severity of the ischaemic insult produced by BCCAo in C57bl/6 strain mice was not sufficient to obliterate the translation of hsp 70i mRNA into hsp 70i protein in hippocampus CA1. Whereas, the severity of the ischaemic insult produced by BCCAo in MF1 mice was not sufficient to produce hsp 70i expression to the same extent as that observed in C57bl/6 strain mice.

4.2 BCCAo in transgenic and viral vector transfected mice

The benefits of genetically modified (transgenic) mice in the understanding of the pathophysiology of cerebral ischaemia have been substantial. The roles of numerous genes and gene products in cerebral ischaemia have been further elucidated using such mice (see Section 1.8). Viral vectors have also been beneficially employed to investigate the role of specific genes in the pathophysiology of cerebral ischaemia (see Section 1.9.5). The second aim of this thesis was to investigate the influence of hsp 70i over-expression on ischaemic outcome following BCCAo. Directed over-expression of hsp 70i was investigated in two systems, first, in transgenic mice over-expressing hsp 70i, and second, in mice with ad hsp 70i gene transfer into the caudate nucleus.

4.2.1 Neuroprotection in hsp 70i transgenic mice

The hsp 70i transgenic mice used in this thesis were produced in an MF1 strain background. The initial study of this thesis described the effects of BCCAo on MF1 strain mice (see Section 3.1). BCCAo in MF1 strain mice was shown to evoke only minimal to moderate ischaemic neuronal damage. Furthermore, ischaemic neuronal damage in MF1 strain mice was similar following 25 and 45-minute BCCAo (circa 15% in caudate nucleus and 25% in hippocampus CA1, see Table 4). On the basis of these findings 25-minute BCCAo was chosen to investigate the ischaemic outcome in hsp 70i transgenic mice and their wild type littermates. Following 25-minute BCCAo, wild type littermate mice displayed similar values of ischaemic neuronal damage in the caudate nucleus, hippocampus CA3 and dentate gyrus to MF1 strain mice subjected to 25-minute BCCAo in a previous study (see Section 3.1). In hippocampus CA1 and CA2 however, wild type littermate mice displayed much lower levels of ischaemic neuronal damage than those observed in MF1 strain mice. Hsp 70i transgenic mice displayed markedly reduced ischaemic neuronal damage compared to wild type littermate mice in three of eight brain regions analysed (lateral caudate nucleus, medial caudate nucleus and posterior thalamus,

see Figure 29). In the initial study in this thesis, significant differences in the susceptibility of MF1 and C57bl/6 strain mice to BCCAo were attributed to differences in PcomA hypoplasticity and MABP during BCCAo. In the present study, markedly reduced ischaemic neuronal damage in hsp 70i transgenic mice compared to wild type littermate mice were unlikely to be attributable to inter-group differences in PcomA hypoplasticity or MABP. In hsp 70i transgenic and wild type littermate mice investigated the incidence of PcomA hypoplasticty was identical (see Figures 30 and 31, Table 14). Whereas, MABP prior to, during and following BCCAo in hsp 70i transgenic and wild type littermate mice was similar (and was marginally lower throughout in hsp 70i transgenic mice, see Figure 32). Moreover, there were no statistically significant differences between hsp 70i transgenic and wild type littermate mice in any of the other physiologic variables measured (see Table 15). Therefore over-expression of hsp 70i might be the major factor contributing to the marked reduction in ischaemic neuronal damage in hsp 70i transgenic mice. However, hsp 70i immunoreactivity was not significantly different in hsp 70i transgenic mice compared to wild type littermate mice in any brain region analysed 72 hours after BCCAo (see Table 16). The best possible explanation for the reduced susceptibility of hsp 70i transgenic mice to BCCAo is increased hsp 70i expression, quicker in transgenic than wild type littermate mice (see Section 4.2.2).

4.2.2 Hsp 70i expression and promoter activity

Where transgenic over-expressing mice are used the nature of the over-expression is very important. Increased basal expression of a given transgene may have an immediate impact upon cellular function following an ischaemic insult. Likewise, stimulation of increased transgene expression elicited by up-regulation of specific transgene promoters may also increase the expression of a given transgene following ischaemic insult. These features are of utmost importance in the study of gene products in the pathophysiology of cerebral ischaemia. The phenomenon of delayed neuronal death following global cerebral

ischaemia has been described in several species (Ito *et al.*, 1975; Pulsinelli and Brierly, 1979; Kirino, 1982; Kirino and Sano, 1984; Smith *et al.*, 1984; Petito *et al.*, 1987; Bonnekoh *et al.*, 1990; Horn and Scholte, 1992). The mechanisms, which mediate this type of cellular death, are not fully understood. Several theories, which may be inter-related, have been hypothesised: (1) glutamate mediated excitotoxicity (Rothman & Olney, 1986; Choi *et al.*, 1988; Danysz *et al.*, 1995; Choi *et al.*, 1999,; Dirnagl *et al.*, 1999); (2) disruption of mitochondrial synthesis due to disrupted axonal transport (Abe *et al.*, 1987); (3) inflammatory attack, mediated by calcium and / or free radicals (MacManus *et al.*, 1993; Chan, 1994; Nitatori *et al.*, 1995). The array of processes evoked in ischaemic brain provide a multitude of candidates which may trigger cell survival or cell death cascades (necrotic or apoptotic). Irrespective of the mechanism, the point at which one or more of these processes is triggered in individual cells or cell populations, impacts upon the utility of potentially protective agents.

The temporal profile of endogenous hsp 70i expression varies with severity of stimulus and vulnerability of brain cells within a given region. Hsp 70i mRNA translation and subsequent transcription to protein occurs over a period of hours. Transcription deficits (of hsp 70i expression) have been reported in neurones destined to die following BCCAo in gerbil (Nowak *et al.*, 1990). Therefore the point at which cell death processes are triggered is paramount. Here, transgenic mice over-expressing hsp 70i are observed to have increased neuronal survival following BCCAo compared with their wild type littermates (see Table 13, Figure 29). These neurones may have been saved primarily by increased basal levels of hsp 70i acting to preserve intracellular protein integrity from the point of ischaemic insult. Furthermore stimulation of the rhombotin 1 promoter regulating hsp 70i expression by ischaemia (or a by-product of ischaemia) may have enabled increased and quicker expression of hsp 70i.

The rhombotin 1 promoter is up-regulated by kainate receptor activation (Hinks *et al.*, 1997) and kainate receptors are activated during ischaemia (Choi *et al.*, 1999; Dirnagl *et al.*, 1999). It is likely both of these processes occurred following BCCAo, meaning early cell death mechanisms may be ameliorated by pre-existing and speedy increases in hsp 70i transgene expression in transgenic mice employed. The endogenous hsp 70i response, which is evident from wild type littermate MF1 strain mice (see Table 16) (and has been previously shown previously in MF1 strain mice a separate study, see Table 8), may ameliorate late or less severe ischaemic cell damage. In this way hsp 70i transgenic mice may have three phases of hsp 70i expression to combat ischaemic cell changes, immediate and intermediate (driven by hsp 70i transgene over-expression) and an endogenous hsp 70i response to BCCAo. While wild type littermate mice only exhibit endogenous hsp 70i expression which may occur after ischaemic cell death has been triggered in some cells. The hypothesis that germ-line transgenic over-expression of hsp 70i is neuroprotective in cerebral ischaemia is consolidated by recent reports of decreased infarct volumes following focal cerebral ischaemia (Radjev *et al.*, 1999; Yenari *et al.*, 1999).

4.2.3 Further studies using genetically modified mice

In two further studies within the laboratory, apoE-deficient and IL-18-deficient mice were employed to investigate their roles in BCCAo (Appendices H and I). A role for apoE in regulating the response to and outcome following brain injury (including ischaemic brain injury) has been suggested following numerous reports (Teasdale *et al.*, 1997; Sheng *et al.*, 1998; Horsburgh *et al.*, 1999; McCarron *et al.*, 1999). The role of IL-18 in cerebral ischaemia is not yet known (Touzani *et al.*, 1999). ApoE-deficient mice were more susceptible to BCCAo than their wild type littermates. IL-18-deficient mice were also more susceptible to BCCAo than their wild type littermates. These results suggested that apoE and IL-18 genes modified the pathophysiological response following BCCAo. Furthermore, intraventricular infusion of exogenous apoE (prior to, during and following

BCCAo) was shown to significantly reduce ischaemic neuronal damage (Horsburgh *et al.*, 2000). A similar rhetoric, whereby exogenous IL-18 was intracerebrally injected into IL-18-deficient mice, did little to ameliorate ischaemic brain damage (and in fact may have been toxic, appendix J). The apparent success of intraventricular infusion of apoE in reducing ischaemic neuronal damage in apoE-deficient mice strongly supported a beneficial role for apoE in the brain response to ischaemia. The failure of intracerebral IL-18 injection to ameliorate ischaemic neuronal damage suggests IL-18 may not be so important in the pathophysiology of ischaemic brain damage. However, these studies highlight a design flaw. For example, following brain injury apoE is markedly increased and secreted (predominantly from astrocytes) into the extracellular space (Poirier, 1994). ApoE mRNA has not been found in neurones to date (Horsburgh *et al.*, 1999), although several investigators have identified apoE in vulnerable neurones following ischaemia (Hall *et al.*, 1995; Horsburgh and Nicholl, 1996). These findings suggest a mechanism for neuronal apoE uptake from the extracellular space (i.e., intraventricularly infused apoE could be taken up by neurones). The cellular source of IL-18 in the brain has only recently been identified *in vitro* (Conti *et al.*, 1999; Prinz and Hanisch, 1999). The cell types implicated are microglia and astrocytes. An antibody to IL-18 has not yet been produced and furthermore, only one study upon the role of IL-18 in cerebral ischaemia has been undertaken (Appendix I). Therefore intracerebral injection of IL-18 might not necessarily lead to increased neuronal IL-18, as no mechanism has been postulated. Sophisticated systems of directly injecting or infusing molecules into the brain have been developed. These systems include the use of vectors (such as viral vectors, see below), which, can be targeted to specific cell types including neurones and glial cells (Hermens and Verhaagan, 1997; Weihl, 1999; Sapolsky and Steinberg, 1999).

4.2.4 Ad hsp 70i gene transfer is neuroprotective

Ad hsp 70i gene transfer was hypothesised to ameliorate ischaemic neuronal damage following BCCAo. Ad egfp gene transfer was hypothesised to have no biological effect upon ischaemic neuronal damage following subsequent BCCAo. These assumptions were based on previous findings. Several studies employing ad vector transfection of a number of different therapeutic genes have been shown to ameliorate ischaemic neuronal damage *in vivo* and *in vitro* (see Section 1.9.5). Moreover, ad gene transfer of β-galactosidase (a commonly used reporter gene, like egfp) has been reported to have no significant effect upon ischaemic outcome (Betz *et al.*, 1995; Kindy *et al.*, 1996; Yang *et al.*, 1999). In this thesis, both ad hsp 70i and ad egfp significantly reduced ischaemic neuronal damage in ipsilateral caudate nucleus compared to contralateral caudate nucleus in mice subjected to 20-minute BCCAo (see Figure 42). While it is entirely unlikely that ad hsp 70i and ad egfp reduce ischaemic neuronal damage of striatal neurones by the same mechanism, the data of the present study cannot clarify this.

4.2.5 Impact of injecting ad vectors into the brain

First generation ad vectors (E1-deleted, used in this thesis) have many advantages including efficient and relatively safe gene transfer into dividing and quiescent cells (Breakfield, 1993; Heistad and Faraci, 1996; Verma & Somia, 1997). E1-deleted ad vectors however, induce innate cellular and humeral immune responses in the periphery (Yang *et al.*, 1994a, 1994b, 1995; Simon *et al.*, 1993; Dai *et al.*, 1995) and in brain (Byrnes *et al.*, 1995, 1996a; Kajiwara *et al.*, 1997, 2000). In peripheral organs, such as the liver, the immune response eliminates E1-deleted ad particles and transduced cells within 14-21 days (Elkon *et al.*, 1997). In brain, E1-deleted ad mediated transgene expression persists for somewhat longer durations (Wood *et al.*, 1996). Geddes *et al.*, (1997) report stable reversion of diabetes insipidus phenotype in Brattleboro rats transfected with ad vectors containing vasopressin four months after injection. The stability of E1-deleted ad

transgene expression is, however, significantly reduced where the subject is subsequently exposed peripherally to the same ad vector (Byrnes *et al.*, 1996b). Moreover, the anatomical site of ad vector injection into the brain significantly affects the immune response. Using replication competent influenza virus Stevenson *et al.*, (1997a) reported that immune response priming in the brain occurred following infection of the cerebrospinal fluid, but not the parenchyma. Stevenson *et al.*, (1997b) subsequently suggested that immune responses in the brain could be region specific.

The immune response consists of two aspects, the cellular immune response and the humeral immune response. In the periphery, cellular immunity to ad vectors is believed to be the predominant mechanism limiting the duration of transgene expression by killing virus infected cells (Kajiwara *et al.*, 2000). Humeral immunity is believed to be the predominant mechanism limiting secondary ad transduction (Kay *et al.*, 1995). In brain, the inflammatory and immune responses to ad vectors are not well understood. Recent studies using ad vectors have shown involvement of the cellular and humeral immune responses. Intracerebroventricular (i.e., into the cerebrospinal fluid and not the parenchyma) injection of E1/E3 deleted ad vectors was reported to induce rapid release of tumour necrosis factor-α, interleukin-1β and interleukin-6 pro-inflammatory cytokines (Cartmell *et al.*, 1999). While, intrastriatal injection of E1-deleted ad vectors containing β-galactosidase gene has been shown to produce a humoral immune response (Kajiwara *et al.*, 2000). Thus anti-ad antibodies and anti-β-galactosidase antibodies were produced.

4.2.6 Hsp 70i expression following ad vector injection into brain

Kitagawa *et al.*, (1998) reported expression of hsp 70i following intrahippocampal and intraventricular injection of E1/E3 deleted ad vectors containing the β-galactosidase gene. Expression of hsp 70i was local to the site of virus injection and β-galactosidase transfection in the hippocampus and lateral ventricle. In this thesis, hsp 70i expression was

observed in mice injected with ad hsp 70i and ad egfp subjected to 10 and 20-minute BCCAo. BCCAo of these durations had been shown previously to induce hsp 70i expression in large numbers of neurons in several brain regions of C57bl/6 strain mice, including the caudate nucleus (see Table 8). In the present study, hsp 70i expression was also abundant in several brain regions, including the caudate nucleus (see Tables 19 and 20). Unfortunately it was not possible to attribute hsp 70i expression observed here to ad or BCCAo alone. However, hsp 70i expression in ipsilateral ad injected caudate nucleus was significantly greater than that in contralateral caudate nucleus in mice subjected to 10 and 20-minute BCCAo (see Figures 44, 45, 46, 47 and 48). This suggests that ad hsp 70i transfection may be a significant factor in attenuating ischaemic neuronal damage in these mice. Hsp 70i expression in ipsilateral ad egfp injected caudate nucleus was not significantly greater than that in contralateral caudate nucleus in mice subjected to 10 and 20-minute BCCAo. The levels of hsp 70i expression in ad egfp transfected mice subjected to 20-minute BCCAo were; however, very similar to those in ad hsp 70i transfected mice. This suggests that ad egfp gene transfer may induce hsp 70i expression, which could ameliorate ischaemic neuronal damage.

4.2.7 Immune responses to ischaemia: effect on ad transgene expression

The expression of the pro-inflammatory cytokines interleukin-1, interleukin-6 and tumour necrosis factor-α in normal physiologic conditions are very low (Touzani *et al.*, 1999). However, these cytokines are up-regulated in the brain following injury, including ischaemia (Stoll *et al.*, 1998; Touzani *et al.*, 1999). The paradigm for the study being discussed here involved intrastriatal injection of ad hsp 70i or ad egfp followed by BCCAo of 10 or 20 minutes duration 14-days later. The impact of ad vector injection into the brain has already been discussed (section 4.2.5) and it is realised that the cellular immune response is believed to limit the duration of transgene expression (Kajiwara *et al.*, 2000). Given the severity of the ischaemic insult (produced in C57bl/6 strain, used here), it is not

unreasonable to assume some inflammatory response may have been elicited in the brain following reperfusion (not tested). If such a response did occur, transfected ad particles and transgene expression might have declined. Comparison of 10 and 20-minute BCCAo mice indicated that there were no significant differences in the level of transgene expression between ischaemic durations.

4.2.8 Importance of mouse strain

The strain of mouse chosen for experiments such as the present is also very important. Mouse strain has been reported to affect vector transgene expression rate (Christenson *et al.*, 1998), immune response (Ohmoto *et al.*, 1999) and susceptibility to BCCAo (Yang *et al.*, 1997; Fujii *et al.*, 1997). C57bl/6 strain mice (used here) have been shown to exhibit increased susceptibility to BCCAo (see Section 3.1). Inter-hemispheric association of ischaemic neuronal damage was also a very important feature of the study at hand, as ad vectors were injected unilaterally and the effects compared to the contralateral hemisphere. C57bl/6 strain mice displayed significant inter-hemispheric association of ischaemic neuronal damage (Appendix E) enabling meaningful comparison between ischaemic neuronal damage between in ipsilateral (ad injected) and in contralateral hemispheres could be made.

4.3 Functional consequences of transgene introduction in mice

Having observed the neuroprotective effects of hsp 70i transgene over-expression (in hsp 70i transgenic mice and in mice with intrastriatal ad hsp 70i gene transfer). The third aim of this thesis was to investigate the impact of transgene over-expression on brain function. Changes in LCGU were measured using ^{14}C-2-deoxyglucose autoradiography. Directed over-expression of transgenes was investigated in two systems. First, transgenic mice over-expressing hsp 70i from birth (i.e., hsp 70i was introduced in the germ-line) were investigated. Second, adult mice were intrastriatally injected with ad egfp (producing transfection of all cell types with egfp) were investigated.

4.3.1 Utility of ^{14}C-2-deoxyglucose autoradiography

^{14}C-2-deoxyglucose autoradiography can be used to determine LCGU in discrete and functionally diverse brain regions simultaneously in conscious, freely moving animals. The ^{14}C-2-deoxyglucose autoradiographic technique has been extensively employed to map functional consequences of various environmental, neuropharmacologic and neurophysiologic interventions. These investigations have been carried out predominantly in the rat (Sokoloff *et al.*, 1977 published their description of the technique in rat). However, the technique has been adapted and used in a range of species, including mouse (Nowaczyk and Des Rosiers, 1981). Moreover, a number of modifications to the Sokoloff *et al.*, (1977) technique have also been reported (Schwartz , 1978a, 1978b; Brown and Wolfson, 1978). In this thesis, a modification of the Nowaczyk and Des Rosier, (1981) approach was used to investigate the functional consequences of germ-line and ad mediated transgene expression in the mouse brain.

Two major modifications to the approach of Nowaczyk and Des Rosier, (1981) were implemented. First, ^{14}C-2-deoxyglucose was injected intraperitoneally (not intravenously). Second, only a terminal blood sample was collected (as opposed to 14 timed arterial

samples throughout the 45-minute experimental period). These modifications were driven by two main concerns. First, the impact of hypovolaemic effects of withdrawing blood from mice. Second, increases in motor function and hyperexcitability elicited by dizocilpine injection in mice. The route of ^{14}C-2-deoxyglucose administration significantly affects the uptake and clearance of the isotope from the blood (Kelly and McCulloch, 1983). The absence of any plasma ^{14}C and plasma glucose data from the experimental period precluded the use of the operational equation of Sokoloff *et al.*, (1977) (see Figure 6). However tissue ^{14}C concentration was measured densitometrically and plasma ^{14}C and glucose concentration were determined from a terminal blood sample. Tissue ^{14}C in a region of interest could therefore be normalised to an area in which ^{14}C uptake was notionally unaltered (in this case the cerebrellar cortical grey matter, Figure 62). Thus the relative rates of ^{14}C-2-deoxyglucose uptake from plasma in individual mice, in individual brain regions could be accounted for. Moreover, because terminal plasma ^{14}C and glucose concentrations were measured, the relationship between tissue ^{14}C and glucose could be explored. In this way tissue ^{14}C (cerebellar cortical grey matter) was observed to correlate well with plasma ^{14}C / glucose (see Figures 50 and 57). While this approach does not offer precise values of LCGU it does provide a reliable estimate without the complications of invasive surgical procedures.

4.3.2 LCGU in hsp 70i transgenic mice

LCGU in transgenic mice over-expressing hsp 70i did not differ significantly compared to wild type littermate mice, in any of the 35 brain regions analysed (see Table 22). Following metabolic activation (produced by dizocilpine injection) there were widespread marked, heterogeneous alterations in LCGU between hsp 70i transgenic and wild type littermate mice in the basal state (see Tables 23 and 24). The patterns of the alterations in LCGU evoked in mouse by dizocilpine were broadly similar to those reported in the rat (Nehls *et al.*, 1988, 1990; Kurumaji *et al.*, 1989). These alterations in LCGU which

Figure 62 **^{14}C in cerebellar cortical grey matter**

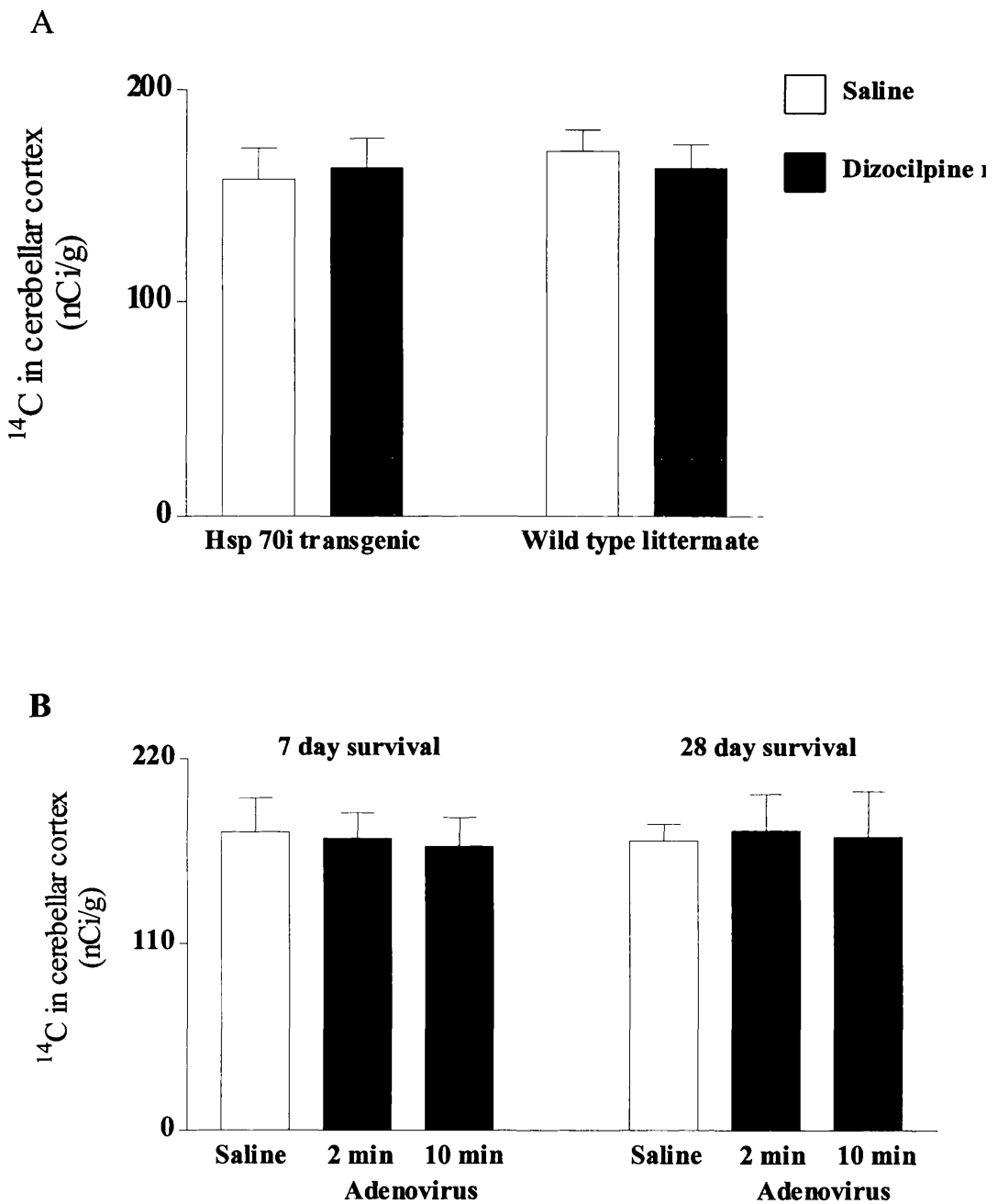

^{14}C concentration was similar in all groups, irrespective of genotype and dizocilpine injection (A) or intrastriatal injection of ad egfp (B).

encompass the Papez circuit (entorhinal cortex → hippocampus → mammillary body → anterior thalamus → entorhinal cortex) (Nehls *et al.*, 1988) are accompanied by a range of neurophysiologic events. Among these neurophysiologic events are immediate early gene induction (Dragunow and Faull, 1990; Gass *et al.*, 1993), ionic homeostasis / cell swelling (Olney *et al.*, 1989) and hsp 70i expression (Sharp *et al.*, 1991).

Metabolic activation with dizocilpine produced significantly altered LCGU in transgenic mice over-expressing hsp 70i compared with wild type littermates, in five of 35 brain regions analysed (see Table 25, Figures 51, 52, 53 and 54). Three of these regions (anterior thalamic nucleus, hippocampus CA1 stratum lacunosum moleculare and hippocampus CA1 stratum oriens) displayed marked increases in LCGU in hsp 70i transgenic mice compared wild type littermate mice. Anterior thalamic nucleus and hippocampus are components of the Papez circuit (which is activated by dizocilpine) and are known to chronically over-express hsp 70i (as the rhombotin 1 promoter is present in these regions, Hinks *et al.*, 1997). Hence the increases in LCGU could be attributed to hsp 70i over-expression. However, this does not explain why other transgene rich areas, activated by dizocilpine, such as caudate nucleus, do not display similar increases in LCGU compared with wild type littermate mice. One hypothesis that could explain this is that dizocilpine activation produces maximal increases in LCGU in areas such as the caudate nucleus, which cannot be influenced by hsp 70i transgene over-expression. Whereas, in areas such as anterior thalamic nucleus, dizocilpine evoked marked increases in LCGU which could be further increased by the presence of hsp 70i transgene. Given hsp 70i is an ATPase, which operates to ameliorate intracellular protein malfolding and trafficking caused by insult or injury, then hsp 70i may enable increased cellular function reflected by increased LCGU.

The two other regions (superior olivary body and nucleus of the lateral lemniscus) displayed marked decreases in LCGU in hsp 70i transgenic mice compared with wild type littermate mice. The reason why LCGU in the superior olivary body and the nucleus of the lateral lemniscus was significantly decreased in transgenic mice over-expressing hsp 70i compared with wild type littermate mice is less clear. It is unlikely that dizocilpine effected these changes in LCGU. While, dizocilpine has effects on some auditory nuclei, no effect was seen relative to vehicle (see Tables 22 and 25) or previously in rat (Kurumaji *et al.*, 1989). It is also unlikely that hsp 70i transgene effected these changes in LCGU. As the rhombotin 1 promoter is not prevalent in these regions (Hinks *et al.*, 1997). In short, it remains unclear why LCGU should decrease significantly in these brain regions.

4.3.3 LCGU in IL-18 deficient mice

In a further study within the laboratory, IL-18 deficient mice were employed to investigate the impact of IL-18 deficiency upon LCGU. The precise role IL-18 in the brain is not yet known (Touzani *et al.*, 1999). In the present study IL-18 deficient mice displayed significantly increased LCGU (compared to their wild type littermates) in 14 of 18 brain regions analysed (Appendix K). Increases in LCGU were observed throughout the forebrain in striatal, cortical and hippocampal structures. These data clearly show that IL-18 deficient mice display widespread heterogeneous increases in LCGU. This suggests that IL-18 may have an inhibitory role in the brain or that IL-18 deficiency stimulates increased cerebral function.

4.3.4 LCGU following intrastriatal ad egfp gene transfer

Two approaches of measuring LCGU in the caudate nucleus following ad egfp gene transfer were employed (see Appendix F). LCGU was measured in the entire caudate nucleus and in circumscribed areas of ad egfp transgene expression and needle damage (see Appendix F). These approaches produced different findings in the same groups of

mice. Where LCGU in the entire caudate nucleus was measured, ad egfp gene transfer had no significant effect (see Figure 58). Where LCGU was measured in circumscribed areas of the caudate nucleus, ad egfp expression effected significant alterations in LCGU (see Figure 60).

Ads bind to an as yet unidentified cell surface receptors (Hermens and Ver Haagen, 1997). The ad then becomes internalised, the viral nucleocapsid is released from endosomes and transported to the nucleus (Greber *et al.*, 1993; Figure 63). Once inside the nucleus the ad replicates to produce daughter virions. Infection with wild type ad results in cell death and release of daughter virions (Figure 64). Whereas, infection with replication-deficient (recombinant, E1-deleted vectors) produces expression of transgene only (Figure 64, although some inflammatory and immune responses have been reported, see Section 4.2.5). In the present study, brain areas in which ad egfp transfection was observed displayed significantly reduced LCGU compared to the contralateral hemisphere at seven and 28-days (see Figure 61). There were no differences in LCGU between hemispheres in saline injected mice. These data suggest that ad egfp gene transfer reduce cerebral function. The mechanisms by which ad egfp transfection leads to these reductions remain unclear at present.

Intrastriatal needle insertion and injection of fluid causes localised structural damage in the caudate nucleus (see Figure 49, Appendix F). In some mice needle insertion also produced small bleeds. On ^{14}C-2-deoxyglucose autoradiograms structural damage and associated bleeding appeared as intense, dark regions, mimicking increased LCGU (Figure 65). Dark regions were observed almost exclusively at 7 days post-injection in mice in which needle extraction was performed at 2 minutes after injection. These regions were considered to be artefacts and represent a major source of error in ^{14}C-2-deoxyglucose densitometry in such experiments. In ad egfp transfected mice a second intriguing feature was observed. LCGU

Figure 63 **Ad infection**

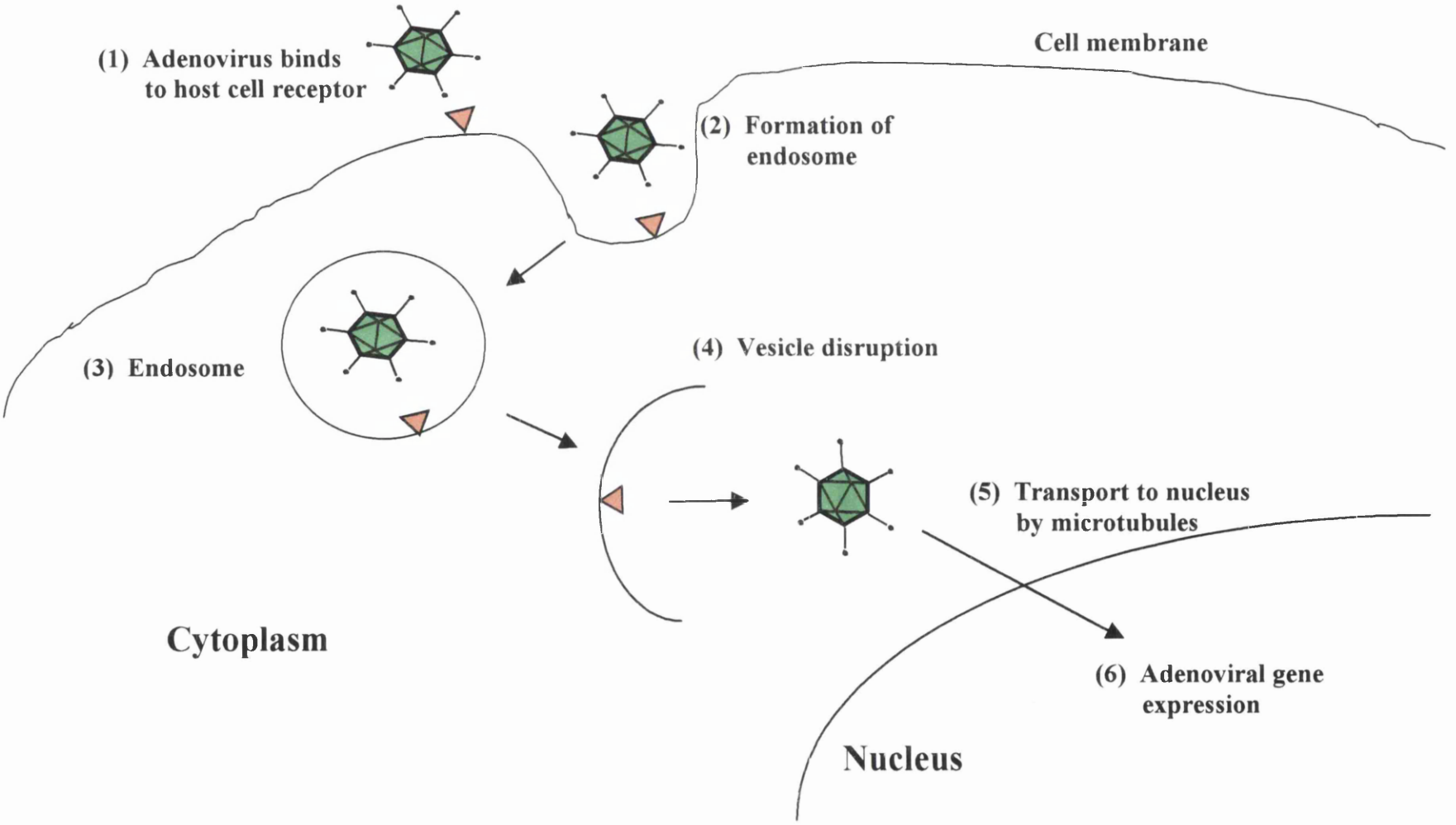

Figure 64 **Wild type and recombinant ad cell cycle**

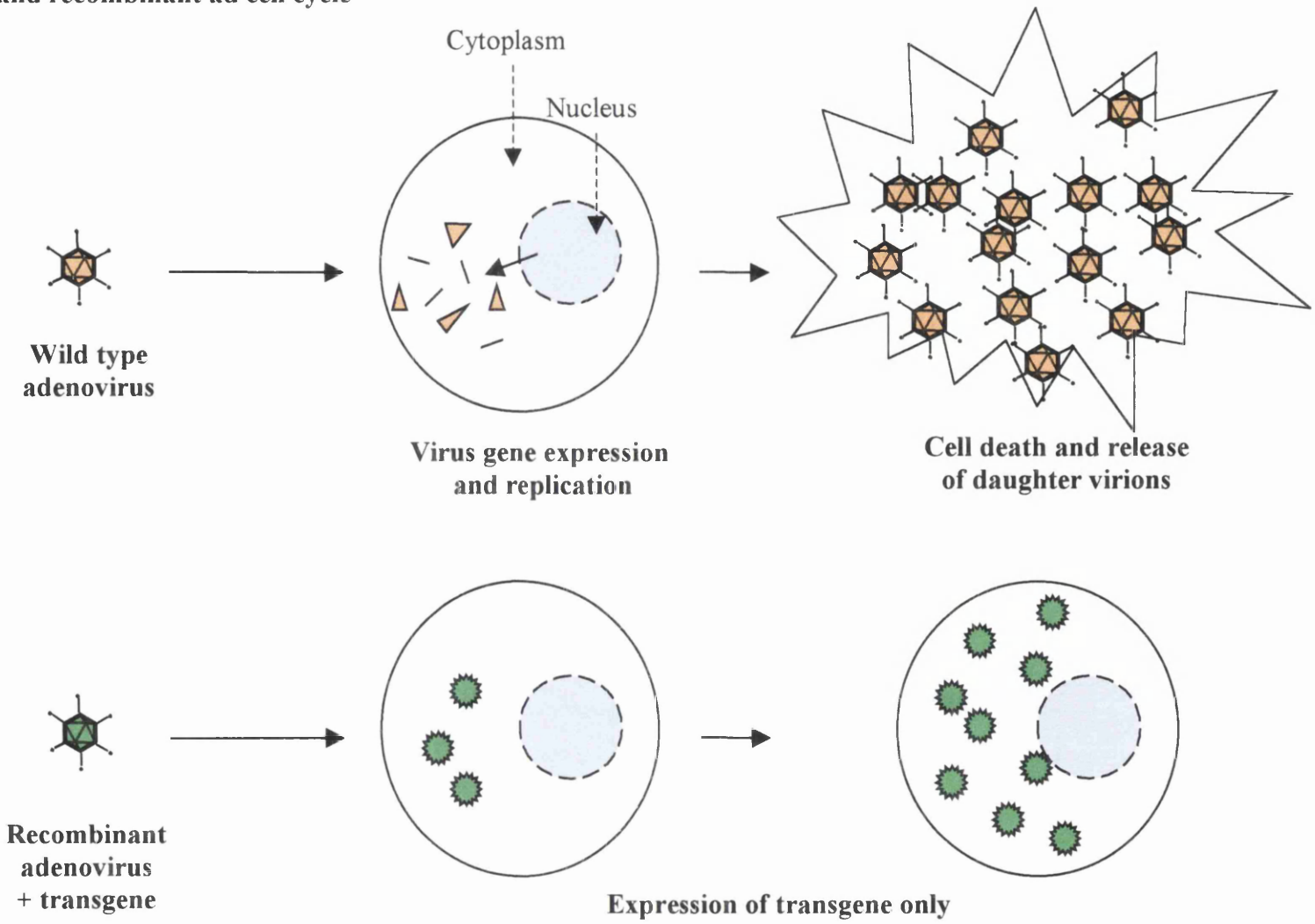

Figure 65 Needle damage on autoradiograms: seven and 28 days post-injection

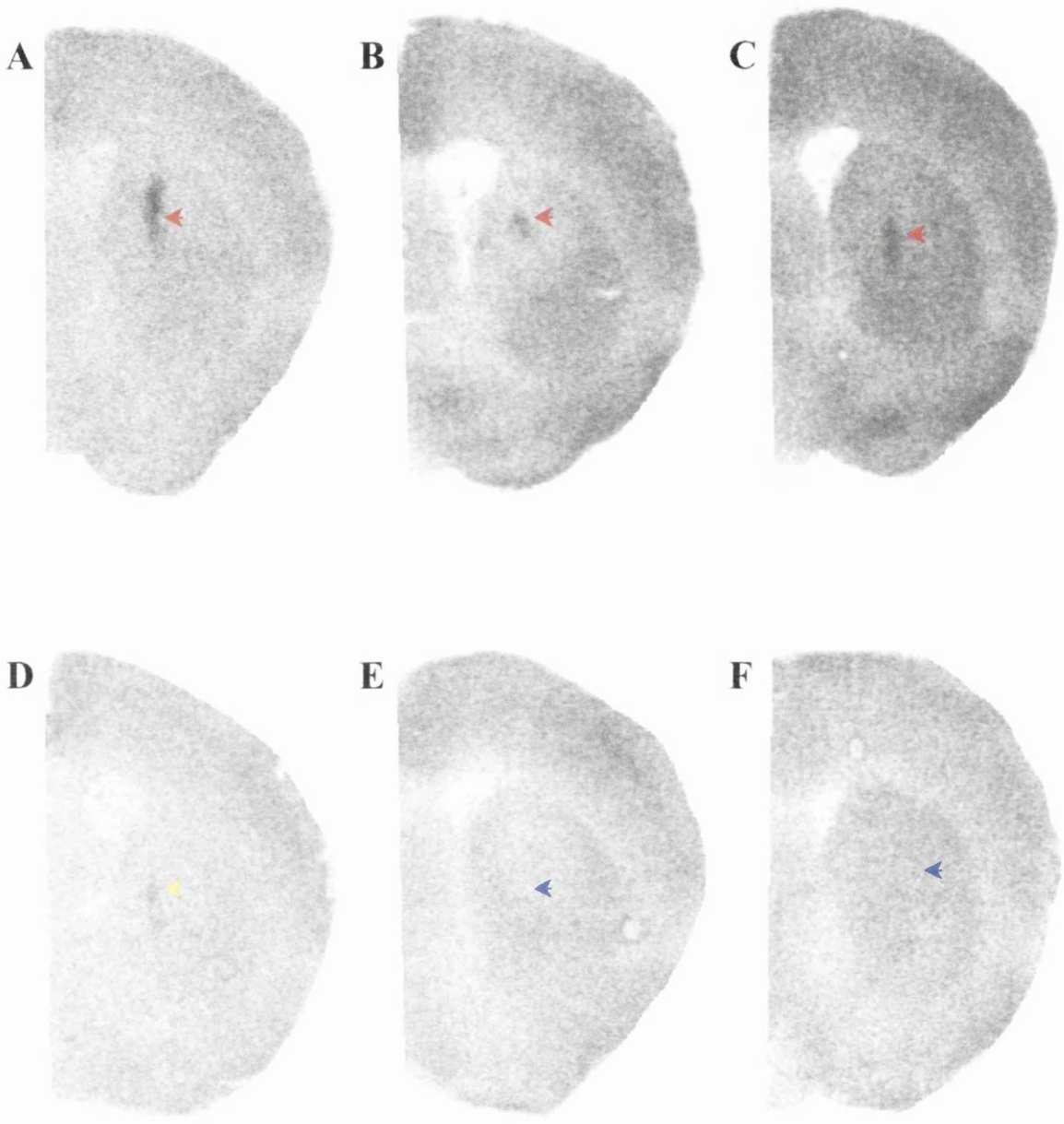

Needle damage at seven days appeared on autoradiograms as dark areas (red arrows; saline A, ad egfp 2 min needle extraction B, ad egfp 10 min needle extraction C). Needle damage at 28 days appeared as dark areas only in saline injected mice (D, yellow arrow). Needle damage at 28 days in ad egfp (2 min and 10 min needle extraction) did not appear as dark areas (E and F, blue arrows).

(measured at 28 days post-injection) in the ipsilateral caudate nucleus was significantly decreased compared to contralateral caudate nucleus (in mice in which needle extraction was performed at two and ten minutes, see Figure 61). While LCGU in saline injected mice was not significantly different between hemispheres at 28 days post-injection. On this occasion it is likely that the areas of reduced LCGU are areas of irreversibly damaged tissue, lacking in functional synapses. This also represents a major source of error in ^{14}C-2-deoxyglucose densitometry in this type of experiment.

4.3.5 LCGU following intrastriatal hsv β-galactosidase gene transfer

In a further study within the laboratory, hsv vectors containing β-galactosidase (reporter gene) were intrastriatally injected into mice to investigate the effect on LCGU. In mice intrastriatally injected with wild type hsv β-galactosidase, LCGU in the ipsilateral caudate nucleus (in regions of β-galactosidase transfection) was not significantly altered compared to LCGU in the contralateral hemisphere at three days post injection (Appendix L). Similarly, in mice intrastriatally injected with attenuated hsv (McKie *et al.*, 1998) β-galactosidase, LCGU in the ipsilateral caudate nucleus (in regions of transfection) was also not significantly altered compared to LCGU in the contralateral hemisphere at three days post-injection (Appendix L). One striking feature of this study was, the compelling difference in the extent of β-galactosidase transfection produced by wild type hsv compared to attenuated hsv (Appendix L). The area of wild type hsv β-galactosidase transfection (at three days post-injection) was similar in magnitude to that observed with attenuated ad egfp transfection at seven and 28 days post-injection (see Figures 55) and 17 days post-injection with BCCAo (see Figure 36).

4.4 Conclusions

The data presented within this thesis clearly fulfil the three main aims proposed at the outset. In fulfilling these aims five major conclusions could be drawn from this work. First, MF1 strain mice are less susceptible to BCCAo than C57bl/6 strain mice. Second, transgenic mice over-expressing hsp 70i display significantly less ischaemic neuronal damage than their wild type littermates following BCCAo. Third, ad gene transfer of hsp 70i ameliorates ischaemic neuronal damage in C57bl/6 strain mice subjected to BCCAo. Fourth, LCGU in transgenic mice over-expressing hsp 70i is unchanged in the basal state, but is altered significantly following metabolic activation with dizocilpine, compared with wild type littermates. Fifth, ad mediated transfection of egfp significantly decreases LCGU in areas of egfp transfection.

LIST OF PUBLICATIONS

Papers

Hakuba, N., Wei, X.Q., **Kelly, S.,** Liew, L.W. and McCulloch, J. (2000) Increased local cerebral glucose utilisation in Il-18 deficient mice. (in preparation).

Hakuba, N., Wei, X.Q., **Kelly, S.,** Liew, L.W. and McCulloch, J. (2000) Increased ischaemic neuronal damage in IL-18 deficient mice following transient forebrain ischaemia. (in preparation).

Horsburgh, K., **Kelly, S.,** McCulloch, J., Higgins, G., Roses, A.D. and Nicoll, J.A.R. (1999) Increased neuronal damage in apolipoprotein E-deficient mice following global ischaemia. *NeuroReport,* **10** (4), 1-5.

Kelly, S., Hughes, D., Harding, T., Rabbitts,T., Sofroniew,M.V., McCulloch, J. and Uney J.B. (2000) Targeting expression of human hsp70i to CA1 and CA2 hippocampal neurones using the LMO-1 promoter: assessment of hsp70i's neuroprotective effects *in vivo* and *in vitro*. (in preparation).

Kelly, S., McCulloch, J., Nicoll, J.A.R. and Horsburgh, K. (2000) MF1 strain mice are less susceptible to global cerebral ischaemia than C57bl/6 strain mice. (in preparation).

Kelly, S., Uney, J.B. and McCulloch, J. (2000) Altered local cerebral glucose utilisation in hsp 70i transgenic mice following dizocilpine maleate administration. (in preparation).

Kelly, S., Uney, J.B. and McCulloch, J. (2000) Adenovirus egfp gene transfer reduces local cerebral glucose utilisation in caudate nucleus. (in preparation).

Kelly, S., Uney, J. and McCulloch, J. (2000) Adenovirus hsp 70i gene transfer is neuroprotective to global cerebral ischaemia. (in preparation).

Abstracts

Hakuba, N., Wei, X.Q., **Kelly, S.,** Liew, L.W. and McCulloch, J. (1999) Cerebral glucose utilisation in interleukin-18 null mice. *Journal of Cerebral Blood Flow and Metabolism*, **19** supplement 1, S299.

Horsburgh, K., **Kelly, S.,** McCulloch, J., Higgins, G., Roses, A.D. and Nicoll, J.A.R. (1998) Apolipoprotein E deficient mice have increased neuronal damage following global ischaemia. *Neurobiology of Ageing*, **19**(4S), S281.

Horsburgh, K., **Kelly, S.,** Nicoll, J.A.R. and McCulloch, J. (1999) Differences in susceptibility of MF1 mice compared to C57bl/6 mice following transient cerebral ischaemia. *Journal of Cerebral Blood Flow and Metabolism*, **19** supplement 1, S589.

Kelly, S., Uney, J.B. and McCulloch, J. (1998) Effect of intense metabolic stress upon heat shock protein 70i transgenic mice: A ^{14}C-2-deoxyglucose autoradiography study. *British Journal of Pharmacology*, **125** proceedings supplement, 2P.

Kelly, S., Uney, J.B. and McCulloch, J. (1999) Subtle differences in susceptibility of hsp 70i transgenic mice compared to their wild type counterparts. *Journal of Cerebral Blood Flow and Metabolism*, **19** supplement 1, S293.

Kelly, S., Horsburgh, K. and McCulloch, J. (1999) Minimal neuronal damage after prolonged bilateral common carotid artery occlusion in MF1 mice. *Journal of Cerebral Blood Flow and Metabolism*, **19** supplement 1, S518.

Riley, P.M., **Kelly, S.,** Hakuba, N., Brown, S.M. and McCulloch, J. (1999) The utility of ^{14}C-2-deoxyglucose autoradiography in assessing dysfunction after intra-striatal HSV vector injection. *29th Annual Meeting, Society for Neuroscience.* 655.2.

Kelly, S., Uney, J.B. and McCulloch, J. (2000) Adenovirus egfp gene transfer reduces local cerebral glucose utilisation in caudate nucleus. (in preparation).

Kelly, S., Uney, J. and McCulloch, J. (2000) Adenovirus hsp 70i gene transfer is neuroprotective to transient forebrain ischaemia. (in preparation).

APPENDICES

Appendix A Stock solutions

Phosphate Buffer (50 millimolar; pH 7.4)

Stock solutions:

A	sodium dihydrogen orthophosphate ($NaH_2PO_42H_2O$)	24 g/l distilled water
B	disodium hydrogen orthophosphate ($Na_2HPO_42H_20$)	28.5 g/ l distilled water

Add 95ml stock A and 405ml stock B to 1.5 litres of distilled water and mix

Phosphate buffered saline (50 millimolar; pH 7.4)

Stock solutions:

A	sodium dihydrogen orthophosphate ($NaH_2PO_42H_2O$)	24 g/l distilled water
B	disodium hydrogen orthophosphate ($Na_2HPO_42H_20$)	28.5 g/ l distilled water

Add 95ml stock A and 405ml stock B to 1.5 litres of 0.9% saline and mix

4% paraformaldehyde

In a fume hood gently heat two litres of phosphate buffer to 65°C. To this add 80g of paraformaldehyde and mix until completely dissolved. Chill mixture to 4°C and filter before use. Fresh fixative was freshly prepared as required.

Appendix B Identification of ischaemic cell change: validation

My ability to identify and score ischaemic cell change following BCCAo in MF1 and C57bl/6 strain mice was compared directly to values obtained by Dr Karen Horsburgh.

MF1

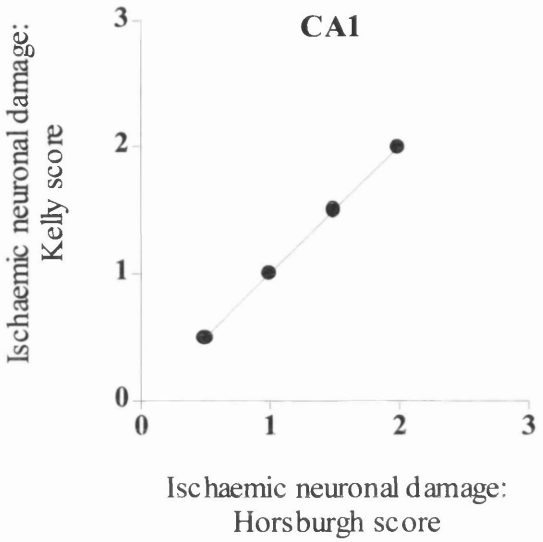

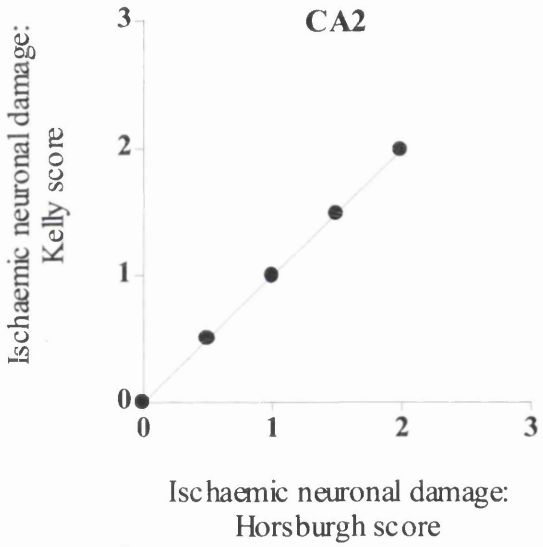

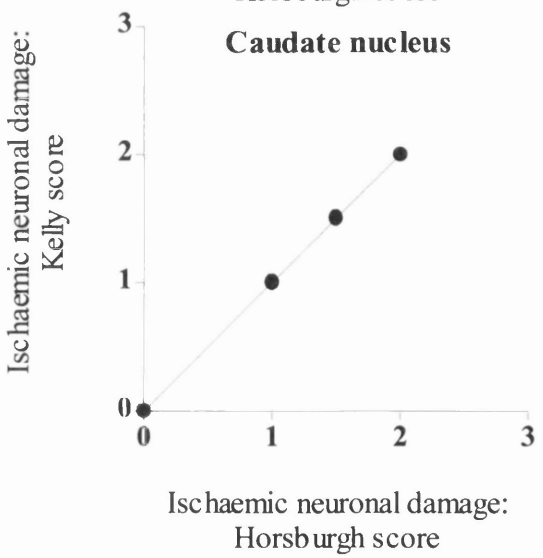

C57bl/6

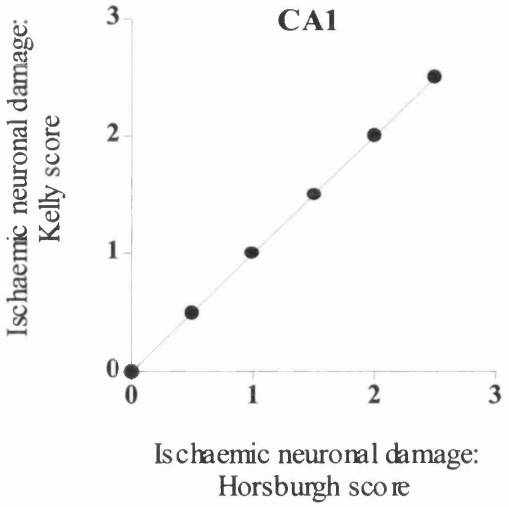

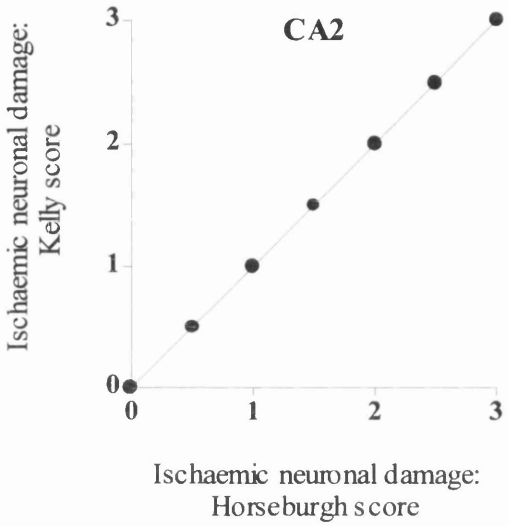

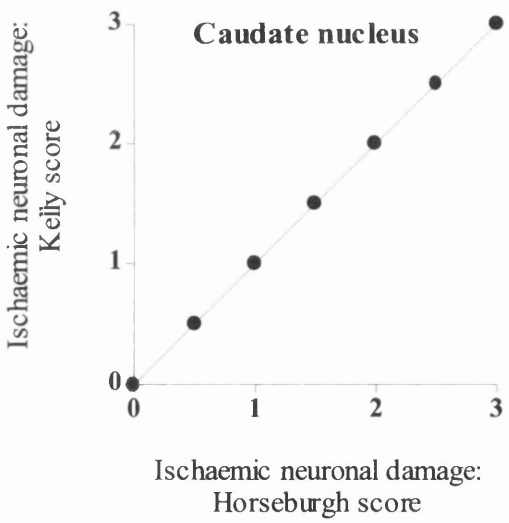

My scores were identical to those of Dr Horsburgh.

Appendix C Identification of ischaemic cell change: consistancy

My ability to consistently identify and score (semi-quantitatively and quantitatively) ischaemic cell change following BCCAo in MF1 and C57bl/6 strain mice (two months apart) was excellent.

MF1 score

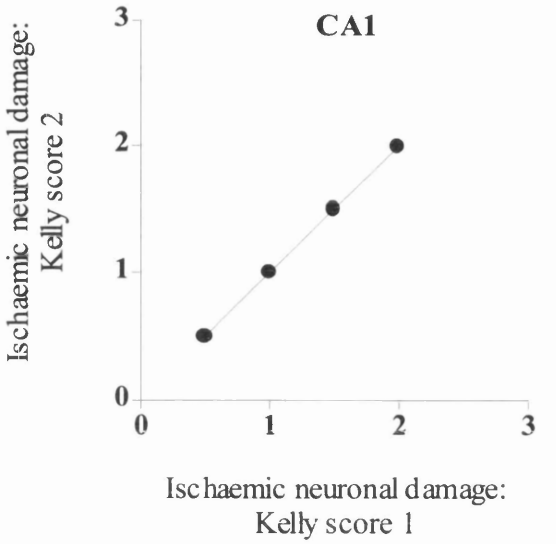

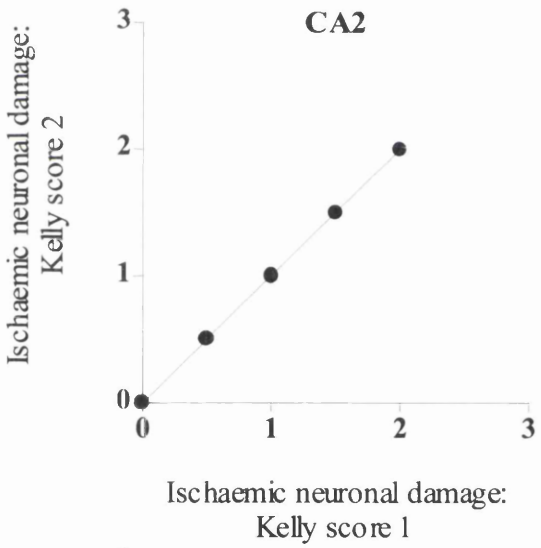

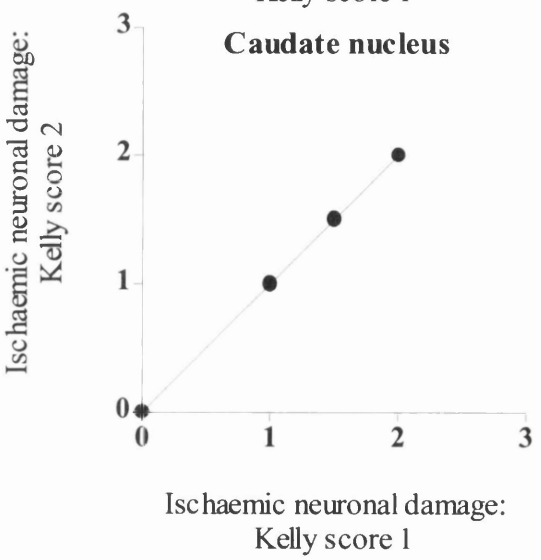

C57bl/6 score

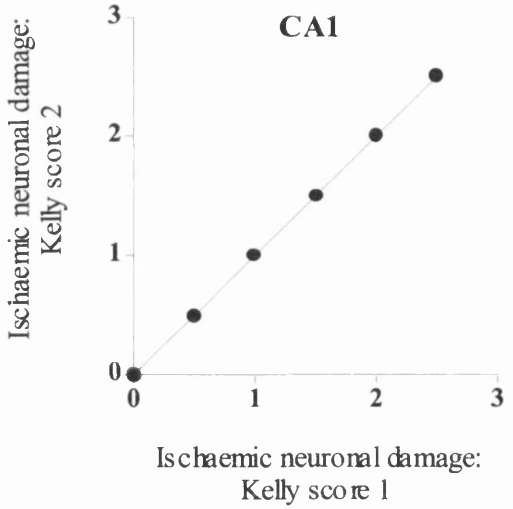

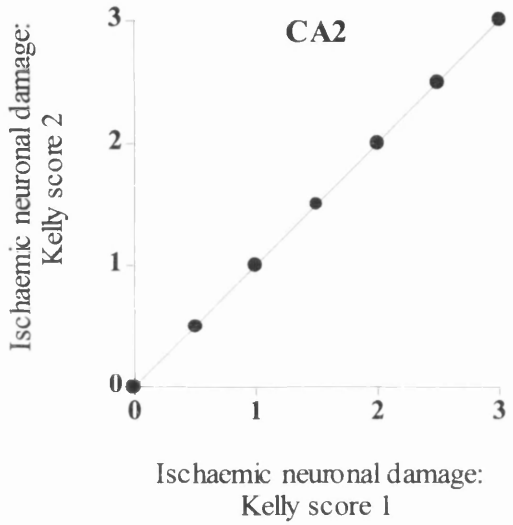

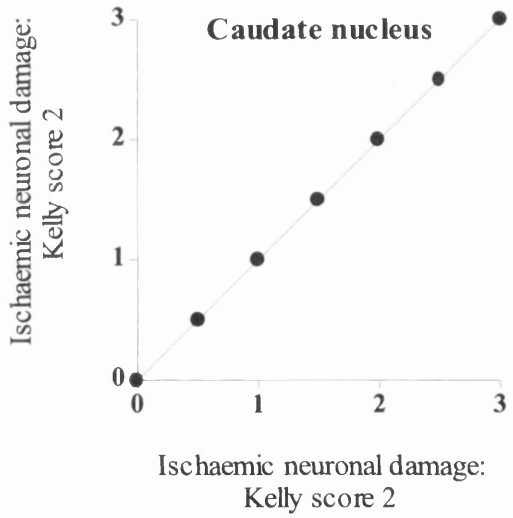

MF1 percent

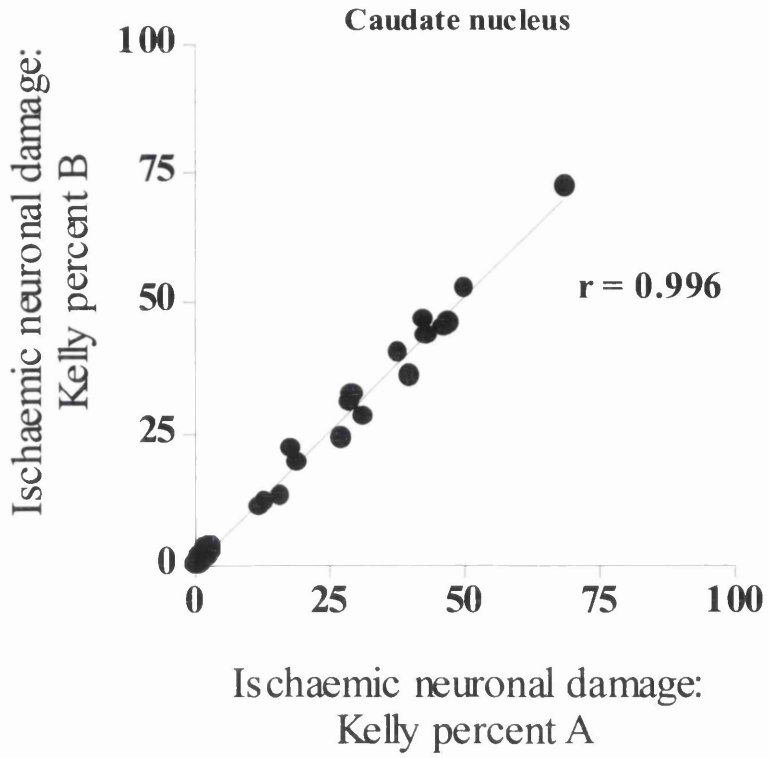
Caudate nucleus
Ischaemic neuronal damage:
Kelly percent B
100
75
50
25
0
r = 0.996
0
25
50
75
100
Ischaemic neuronal damage:
Kelly percent A

Appendix D Optimising anti-hsp 70i antibody

The optimal concentration of anti-hsp 70i antibody was determined for each study in which hsp 70i immunohistochemical detection was required. A range of anti-hsp 70i antibody concentrations (0% A, 0.02% B, 0.04% C, 0.1% D, 0.2% E, 0.4% F and 1% G) was run on each occasion. Zero percent anti-hsp 70i antibody was run as a negative control. In the first study using anti-hsp 70i antibody all dilutions were run on ischaemic tissue (positive control) and non-ischaemic (sham, negative control). Moreover, another established and commonly used monoclonal antibody (anti-synaptophysin antibody) was run on these tissues to ensure the proper procedure was followed. Where zero percent anti-hsp 70i antibody was incubated on ischaemic and non-ischaemic tissue there was no immunohistochemical detection of hsp 70i. Where anti-hsp 70i was incubated on non-ischaemic tissue there was also no immunohistochemical detection of hsp 70i. Where anti-hsp 70i was incubated on ischaemic tissue immunohistochemical detection of hsp 70i at all concentrations. Using a light microscope, each concentration of anti-hsp 70i antibody was analysed. One part anti-hsp 70i in 1000 (0.1%, D) offered the best contrast of immunohistochemical staining of neurones and fibres with minimal or no background in all studies.

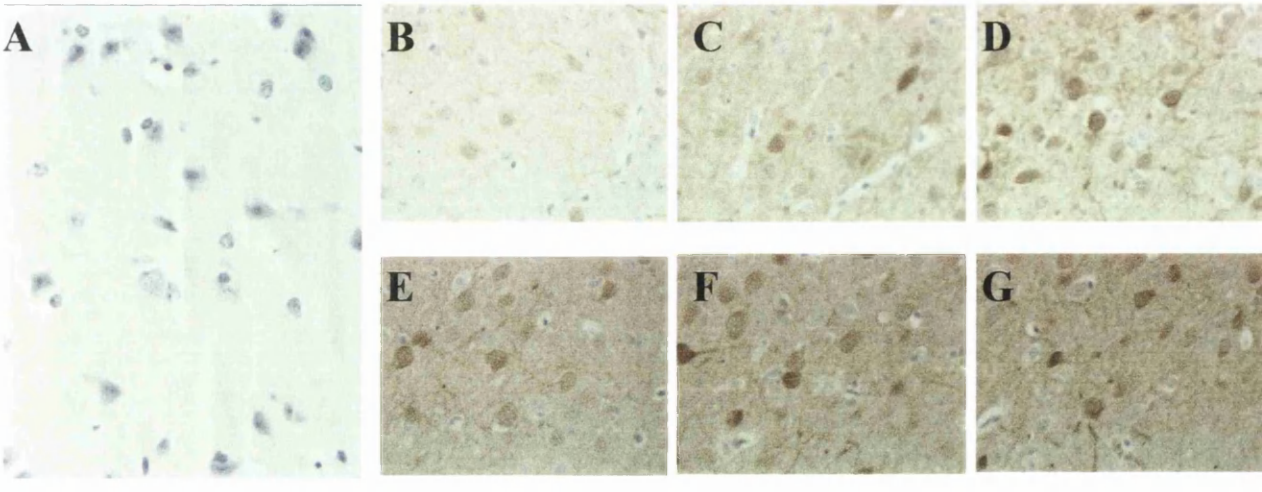

Brown stain = hsp 70i immunoreactive cells; purple stain = haematoxylin counterstain

Appendix E Inter-hemispheric association of ischaemic neuronal damage

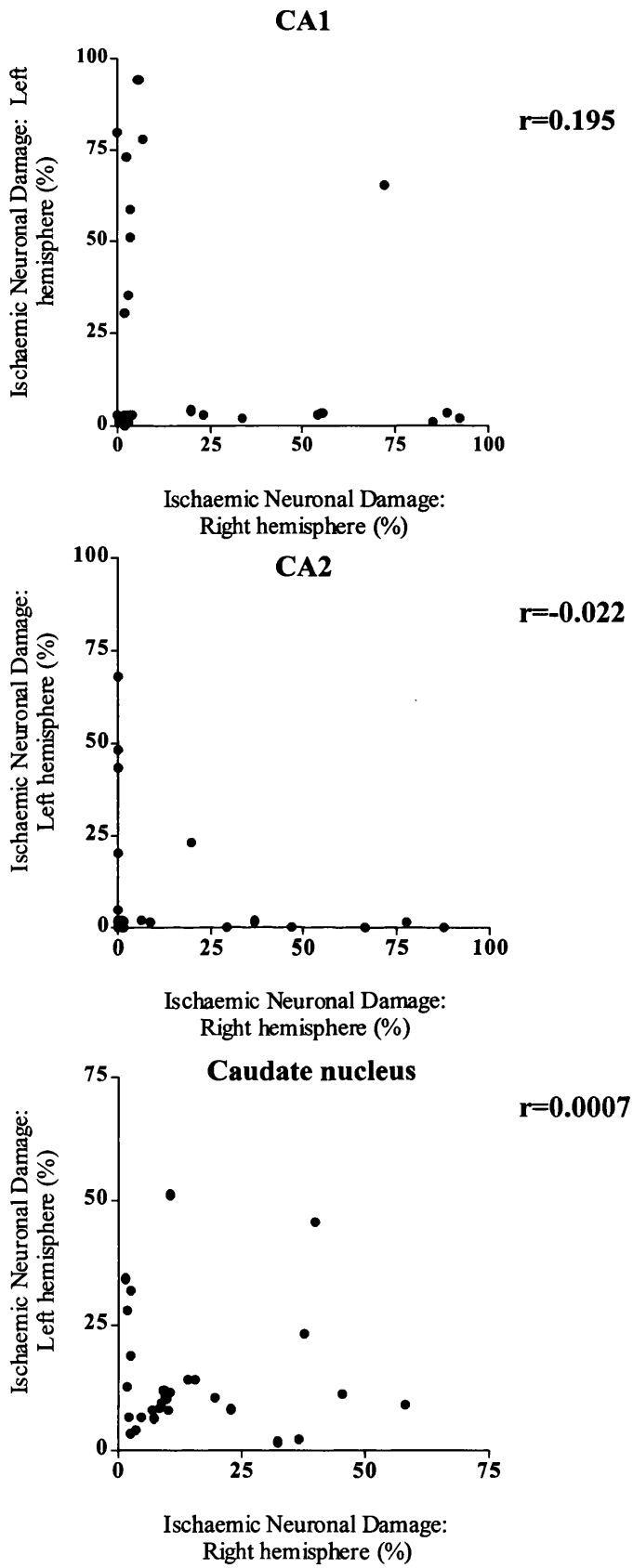

Inter-hemispheric association of ischaemic neuronal damage in MF1 strain mice: 25-45 minute BCCAo. P>0.05 Spearman rank correlation.

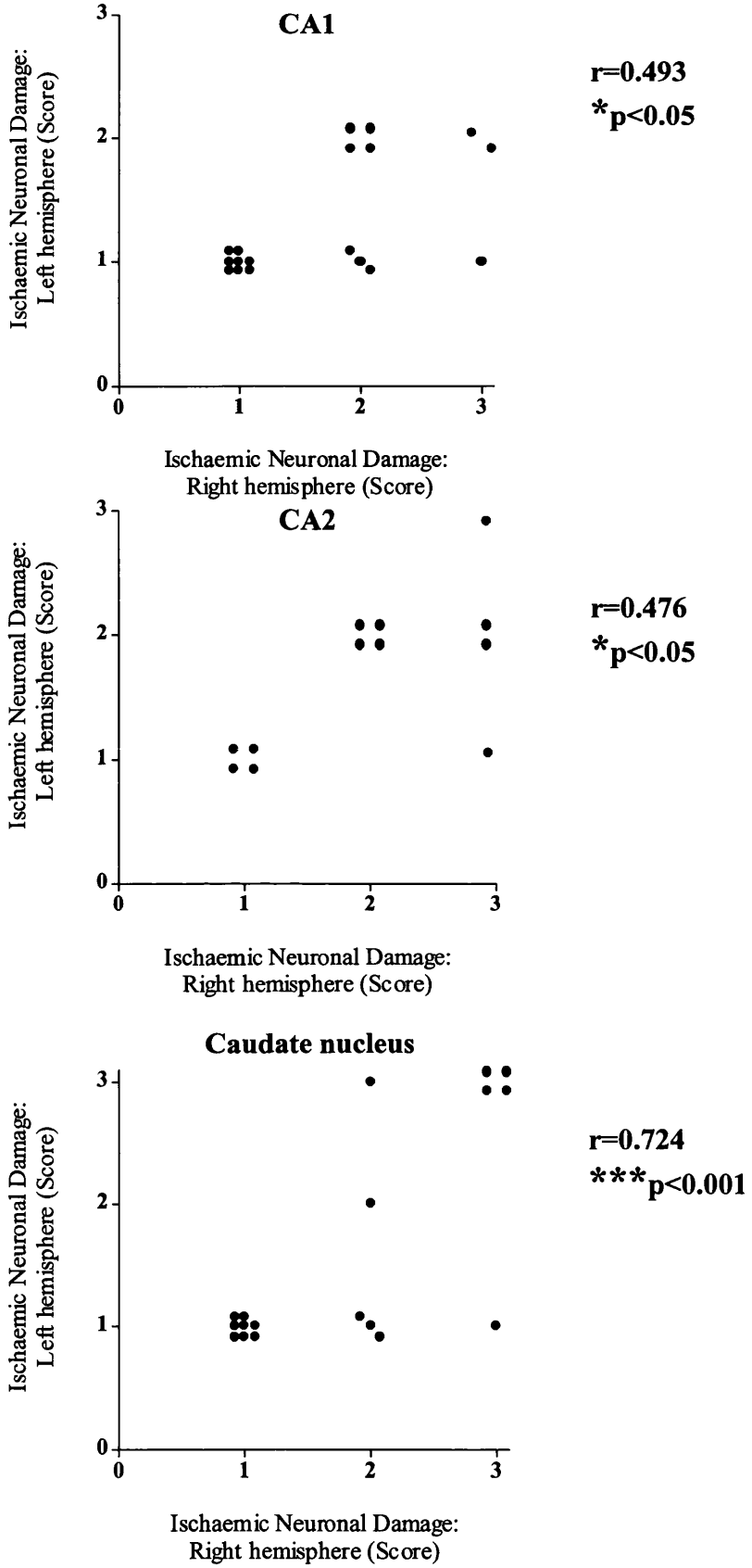

Inter-hemispheric association of ischaemic neuronal damage in C57bl/6 strain mice: 10-20 minute BCCAo. *p<0.05, ***p<0.0001 Pearson rank correlation.

Appendix F Delineation of ad egfp transfection and needle damage

Densitometric analysis of circumscribed regions of ad egfp transfection and of needle damage was required to gain an accurate reflection of the effect of ad gene upon LCGU. Defined regions of decreased and increased optical density could be observed macroscopically on all autoradiograms (A). These areas were correlated to areas of ad egfp transfection and of needle damage on adjacent sections using fluorescence light microscopy (B) and light microscopy of haematoxylin and eosin stained sections (C). Once confirmed, optical density readings of each zone were calculated using a micro computer imaging device.

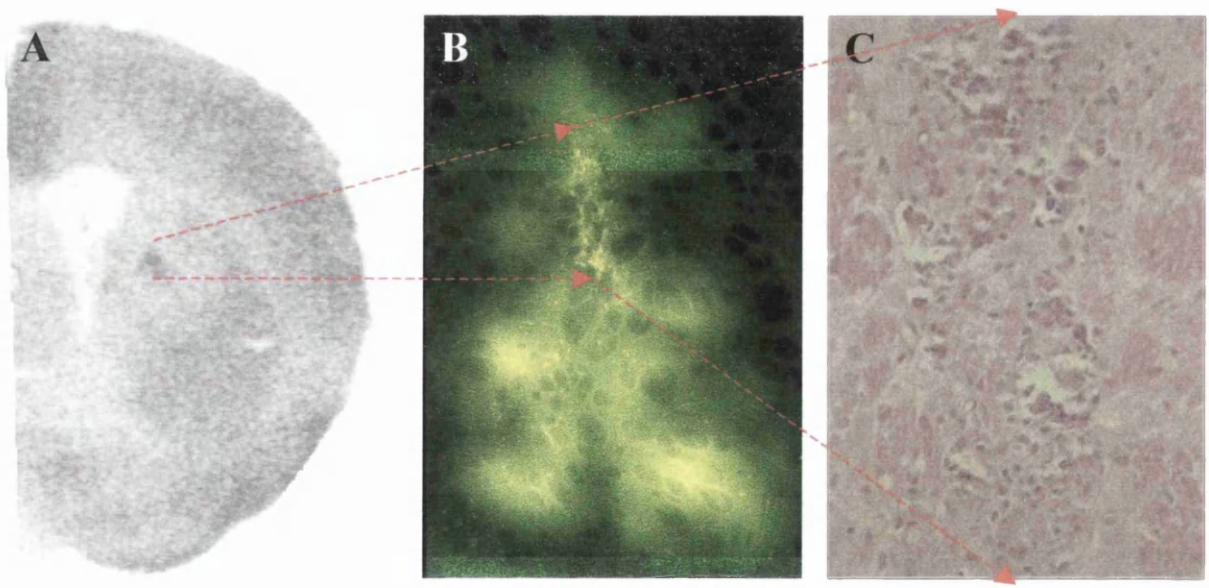

Appendix G Hsp 70i immunoreactivity in white matter, thalamus and cortex of ad hsp 70i transfected mice: 20-minute BCCAo

Hsp 70i was detected in several brain regions other than caudate nucleus in ad hsp 70i transfected mice subjected to 20-minute BCCAo. These regions included; subcortical white matter (A), white matter bundle in the caudate nucleus (B), anterior thalamus (C), somatosensory cortex (D). (X 400 original magnification A and B; X200 original magnification C; X100 original magnification D).

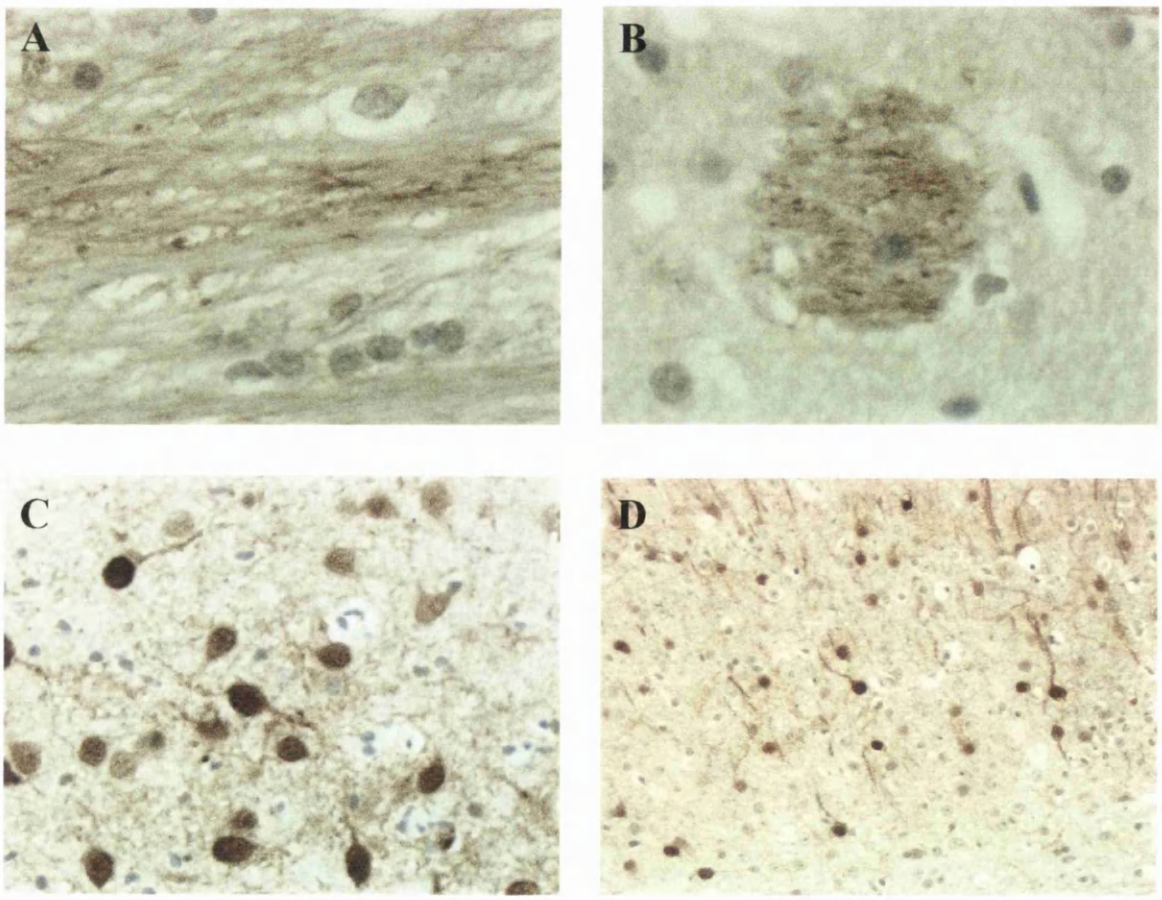

Brown stain = hsp 70i immunoreactive cells.

Appendix H Increased ischaemic neuronal damage in apoE-deficient mice

Apolipoprotein E-deficient mice displayed significantly increased ischaemic neuronal damage than their wild type littermates following 17-minute BCCAo, in six of seven brain regions analysed.

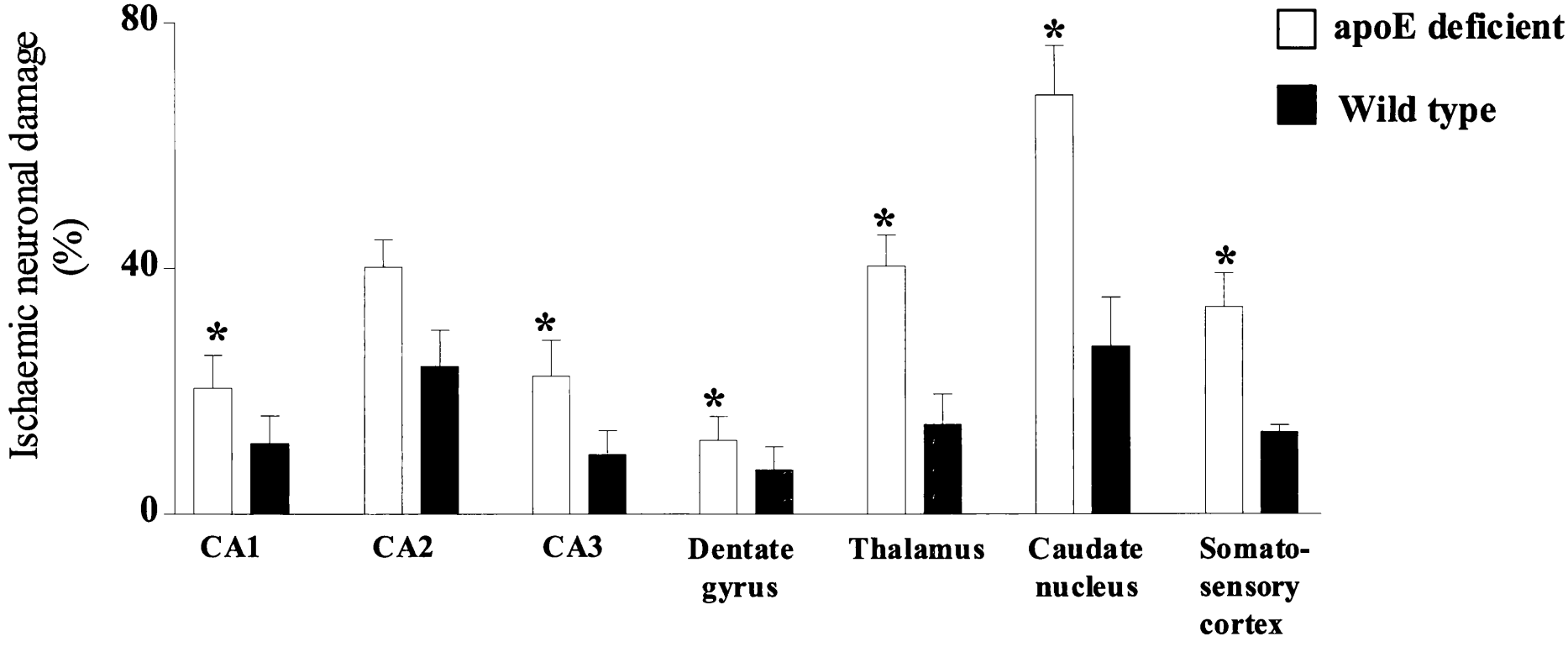

Data are presented as mean ± standard error of the mean (n = 8 per group). *p<0.05 Mann-Whitney test.

Appendix I Increased ischaemic neuronal damage in IL-18 deficient mice

Interleukin-18 deficient mice displayed significantly increased ischaemic neuronal damage than their wild type littermates following 25-minute BCCAo, in 2 of 4 brain regions analysed.

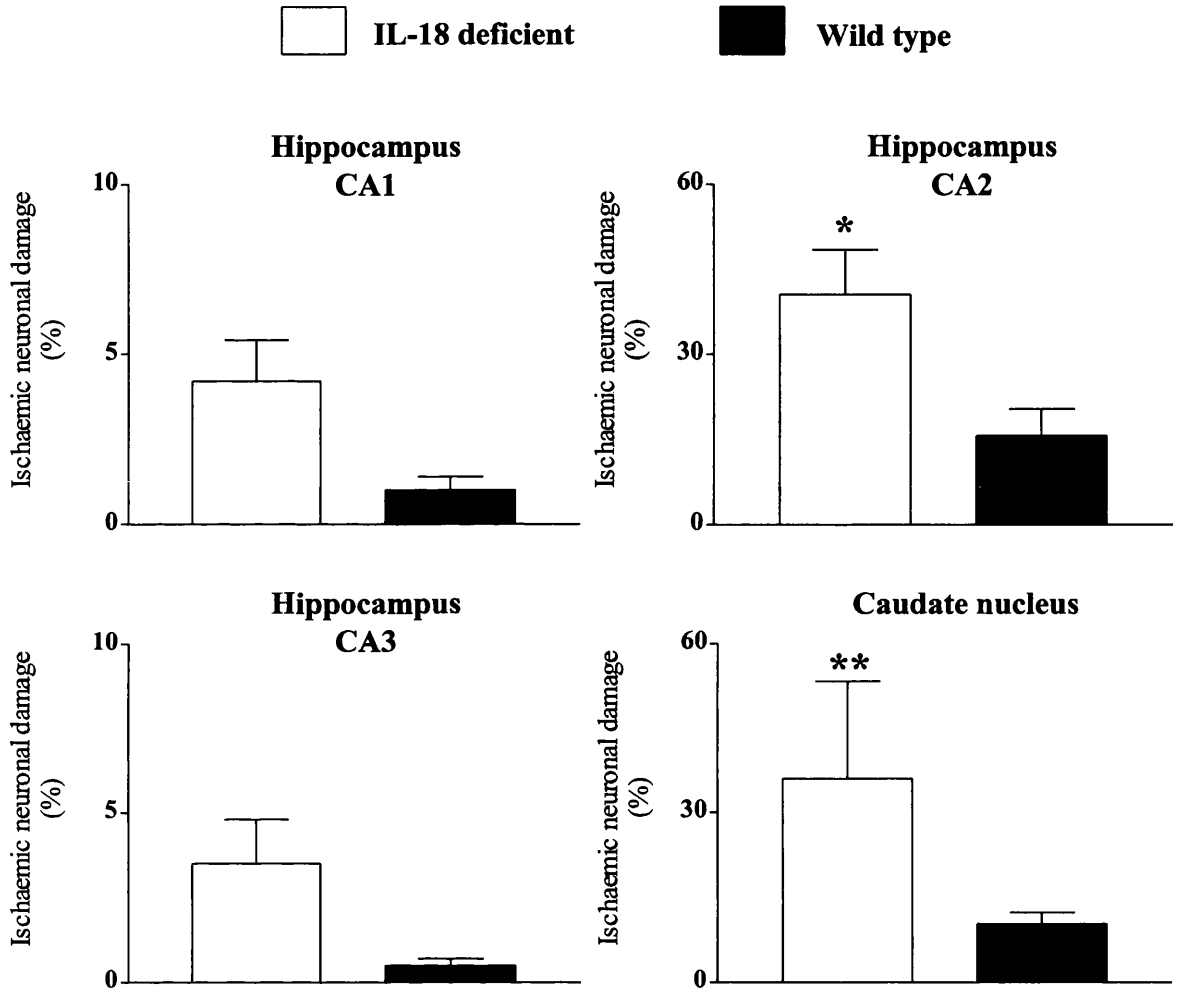

Data are presented as mean ± standard error of the mean (n = 6 per group).

*p<0.05; **p<0.01 Student's *t*-test.

Appendix J Intrastriatal injection of IL-18 has no effect on ischaemic neuronal damage in caudate nucleus

Intrastriatal injection of one microlitre of IL-18 (0.5μM, 5.0μM, and 50μM) had no significant effect upon ischaemic neuronal following 25-minute BCCAo compared with saline. However, 2 out of 2 mice intrastriatally injected with 500μM of IL-18 deficient mice died shortly after injection. This suggests that increased concentrations of IL-18 may be neurotoxic.

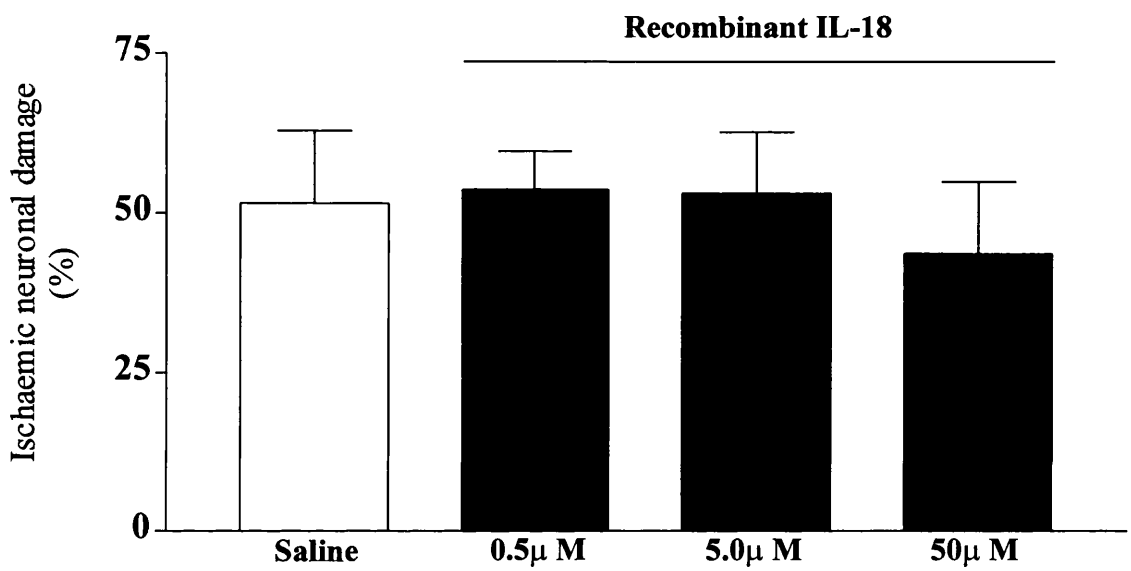

Data are expressed as mean ± standard error of the mean. $p>0.05$ unpaired Student's *t*-test. (n = 6 per group).

Appendix K Increased LCGU in IL-18 deficient mice

IL-18 deficient mice displayed significantly increased LCGU than their wild type littermates in 14 of 18 brain regions analysed.

	interleukin-18 deficient (n=6)	**wild type littermates** (n=6)	
Caudate nucleus	2.10 ± 0.02	2.57 ± 0.14	***
Sensory motor cortex	2.76 ± 0.19	3.65 ± 0.26	***
Dorsal CA1 stratum lacunosum moleculare	2.63 ± 0.19	3.05 ± 0.17	***
Dorsal hippocampus CA1	1.76 ± 0.06	2.27 ± 0.22	***
Hippocampus CA2	1.69 ± 0.04	2.64 ± 0.17	***
Hippocampus CA3	1.82 ± 0.07	2.09 ± 0.13	***
Parietal cortex	2.81 ± 0.13	3.61 ± 0.35	***
Auditory cortex	2.93 ± 0.18	3.62 ± 0.18	***
Dentate gyrus	1.80 ± 0.21	2.35 ± 0.29	***
Substantia nigra pars compacta	2.52 ± 0.11	2.85 ± 0.22	**
Substantia nigra pars reticulata	1.65 ± 0.16	1.99 ± 0.20	**
Subthalamic nucleus	2.62 ± 0.12	2.81 ± 0.08	*
Medial geniculate body	2.12 ± 0.23	2.45 ± 0.24	*
Red nucleus	2.14 ± 0.17	2.50 ± 0.17	*
Genu	0.92 ± 0.02	0.92 ± 0.07	
Globus pallidus	1.97 ± 0.13	2.01 ± 0.31	
Ventral thalamus	2.13 ± 0.21	2.16 ± 0.20	
Corpus callosum	0.98 ± 0.03	0.95 ± 0.08	

Data are expressed as mean ^{14}C region of interest / ^{14}C hypothalamus ± standard error of the mean. *p<0.05; **p<0.01; ***p<0.001 Student's *t*-test.

Appendix L No change in LCGU following intrastriatal hsv β-galactosidase gene transfer

Intrastriatal injection of hsv (wild type and attenuated, 1716) did not significantly alter LCGU in the caudate nucleus or any of the other eight brain regions analysed.

	3 Day survival			
	Wild type HSV β-galactosidase (n=4)		Attenuated (1716) HSV β-galactosidase (n=4)	
	IPSI	CONTRA	IPSI	CONTRA
Caudate nucleus	1.28 ± 0.05	1.27 ± 0.06	1.26 ± 0.01	1.24 ± 0.10
Globus pallidus	0.74 ± 0.03	0.74 ± 0.02	0.77 ± 0.11	0.78 ± 0.09
Substantia nigra pars compacta	0.96 ± 0.13	0.98 ± 0.17	0.98 ± 0.05	0.97 ± 0.03
Substantia nigra pars reticulata	0.59 ± 0.05	0.59 ± 0.05	0.71 ± 0.05	0.71 ± 0.07
Hippocampus CA1	1.09 ± 0.10	1.06 ± 0.08	1.10 ± 0.05	1.08 ± 0.05
Genu of corpus callosum	0.59 ± 0.05	0.61 ± 0.02	0.68 ± 0.05	0.71 ± 0.07
Thalamus	1.34 ± 0.03	1.31 ± 0.03	1.45 ± 0.12	1.46 ± 0.14
Sensory motor cortex	1.55 ± 0.09	1.42 ± 0.12	1.54 ± 0.11	1.54 ± 0.13
Hypothalamus	0.81 ± 0.01	0.87 ± 0.01	0.93 ± 0.13	0.92 ± 0.13

Data are expressed as mean ratio of ^{14}C region of interest / ^{14}C cerebellar cortex ± standard error of the mean. (HSV = herpes simplex virus). $p>0.05$ paired Student's *t*-test (ipsilateral versus contralateral).

β-galactosidase transfection produced by wild type hsv was much greater than produced by attenuated (1716) hsv.

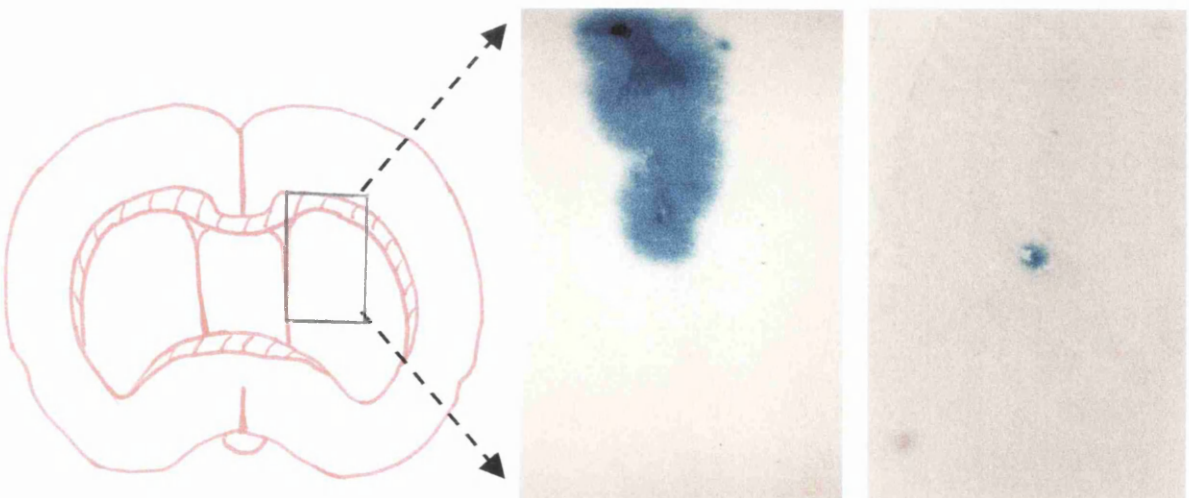

Wild type hsv **Attenuated hsv**

REFERENCES

Abe, K., Kawagoe, J., Araki, T., Aoki, M. and Kogure, K. (1992) Differential expression of heat shock protein 70 gene between the cortex and caudate after transient focal cerebral ischaemia in rats. *Neurological Research*, **14**, 381-385.

Abe, K., Kawagoe, J., Araki, T., Aoki, M. and Kogure, K. (1993) Dissociation of HSP70 and HSC70 heat shock MRNA inductions as an early biochemical marker of ischemic neuronal death. *Neuroscience Letters*, **149**, 165-168.

Abe, K., Kogure, K., Yamamoto, H., Imazawa, M. and Miyamoto, Z. (1987) Mechanism of arachidonic liberation during ischemia in gerbil cerebral cortex. *Journal of Neurochemistry*, **48**, 503-509.

Abe, K., Tanzi, R.E. and Kogure, K. (1991) Induction of HSP70 MRNA after transient ischemia in gerbil brain. *Neuroscience Letters*, **125**, 166-168.

Abravaya, K., Myers, M.P., Murphy, S.P. and Morimoto, R.I. (1992) The human heat shock protein hsp70 interacts with HSF, the transcription factor that regulates heat shock gene expression. *Genes and Development*, **6**, 1153-1164.

Abremski, K. and Hoess, R. (1984) Bacteriophage P1 site-specific recombination. Purification and properties of the cre recombinase protein. *Journal of Biological Chemistry* **259**, 1509-1514.

Akli, S., Caillaud, C., Vigne, E., Stratford-Perricaudet, L.D., Perricaudet, M. and Peschanski, M.R. (1993) Transfer of a foreign gene into the brain using adenovirus vectors. *Nature Genetics*, **3**, 224-228.

Ali, A., Bharadwaj, S., O'Carroll, R. and Ovsenek, N. (1998) HSP90 interacts with and regulates the activity of heat shock factor 1 in *Xenopus* oocytes. *Molecular and Cellular Biology*. **18**, 4949-4960.

Amin, V., Cumming, D.V.E. and Latchman, D.S. (1996) Over-expression of heat shock protein 70 protects neuronal cells against both thermal and ischaemic stress but with different efficiencies. *Neuroscience Letters*, **206**, 45-48.

Andersen, J.K., Garber, D.A., Meaney, C.A. and Breakfield, X.O. (1992) Gene transfer into mammalian nervous system using herpes simplex virus vectors: Extended expression of bacterial LacZ in neurons using the non-specific enolase promoter. *Human Gene Therapy*, **3**, 487-499.

Anderson, W.F. (1984) Prospects for human gene therapy. *Science* **226**, 401-409.

Aoki, M., Abe, K., Kawague, J., Sato, S., Nakamura, S. and Kogure, K. (1993a) Temporal profile of the induction of heat shock protein 70 and heat shock cognate protein 70 MRNAS after transient ischemia in gerbil brain. *Brain Research*, **601**, 185-192.

Aoki, M., Abe, K., Lie, X-H., Lee, T-H., Kato, H and Kogure, K. (1993b) Reduction of HSP70 and HSC70 MRNA inductions by bifemelane hydrochloride after transient ischemia in gerbil brain. *Neuroscience Letters*, **154**, 69-72.

Araki, T., Kato, H. and Kogure, K. (1989) Selective neuronal vulnerability following transient cerebral ischemia in the gerbil: distribution and time course. *Acta Neuropathlogica Scandinavica*, **80**, 548-553.

Arends, M.J., Morris, R.G. and Wyllie, A.H. (1990) Apoptosis. The role of the endonuclease. *American Journal of Pathology*, **136**, 593-608.

Armentano, D., Zabner, J., Sacks, C., Sookdeo, C.C., Smith, M.P., George, J.A., Wadsworth, S.C., Smith, A.E. and Gregory, R.J. (1997) Effect of the E4 region on the persistence of transgene expression from adenovirus vectors. *Proceedings of the National Academy of Sciences, USA,* **71**, 2408-2416.

Armstrong, J.N., Plumier, J.C.L., Robertson, H.A. and Currie, R.W. (1996) The inducible 70, 000 molecular/weight heat shock protein is expressed in the degenerating dentate hilus and piriform cortex after systemic administration of kainic acid in the rat. *Neuroscience*, **74**, 685-693.

Ashburner, M. (1970) Patterns of puffing activity in the salivary gland chromosomes of *Drosophila*. V. Responses to environmental treatments. *Chromosoma*, **31**, 356-376.

Ashburner, M. (1982) The effects of heat shock and other stress on gene activity: An introduction. In *Heat Shock from Bacteria to Man* (editors, Schlesinger, M. J., Ashburner, M. and Tissieres, A.) pp. 1-9. Cold Spring Harbor Laboratory, New York.

Attwell, D., Barbour, B. and Szatkowski, M. (1993) Nonvesicular release of neurotransmitter. *Neuron*, **11**, 401-477.

Auer, R.N. (1998) Histopathology of cerebral ischemia. In *Cerebrovascular Disease* (editors, Ginsberg, M.D. and Bogousslavasky, J.) pp 90-106 Blackwell Science, Oxford.

Auer, R.N. and Benveniste, H. (1997) Hypoxia and related conditions. In *Greenfield's Neuropathology*, sixth edition (editors Graham, D.I. and Lantos, P.L) pp263-314. Arnold, London.

Auer, R.N., Kalimo, H., Olsson, Y. and Wieloch, T. (1985) The dentate gyrus I hypoglycemia. Pathology implicating excitotoxin-mediated neuronal necrosis. *Acta Neuropathologica Berlin*, **67**, 279-288.

Austin, S., Ziese, M. and Sternberg, N. (1981) A novel role for site specific recombination in maintenance of bacterial replicons. *Cell* **25**, 729-736.

Bacchetti, S., and Graham, F.L. (1977) Transfer of the gene for thymidine kinase-deficient human cells by purified herpes simplex viral DNA. *Proceedings of the National Academy of Sciences, USA,* **74**, 1590-1594.

Bachelard, H.S. (1971) Specificity and kinetic properties of monosaccaride uptake into guinea pig cerebral cortex *in vitro*. *Journal of Neurochemistry*, **18**, 213-222.

Bajocchi, G., Feldman, S.H., Crystal, R.G. and Mastrangeli, A. (1993) Direct *in vivo* gene transfer to ependymal cells in the central nervous system using recombinant adenovirus vectors. *Nature Genetics*, **3**, 229-234.

Bamford, J., Sandercock, P.D.M., Burn, J. and Warlow, C. (1990) A prospective study of acute cerebrovascular disease in the community: the Oxfordshire Community Stroke Project, 1981-86. *Journal of Neurology, Neurosurgery and Psychiatry*, **53**, 16-22.

Banbury Conference on Genetic Background in Mice. (1997) Mutant mice and neuroscience; recommendations concerning genetic background. *Neuron*, **19**, 755-759.

Barnett, T., Altschuler, M., McDaniel, C.N. and Mascarentes, J.P. (1980) Heat shock induced proteins in plant cells. *Developmental Genetics*. **1**, 331-340.

Barone, F.C., Knudsen, D.J., Nelson, A.H., Feurerstein, G.Z. and Willette, R.N. (1993) Mouse strain differences in susceptibility to cerebral ischemia are related to cerebral vascular anatomy. *Journal of Cerebral Blood Flow and Metabolism*, **13**, 683-692.

Bart, R.D., Sheng, H., Laskowitz, D.T., Pearlstein, R.D. and Warner, D.S. (1998) Regional CBF in Apolipoprotein E-deficient and wild type mice during focal cerebral ischaemia. *Neuroreport*, **9**, 2615-2120c.

Beaucamp, N., Harding, T.C., Geddes, B.J., Williams, J. and Uney, J.B. (1998) Overexpression of hsp 70i facilitates reactivation of intracellular proteins in neurones and protects them from denaturing stress. *FEBS Letters*, **441**, 215-219.

Beerman, W. (1956) Nuclear differentiation and functional morphology of chromosomes. *Cold Spring Harbor Symposia on Quantitative Biology*, **21**, 217-232.

Berendes, H.D. (1965a) The induction of changes in chromosomal activity in different polytene types of cell in *Drosophila hydei. Developmental Biology*, **11**, 371-384.

Berendes, H.D. and Holt, T.K.H. (1964) The induction of chromosomal activities by temperature shocks. *Genen en Phaenen* **9**, 1-7.

Berendes, H.D., Van Breugel, F.M.H. and Holt, T.K.H. (1965b) Experimental puffs in *Drosophila hydei* salivary gland chromosomes. *Chromosoma,* **16**, 35-46.

Betz, A.L., Yang, B. and Davidson, J. (1995) Attenuation of stroke size in rats using an adenoviral vector to induce overexpression of interleukin-1 receptor in brain. *Journal of Cerebral Blood Flow and Metabolism*, **15**, 547-553.

Blomqvist, P. and Wieloch, T. (1985) Ischemic brain damage in rates following cardiac arrest using a long-term recovery model. *Journal of Cerebral Blood Flow and Metabolism*, **5**, 420-431.

Bogousslavsky, J., Perentes, E., Deruaz, J.P. and Regli, F. (1982) Mitochondrial myopathy and cardiomyopathy with neurodegenerative features and multiple brain infarcts. *Journal of Neurological Science*, **55**, 351-357.

Bonnekoh, P., Barbier, A., Oschlies, U. and Hossmann, K.A. (1990) Selective vulnerability in the gerbil hippocampus: morphological changes after 5-min ischemia and long survival times. *Acta Neuropatholica Berlin*, **80**, 18-25.

Böttiger, B.W., Motsch, J., Böhrer, H., Böker, T., Aulmann, M., Naworth, P.P.. and Martin, E. (1995) Activation of blood coagulation after cardiac arrest is not balanced adequately by activation of endogenous fibrinolysis. *Circulation*, **92**, 2572-2578.

Böttiger, B.W., Teschendorf, P., Krumnikl, J.J., Vogel, P., Galmbacher, R., Schmitz, B., Motsch, J., Martin, E. and Gass P. (1999) Global cerebral ischemia due to cardiocirculatory arrest in mice causes neuronal degeneration and early induction of transcription factor genes in the hippocampus. *Molecular Brain Research*, **65**, 135-142.

Bouche, G., Amalric, F., Caizergues-Ferres, M. and Zalta, J.P. (1979) Effects of heat shock on gene expression and subcellular protein distribution in Chinese hamster ovary cells. *Nucleic Acid Research* **7**, 1739-1747.

Brinker, G., Pillekamp, F. and Hossman, K.A. (1999) Brain haemorrhages after rt-PA treatment of embolic stroke in spontaneously hypertensive rats. *Neuroreport*, **10**, 1943-1946.

Brinster, R.L. (1972) Cultivation of the mammalian embryo. In *Growth, Nutrition and Metabolism of Cells in Culture,* Vol. II. (editors, Rothblat, G. and Cristofalo, V.) pp. 251-283, Academic Press, Inc., New York.

Brinster, R.L. (1974) The effect of cells transferred into the mouse blastocyst on subsequent development. *Journal of Experimental Medicine*, **140**, 1049-1056.

Brinster, R.L., Chen, H.Y., Trumbauer, M., Senear, A.W., Warren, R. and Palmiter, R.D. (1981) Somatic expression of herpes thymidine kinase in mice following injection of a fusion gene into eggs. *Cell*, **27**, 223-231.

Brown, L.L. and Wolfson, L.t. (1978) Apomorphine increase glucose utilization in the substantia nigra, subthalmic nucleus, and corpus striatum of Rat. *Brain Research*, **140**, 188-193.

Browne, S.E., Ayata, C., Huang, P.L., Moskowitz, M.A. and Beal, M.F. (1999) The cerebral metabolic consequences of nitric oxide synthase deficiently: glucose utilization endothelial and neuronal nitric oxide synthase null mice. *Journal of Cerebral Blood Flow and Metabolism*, **19**, 144-148.

Bruce, A.J., Boling, W., Kindy, M.S., Peschon, J., Kraemer, P.J., Carpenter, M.K., Holtsberg, F.W. Mattson, M.P. (1996) Altered neuronal and microglial responses to excitotoxic and ischemic brain injury in mice lacking TNF receptors. *Nature Medicine*, **2**, 788-794.

Burcin, M.M., Schiedner, G., Kochanek, S., Tsai, S.Y. and O'Malley, B.W. (1999) Adenovirus-mediated regulable target gene expression in vivo. *Proceedings of the National Academy of Sciences, USA,* **96**, 355-360.

Busto, R., Dietrich, W.D., Globus, M.Y., Valdes, I., Scheinberg, P. and Ginsberg, M.D. (1987) Small differences in intraischemic brain temperature critically determine the extent of ischemic neuronal injury. *Journal of Cerebral Blood Flow and Metabolism*, **7**, 729-738.

Byrnes, A.P., MacLaren, R.E and Charlton, H.M. (1996) Immunological instability of persistent adenovirus vectors in the brain: peripheral exposure to vector leads to renewed inflammation, reduced gene expression, and demyelination. *Journal of Neuroscience*, **16**, 3045-3055.

Byrnes, A.P., Rusby, J.E., Wood, M.J.A. and Charlton, H.M. (1995) Adenovirus gene transfer causes inflammation in the brain. *Neuroscience*, **66**, 1015-1024.

Byrnes, A.P., J.E., Wood, M.J.A. and Charlton, H.M. (1996) Role of T cell inflammation caused by adenovirus in the brain. *Gene Therapy*, **3**, 644-651.

Cahill, G.F. and Aoki, T.T. (1980) Alternate fuel utilisation by the brain. In: *Cerebral Metabolism and Neural Function.* (Editors. Passonneau, J.V, Hawkins, R.A., Lust, W.D. and Welsh, F.A.) pp. 234-242. Williams & Williams, Baltimore.

Camarata, P.J., Heros, R.C. and Latchaw, R.E. (1994) "Brain Attack": The rationale for treating stroke as a medical emergency. *Neurosurgery*, **34**, 144-158.

Cartmell, T., Southgate, T., Rees, G.S., Castro, M.G., Lowenstein, P.R. and Luheshi, G.N. (1999) Interleukin-1 mediates a rapid inflammatory response after injection of adenoviral vectors into the brain. *Journal of Neuroscience*, **9**, 1517-1523.

Chan, P.H. (1994) Oxygen radicals in focal cerebral ischemia. *Brain Pathology*, **4**, 59-65.

Choi, D.W. (1988) Calcium-mediated neurotoxicity: relationship to specific channel types and role in ischemic damage. *Trends in Neuroscience*, **11**, 465-469.

Choi, D.W. (1997) Background genes: out of sight, but not out of brain. *Trends in Neuroscience*, **20**, 499-500.

Choi, D.W. and Koh, J.Y. (1998) Zinc and brain injury. *Annual Review of Neuroscience*, **21**, 347-375.

Chopp, M., Chen, H., Ho, K-L., Dereski, M.O., Brown, E., Hetzel, F.W. and Welch, K.M.A. (1989) Transient hyperthermia protects against subsequent forebrain ischemic cell damage in the rat. *Neurology*, **39**, 1396-1398.

Christenson, S.D., Lake, K.D., Ooboshi, H., Faraci, F.M., Davidson, B.L. and Heistad, D.D. (1998) Adenovirus-mediated gene transfer in vivio to cerebral blood flow vessels and perivascular tissue in mice. *Stroke*, **29**, 1411-1415.

Church, A.C. and Feller, D. (1979) The influence of mouse genotype on the changes in brain cyclic nucleotide levels induced by acute alcohol administration. *Pharmacology Biochemistry Behavior*, **10**, 335-338.

Ciment, J. (2000) Gene therapy experiments put on "clinical hold". *British Medical Journal*, **320**, 336.

Clarke, D.D., Lagtha, A.L. and Maker, H.S. (1989) *Intermediary metabolism in basic neurochemistry: Molecular, cellular and medical aspects,* 4th edition. (Editor, Siegel, G.J.) pp. 541-564. Raven Press Ltd., New York.

Clarke, P.G.H. (1990) Developmental cell death: morphological diversity and multiple mechanisms. *Anatomical Embryology, Berlin*, **181**, 195-213.

Clever, U. and Karlson, P. (1960) Induktion von puffveranderungen in den speicheld rusenchromosomen von Chironimus tentans durch ecdyson. *Experimental Cell Research*, **20**, 623-626.

Cohen, J.J. (1991) Programmed cell death in the immune system. *Advances in Immunology*, **50**, 55-85.

Colbourne, F. and Corbett, D. (1994) Delayed and prolonged post-ischemic hypothermia is neuroprotective in the gerbil. *Brain Research*, **654**, 265-72.

Colbourne, F. and Corbett, D. (1995) Delayed postischemic hypothermia: A six month survival study using behavioral and histologic assessments of neuroprotection. *Journal of Neuroscience*, **15**, 7250-7260.

Colbourne, F., Sutherland, G.R., and Auer, R.N. (1999) Electron microscopic evidence against apoptosis as the mechanism of neuronal death in global ischemia. *Journal of Neuroscience*, **19**, 4200-4210.

Commander, H. (2000) Biotechnology industry responds to gene therapy death. *Nature Medicine*, **6**, 118.

Connolly, E.S.Jr., Winfree, C.J., Prestigiacomo, C.J., Kim, S.C., Choudhri, T.F., Hoh, B.L., Nakay, Y., Soloman, R.A. and Pinsky, D.J. (1997) Exacerbation of cerebral injury in mice that express the P-selectin gene: identification of P-selectin blockade as a new target for the treatment of stroke. *Circulation Research*, **81**, 304-310.

Connolly, E.S.Jr., Winfree, C.J., Springer, T.A., Naka, Y., Liao, H., Yan, S.D., Stern, D.M., Solomon, R.A., Gutierrez-Ramos, J.C. and Pinsky, D.J. (1996) Cerebral protection in homozygous null ICAM-1 mice after middle cerebral artery occlusion: role of neutrophil adhesion in the pathogenesis of stroke. *Journal of Clinical Investigation*, **97**, 209-216.

Constantini, F., Chada, K. and Magram, J. (1986) Correction of murine β-thalassemia by gene transfer into the germ line. *Science*, **233**, 1192-1194.

Constantini, F. and Lacy, E. (1981) Introduction of a rabbit β-globin gene into the mouse germ line. *Nature* **294**, 92-94.

Conti, B., Park, L.C.H., Calingasan, N.Y., Kim, Y., Kim. H., Bae, Y., Gibson, G.E. and Joh, T.H. (1999) Cultures of astrocytes and microglia express interleukin 18. *Molecular Brain Research,* **67**, 46-52.

Cooper, S.J. and Francis, R.L. (1979) Food-choice in a food-preference test: comparison of two mouse strains and the effects of chlordiazepoxide treatment. *Psychopharmacology*, **65**, 89-93.

Cosgrove, J.W., Heikkila, J.J. and Brown, I.R. (1982) Translation of mRNA associated with monosomes and residual polysomes following disaggregation of brain polysomes by LSD and hyperthermia. *Neurochemistry Research*, **7**, 505-18.

Crain, B.J., Westerkam, W.D., Harrison, A.H. (1988) Selective neuronal death after transient forebrain ischemia in the Mongolian gerbil: a silver impregnation study. *Neuroscience*, **27**, 387-402.

Crawley, J.N. (1996) Unusual behavioural phenotypes of inbred mouse strains. *Trends in Neuroscience*, **19**, 181-182.

Crawley, J.N. (1999) Behavioral phenotyping of transgenic and knockout mice: Experimental design and evaluation of general health, sensory functions, motor abilities and specific behavioural tests. *Brain Research*, **835**, 18-26.

Crawely, J.N., Bellknap, J.K., Collins, A., Crabbe, J.C., Frankel, W., Henderson, N., Hitzemann, R.J., Maxson, S.C., Miner, L.L., Silva, A.J., Wehner, J.M., Wynshaw-Boris, A. and Paylor, R. (1997) Behavioural phenotypes of inbred strains of mice. *Psychopharmacology*, **132**, 107-124.

Crawley, J.N. and Davis, L.G. (1982) Baseline exploratory activity predicts anxiolytic responsiveness to diazepam in five mouse strains. *Brain Research Bulletin*, **8**, 609-612.

Currie, R.W. and White, F.P. (1981) Trauma-induced protein in rat tissues: A physiological role for 'heat shock' protein? *Science*, **214**, 327-330.

Currie, R.W. and White, F.P. (1983) Characterization of the synthesis and accumulation of a 71-kilodalton protein induced in rat tissues after hypothermia. *Canadian Journal of Biochemical and Cellular Biology*, **61**, 438-446.

Crusio, W.E. (1996) Gene-targeting studies: New methods, old problems. *Trends in Neuroscience*, **19**, 186-187.

Crusio, W.E., Bar, I.M., Schwegler, H. and Buselmaier, W. (1990) A multivariate morphometric analysis of hippocampal anatomical variation in C57BL/6 in equilibrium BALB/c chimeric mice. *Brain Research*, **10**, 343-346.

Czarnecka-Verner, E., Yuan, C.X., Foxand, P.C. and Gurley, W.B. (1995) Isolation and characterization of six heat shock transcription factor cDNA clones from soybean. *Plant Molecular Biology*, **29**, 37-51.

Dai, Y., Schwarz, E.M., Gu, D., Zhang, W.W., Sarvetnick, N., Verma, I.M. (1995) Cellular and humoral immune responses to adenoviral vectors containing factor IX gene: tolerization of factor IX and vector antigens allows for long-term expression. *Proceedings of the National Academy of Sciences, U.S.A*, **92**, 1401-1405.

***Danysz, W., Parsons, C.G., Bresink, I. And Quack, G. (1995) A revived target for drug development? Glutamate in CNS Disorders. *DN & P*, **8**, 261-277.

Dash, R., Lawrence, M., Ho, D.Y. and Sapolsky, R. (1996) A herpes simplex virus vector overexpressing the glucose transporter gene protects the rat dentate gyrus from an antimetabolite toxin. *Experimental Neurology*, **137**, 43-48.

Davidson, B.L., Allen, E.D., Kozarsky, K.F., Wilson, J.M. Roessler, B.J. (1993) A model system for *in vivo* gene transfer into the CNS using an adenoviral vector. *Nature Genetics*, **3**, 219-223.

De Garavilla,L., Babbs, C. and Tacker, W. (1984) An experimental circulatory arrest in the rat to evaluate calcium antagonists in cerebral resuscitation, *American Journal of Emergency Medicine*, **2**, 321-326.

Dedieu, L.F., Vigne, E., Torrent, C., Jullien, C., Mahfouz, I., Caillaud, J.M., Aubailly, N., Orsini, C., Guillaume, J.M., Opolon, P., Perricadet, M. and Yeh, P. (1997) long-term gene delivery into the livers of immunocompetent mice with E1/E4-defective adenoviruses. *Journal of Virology*, **71**, 4626-4637.

Deshpande, J., Bergstedt, K., Linden, T., Kalimo, H. and Wieloch, T. (1992) Ultrastructural changes in the hippocampal CA1 region following transient cerebral ischemia: evidence against programmed cell death. *Experimental Brain Research*, **88**, 91-1053.

Dewar, D., Yam, P. and McCulloch, J. (1999) Drug development for stroke: importance of protecting cerebral white matter.. *European Journal of Parmacology*, **30**, 41-50.

Dienel, G.A., Kiessling, M., Jacewicz, M. and Pulsinelli, W.A. (1986) Synthesis of heat shock proteins in rat brain cortex after transient ischemia. *Journal of Cerebral Blood Flow and Metabolism*, **6**, 505-510.

Dienel, G.A., Pulsinelli., W.A. and Duffy, T.E. (1980) Regional protein synthesis in rat brain following acute hemispheric ischemia. *Journal of Neurochemistry*, **35**, 1216-1226.

Dietrich, W.D., Busto, R., Alonso, O., Globus, M.Y. and Ginsberg, M.D. (1994) Intraischemic but not postischemic brain hypothermia protects chronicall following global forebrain ischemia in rats. *Journal of Cerebral Blood Flow and Metabolism*, **13**, 541-549.

Dietrich, W.D., Busto, R., Valdés, I. and Loor, Y. (1990) Effects of normothermic versus mild hyperthermic forebrain ischemia in rats. *Stroke*, **21**, 1318-1325.

Di Santo, J.P., Muller, W., Guy-Grand, D., Fischer, A. and Rajewsky, K. (1995) Lymphoif development in mice with a targeted deletion of the interleukin 2 receptor γ chain. *Proceedings of the National Academy of Sciences, USA,* **92**, 377-381.

Doetschman, T., Gregg, R.G., Maeda, N., Hooper, M.L., Melton, D.W., Thompson, S. and Smithies, O. (1987) Targeted correction of a mutant HPRT gene in mouse embryonic stem cells. *Nature*, **330**, 576-578.

Dragunow, M. and Faull, R.L.M. (1990) MK-801 induces c-fos protein in thalamic and neocortical neurons of rat brain. *Neuroscience Letters*, **111**, 39-45.

Edvinson, L., MacKenzie, E.T. and McCulloch, J. (1993) *Cerebral Blood Flow and Metabolism.* Raven Press, New York.

Eliason, M.J., Sampei, K., Mandir, A.S., Hurn, P.D., Traystman, R.J., Bao, J., Pieper, A., Wang, Z.O., Dawson, T.M., Snyder, S.H. and Dawson, V.L. (1997) Poly(ADP-ribose) polymerase gene disruption renders mice resistant to cerebral ischemia. *Nature Medicine*, **3**, 1089-1095.

Elkon, K.B., Liu, C.C., Gall, J.G., Trevejo, J., Marino, M.W., Abrahamsen, K.A., Song, X., Zhou, J.L., Old, L.J., Crystral, R.G. and Falck-Pedersen E. (1997) Tumor necrosis factor alpha plays a central role in immune-mediated clearance of adenoviral vectors. *Proceedings of the National Academy of Sciences, U.S.A.,* **94**, 9814-9819.

Englehardt, J.E., Wilson, J.M. and Doranz, B. (1994) Ablation of E2A in recombinant adenoviruses improves transgene persistence and decreases inflammatory response in mouse liver. *Proceedings of the National Academy of Sciences, USA,* **91**, 6196-6200.

Evans, M.J. and Kaufman, M.H. (1981) Establishment in culture of pluripotential cells from mouse embryos. *Nature*, **292**, 154-156.

Ferrer, I., Soriano, M.A., Vidal, A. and Planas, A.M. (1995) Survival of parvalbumin-immunoreactive neurons in the gerbil hippocampus following transient forebrain ischemia does not depend on HSP-70 protein induction. *Brain Research,* **692**, 41-46.

Fink, D.J., Sternberg, L.R., Weber, P.C., Mata, M., Goins, W.F. and Glorioso, J.S. (1992) *in vivo* expression of β-galactosidase in hippocampal neurons by HSV-mediated gene transfer. *Human Gene Therapy*, **3**, 11-19.

Fink, K. and Zeuthen, E. (1978) Heat shock protein in *Tetrahymena. ICN-UCLA Symposia on Molecular and Cellular Biology*, **12**, 103-115.

Fisher, K.J., Choi, H., Burda, J., Chen, S.J. and Wilson, J.M. (1996) Recombinant adenovirus deleted of all genes for gene therapy of cystic fibrosis. *Virology*, **217**, 11-22.

Fisher, L.J. (1995) Engineered cells: a promising therapeutic approach for neural disease. *Restorative Neurology and Neuroscience*, **8**, 49-57.

Fotaki, M.E., Pink, J.R. and Mous, J. (1997) Tetracycline-responsive gene expression in mouse brain after amplicon-mediated gene transfer. *Gene Therapy*, **4**, 901-908.

Fox, J.L. (1999) Gene therapy safety issues come to fore. *Nature Biotechnology*, **17**, 1153.

Fox, J.L. (2000) Investigation of gene therapy begins. *Nature Biotechnology*, **18**, 143-144.

Franklin, K.B.J. and Paxinos, G. (1997) The mouse brain in sterotaxic coordinates. Academic Press, New York.

Freedman, M.S., Clark, B.D., Cruz, T.F., Gurd, J.W. and Brown, I.R. (1981) Selective effects of LSD and hyperhermia on the synthesis of synaptic proteins and glycoproteins. *Brain Research*, **207**, 129-45.

Fritsch, E.F. and Temin, H.M. (1977) Inhibition of viral DNA synthesis in stationary chicken embryo fibroblasts infected with avian retroviruses. *Journal of Virology*, **24**, 461-469.

Fujii, M., Hara, H., Meng, W., Vonsattel, J.P., Huang, Z. and Moskowitz, M.A. (1997) Strain-Related Differences in Susceptibility to Transient Forebrain Ischemia in SV-129 and C57Black/6 Mice. *Stroke*, **28**, 1805-1811.

Fujimura, M., Morita-Fujimura, Y., Kawase, M., Copin, J.C., Calagui, B., Epstein, C.J. and Chan, P.H. (1999) Manganese superoxide dismutase mediates the early release of mitochondrial cytochrome C and subsequent DNA fragmentation after permanent focal cerebral ischaemia in mice. *Journal of Neuroscience*, **19**, 3414-3422.

Gage, F.H. and Fisher, L.J. (1991) Intracerebral grafting: a tool for the neurobiologist. *Neuron*, **6**, 1-12.

Gage, F.H., Kawaja, M.D. and Fisher, L.J. (1991) Genetically modified cells: applications for intracerebral grafting. *Trends in Neuroscience*, **14**, 328-333.

Gage, F.H., Wolff, J.A., Rosenberg, M.B., Xy, L., Yee, J.L., Shults, C. and Friedman, T. (1987) Grafting genetically modified cells to the brain: possibilities for the future. *Neuroscience*, **23**, 795-807.

Gaitonde, M.K., Evinson, E. and Evans, G.M. (1983) The rate of utilization glucose via hexosemonophosphate shunt in brain. *Journal of Neurochemistry*, **41**, 1253-1260.

Gallo, G.J., Prentice, H. and Kingston, R.E. (1993) Heat shock factor is required for growth at normal temperatures in the fission yeast Schizosaccharomyces pombe. *Molecular and Cellular Biology*, **13**, 749-761.

Gardner, R.L. (1968) Mouse chimaeras obtained by the injection of cells into the blastocyst. *Nature*, **220**, 596-597.

Gardner, R.L. (1972) An investigation of the inner cell mass and trophoblast tissues following their isolation from the mouse blastocyst. *Journal of Embryology and Experimental Morphology* **28**, 279-312.

Gaspary, H., Graham, S.H., Sagar, S.M. and Sharp, F.R. (1995) HSP70 heat shock protein induction following global ischemia in the rat. *Molecular Brain Research*, **28**, 327-332.

Gass, P., Spranger, M., Herdegen, T., Bravo, R., Köck, P., Hacke, W. and Kiessling, M. (1992) Induction of FOS and JUN proteins following focal ischemia in the rat cortex: differential effect of MK-801. *Acta Neuropathologica Berlin*, **84**, 545-553.

Gavrieli, Y., Sherman, Y. and Ben-Sasson, S.A. (1992) Identification of programmed cell death *in situ* via specific labeling of nuclear DNA fragmentation. *Journal of Cell Biology*, **119**, 493-501.

Geddes, B.J., Harding, T.C., Lightman, S.L. and Uney, J.B. (1997) Long-term gene therapy in the CNS: reversal of hypothalamic diabetes insipidus in Brattleboro rat by using an adenovirus expressing arginine vasopressin. *Nature Medicine*, **3**, 1402-1404.

Gerlai. R. (1996) Gene-targeting studies of mammalian behavior: is it the mutation or background genotype? *Trends in Neuroscience*, **19**, 177-181.

Gerlai. R. (1996) Gene-targeting in neuroscience: the systemic approach. *Trends in Neuroscience*, **19**, 188-189.

Ginsberg, M.D. (1999) On ischaemic brain injury in genetically altered mice. *Arteriosclerosois, Thrombosis and Vascular Biology*, **19**, 2581-2583.

Ginsberg, M.D., Sternau, L.L., Globus, M.Y-T., Dietrich, W.D. and Busto, R. (1992) Therapeutic Modulation of Brain Temperature: Relevance to Ischemic Brain Injury. *Cerebrovascular and Brain Metabolism Reviews*, **4**, 189-225.

Gold, R., Schmied, M., Rothe, G., Zischler, H., Breitschopf, H., Wekerle, H. and Lassmann, H. (1993) Detection of DNA fragmentation in apoptosis: Application of *in situ* nick translation to cell culture systems and tissue sections. *Journal of Histochemistry and Cytochemistry*, **41**, 1023-30.

Goldenstein, G.W., Wolinsky, J.S., Csejtey, J. and Diamond, I. (1975) Isolation of metabolically active capillaries from rat brain. *Journal of Neurochemistry*, **25**, 715-717.

Gonzalez, M.F., Schiraishie, K., Hissanaga, K., Sagar, S.M., Mandabach, M. and Sharp, F.R. (1989) Heat shock proteins as markers of neural injury. *Molecular Brain Research*, **6**, 93-100.

Gordon, J.W. and Ruddle, F.H. (1981) Integration and stable germ line transmission of genes injected into mouse pronuclei. *Science*, **214**, 1244-1246.

Gordon, J.W., Scangos, G.A., Plotkin, D.J., Barbosa, J.A. and Ruddle, F.H. (1980) Genetic transformation of mouse embryos by microinjection of purified DNA. *Proceedings of the National Academy of Sciences, USA,* **77**, 7380-7384.

Gossen, M. and Bujard, H. (1992) Tight control of gene expression in mammalian cells by tetracycline responsive promoters. *Proceedings of the National Academy of Sciences, USA,* **89**, 5547-5551.

Gossler, A., Doetschman, T., Korn, A., Serfling, E. and Kemler, R. (1986) Transgenesis by means of blastocyst derived embryonic stem cell lines. *Proceedings of the National Academy of Sciences, USA,* **83**, 9065-9069.

Graham, F.L. and Van der Eb, A.J. (1973) Anew technique for the assay of infectivity of human adenovirus 5 DNA. *Virology*, **52**, 456-467.

Greber, U.F., Willets, M., Webster, P. and Helenius, A. (1993) Stepwise dismantling of adenovirus 2 during entry into cells. *Cell*, **75**, 477-486.

Greenberg, J.M., Boehm, T., Sofroniew, M.V., Keynes, R.J., Barton, S.C., Norris, M.L., Surani, M.A., Spillantini, M-G. and Rabbitts, T.H. (1990) Segemental and developmental regulation of a presumptive T-cell oncogene in the central nervous system. *Nature*, **344**, 158-160.

Gu, H., Marth, J.D., Orban, P.C., Mossman, H and Rajewsky, K. (1994) Deletion of a DNA polymerase β gene segment in T cells using cell type-specific gene targeting. *Science* **265**, 103-106.

Gu, H., Zou, Y-R. and Rajewsky, K. (1993) Independent control of immunoglobulin switch recombination at individual switch regions evidenced through Cre-*loxP*-mediated gene targeting. *Cell*, **73**, 1155-1164.

Hagan, P., Barks, J., Yabut, M., Davidson, B.L., Roessler, B. and Silverstein, F.S. (1996) Adenovirus-mediated overexpression of Interleukin 1 receptor antagonist reduces susceptibility to excitotoxic brain injury in perinatal rats. *Neuroscience*, **75**, 1033-1045.

Hall, E.D., Oostveen, J.A., Dunn, E. and Carter, D.B. (1995) Increased amyloid protein precursor and apolipoprotein E immunoreactivity in the selectively vulnerable hippocampus following transient forebrain ischemia in gerbils. *Experimental Neurology*, **135**, 17-27.

Hara, H., Fink, K., Endres, M., Friedlander, R.M., Gagliardini, V., Yuan, J. and Moskowitz, M.A. (1997) Attenuation of transient focal cerebral ischemic injury in transgenic mice expressing a mutant ICE inhibitory protein. *Journal of Cerebral Blood Flow and Metabolism*, **17**, 370-375.

Hara, H., Huang, P.L., Panahian, N., Fishman, M.C. and Moskowitz, M.A. (1996) Reduced brain edema and infarction volume in mice lacking the neuronal isoform of nitric oxide synthase after transient MCA occlusion. *Journal of Cerebral Blood Flow and Metabolism*, **16**, 605-611.

Harding, T.C., Geddes, B.J., Murphy, D., Knight, D. and Uney, J.B. (1998) Switching transgene expression in the brain using an adenoviral tetracycline-regulatable system. *Nature Biotechnology*, **16**, 553-555.

Harding, T.C., Geddes, B.J., Noel, J.D., Murphy, D. and Uney, J.B. (1997) Tetracycline-regulated transgene expression in hippocampal neurones following transfection with adenoviral vectors. *Journal of Neurochemistry*, **69**, 2620-2623.

Hata, R, Gass, P., Mies, G. and Hossman, C. (1998) Attenuated *c-fos* mRNA induction after middle cerebral artery occlusion in CREB knockout mice does not modulate focal ischemic injury. *Journal of Cerebral Blood Flow and Metabolism*, **18**, 1325-1335.

Heikkila, J.J. and Brown, I.R. (1979a) Hyperthermia and disaggregation of brain polysomes induced by bacterial pyrogen. *Life Sciences*, **25**, 347-352.

Heikkila, J.J. and Brown, I.R. (1979b) Disaggregation of brain polysomes after LSD in vivo. Involvement of LSD-induced hypothermia. *Neurochemical Research*, **4**, 763-76.

Heikkila, J.J., Holbrook, L. and Brown, I.R. (1979) Disaggregation of polysomes in fetal organs and maternal brain after administration of d-lysergic acid diethylamide in vivo. *Journal of Neurochemistry*, **32**, 1793-1799.

Heistad, D.D. and Faraci, F.M. (1996) Gene therapy for cerebral vascular disease. *Stroke*, **27**, 1688-1693.

Herbert, F. (1969) *Dune*, Putnam, New York.

Hermens, W.T.J.M.C. and Verhaagen, J. (1998) Viral vectors, tools for gene transfer in the central nervous system. *Progress in Neurobiology*, **55**, 399-432.

Hightower, L.E. and Smith, M.D. (1978) Effects of canavanine on protein metabolism in Newcastle disease-virus infected chicken embryo cells. In *Negative Strand Viruses and the Host Cell.* (editors, Mahey, B.W.J. and Barry, R.D.) pp. 395-405. Academic Press, London.

Hightower, L.E. and White, F.P. (1981) Cellular responses to stress: Comparison of a family of 71-73 kilodalton proteins rapidly synthesised in rat tissue slices and canavanine-treated cells in culture. *Journal of Cellular Physiology*, **108**, 261.

Himori, N., Moreau, J.L. and Martineo, J.R. (1991) Cerebral ischemia decreases the behavioural effects and mortality rate elicited by activation of NMDA receptors in mice. *Neuropharmacology*, **30**, 1179-1186.

Himori, N., Watanabe, H., Akaike, N., Kurosawa, M., Hoh, J. and Tanaka, T. (1990) Cerebral ischemia model with conscious mice: involvement with NMDA receptor activation and derangement of learning and memory ability. *Journal of Pharmacological Methods*, **23**, 311-327.

Hinks, G.L., Shah, B., French, S.J., Campos, L.S., Staley, K., Hughes, J. and Sofroniew, M.V. (1997) Expression of LIM protein genes Lmo1, Lmo2, and Lmo3 in adult mouse hippocampus and other forebrain regions: differential regulation by seizure activity. *Journal of Neuroscience*, **17**, 5549-5559.

Ho, D.Y., Lawrence, M.S., Meier, T.J., Fink, S.L., Dash, R., Saydam, T.C. and Sapolsky, R.M. (1995a) Use of herpes simplex virus vectors for protection from necrotic neuron death. In *Viral Vectors: Gene Therapy and Neuroscience Applications.* (editors, Kaplitt, M.G. and Loewry, A.D.) pp. 133-155. Academic Press, San Diego.

Ho, D.Y., McLaughlin, J.R. and Sapolsky, R.M. (1996) Inducible gene expression from defective herpes simplex virus vectors using the tetracycline responsive promoter system. *Molecular Brain Research*, **41**, 200-209.

Ho, D.Y., Saydam, T., Fink, S., Lawrence, M.S. and Sapolsky, R.M. (1995b) Defective herpes simplex virus vectors expressing the rat brain glucose transporter protect cultured neurons from necrotic insults. *Journal of Neurochemistry*, **65**, 842-850..

Hockenbery, D. (1995) Defining apoptosis. *American Journal of Pathology*, **146**, 16-18.

Hollan, T. (2000) Researchers and regulators reflect on first gene therapy death. *Nature Medicine*, **6**, 6.

Holsztynska, E.J., Weber, W.W. and Domino, E.F. (1991) Genetic polymorphism of cytochrome P-450-dependent phencyclidine hydroxylation in mice. Comparison of phencyclidine hydroxylation in humans. *Drug Metabolism and Disposition*, **19**, 48-53.

Honkaniemi, J., Massa, S.M., Breckinridge, M. and Sharp, F.P. (1996) Global ischemia induces apoptosis-associated genes in hippocampus. *Molecular Brain Research*, **42**, 79-88.

Hooper, M., Hardy, K., Handyside, A., Hunter, S. and Monk, M. (1987) HPRT-deficient (Lesch-Nyhan0 mouse embryos derived from germline colonization by cultured cells. *Nature*, **326**, 292-295.

Horn, M. and Schlote, W. (1992) Delayed neuronal death and delayed neuronal recovery in the human brain following global ischemia. *Acta Neuropathologia Berlin,* **85**, 79-87.

Horsburgh, K., Kelly, S., McCulloch, J., Higgins, G.A., Roses, A.D. and Nicoll, J.A.R. (1999) Increased neuronal damage in Apolipoprotein E-deficient mice following global ischaemia. *NeuroReport*, **10**, 837-841.

Horsburgh, K., McCulloch, J., Nilsen, M., McCraken, E., Large, C., Roses, A.D. and Nicholls, J.A. (2000) Intraventricular infusion of apolipoprotein E ameliorates acute neuronal damage after global cerebral ischemia in mice. *Journal of Cerebral Blood Flow and Metabolism,* **20**, 458-462.

Horsburgh, K. and Nicol, J.A. (1996) Selective alterations in the cellular distribution of apolipoprotein E immunoreactivity following transient cerebral ischaemia in the rat. *Neuropathology and Applied Neurobiology,* **22**, 342-349.

Huang, Q., Vonsattel, J., Schaffer, P.A., Martuza, R.L., Breakfield, X.O. and DiFiglia, M. (1992) Introduction of a foreign gene (*Escherichia coli* LacZ) into rat neostriatal neurons using herpes simplex virus mutants: a light and electron microscopic study. *Experimental Neurology*, **115**, 303-316.

Huang, Z, Huang, P.L., Ma, J., Meng, W., Ayata, C., Fishman, M.C. and Moskowitz, M.A. (1996) Enlarged infarcts in endothelial nitric oxide synthase knockout mice are attenuated by nitro-L-arginine. *Journal of Cerebral Blood Flow and Metabolism*, **16**, 981-987.

Huang, Z, Huang, P.L., Panahian, N., Dalkara, T., Fisnman, M.C. and Moskowitz, M.A. (1994) Effects of cerebral ischaemia in mice deficient in neuronal nitric oxide synthase. *Science*, **265**, 1883-1885.

Iadecola, C., Salkowski, C.A., Zhang, F., Aber, T., Nagayama, M., Vogel, S.N., and Ross, M.E. (1999) The transcription factor interferon regulatory factor 1 is expressed after cerebral ischemia and contributes to ischemic brain injury. *Journal of Experimental Medicine*, **189**, 719-727.

Iadecola, C., Zhang, F., Casey, R., Nagayama, M. and Ross, M.E. (1997) Delayed reduction of ischaemic brain injury and neurological deficits in mice lacking the inducible nitric oxide synthase gene. *Journal of Neuroscience*, **17**, 9157-9164.

Inamura, K., Olsson, Y., Siesjö, B.K. (1987) Substantia nigra damage induced by ischemia in hyperglycemic rats. A light and electron microscpoic study. *Acta Neuropathologica Berlin*, **75**, 131-139.

Inamura, K., Smith, M-L., Olsson, Y. and Siesjö, B.K. (1988) Pathogenesis of substantia nigra lesions following hyperglycemic ischemia: changes in energy metabolites, cerebral blood flow, and morphology of pars reticulata in a rat model of ischemia. *Journal of Cerebral Blood Flow and Metabolism*, **8**, 375-384.

Ish-Horowicz, D., Holden, J.J. and Gehring, W.J. (1977) Deletions of two heat-activated loci in *Drosophila melanogaster* and their effect on heat-induced protein synthesis. *Cell* **17**, 643-652.

Ish-Horowicz, D., Pinchin, S.M., Gausz, J., Gyurkovics, H., Bencze, G., Goldschmidt-Clermont, M. and Holden, J.J. (1979) Deletion mapping of the two *Drosophila melanogaster* loci that code 70,000 Dalton heat induced protein. *Cell* **17**, 565-571.

Ito, U., Spatz, M., Walker, J.T. and Klatzo, I. (1975) Experimental cerebral ischemia in Mongolian gerbils. I. Light-microscopic observations. *Acta Neuropathologica Berlin*, **32**, 209-223.

Iwai, T., Hara, A., Niwa, M., Nozaki, M., Uematsu, T., Sakai, N., and Yamada, H. (1995) Temporal profile of nuclear DNA fragmentation in situ in gerbil hippocampus following transient forebrain ischemia. *Brain Research*, **671**, 305-308.

Jacewizc, M., Kiessling, M. and Pulsinelli, W.A. (1986) Selective gene expression in focal cerebral ischemia. *Journal of Cerebral Blood Flow and Metabolism*, **6**, 263-272.

Jackson, P. and Blythe, B. (1993) Immunolabelling techniques for light microscopy. In *Immunocytochemistry: A Practical Approach* (editor Beesley, J.E.). pp. 15-41., Oxford University Press.

Jaenisch, R. (1976) Germ line integration and Mendelian transmission of the exogenous Moloney leukaemia virus. *Proceedings of the National Academy of Sciences, USA,* **73**, 1260-1264.

Jaenisch, R. and Mintz, B. (1974) Simian virus 40 DNA of healthy adult mice derived from pre-implantation blastocysts injected with viral DNA. *Proceedings of the National Academy of Sciences, USA,* **71**, 1250-1254.

Jia, W.W., Wang, Y., Qiang, D., Tufaro, F., Remington, R. and Cynader, M. (1996) A bcl-2 expressing viral vector protects cortical neurons from excitotoxicity even when administered several hours after the toxic insult. *Molecular Brain Research*, **42**, 350-353.

Johansen , F.F., Jørgensen, M.B., von Lubitz, D.K.J.E. Diemer, N.H. (1984) Selective dendrite damage in hippocampal CA1 stratum radiatum with unchanged axon ultrastructure and glutamate uptake after transient cerebral ischemia in the rat. *Brain Research*, **291**, 373-377.

Johansen, F.F., Toner, N., Berg, M., Zimmer, J. and Diemer, N.H. (1993) Hypothermia protects somatostatinergic neurons in rat dentate hilus from zinc accumulation and cell death after cerebral ischemia. *Molecular Chemical Neuropathology*, **18**, 161-172.

Johnson, R.S., Sheng, M., Greenberg, M.E., Kolodner, R.D., Papaioannou, V.E. and Spiegelman, B.M. (1989) Targeting of nonexpressed genes in embryonic stem cells via homologous. *Science* **245**, 1234-1236.

Joyner, A.L. and Bernstein, A. (1983) Retrovirus transduction: Generation of infectious retroviruses expressing dominant and selectable genes is associated with in vivo recombination and deletion events. *Molecular and Cellular Biology*, **3**, 2180-2190.

Kajiwara, K., Byrnes, A.P., Charlton, H.M., Wood, M.J.A. and Wood, K.J. (1997) Immune responses to adenoviral vectors during gene transfer in the brain. *Human Gene Therapy,* **8**, 253-265.

Kajiwara, K., Byrnes, A.P., Ohmoto, Y., Charlton, H.M., Wood, M.J.A. and Wood, K.J. (1999) Humoral immune responses to adenovirus vectors in the brain.. *Journal of Neuroimmunology*, **103**, 8-15.

Kaplitt, M.G., Leone, P., Samulski, R.J., Xiao, X., Pfaff, D.W., O'Malley, K.L. and During, M.J. (1994) Long-term gene expression and phenotypic correction using adeno-associated virus vectors in the mammalian brain. *Nature Genetics*, **8**, 148-154.

Kawagoe, J., Abe, K. and Kogure, K. (1993) Regional difference of HSP70 and HSC70 heat shock mRNA inductions in rat hippocampus after transient global ischemia. *Neuroscience Letters*, **153**, 165-8.

Kawai, K., Nitecka, L., Ruetzler, C.A., Nagashima, G., Joo, F., Mies, G., Nowak, T.S., Jnr., Saito, N., Lohr, J.M. and Klatzo, I. (1992) Global cerebral ischemia associated with cardiac arrest in the rat.I. Dynamics of early neuronal changes. *Journal of Cerebral Blood Flow Metabolism*, **12**, 238-249.

Kay, M.A., Holterman, A.-X., Meuse, L., Gown, A., Ochs, H.D., Linsley, P.S. and Wilson, C.B. (1995) Long-term hepatic adenovirus-mediated gene expression in mice following CTLA41g administration. *Nature Genetics*, **11**, 191-197.

Kelley, P. and Schlesinger, M.J. (1978) The effect of amino-acid analogues and heat shock on gene expression in chicken embryo fibroblasts. *Cell*, **15**, 1277-1286.

Kelly, P.A.T. and McCulloch, J. (1982) A potential error in modifications of the [14^C]2-deoxyglucose technique. *Brain Research*, **260**, 172-7.

Kennedy, C., Sakurada, O., Shinohara, M., Jehle, J. and Sokoloff, L. (1978) Local cerebral glucose utilization in the normal conscious macaque monkey. *Annals of Neurology*, **4**, 293-301.

Kerr, J.F.R., Wylie, A.H. and Currie, A.R. (1972) Apoptosis: A basic biological phenomenon with wide ranging implications in tissue kinetic. *British Journal of Cancer*, **26**, 239-57.

Kety, S.S. (1948) Blood-tissue exchange methods: Theory of blood-tissue exchange and its application to measurement of blood flow. In: *Methods in Medical Research.* (editor, Bruner, H.D.) Year Book Publishers Inc., Chicago.

Kihara, S., Shiraishi, T., Nakagawa, S., Toda, K. and Tabuchi, K. (1994) Visualization of DNA double strand breaks in the gerbil hippocampal CA1 following transient ischemia. *Neuroscience Letters*, **175**, 133-136.

Kim, J., Nueda, A., Meng, Y-H., Dynan, W.s. and Mivechi, N.F. (1997) Analysis of the phosphorylation of human heat shock transcription factor –1 by MAP kinase family members. *Journal of Cellular Biochemistry*, **67**, 43-54.

Kindy, M.S., Yu, J., Miller, R.J., Roos, R.P. and Ghadge, G.D. (1996) Adenoviral vectors in ischaemic injury. In: *Pharmacology of Cerebral Ischemia.* (editor, Krieglstein, J.) pp. 525-535. Medical Pharmacology, Stuttgart.

Kinouchi, H., Epstein, C.J., Mizui, T., Carlson, E., Chen, S.F. and Chan, P.H. (1991) Attenuation of focal ischemic injury in transgenic mice overexpressing CuZn superoxide dismutase. *Proceedings of the National Academy of Sciences, USA,* **88**, 11158-11162.

Kirino, T. (1982) Delayed neuronal death in the gerbil hippocampus following ischemia. *Brain Research*, **239**, 57-69.

Kirino, T., and Sano, K. (1984a) Selective vulnerability in the gerbil hippocampus following transient ischemia. *Acta Neuropathologica Berlin*, **62**, 201-208.

Kirino, T., and Sano, K. (1984b) Fine structural nature of delayed neuronal death following ischemia in the gerbil hippocampus. *Acta Neuropathologica Berlin*, **62**, 209-218.

Kirino, T., Tsujita, Y. and Tamura, A. (1991) Induced tolerance to ischemia in gerbil hippocampal neurons. *Journal of Cerebral Blood Flow and Metabolism, II*, 299-307.

Kitagawa, K., Matsumoto, M., Tagaya, M., Kuwabara, K., Hata, R., Handa, N., Fukunaga, R., Kimura, K. and Kamada, T. (1991) Hyperthermia-Induced neuronal protection against ischemic injury in gerbils. *Journal of Cerebral Blood Flow and Metabolism*, **11**, 449-452.

Kitagawa, K., Matsumoto, M., Mabuchi, T., Yagita, Y., Ohtsuki, T., Hori, M., Yang, G., Tanabe, H., Martinou, J.C., Hori, M. and Yanagihara, T. (1998) Deficiency of intracellular adhesion molecule 1 attenuates microcirculatory disturbance and infarction size in focal cerebral ischemia. *Journal of Cerebral Blood Flow and Metabolism*, **18**, 1336-1345.

Kitagawa, K., Matsumoto, M., Tsujimoto, Y., Ohtsuki, T., Kuwabara, K., Matsushita, K., Yang, G., Tanabe, H., Martinou, J.C., Hori, M. and Yanagihara, T. (1998) Amelioration of hippocampal neuronal damage after global ischemia by neuronal overexpression of BCL-2 in transgenic mice. *Stroke*, **29**, 2616-2621.

Kitagawa, H., Setoguchi, Y., Fukuchi, Y., Mitsumoto, Y., Koga, N., Mori, T. and Abe, K. (1998) Induction of DNA fragmentation and HSP72 immunoreactivity by adenovirus-mediated gene transfer in normal gerbil hippocampus and ventricle. *Journal of Neuroscience Research*, **54**, 38-45.

Kleihues, P. and Hossman, K-A. (1971) Protein synthesis in the cat brain after prolonged cerebral ischemia. *Brain Research*, **35**, 409-418.

Kochanek, S., Clemens, P.R., Mitani, K., Chen, H., Chan, S. and Caskey, C.T. (1996) A new adenoviral vector: Replacement of all viral coding sequences with 28 Kb of DNA independent expression in both full-length dystrophan and β-galactosidase. *Proceedings of the National Academy of Sciences, USA,* **93**, 5731-5736.

Koller, B.H., Hagemann, L.J., Doetschman, T., Hagaman, J.R., Huang, S., Williams, P.J., First, N.L., Maeda, N. Smithies, O. (1989) Germ-line transmission of a planned alteration made in a hypoxanthine phosphoribosyltransferase gene by homologous recombination embryonic stem cells. *Proceedings of the National Academy of Sciences, USA,* **86**, 8927-8931.

Kondo, T., Sharp, F.R., Honkaniemi, J., Mikawa, S., Epstein, C.J. and Chan, P.H. (1997) DNA fragmentation and Prolonged expression of c-fos, c-jun, and hsp70 in kainic acid-induced neuronal cell death in transgenic mice overexpressing human CuZu-superoxide dismutase. *Journal of Cerebral Blood Flow and Metabolism,* **17**, 241-256.

Kreutzberg, G.W., Blakemore, W.F. and Graeber, M. (1997) Cellular pathology of the central nervous system. In *Greenfield's Neuropathology*, (editors, Graham, D.I. and Lantos, P.L.), Arnold, London.

Kristián, T., Bo, K., Siesjö, M.D. (1998) Calcium in ischemic cell death. *Stroke*, **29**, 705-718.

Kuehn, M.R., Bradley, A., Robertson, E.J. and Evans, M.J. (1987) A potential animal model for Lesch-Nyhan syndrome through introduction of HPRT mutations into mice. *Nature*, **326**, 295-298.

Kuriyama, M., Umezaki, H., Fukuda, Y., Osume, M., Koike, K., Tateishi, J. and Igata, A. (1984) Mitochondrial encephalomyelopathy with lactate-pyruvate elevation and brain infarctions. *Neurology*, **34**, 72-77.

Kuroiwa, T., Bonnekoh, P and Hossman, K-A. (1990) Prevention of postischemic hyperthermia prevents ischemic injury of CA1 neurons in gerbils. *Journal of Cerebral Blood Flow Metabolism*, **10**, 550-556.

Kurumaji, A., Nehls, D.G., Park, C.K. and McCulloch, J. (1989) Effects of NMDA antagonists, MK-801 and CPP, upon local cerebral glucose use. *Brain Research*, **496**, 268-284.

Larson, J.S., Schuetz, T.J. and Kingston, R.E. (1988) Activation in vitro of sequence-specific DNA binding by a human regulatory factor. *Nature*, **335**, 372-375.

Lasko, M., Sauer, B., Mosigner, B., Lee, E.J., Manning, R.W., Yu, S-H., Mulder, K.L. and Westphal, H. (1992) Targeted oncogene activation by site-specific recombination in transgenic mice. *Proceedings of the National Academy of Sciences, USA,* **89**, 6232-6236.

Latchman, D.S. (1998) Stress proteins: An overview. In *Stress proteins* (editor, Latchman, D.S.) pp. 1-7, Springer- Verlay Press, New York.

Lathe, R. (1996) Mice, gene targeting and behaviour: more than just genetic background. *Trends in Neuroscience*, **19**, 183-186.

Lawrence, M.S., Ho, D., Dash, R. and Sapolsky, R.M. (1995) Herpes simplex virus vectors overexpressing the glucose transporter gene protect against seizure-induced neuron loss. *Proceedings of the National Academy of Sciences, USA,* **92**, 7247-7251.

Lawrence, M.S., Ho, D.Y., Sun, GH., Steinberg, G.K. and Sapolsky, R.M. (1996a) Overexpression of Bcl-2 with herpes simplex virus vectors protects CNS neurons against neurologic insults in vitro and in vivo. *Journal of Neuroscience*, **16**, 486-493.

Lawrence, M.S., Sun, G.H., Kunis, D.M., Saydam, D.M., Ho, D.Y ., Sapolsky, R.M. and Steinberg, G.K. (1996b) Overexpression of the glucose transporter gene with a herpes simplex viral vector protects striatal neurons against stroke. *Journal of Cerebral Blood Flow and Metabolism*, **181**, 181-185.

Le Gal La Salle, G., Robert, J.J., Berrard, S., Ridoux, V., Stratford-Perricaudet, L.D., Perricaudet, M. Mallet, J. (1993) An adenovirus vector for gene transfer into neurons and glia in the brain. *Science*, **259**, 988-990.

Lee, J.Y., Park, J., Kim, Y.H., Kim, D.K., Kim, C.G. and Koh, J.Y. (2000) Induction by synaptic zinc of heat shock protein-70 in hippocampus after kainate seizures. *Experimental Neurology*, **161**, 433-41.

Lemeaux, P.G., Herendeen, S.L., Bloch, P.L. and Neidhart, F.C. (1978) Transient rates of synthesis of individual peptides in *E.coli* following temperature shifts. *Cell*, **13**, 427-434.

Levine, S. and Payan, H. (1996) Effects of ischemia and other procedure on the brain and retina of the gerbil. *Experimental Neurology*, **16**, 255-262.

Levine, S. and Sohn, D. (1969) Cerebral ischemia in infant and adult gerbils: relation to an incomplete circle of Willis. *Archives of Pathology*, **87**, 315-317.

Lewis, M.J., Helmsing, P. and Ashburner, M. (1975) Parallel changes in puffing activity and patterns of protein synthesis in salivary glands of *Drosophila*. *Proceedings of the National Academy of Sciences, USA,* **72**, 3604-3608.

Linnik, M.D., Zahos, P., Geshwind, M.D. and Federoff, H.J. (1995) Expression of Bcl-2 from a defective herpes simplex virus-1 vector limits neuronal death in focal ischemia. *Stroke*, **26**, 1670-1674.

Lis, J., Prestige, L. and Hogness, D.S. (1978) A novel arrangement of tandemly repeated genes at a major heat shock site in *Drosophila melanogaster*. *Cell*, **14**, 901-919.

Lisovoski, F., Wahram, J.P., Pages, J.C., Cadusseau, J., Rieu, M., Weber, M., Kahn, A. and Peschanski, (1997) Long-term histological follow-up of genetically modified myoblasts grafted into the brain. *Molecular Brain Research*, **44**, 125-133.

Liu, J., Solway, K., Messing, R.O. and Sharp, F.R. (1998) Increased neurogenesis in the dentate gyrus after transient global ischemia in gerbils. *Journal of Neuroscience*, **18**, 7768-7778.

Livy, D.J. and Wahlsten, D. (1991) Tests of Genetic Allelism between four inbred mouse strains with absent corpus callosum. *Journal of Heredity*, **82**, 459-464.

Ljunggren, B., Schutz, H. and Siesjo, B.K. (1974) Changes in energy state and acid-base parameters of the rat brain during complete compression ischemia. *Brain Research*, **73**, 277-289.

Longa, E.Z., Weinstein, P.R., Carlson, S. and Cummins, R. (1989) Reversible middle cerebral artery occlusion without craniectomy in rats. *Stroke*, **20**, 84-91.

Lowensein, D.H., Chan, P.H. and Miles, M.F. (1991) The stress response in cultural neurons: Characterisation and evidence for a protective role in excitotoxicity. *Neuron*, **7**, 1053-1060.

Lowry, O.H., Passonneau, J.V., Hasselberger, F.X. and Schulz, D.W. (1964) Effects of ischemia on known substrates and cofactors of the glycolytic pathway in brain. *Journal of Biological Chemistry*, **239**, 18-30.

MacManus, J.P., Buchan, A.M., Hill, I.E., Rasquinha, I. and Preston, E. (1993) Global ischemia can cause DNA fragmentation indicative of apoptosis in rat brain. *Neuroscience Letters*, **164**, 89-92.

MacManus, J.P., Hill, I.E., Preston, E., Rasquinha, I., Walker, T. and Buchan, A.M. (1995) Differences in DNA fragmentation following transient cerebral or decapitation ischemia in rats. *Journal of Cerebral Blood Flow Metabolism*, **15**, 728-737.

MacManus, J.P. and Linnik, M.D. (1997) Gene expression induced by cerebral ischemia: an apoptotic perspective. *Journal of Cerebral Blood Flow Metabolism*, **17**, 815-832.

Maeda, R., Hata, R. and Hossman, K-A. (1998) Differences in the cerebrovascular anatomy of C57Black/6 and SV129 mice. *NeuroReport*, **9**, 1317-1319.

Maeda, R., Hata, R. and Hossman, K-A. (1999) Regional metabolic disturbances and cerebrovascular anatomy after permanent middle cerebral artery occlusion in C57Black/6 and SV129 Mice. *Neurobiology of Disease*, **6**, 101-108.

Maitland, N.J. and McDougall, J.K. (1977) Biochemical transformation of mouse cells by fragments of herpes simplex virus DNA. *Cell*, **11**, 233-241.

Mailhos, C., Howard, M.K. and Latchman, D.S. (1994) Heat shock proteins hsp90 and hsp70 protect neuronal cells from thermal stress but not from programmed cell death. *Journal of Neurochemistry*, **63**, 1787-1795.

Majno, G. and Joris, I. (1995) Apoptosis, oncosis, and necrosis. *American Journal of Pathology*, **146**, 16-18.

Mann, R., Mulligan, R.C. and Baltimore, D. (1983) Construction of a retrovirus packaging mutant and its use to produce helper-free defective retrovirus. *Cell*, **33**, 153-159.

Mansour, S.L., Thomas, K.R. and Capecchi, M.R. (1988) Disruption of the proto-oncogene *int-2* in mouse embryo-derived stem cells: a general strategy for targeting mutations to non-selectable genes. *Nature*, **336**, 348-352.

Marcel, T. and Grausz, J.D. (1997) The TMC worldwide gene therapy enrolment report, end 1996. *Human Gene Therapy*, **8**, 775-800.

Martin, G.R. (1981) Isolation of a pluripotent cell line from early mouse embryos cultured in medium conditioned by teratocarcinoma stem cells. *Proceedings of the National Academy of Sciences, USA,* **78**, 7624-7638.

Massa, S.M., Swanson, R.A. and Sharp, F.R. (1996) The stress gene response in brain. *Cerebrovascular and Brain Metabolism Reviews*, **8**, 95-158.

Mathis, C., Neumann, PE.E., Gershenfeld, H., Paul, S.M. and Crawley, J.N. (1995) Genetic analysis of anxiety-related drugs in AXB and BXA recombinant inbred mouse strains. *Behavioural Genetics*, **25**, 557-68.

Mathis, C., Paul, S.M. and Crawley, J.N. (1994) Characterization of benzodiazepine-sensitive behaviors n the A/J and C57BL/6J inbred strains of mice. *Behavioural Genetics*, **24**, 171-80.

McAlister, L., Strausberg, S., Kulaga, A. and Finklestein, D.B. (1979) Altered patterns of synthesis induced by heat shock in yeast. *Current Genetics,* **1**, 63-74.

McCarron, M.O., Delong, D. and Alberts, M.J. (1999) *APOE* genotype as a risk factor for ischemic cerebrovascular disease. A meta-analysis. *Neurology*, **53**, 1308-1311.

McCulloch, J. (1994) Amelioration of ischemic and hemorrhagic injury by pharmacological intervention. In *Brain Lesions in the Newborn*, (editors, Lou, H.C., Gresien, G. and Falck Larson, J) pp. 485-495, Alfred Benzon Symposium 37, Munksgaard, Copenhagen.

McCulloch, J. (1982) Mapping functional alterations in the CNS with [^{14}C]-deoxyglucose. In: *Handbook of Psychopharmacology: New Techniques In Psychopharmacology*. (editors, Iversen, L.L., Iversen, S.D. and Snyder, S.H.) pp. 321-410. Plenum Press, New York and London.

McKie, E.A., Graham, D.I. and Brown, S.M. (1998) Selective astrocytic transgene expression in vitro and in vivo from the GFAP promoter in a HSV RL1 null mutant vector – potential glioblastoma targeting. *Gene Therapy*, **5**, 440-450.

McKenzie, S., Lindquist, S.L., Henikoff, S. and Meselson, M. (1975) Localisation of RNA from heat-induced polysomes at puff sites in *Drosophila melanogaster*. *Proceedings of the National Academy of Sciences, USA,* **72**, 1117-1121.

McKenzie, S., Lindquist, S.L. and Meselson, M. (1977) Translation *in vitro* of *Drosophila* heat shock messages. *Journal of Molecular Biology*, **117**, 279-283.

Meier, T., Ho, D.Y., Park, T.S. and Sapolsky, R.M. (1998) Gene transfer of calbindin D28K cDNA via herpes simplex virus amplicon decreases calcium ion mobilization and enhances neuronal survival following glutaminergic challenge but not following cyanide. *Journal of Neurochemistry*, **70**, 1013-1020.

Meier, T., Ho, D.Y. and Sapolsky, R.M. (1997) Increased expression of calbindin D28K via herpes simplex virus amplicon vector decreases calcium ion mobilization and neuronal survival following hypoglycaemic challenge. *Journal of Neurochemistry*, **69**, 1039-1045.

Miller, A.D., Jolly, D.J., Friedmann, T. and Verma, I.M. (1983) A transmissible retrovirus expressing human hypoxanthine phosphoribosyltransferase (HPRT): Gene transfer into cells obtained from humans deficient in HPRT. *Proceedings of the National Academy of Sciences, USA,* **80**, 4709-4713.

Miller, D.G., Adam, M.A. and Miller, A.D. (1990) Gene transfer by retrovirus vectors occurs only in cells that are actively replicating at the time of infection. *Molecular and Cellular Biology*, **10**, 4239-4242.

Miller, M.J., Xuong, N-H. and Geiduschek, E.P. (1979) A response of protein synthesis to temperature shift in yeast *Saccharomyces cerevisiae*. *Proceedings of the National Academy of Sciences, USA,* **76**, 5222-5225.

Minson, A.C., Wildy, P., Buchan, A. and Darby, G. (1978) Introduction of the herpes simplex virus thymidine kinase gene into mouse cells using virus DNA or transformed cell DNA. *Cell*, **13**, 581-587.

Mintz, B. (1962) Formation of genotypically mosaic mouse embryos. *American Zoologist* **2**, 432.

Mintz, B. and Illmensee, K. (1975) Normal genetically mosaic mice produced from malignant teratocarcinoma cells. *Proceedings of the National Academy of Sciences, USA,* **72**, 3585-3589.

Mirault, M.E. Goldschmidt-Clermont, M., Moran, L., Arrigo, A.P. and Tissieres, A. (1978) The effect of heat shock on gene expression in *Drosophila melanogaster. Cold Spring Harbor Symposia on Quantitative Biology*, **42**, 819-827.

Mivechi, N.F., Uvyang, H. and Hahn, G.M. (1992) Lower heat shock factor activation and binding and faster rate of HSP-70 A messenger RNA turnover in heat sensitive human leukaemia's. *Cancer Research*, **52**, 6815-6822.

Morimoto, R.I. (1998) Regulation of the heat shock transcriptional response: cross talk between a family of heat shock factors, molecular chaperones, and negative regulators. *Genes and Development*, **12**, 3788-3796.

Morimoto, R.I., Jurivich, D.A., Kroger, P.E., Mathur, S.K. Murphy, S.P., Nakai, A., Sarge, A.K., Abravaya, K. and Sistonen, L.T. (1994) Regulation of heat shock gene transcription by a family of heat shock factors. In *The biology of heat shock proteins and molecular chaperones.* (editors, Morimoto, R.I., Tissieres, A. and Georgopoulos) pp. 417-455. Cold Spring Harbor Laboratory Press, Cold Spring Harbour, NY.

Morimoto, R.I., Kroeger, P.E, and Cotto, J.J. (1996) The transcriptional regulation of heat shock genes: a plethora of heat shock factors and regulatory conditions. In *Stress-inducible cellular responses* (editors, Feige, U., Morimoto, R., Yahara, I. And Pollaj, B.S.) pp. 139-163, Birkhauser, Boston, MA. .

Morimoto, R.I., Tissieres, A. and Georgopoulos, C. (1990) The stress response, function of the proteins, and perspectives, in *Stress proteins in biology and medicine* (editors,. Morimoto, R.I., Tissieres, A. and Georgopoulos, C.) pp. 1-36. cold Spring Harbor Laboratory Press, Cold Spring Harbor, NY.

Mosser, D.D., Duchaine, J. and Massie, B. (1993) The DNA-binding activity of the human heat shock transcription factor is regulated in vivo by hsp70. *Molecular and Cellular Biology.* **13**, 5427-5438.

Mukoyama, M., Kazui, H., Sunohara, N., Yoshida, M., Nonaka, I. And Satoyoshi. (1986) Mitochondrial myopathy, encephalopathy, latic acidosis, and strokelike episodes with acanthocytosis: a clinicopathological study of a unique case. *Journal of Neurology*, **233**, 228-232.

Murakami, K., Kondo, T., Kawase, M. and Chan, P.H. (1998a) The development of a new mouse model of global ischemia: focus on the relationships between ischemia duration, anasthesia, cerebral vasculature, and neuronal injury following global ischemia in mice. *Brain Research*, **780**, 304-310.

Murakami, K., Kondo, T., Kawase, M., Li, Y Sato, S., Chen, S.F., and Chan, P.H. (1998b) Mitochondrial susceptibility to oxidative stress exacerbates cerebral infarction that follows permanent focal cerebral ischemia in mutant mice with manganese superoxide dismutase deficiency. *Journal of Neuroscience*, **18**, 205-213.

Nagayama, M., Aber, T., Nagayama, T., Ross, M.E. and Iadecola, C. (1999) Age-dependant increase in ischemic brain injury in wild-type mice and mice lacking the inducible nitric oxide synthase gene. *Journal of Cerebral Blood Flow and Metabolism*, **19**, 661-666.

Nakai, A. and Morimoto, R.I. (1993) Characterisation of a novel chicken heat shock transcription factor, heat shock factor 3, suggests a new regulatory pathway. *Molecular and Cellular Biology*, **13**, 1983-1987.

Nakai, A., Tanabe, M., Kawazoe, Y., Inazawa, J., Morimoto, R.I. and Nagata, K. (1997) HSF4, a new member of the human heat shock factor family which lacks properties of a transcriptional activator. *Molecular and Cellular Biology*, **17**, 469-481.

Naldini, L., Blomer, U., Gallay, P., Ory, D., Mulligan, R., Gage, F.H., Verma, I.M. and Trono, D. (1996) *In vivo* gene delivery and stable transduction of nondividing cells by a lentiviral vector. *Science*, **272**, 263-267.

National Institute of Neurological Disorders; Stroke rt-PA Stroke Study Group. (1995) Tissue plasminogen activator for acute ischemic stroke. *The New England Journal of Medicine*, **333**, 1581-1587.

Nehls, D.G., Kurumaji, A., Park, C.K. and McCulloch, J. (1988) Differential effects of competitive and non-competitive *N*-methyl-D-aspartate antagonists on glucose use in the limbic system. *Neuroscience Letters*, **91**, 204-210.

Nehls, D.G., Park, C.K., MacCormack, A.G. and McCulloch, J. (1990) The effects of *N*-methyl-D-aspartate receptor blockade with MK-801 upon the relationship between cerebral blood flow and glucose utilisation. *Brain Research*, **511**, 271-279.

Nevander, G., Ingvar, M., Auer, R.N. and Siesjö, B.K. (1985) Status epilepticus in well oxygenated rats causes neuronal necrosis. *Annals of Neurology*, **18**, 281-290.

Nicholas, J.S. and Hall, B.V. (1942) Experiments on developing rats: The development of isolated blastomeres and fused eggs. *Journal of Experimental Zoology* **90**, 441-458.

Nicholls, D. and Attwell, D. (1990) The release and uptake of excitatory amino acids. *Trends Pharmacological Science*, **11**, 462-8.

Nitatori, T., Sato, N., Waguri, S., Karasawa, Y., Araki, H., Shibanai, K., Kominami, E. and Uchiyama, Y. (1995) Delayed neuronal death in the CA1 pyramidal cell layer of the gerbil hippocampus following transient ischemia is apoptosis. *Journal of Neuroscience*, **15**, 1001-1011.

Nowak, T.S. Jr (1985) Synthesis of a stress protein following transient ischemia in the gerbil. *Journal of Neurochemistry*, **45**, 1635-1641.

Nowak, T.S. Jr (1990) Localisation of 70kDa stress protein mRNA induction in gerbil brain after ischemia. *Journal of Cerebral Blood Flow and Metabolism*, **11**, 432-439.

Nowacyzk, T. and Des Rosiers, M.H. (1981) Application of the 2-deoxy-D-[14C]-glucose method to the mouse for measuring local cerebral glucose utilitzation. *European Neurology*, **20**, 169-172.

Nyberg-Hoffman, C. and Aguiler-Cordiova, E. (1999) Instability of adenoviral vectors during transport and its implication for clinical studies. *Nature Medicine*, **5**, 955-957.

Ohmoto, Y., Wood, M.J., Charlton, H.M., Kajiwara, K., Perry, V.H. and Wood, K.J. (1999) Variation in the immune response to adenoviral vectors in the brain: influence of mouse strain, environmental conditions and priming. *Gene Therapy*, **6**, 471-81.

Okamoto, M., Matsumoto, M., Ohtsuki, T., Taguchi, A., Mikoshiba, K., Yanagihata, T and Kamada, T. (1993) Internucleosomal DNA cleavage involved in ischemia-induced neuronal death. *Biochemical and Biophysical Research and Communication*, **196**, 1356-1362.

Oldendorf, W.H. (1971) Brain uptake of radiolabelled amino acids, amines and hexoses after arterial injection. *American Journal of Physiology*, **221**, 1629-1639.

Oldstone, M.B.A. (1998) *Viruses, Plagues and History*, Oxford University Press, New York and London.

Olney, J.W. (1969a) Glutamate-induced retinal degeneration in neonatal mice. Electron microscopy of the acutely evolving lesions. *Journal of Neuropathology and Experimental Neurology*, **28**, 455-474.

Olney, J.W. (1969b) Brain lesions, obesity, and other disturbances in mice treated with monosodium glutamate. *Science*, **164**, 719-721.

Olney, J.W. (1971) Glutamate-induced neuronal necrosis in the infant mouse hypothalamus. *Journal of Neuropathology and Experimental Neurology*, **30**, 75-90.

Olney, J.W., Ho, O.L. and Rhee, V. (1971) Cytotoxic effects of acidic and sulphur containing amino acids on the infant mouse central nervous system. *Experimental Brain Research*, **14**, 61-76.

Olney, J.W., Labruyere, J. and Price, M.T. (1989) Pathological changes induced in cerebrocortical neurons by phencyclidine and related drugs. *Science*, **244**, 1360-62.

Orban, P.C., Chui, D. and Marth, J.D. (1992) Tissue- and site-specific DNA recombination in transgenic mice. *Proceedings of the National Academy of Sciences, USA*, **89**, 6861-6865.

Palmiter R.D., Brinster, R.L., Hammer, R.E., Trumbauer, M.E., Rosenfeld, M.G., Birnberg, N.C. and Evans, R.M. (1982) Dramatic growth of mice that develop from eggs microinjected with metallothionein-growth hormone fusion genes. *Nature*, **300**, 611-615.

Panahian, N., Yoshida, T., Huang, P.L., Hedley-White, E.T., Dalkara, T., Fishman, M.C., and Moskowitz, M.A. (1996) Attenuated hippocampal damage after global cerebral ischemia in mice mutant in neuronal nitric oxide synthase. *Neuroscience*, **72**, 343-354.

Panahian, N., Yoshimura, M. and Maines, M.D. (1999) Overexpression of heme oxygenase-1 is neuroprotective in a model of permanent middle cerebral artery occlusion in transgenic mice. *Journal of Neurochemistry*, **72**, 1187-1203.

Papadopoulos, M., Sun, X., Cao., J., Mivechi, N.F. and Giffard, R.G. (1996) Over-expression of HSP-70 protects astrocytes from combined oxygen-glucose deprivation. *NeuroReport*, **7**, 429-432.

Pavlakis, S.G., Phillips, P.C., DiMauro, S., De Vivo, D.C. and Rowland, L.P. (1984) Mitochondrial myopathy, encephalopathy, latic acidosis, and strokelike episodes: a distinctive clinical syndrome. *Annals of Neurology*, **16**, 481-488.

Petito, C.K., Feldmann, E., Pulsinelli, W.A. and Plum, F. (1987) Delayed hippocampal damage in humans following cardiorespiratory arrest. *Neurology*, **37**, 1281-1286.

Petty, M.A. and Wettstein, J.G. (1999) White matter ischaemia. *Brain Research Reviews*, **31**, 58-64.

Phillips, R.G., Meier, T.J., Giuli, L.C., McLaughlin, J.R., Ho, D.Y., and Sapolsky, R.M. (1999) Calbindin D28K gene-transfer via herpes simplex virus amplicon vector decreases hippocampal damage in vivo following neurotoxic insults. *Journal of Neurochemistry*, **73**, 1200-05.

Planas, A.M., Soriano, M.A., Ferrer, I., Rodrigues and Farre, E. (1994) Regional expression of inducible heat shock protein-70 m RNA in the rat brain following administration of convulsant drugs. *Molecular Brain Research*, **27**, 127-37.

Plumier, J-C. L., Krueger, A.M., Currie, R.W., Kontoyianis, D., Kollias, G. and Pagoulatos, G.N. (1997) Transgenic mice expressing the human inducible hsp70 have hippocampal neurones resistant to ischemic injury. *Cell Stress and Chaperones*, **2**, 162-167.

Poirer, J. (1994) Apolipoprotein E in animal models of CNS injury and in Alzheimer's disease. *Trends in Neuroscience*, **17**, 525-30.

Prestigiacomo,C.J., Kim, S.C., Connolly, E.S.J., Liao, H., Yan, S.F. and Pinsky, D.J. (1999) CD18-mediated neutrophil recruitment contributes to the pathogenesis of reperfused but not nonreperfused stroke. *Stroke*, **30**, 1110-1117.

Prinz, M. and Hanisch, U-K. (1999) Murine microglial cells produce and respond to interleukin-18. *Journal of Neurochemistry*, **72**, 2215-2218.

Pulsinelli, W.A. and Brierley, J.B, (1979) A new model of bilateral hemispheric ischemia in the unanesthetized rat. *Stroke*, **10**, 267-272.

Pulsinelli, W.A., Brierley, J.B. and Plum, F. (1982) Temporal profile of neuronal damage in a model of transient forebrain ischemia. *Annals of Neurology*, **11**, 491-498.

Radjev, S., Hara, K., Solway, K.E., Mestril, R., Dillman, W.H., Weinstein, P.R. and Sharp, F.R. (1999) Cerebral protection in transgenic mice overexpressing heat shock protein 72 after focal ischemia. *Journal of Cerebral Blood Flow and Metabolism*, **19** (Supplement 1), S289.

Rendahl, K.G., Leff, S.E., Otten, G.R., Spratt, S.K., Bohl, D., Van Roey, M., Donahue, B.A., Cohen, L.K., Mandel, R.J., Danos, O. and Snyder, R.O. (1998) Regulation of gene expression in vivo following transduction by two separate rAAV vectors. *Nature Biotechnology*, **16**, 757-761.

Reventos, J. and Gordon, J.W. (1990) Introduction of genes into the mouse germ line. *Acta Paediatrica Scandinavica (supplementum)*, **366**, 45-56.

Ritossa, F. (1962) A new puffing pattern induced by temperature shock and DNP in *Drosophila. Experientia*, **18**, 571-573.

Ritossa, F. (1964) Experimental activation of specific loci in polytene chromosomes of *Drosophila Experimental Cell Research*, **35**, 601-607.

Robertson, E., Bradley, A., Kuehn, M. and Evans, M. (1986) Germ-line transmission of genes introduced into cultured pluripotential cells by retroviral vector. *Nature*, **323**, 445-448.

Robinson, R.G., Shoemaker, W.J., Schlumpf, M., Valk, T. and Bloom, F.E. (1975) Experimental early infarction in rat brain: effect on catecholamines and behaviour. *Nature*, **255**, 332-334.

Rothman, S.M. and Olney, J.W. (1986) Glutamate and the pathophysiology of hypoxic-ischemic brain damage. *Annals of Neurology*, **19**, 105-111.

Rottenberg, A. (1996) Reverse peidpiperase: is the knockout mouse leading neuroscientist to a watery end? *Trends in Neuroscience*, **19**, 471-472.

Roy, M. and Sapolsky, R.M. (1999) The neuroprotective capabilities of viral anti-apoptotic genes. *Society for Neuroscience Abstracts*, **25**, 451.10

Sapolsky, R.M. and Steinberg, G.K. (1999) Gene therapy using viral vectors for acute neurologic insults. *Neurology*, **53**, 1922-1931.

Sarge, K.D., Zimarino, V., Holm, K., Wu, C. and Morimoto, R.I. (1991) Cloning and characterization of two mouse heat shock factors with distinct inducible and constitutive DNA-binding ability. *Genes and Development*, **5**, 1902-1911.

Sauer, B and Henderson, N. (1988) Site-specific DNA recombination in mammalian cells by the Cre recombinase of bacteriophage P1. *Proceedings of the National Academy of Sciences, USA,* **85**, 5166-5170.

Sauer, B and Henderson, N. (1989) Cre-stimulated recombination at *loxP*-containing DNA sequences placed into the mammalian genome. *Nucleic Acids Research*, **17**, 147-161.

Scheidner, A., Martin-Villalba, A., Weih, F., Vogel, J., Writh, T. and Schwaninger, M. (1998) NF-κB is activated and promotes cell death in focal cerebral ischemic injury. *Nature Medicine*, **5**, 554-559.

Scheidner, G., Morral, N., Parks, R.J., Wu, Y., Koopmans, S.C., Langston, C., Graham, F.L., Beaudet, A.L. and Kochanek, S. (1998) Genomic DNA transfer with a high-capacity adenovirus vector results in improved in vivo gene expression and decreased toxicity. *Nature Genetics*, **18**, 180.

Schuetz, T.J., Gallo, G.J., Sheldon, L., Tempst, P., and Kingston, R.E. (1991) Isolation of a cDNA for HSF2: evidence for two heat shock factor genes in humans. *Proceedings of the National Academy of Sciences, USA,* **88**, 6911-6915.

Schwartz, W.J. (1978a) 6-Hydroxydopamine lesions of rat locus coeruleus after brain glucose consumption, as measured by the 2-deoxy-*d*-[^{14}C]-glucose tracer technique. *Neuroscience Letters*, **7**, 141-150.

Schwartz, W.J. (1978b) A role for the dopaminergic nigrostriatal bundle in the pathogenisis of altered brain glucose consumption after lateral hypothalamic lesion. Evidence using the ^{14}C-labelled deoxyglucose technique. *Brain Research*, **158**, 129-147.

Schwartz, W.J., Smith, C.B., Davidsen, L., Savaki, H.E., Sokoloff, L., Mata, M., Fink, D.J. and Gainer, H. (1979) Metabolic mapping of functional activity in the hypothalamo-neurohyphyseal system of the rat. *Science*, **205**, 723-725.

Scope, R., Wolfer, D.P., Lipp, H.P. and Leisinger-Trigona, M.C. (1991) Swimming navigation and structural variation of the infrapyramidal mossy fibers in the hippocampus of the mouse. *Hippocampus*, **1**, 315-28.

Seale T.W., McLananhan, K., Johnson, P., Carney, J.M. and Rennert, O.M. (1984) Systematic comparison of apomorphine-induced behavioral changes in two mouse strains with inherited differences in brain dopamine receptors. *Pharmacology Biochem Behavioral Genetics*, **21**, 237-44.

Sen, S. (1992) Programmed cell death: concept, mechanism and control. *Biological Reviews*, **67**, 287-319.

Sharp, F.R., Jasper, P., Hall, J., Noble, L. and Sagar, S.M. (1991) MK-801 and ketamine induce heat shock protein HSP72 in injured neurons in posterior cingulate and retrosplenial cortex. *Annals of Neurology*, **30**, 801-9.

Sharp, F.R., Massa, S.M. and Swanson, R.A. (1999) Heat-shock protein protection. *Trends in Neuroscience*, **22**, 97-99.

Sheng, H., Laskowitz, D.T., Bennett, E., Schmechel, D.E., Bart, R.D., Saunders, A.M., Pearlstein, R.D., Roses, A.D. and Warner, D.S. (1998) Apolipoprotein E isoform-specific differences in outcome from focal ischemia in transgenic mice. *Journal of Cerebral Blood Flow and Metabolism*, **18**, 361-366.

Shielke, G.P., Yang, G.Y., Shivers, B.D and Betz, A.L. (1998) Reduced ischemic brain injury in interleukin-1β converting enzyme-deficient mice. *Journal of Cerebral Blood Flow and Metabolism*, **18**, 180-185.

Siesjö, B.K. (1978) *Brain Energy Metabolism*, John Wiley & Sons, New York.

Siesjö, B.K., Katsura, K. and Kristian, T. (1995) The biochemical basis of cerebral ischemic damage. *Journal of Neurosurgical Anesthesiology*, **7**, 47-52.

Simon, R.H., Engelhardt, J.F., Yang, Y., Zepeda, M., Weber-Pendleton, S., Grossman, M. and Wilson, J.M. (1993) Adenovirus-mediated transfer of the CFTR gene to lung of nonhuman primates: toxicity study. *Human Gene Therapy*, **4**, 771-780.

Simon, R.P., Schmidley, J.W., Swan, J.H. and Meldrum, B.S. (1986) Neuronal alterations in hippocampus following severe hypoglycaemia: a light microscopic and ultrastructural study in the rat. *Neuropathology and Applied Neurobiology*, **12**, 11-26.

Smaglik, P. (1999) Tighter watch urged on adenoviral vectors. *Nature*, **402**, 707.

Smith, M.-L., Auer, R.N. and Siesjö, B.K. (1984) The density and distribution of ischemic brain injury in the rat following 2 – 10 min of Forebrain Ischemia. *Acta Neuropathologica Berlin*, **64**, 319-322.

Smithies, O., Gregg, R.G., Boggs, S.S., Koralewski, M.A. and Kucherlapati, R.S. (1985) Insertion of DNA sequences into the human chromosomal β-globin locus by homologous recombination. *Nature*, **317**, 230-234.

Sokoloff, L. (1977) Relation between physiological function and energy metabolism in the central nervous system. *Journal of Neurochemistry*, **29**, 13-26.

Sokoloff, L. (1979) Mapping cerebral functional activity with radioactive deoxyglucose. *Trends in Neuroscience*, **1**, 75-79.

Sokoloff, L., Reivich, M., Kennedy, C., Des Rosiers, M.H., Patlak, C.S., Pettigrew, K.D., Sakurada, O. and Shinohara, M. (1977) The [^{14}C]-deoxyglucose method for the measurement of local cerebral glucose utilisation: theory, procedure and normal values in the conscious and anaesthetized albino rat. *Journal of Neurochemistry*, **28**, 897-916.

Sorger, P.K., Lewis, M.J. and Pelham, H.R. (1987) Heat shock factor is regulated differently in yeast and HeLa cells. *Nature*, **329**, 81-4.

Sorger, P.K. and Pelham, H.R. (1988) Yeast heat shock factor is an essential DNA-binding protein that exhibits temperature-dependent phosphorylation. *Cell*, **54**, 855-864.

Soriano, M.A., Tortosa, A., Planas, A.M., Rodriguez-Farre, E. and Ferrer, I. (1994) Induction of HSP70 protein in the hippocampus of the developing gerbil following transient forebrain ischemia. *Brain Research,* **653**, 191-198.

Soriano S.G., Coxon, A., Wang, Y.F., Frosch, M.P., Lipton, S.A., Hickey, P.R., and Mayadas, T.N. (1999) Mice deficient in Mac-1 (CD11b/CD18) are less susceptible to cerebral ischemia/reperfusion injury. *Stroke*, **30**, 134-139.

Soriano, S.G., Wang, Y.F., Lipton, S.A., Dikkes, P., Gutierrez-Ramos, J.C. and Hickey, P.R. (1998) ICAM-1 dependant pathway is not involved in the development of neuronal apoptosis after transient focal cerebral ischemia. *Brain Research*, **780**, 337-341.

Spralding, A., Penman, S. and Pardue, M.L. (1975) Analysis of *Drosophila* mRNAs by in situ hybridisation: Sequences transcribed in normal and heat shock cultured cells. *Cell*, **4**, 395-404.

Sternberg, N. and Hamilton, D. (1981) Bacteriophage P1 site-specific recombination I. Recombination between *loxP* sites. *Journal of Molecular Biology*, **150**, 467-486.

Stevenson, P.G., Freeman, S., Bangham, C.R. and Hawakes, S. (1997a) Virus dissemination through the brain parenchyma without immunologic control. *Journal of Immunology*, **159**, 1876-1884.

Stevenson, P.G., Hawkes, S., Sloan, D.J. and Bangham, C.R. (1997b) The immunogenicity of intracerebral virus infection depends on anatomical site. *Journal of Virology*, **71**, 145-151.

Stoll, G., Jander, S., and Schroeter, M. (1998) Inflammation and glial responses in ischemic brain lesion. *Progress in Neurobiology*, **56**, 149-171.

Suzuki, R., Yamaguchi, T., Kirino, T., Orzi, F. and Klatzo, I. (1983a) The effects of 5-min ischemia in Mongolian gerbils. I. Blood brain barrier, cerebral blood flow, and local cerebral glucose utilization changes. *Acta Neuropathologica Berlin*, **60**, 207-216.

Suzuki, R., Yamaguchi, T., Li, C-L. and Klatzo, I. (1983b) The effects of 5-min ischemia in Mongolian gerbils. II. Changes of spontaneous neuronal activity in the cerebral cortex and CA1 sector of the hippocampus. *Acta Neuropathologica Berlin*, **60**, 217-222.

Tamura, A., Graham, D.I., McCulloch, J. and Teasdale, G.M. (1981a) Focal cerebral ischaemia in the rat: I. Description of technique and early neuropathological consequences following middle cerebral artery occlusion. *Journal of Cerebral Blood Flow and Metabolism*, **1**, 53-60.

Tamura, A., Kawai, K. and Takagi, K. (1995) Animal models used in cerebral ischemia and stroke research. In *Clinical Pharmacology of Cerebral Ischemia*, (editors, Ter Horst, G.J. and Korf, J), Humana Press Inc., Totowa, New Jersey..

Tarkowski, A.K. (1961) Mouse chimaeras developed from fused eggs. *Nature*, **190**, 857-860.

Teasdale, G.M., Nicholl, J.A., Murray, G. and Fiddes, M. (1997) Association of apolipoprotein E polymorphism with outcome after head injury. *Lancet*, **350**, 1069-1071.

Thilman, R., Xie, Y., Kleihues, P. and Keissling, M. (1986) Persistent inhibition of protein synthesis precedes delayed neuronal death in postischemic gerbil hippocampus. *Acta Neuropathologica Berlin*, **71**, 88-93.

Thomas, K.R. and Capecchi, M.R. (1987) Site-directed mutagenesis by gene targeting in mouse embryo-derived stem cells. *Cell*, **51**, 503-512.

Thompson, S., Clarke, A.R., Pow, A.M., Hooper, M.L. and Melton, D.W. (1989) Germ line transmission and expression of a corrected HPRT gene produced by gene targeting in embryonic stem cells. *Cell*, **56**, 313-321.

Tissieres, A., Mitchell, H.K. and Tracy, U. (1974) Protein synthesis in salivary glands of *Drosophila melanogaster*: Relation to chromosome puffs. *Journal of Molecular Biology*, **84**, 389-398.

Tolliver, B.K. and Carney, J.M. (1994) Comparison of cocaine and GBR 12935: effects on locomotor activity and stereotypy in two inbred mouse strains. *Pharmacology Biochemistry and Behavior*, **48**, 733-9.

Tomimoto, H., Yamamoto, K., Homburger, H.A. and Yanagihara, T. (1993) Immunoelectron microscopic investigation of creatine kinase BBisoenzyme after cerebral ischemia in gerbils. *Acta Neuropathologica Berlin*, **86**, 447-455.

Tonder, N., Johansen, F.F., Frederickson, C.J., Zimmer, J. and Diemer, N.H. (1990) Possible role of zinc in the selective degeneration of dentate hilar neurons after cerebral ischemia in the adult rat. *Neuroscience Letters*, **109**, 247-252.

Touzani, O., Boutin, H., Chuquet, J. and Rothwell, N. (1999) Potential mechanisms of interleukin-1 involvement in cerebral ischaemia. *Journal of Neuroimmunology*, **100**, 203-15.

Tower, D.B. (1958) The effects of 2-deoxy-d-glucose on metabolism of slices of cerebral cortex incubated *in vitro*. *Journal of Neurochemistry*, **3**, 185-191.

Treuter, E.L., Nover, L., Ohme, K. and Scharf, K.D. (1993) Promoter specificity and deletion analysis of three tomato heat stress transcription factors. *Molecular & General Genetics*, **240**, 113-125.

Van der Neut, R. (1997) Targeted gene disruption: applications in neurobiology. *Journal of Neuroscience Methods*, **71**, 19-27.

Vass, K., Welch, W.J. and Nowak Jr, T.S. (1988) Localisation of 70-kDa stress protein induction in gerbil brain after ischemia. *Acta Neuropathologica Berlin*, **77**, 128-135.

Verma, I.M. and Somia, N. (1997) Gene therapy: problems and prospects. *Nature*, **389**, 239-242.

Wagner, M., Hermanns, I., Bittinger, F. and Kirkpatrick, C.J. (1999) Induction of stress proteins in human endothelial cells by heavy metal ions and heat shock. *American Journal of Physiology*, **277**, L1026-L1033.

Wahlsten, D. and Schalomon, P.M. (1994) A new hybrid mouse model for agenesis of the corpus callosum. *Behavioral Brain Research*, **20**, 111-117.

Wainwright, P. and Deeks, S. (1984) A comparison of corpus callosum development in the BALB/cCF and C57BL/6J inbred mouse strains. *Growth*, **48**, 192-197.

Walsh, C. (1980) Appearance of heat shock proteins during the incubation of multiple flagella in *Naegleria gruberi*. *Journal of Biological Chemistry*, **225**, 2629-2632.

Walters, L. (1986) The ethics of human gene therapy.. *Nature*, **320**, 225-27.

Watkins, J.C. and Evans, R.H. (1981) Excitatory amino acid tansmitters. *Annual Reviews in Pharmacological Toxicology*, **21**, 165-204.

Wehner, J.M. and Silva, A. (1996) Importance of strain differences in evaluations of learning and memory processes in null mutants. *Mental Retardation and Developmental Disabilities Research Review*, **2**, 243-248.

Weihl, C., MacDonald, R.L., Stoodley, M., Luders, J. and Lin, G. (1999) Gene Therapy for cerebrovascular disease. *Neurosurgery*, **44**, 239-253.

Welch, W.J. and Suhun, J.P. (1986) Cellular and biochemical events in mammalian cells during and after recovery from physiological stress. *Journal of Cell Biology*, **259**, 4501-4513.

Wigler, M., Silverstein, S., Lee, L., Pellicer, A., Cheng, Y. and Axel, R. (1977) Transfer of purified herpes virus thymidine kinase gene to cultured mouse cells. *Cell*, **11**, 223-232.

Williamson, B. (1982) Gene Therapy. *Nature*, **298**, 416-418.

White, F.P. (1980a) The induction of 'stress' proteins in organ slices from brain, heart and lung as a function of postnatal development. *Journal of Neuroscience*, **1**, 1312-1319.

White, F.P. (1980b) The synthesis and possible transport of specific proteins by cells associated with brain capillaries. *Journal of Neurochemistry*, **35**, 88-94.

White, F.P. (1981) Differences in protein synthesised in vivo and in vitro by cells associated with the cerebral microvasculature: A protein synthesised in response to trauma? *Neuroscience*, **5**, 1793-1799.

Wood, M.J., Charlton, H.M., Wood, K.J., Kajiwara, K. and Byrnes, A.P. (1996) Immune responses to adenovirus in the nervous system. *Trends in Neuroscience*, **19**, 497-501.

Woznicki, D.T. and Walker, J.B. (1980) Utilization of Cyclocreatine Phosphate, an Analogue of Creatine Phosphate, by Mouse Brain During Ischemia and Its Sparing Action on Brain Energy Reserves. *Journal of Neurochemistry*, **34**, 1247-1253.

Wroblewski, J.T. and Danysz, W. (1989) Modulation of glutamate receptors: Molecular mechanisms and functional implications. *Annual Reviews in Pharmacological Toxicology*, **29**, 441-74.

Wu, C. (1984) Two protein-binding sites in chromatin implicated in the activation of heat-shock genes. *Nature*, **309**, 229-234.

Wu, C. (1995) Heat shock transcription factors: structure and regulation. *Annual Review of Cell and Developmental Biology*, **11**, 441-469.

Wyllie, A.H., Kerr, J.F.R. and Currie, A.E. (1980) Cell death: the significance of apoptosis. *International Reviews in Cytology*, **68**, 251-306.

Xie, Y., Zacharias, E., Hoff, P., and Tegtmeier, F. (1995) Ion channel involvement in anoxic depolarisation induced by cardiac arrest in rat brain. *Journal of Cerebral Blood Flow and Metabolism,* **15**, 587-594.

Xu, D. and Cocker, S. (1997) Elevation of neuronal expression of NAIP reduces ischemic damage in the rat hippocampus. *Nature Medicine*, **3**, 997-1001.

Xu, L. and Giffard, R.G. (1997) HSP70 protects murine astrocytes from glucose deprivation injury. *Neuroscience Letters*, **224**, 9-12.

Yamamori, T., Ito, K., Nakamura, Y. and Yura, T. (1978) Transient regulation of protein synthesis in *Escherichia coli* upon shift-up of growth temperature. *Journal of Bacteriology*, **34**, 1133-1140.

Yamamoto, K., Hayakawa, T., Mogami, H., Akai, F. and Yanagihara, T. (1990) Ultrastructural investigation of the CA1 region of the hippocampus after transient cerebral ischemia in gerbils. *Acta Neuropathologica Berlin*, **80**, 487-492.

Yamamoto, K., Morimoto, K. and Yanagihara, T. (1986) Cerebral ischemia in the gerbil: Transmission electron microscopic and immunoelectron microscopic investigation. *Brain Research*, **384**, 1-10.

Yang, G-Y., Mao, Y., Zhou, L-F., Gong, C., Ge, H-L. and Betz, A.L. (1999) Expression of intercellular adhesion molecule 1 (ICAM-1) is reduced in permanent focal cerebral ischemic mouse brain using an adenoviral vector to induce overexpression in interleukin-1 receptor antagonist. *Molecular Brain Research,* **65**, 143-150.

Yang, Y., Nunes, F.A., Berensci, K., Furth, E.E., Gonczol, E. and Wilson, J.M. (1994) Cellular immunity to viral antigens limits E1-deleted adenoviruses for gene therapy. *Proceedings of the National Academy of Sciences, USA,* **91**, 4407-4411.

Yang, Y., Nunes, F.A., Berensci, K., Gonczol, E., Engelhardt, J. and Wilson, J.M. (1994) Inactivation of E2a in recombinant adenoviruses limits cellular immunity and improves the prospect of gene therapy for cystic fibrosis. *Nature Genetics*, **7**, 362-369.

Yang, G., Kitagawa, K., Matsushita, K., Mabuchi, T., Yagita, Y., Yanagihara, T. and Matsumoto, M. (1996) C57BL/6 strain is most susceptible to cerebral ischemia following bilateral common carotid occlusion among seven mouse strains: selective neuronal death in the murine transient forebrain ischemia. *Brain Research*, **752**, 209-218.

Yang, Y., Li, Q., Ertl, H.C. and Wilson, J.M. (1995) Cellular and humural immune response to viral antigens create barriers to lung-directed gene therapy with recombinant adenoviruses. *Journal of Virology*, **69**, 2004-15.

Yang, G., Zhao, Y., Davidson, B.L. and Betz, A.L. (1997) Overexpression of interleukin-1 receptor anatagonist in the mouse brain reduces ischemic brain injury. *Brain Research*, **751**, 181-188.

Yanagihara, T. (1976) Cerebral ischemia in gerbils: Differential vulnerability of protein, RNA and lipidsynthesis. *Stroke*, **7**, 260-263.

Yanagihara, T. (1978) Experimental stroke in gerbils: effect of translation and transcription. *Brain Research*, **158**, 435-444.

Yenari, M.A., Fink, S., Sun, G., Chang, L.K., Patel, M.K., Kunis, D.M., Onley, D., Ho, D.Y., Sapolsky, R.M. and Steinberg, G.K. (1998) Gene therapy with hsp72 is neuroprotective in rat models of stroke and epilepsy. *Annals of Neurology*, **44**, 584-591.

Yenari, M.A., Lee, J.E., Sun, G.H., Steinberg, G.K. and Gifford, R.G. (1999) Transgenic mice which overexpress HSP70 are protected against some but not all central nervous system insults. *Journal of Cerebral Blood Flow and Metabolism*, **19** (supplement1), S273.

Yenari, M.A., Minami, M., Sun, G., Sapolsky, R.M. and Steinberg, G.K. (1999) Calbindin D28K overexpression attenuates striatal neuron death following transient focal cerebral ischaemia. *Society for Neuroscience Abstracts*, **25**, 841.5.

Zhang, R.L., Chopp, M., Zhang, Z.G., Jiang, Q. and Ewing, J.R. (1997) A rat model of focal embolic cerebral ischemia. *Brain Research*, **766**, 83-92.

Zhang, Z., Chopp, M., Zhang, R.L. and Goussev, A. (1997) A mouse model of embolic focal cerebral ischemia. *Journal of Cerebral Blood Flow and Metabolism*, **17**, 1081-8.

Zijlstra, M., Li, E., Sajjadi, F., Subramani, S. and Jaenisch, R. (1989) Ger-line transmission of a disrupted β_2-microglobulin gene produced by homologous recombination in embryonic stem cells. *Nature*, **342**, 435-438.

Zimarino, V.and Wu, C. (1987) Induction of sequence specific binding of Drosophila heat shock activator protein without protein synthesis. *Nature*, **327**, 727-730.

Zimmer, A. (1996) Gene targeting and behaviour; a genetic problem requires a genetic solution. *Trends in Neuroscience*, **19**, 470-472.

Zimmer, A. and Gruss, P. (1989) Production of chimaeric mice containing embryonic stem (ES) cells carrying a homeobox *Hox 1.1* allele mutated by homologous recombination. *Nature*, **338**, 150-153.

Zou, J., Guo, Y., Guettouche, T., Smith, D.F. and Voellmy. (1998) Repression of heat shock transcription factor HSF1 activation by HSP90 (HSP90 complex) that forms a stress sensitive complex with HSF1. *Cell*, **94**, 471-480.

Zupane, G.K. (1999) Neurogenesis, cell death and regeneration in the adult gymnotiform brain. *Journal of Experimental Biology*, **202**, 1435-1446.